SCHOOL OF ENVIRONMENTAL SCIENCES

DEPARTMENT OF HYDROLOGY AND WATER RESOURCES

ISOTOPIC SIGNATURES AND TRACE METALS IN GEOTHERMAL SPRINGS AND THEIR ENVIRONMENTAL MEDIA WITHIN SOUTPANSBERG

BY

DUROWOJU OLATUNDE SAMOD

Student No: 11634830

A THESIS SUBMITTED TO THE DEPARTMENT OF HYDROLOGY AND WATER RESOURCES, SCHOOL OF ENVIRONMENTAL SCIENCES, UNIVERSITY OF VENDA, IN FULFILMENT OF THE REQUIREMENTS FOR PhD IN ENVIRONMENTAL SCIENCES

PROMOTER: PROFESSOR J.O. ODIYO

CO-PROMOTER: SENIOR PROFESSOR G.E. EKOSSE

JULY 2019

DECLARATION

I, Durowoju Olatunde Samod, student number 11634830, hereby declare that this thesis submitted to the Department of Hydrology and Water Resources, School of Environmental Sciences, University of Venda, for the PhD in Environmental Sciences is my own work and has not been previously submitted, in whole or in part, to any university for any degree; and all reference materials contained herein have been duly acknowledged.

…….. ……..

Student's signature Date

Durowoju OS

DEDICATION

This thesis is dedicated to Almighty God, the one who has known me even before I was formed in my mother's womb and has destined me for greatness.

ACKNOWLEDGEMENTS

"… I can do all things through Christ who strengthens me - Philippians 4;13 (NKJV)". I would like to express my profound gratitude to Almighty God, the author and finisher of my faith for this PhD thesis, to you alone be all the glory.

I would like to acknowledge my indebtedness and render my warmest thanks to my promoter, Professor John Ogony Odiyo and co-promoter Senior Professor Georges-Ivo Ekosse, who made this work possible. Their fatherly guidance and professional advice have been invaluable throughout all stages of the work.

I am sincerely grateful to Dr. E.O. Popoola for her untiring attention to my academic pursuits from my undergraduate studies and laying the foundation for my coming to University of Venda. I wish to say a big thank you for her motherly advice and motivation towards these great strides.

The financial assistance of the Water Research Commission (WRC) through a research project number K5/2739 that supported this PhD research is hereby acknowledged. The University of Venda, through its Research and Publications Committee (RPC) is also acknowledged for its financial support. I thank also, the staff of the Directorate of Research and Innovation at the University of Venda.

I would also like to thank the staff of the Department of Hydrology and Water Resources of University of Venda, particularly the Departmental Coordinator, Ms Rachel Makungo, for not neglecting me and standing by me like a family from the beginning of this research. Mr. Nkuna and Ms. Elle, thank you very much for the field work and willingness to support when the need arises. Also, my appreciation goes to Ms N. Mulovhedzi and Ms M.A Mudzusi from the school of Environmental Sciences Dean's office, thank you all for your support.

My profound gratitude goes to the Environmental Isotope Group (EIG), iThemba Laboratories in Johannesburg and Agricultural Research Council (ARC) in Pretoria, South Africa, where the samples were analysed after pretreatment at the University of Venda. While in the laboratory, I would like to especially appreciate; Mr. Matema (ARC), Mr. Mike

(iThemba Labs), Mr. Hosborn (iThemba Labs) for their technical advice and encouragement towards the completion of this analysis.

I wish to express my gratitude to Dr. NN Bukalo for her listening ears, extended discussions and valuable suggestions which have contributed greatly to the enrichment of the thesis. I am not taking them for granted. Thank you for being there most of the time. Also, big thanks to Dr. JN Edokpayi and Dr. OM Oyebanjo for taking time to read through the first draft of this thesis, thank you so much.

To my wonderful family, particularly my parents (Mr. and Mrs. Durowoju) for their love and support throughout my life. Thank you both for giving me strength to reach for the stars and chase my dreams. Special shout out to my siblings; my younger brother, Abiodun Durowoju; my youngest brother and his wife, Olusegun and Amber Durowoju; my younger sister, Olaide Durowoju deserve my wholehearted thanks as well. You guys deserve some accolades!!!

I smoothly went through my studies along with my colleagues, Ojelade Babatunde, Onipe Tobiloba, Mathivha Fhumulani, Doyin Alayande, Osidele Olujimi, Bilonda Mireille, Etta Elizabeth, Adebayo Kemi, Unahumare Solomon, Kom Zongho, Kalobo Denis, whose friendship and hospitality were so precious to me. They enabled me to enjoy being away from home in so many ways. Also, I thank many whose names are not mentioned above, but whose help was more useful and much appreciated.

The endless support of all my friends, especially Mr. & Mrs. Ibeh, Mr. & Mrs. Ihidero, Mr. & Mrs. Taiwo, Mr. & Mrs. Adekunle, Mr. & Mrs. Edafe, are acknowledged. I appreciate their words of encouragement towards my educational career. In this vein, I would like to appreciate the following families for their support both physically and spiritually: Prof. & Mrs. Osefuiah, Mr. & Mrs. Elesinnla, Mrs. Saka, Mr. & Mrs. Obijole, Mr. & Mrs. Ogunode and Mr. & Mrs. Adegoke. No words could ever repay your priceless encouragement towards this achievement.

Special thanks to my lovely wife, Mrs. KG Durowoju, for her continued prayers, support and understanding, but also for editorial proof reading of manuscripts and thesis. Thank you very much for your understanding and love, loudly I say unto you, THANK YOU.

ABSTRACT

Geothermal springs are natural geological phenomena that occur throughout the world. South Africa is endowed with several springs of this nature. Thirty-one percent of all geothermal springs in the country are found in Limpopo province. The springs are classified according to the residing mountain: Soutpansberg, Waterberg and Drakensberg. This study focused on the geothermal springs within the Soutpansberg region; that is, Mphephu, Siloam, Sagole and Tshipise. The study was aimed at elucidating on the isotopic signatures and trace metals concentrations from the geothermal springs to their environmental media in Soutpansberg region. This study also assessed the interconnectivity of the isotopic signatures within the ecosystem and evaluated the potential human health risks associated with trace metals from geothermal springs and surrounding soils in the study areas.

Geothermal springs and boreholes were sampled for a period of twelve months (May 2016 – May, 2017) to accommodate two major seasons in the study areas. The surrounding soils were sampled vertically from a depth of 10 cm to 50 cm for trace metals and isotopic compositions. Three different plants were sampled at each of the study sites, namely, Amarula tree, Guava tree and Mango tree at Siloam; Acacia tree, Fig tree and Amarula tree at Mphephu; Amarula tree, Lowveld mangosteen and Leadwood tree at Sagole; Sausage tree, Amarula tree and Acacia tree at Tshipise. To achieve the objectives, the physicochemical, geochemical and isotopic compositions of the geothermal springs, boreholes, soils and vegetation were analysed using ion chromatography (IC) (Dionex Model DX 500), inductively coupled plasma-mass spectrometer (ICP-MS)**,** HTP-Elemental analyzer, Liquid water isotope analyzer (LWIA-45-EP) and Liquid scintillation analyzer. The temperature, electrical conductivity (EC), pH and total dissolved solid (TDS) of the geothermal springs and boreholes samples were measeured *in situ* and in the laboratory. Trace metals analysed in geothermal springs, boreholes, soil and vegetation include Beryllium (Be), Chromium (Cr), Manganese (Mn), Cobalt (Co), Nickel (Ni), Copper (Cu), Arsenic (As), Selenium (Se), Cadmium (Cd), Antimony (Sb), Barium (Ba), Vanadium (V), Zinc (Zn), and Mercury (Hg).

Results obtained from this study in the studied geothermal springs and boreholes were classified according to their temperature as hot and scalding; except for tepid boreholes. This study has provided comprehensive physicochemical, geochemical and isotopic compositions of the geothermal springs within the Soutpansberg region (Siloam, Mphephu, Sagole and Tshipise). The local meteoric line ($\delta D = 7.56\delta^{18}O + 10.64$) was generated from rainwater in Vhembe district. This is a crucial component for depicting the source and flow path of the geothermal springs/boreholes; and could be used for future isotopic hydrological studies within the locality. Rain formation processes within Soutpansberg occurred under isotopic equilibrium conditions with minor evaporation effect during rainfall. The δD and $\delta^{18}O$ values of the geothermal spring water/boreholes confirm that the waters are of meteoric origin, which implies that rainfall is the fundamental component of these groundwaters because they were derived from the infiltration of rainwater, with significant contribution of another type of water in the deeper part of the aquifer. Na-Cl and Na-HCO_3 were established as the water types, which are typical of marine and deep groundwaters which are influenced by the ion - exchange process. The reservoir/aquifer temperature of these springs ranges between 95 – 185°C (Na-K geothermometer), which implies most of the waters are mature water (not native). Hence, geothermal springs water is a mixture of the rainwater and salt water.

Radiocarbon values of the geothermal springs ranged from 2700 to 7350 BP, this implies that they are submodern and a mixture of submodern and modern waters. Tritium relative age also corroborates with radiocarbon age, that is the groundwaters were recharged before and after 1952. This gives an indication that the rainfall contributes to the geothermal springs recharge. Various radiocarbon correction models were employed and constrained by tritium relative age. Ingerson and Pearson, Eichinger and Fontes and Garnier correction models have been shown to be the most appropriate models for radiocarbon correction of groundwater in this semi-arid region. Although, geothermal springs water and boreholes are not fit for drinking due to high fluoride content, they could be used for the following: domestic uses (drinking exclusive) due to its softness, direct heating in refrigeration, green-housing, spa, therapeutic uses, aquaculture, sericulture, concrete curing, coal washing and power generation. In contrast with mentioned uses,

the studied geothermal springs are currently used for domestic purposes (drinking inclusive), limited irrigation and spa (swimming and relaxation).

This is an eco-hydrological study that shows the interconnectivity of isotopic signatures among water (rainwater, geothermal springs and boreholes), soils and vegetation. The soil-water reflects the rainwater/geothermal springs water in isotopic composition, which is more depleted as a result of isotopic fractionation in soil. δD values of soil-water increase, whereas $\delta^{13}C$ values in soil-water decrease with the soil depth at all sites. Two equations connecting δD and $\delta^{13}C$ in soil-water were deduced per season for soil-water; $\delta^{13}C = 0.0812\delta D - 10.657$ in winter; $\delta^{13}C = -0.0278\delta D - 21.945$ for summer. $\delta^{13}C$ in soil-water is induced by Crassulacean Acid Metabolism (CAM) (mixture of C3 and C4 photosynthetic cycles) with a stronger C4 trend, which corroborates with $\delta^{13}C$ of the geothermal springs. From literature, Amarula and Acacia trees have been documented for isotopic compositions, while this study has given additional information on other plants including Lowveld, Leadwood, Sausage, Fig, Guava and Mango trees. These plants are categorised as C3, C4 and CAM plants. C3 plants include Amarula, Lowveld and Leadwood trees; C4 plants include Acacia and Sausage trees; and CAM plants include Fig, Guava and Mango trees. This study shows that with CAM soils, there is a possibility of having either C3, C4 or CAM vegetation. This finding has shown that the δD and $\delta^{13}C$ isotopes in water, soil and vegetation are interrelated, which has been statistically justified.

This study has shown the potential human health risks associated with trace metals concentrations from geothermal springs and their surrounding soils. From the geothermal spring's water, it was found that As, Cr and Cd were the highest contributors to the cancer risk with children having a higher risk than adults. Whereas in soils, it was found that Cr, As and Co were the highest contributors to the cancer risk in the studied communities. Therefore, the cancer risk is high in the general population; that is 1 in 72-162 individuals in children and 1 in 7-107 individuals for adults. The ingestion route seems to be the major contributor to excess lifetime cancer risk followed by the dermal pathway. Therefore, proper monitoring and control measures to protect human health, particularly in children, should be implemented for safety. The study also explored the use of surrounding trees

for phytoremediation and found their uptake capacity to be high, thus, they could be used as bio-indicators to assess the level of contamination of trace metals in the soil.

In conclusion, this study has eludicated on the isotopic signatures and trace metals concentrations from the geothermal springs and their surrounding soils and vegetation within Soutpansberg. This study has contributed towards the advancement and enhancement of the existing knowledge of the geothermal systems, such that water resource management could be applied successfully in the respective areas with similar characteristics for the benefit of the local communities and society at large. Hence, this study recommends that proper monitoring and control measures need to be put in place to protect human health, especially in children.

Keyword: Isotopic composition, interconnectivity, local meteoric water line, phytoremediation, rainwater, Soutpansberg Group, trace metals, potential health risk.

RESEARCH OUTPUTS

The following is a list of research outputs emanating from this PhD thesis as contributions to the scientific community/body of knowledge:

a. Refeered/peer reviewed journal articles

- **Durowoju OS**, Odiyo JO and Ekosse GE (**2019**). Determination of isotopic composition of rainwater to generate local meteoric water line in Thohoyandou, Limpopo Province, South Africa, ***Water SA***, 45(2), DOI: 10.4314/wsa.v45i2.04
- **Durowoju OS**, Butler M, Ekosse GE and Odiyo JO (**2019**). Hydrochemical processes and isotopic study of geothermal springs within Soutpansberg, Limpopo Province, South Africa, ***Applied Sciences***, DOI: 10.3390/app9081688

b. Conference proceedings

- **Durowoju OS**, Odiyo JO and Ekosse GE (**2018**). Geochemical and Isotopic Compositions of the Geothermal Springs within Soutpansberg, Limpopo Province, South Africa, conference proceedings of the first international conference on sustainable management of natural resources (ICSMNR 2018), 15 -17 October 2018, Bolivia lodge, Polokwane, South Africa.
- **Durowoju OS**, Odiyo JO and Ekosse GE (**2018**). Environmental isotopic investigation of the Geothermal springs within Soutpansberg, Limpopo Province, South Africa. First Pan African International Research Congress (1st PAIRC), Kisumu, Kenya, 18th – 21st June, 2018, Book of Programme and Abstract, Page 426, ISBN 978-9966-114-73-0

c. Technical/Scientific Report

- Odiyo JO, **Durowoju OS** and Ekosse GE (**2017 – 2019**). Impacts of trace metals from geothermal springs to their surrounding soil and vegetation within Soutpansberg, **WRC project K5/2739** (Final report).

Table of Contents

LIST OF FIGURES

LIST OF TABLES

LIST OF ABBREVIATIONS

BP – Before Present

BH 1&2 – Siloam tepid boreholes

C3 - Calvin photosynthesis

C4 - Hatch-Slack photosynthesis

^{14}C – Carbon-14

^{13}C - Carbon-13

CAM - Crassulacean Acid Metabolism

CFC – Chlorofluorocarbon

D – Deuterium

DIC – Dissolved inorganic carbon

EIG - Environmental Isotope Group

FA – Factor Analysis

GMWL - Global Meteoric Water Line

H_2O_2 – Hydrogen peroxide

HAC - Hierarchical Agglomerative Analysis

HI – Hazard Index

HQ – Hazard quotient

HNO_3 - Nitric acid

HQ - Hazard Quotient

IAEA - International Atomic Energy Agency

ICP-MS - Inductively Coupled Plasma – Mass Spectroscopy

ICP-OES – Inductively Coupled Plasma- Optical Emission Spectroscopy

ISO – International Organisation for Standardisation

IRIS - Isotope Ratio Infrared Spectroscopy

IRMS - Isotope Ratio Mass Spectrometer

LMWL – Local meteoric water line

MCL – Maximum contaminant level

MDL – Maximum detention limit

MPS – Mphephu Summer

MPW – Mphephu Winter

^{14}N – Atmospheric nitrogen

n – thermal neutron

NBS - National Bureau of Standards

NIST - National Institute of Standards and Technology

^{18}O – Oxygen-18

p – proton

PCA - Principal Component Analysis

PDB - PeeDee Belemnite

PmC – Percent modern carbon

QC/QC – Quality Assurance/Quality Control

RAGS - Risk Assessment Guidance for Superfund

RFD - Reference Dose

SABS – South African Bureau of Standards

SANS - South African National Standards

SAW – Siloam

SCC – Siloam community tap water

SGS – Sagole Summer

SGW – Sagole Winter

SH 1&2 – Siloam hot boreholes

SLAP - Standard Light Antarctic Precipitation

SMOW - Standard Mean Ocean Water

TSS – Tshipise Summer

TSW – Tshipise Winter

TTP – Tshipise tap water

TU - Tritium Unit

USEPA - United States Environmental Protection Agency

VPDB - Vienna PeeDee Limestone

VSMOW - Vienna Standard Mean Ocean Water

LIST OF APPENDICES

LIST OF UNITS AND SYMBOLS

Bq/gC – Disintegartion per second per gram of Carbon

cm - centimeter

µl - Microliter

µm - Micrometre

kV - Kilovolt

mHz - Mega Hertz

ml - Millilitre

^{o}C - Degrees Celsius

δ - Per mil deviation

° - Degree

µg/L - Microgram per liter

µS/cm - Micro-Siemen per centimeter

mg/Kg - Milligram per kilogram

mg/L - Milligram per liter

mS/cm - Micro-Siemen per centimeter

pMC - percent modern carbon

ppm – Part per million

TU - Tritium Units

CHAPTER ONE
INTRODUCTION

1.1 Preamble

This chapter presents background, problem statement, motivation, the main objective, specific objectives and hypotheses of the study. In addition, descriptive summary of the study areas such as climate, geology, land use and vegetation type were incorporated in this chapter.

1.2 Background

Geothermal springs are natural geological phenomena which occur on all continents. They originate either from geologic platonic activity (volcanic origin) or from rainwater that percolates into the ground through permeable rocks or via conduits such as joints, faults and fracture zones in less permeable rocks (meteoric origin) (LaMoreaux and Tanner, 2001). Waters recharged at different times, in different locations or flow paths have distinctive isotopic fingerprints. Both biological cycling of solutes and water/rock inter-reactions often change isotopic ratios of the solutes in predictable and recognisable directions; which can often be reconstructed using their isotopic compositions (Blasch and Bryson, 2007). Environmental isotopes could be natural and anthropogenic in nature and their distribution in the hydrosphere can assist in the solution of hydrogeochemical problems (Kendall and McDonnell, 1998; Huang and Zhang, 2015). Environmental isotope geochemistry shows the variation of isotopic composition of elements that are obtained from physicochemical processes rather than nuclear processes (White, 2015). Hence, they can be a useful tool to help deduce geochemical processes.

Stable carbon (^{13}C), oxygen (^{18}O) and hydrogen (^{2}H) isotopic compositions of organic matter and inorganic compounds such as CO_2 and H_2O are altered during vegetation–soil–atmosphere exchange processes, such as evapotranspiration, carbon assimilation and respiration. This leaves an isotopic imprint on soil, plant and atmospheric carbon and water pools and associated fluxes. These isotopic fingerprints can then be used to trace different processes involved in the transfer of carbon and water across the plant–soil–atmosphere continuum. Particularly, the multiple-isotope approach, i.e. the simultaneous measurements of stable isotope composition of different elements ($\delta^{2}H$, $\delta^{18}O$ and/or

$\delta^{13}C$), provides a unique way to investigate the interrelation between water and carbon fluxes (Ehleringer *et al.,* 1993; Griffiths, 1998; Flanagan *et al.,* 2005; Yakir and Sternberg, 2000). The use of biological archives may enable extrapolation of this information to long time scales, such as the Anthropocene (Werner *et al.,* 2011).

Some of the applications of environmental isotopic compositions of low-mass (light) elements such as oxygen, hydrogen, carbon, nitrogen, and sulfur include the identification and determination of the mechanisms responsible for streamflow generation and weathering reactions that mobilise solutes along the flow paths (Kendall and McDonnell, 1998), characterisation of water flow paths (Scholl *et al.,* 2011), determination of the role of atmospheric deposition in controlling water chemistry (Muhammad and Sadiq, 2014), identification of the sources of solutes in contaminated system and assessment of biological cycling of nutrients within an ecosystem (Kendall and McDonnell, 1998; Voss *et al.,* 2000; Gustafson *et al.,* 2007; Goldsmith *et al.,* 2011). They have been used in a wide range of research disciplines at different and complementary temporal and spatial scales. For instance, tracing biogeochemical processes across spatio-temporal scales (Yakir and Sternberg, 2000), assessing the origin of water vapour (Lui *et al.,* 2010), solving water balance of lakes (Jasechko *et al.,* 2013), analysis of isotopic composition of soil surface and leaf water (Yepez *et al.,* 2005; Rothfuss *et al.,* 2010; Dubbert *et al.,* 2013; Hu *et al.,* 2014; Huang and Zhang, 2015) as well as investigating the groundwater recharge (Blasch and Bryson, 2007).

In South Africa (SA), Limpopo Province has the highest number of geothermal springs. These springs are classified according to the dominating mountains; namely, Soutpansberg, Waterberg and Drakensberg (Durowoju *et al.,* 2015). There are eighty-three (83) known geothermal springs in SA, out of which twenty-four (24) are located in Limpopo Province (Kent, 1949; Olivier *et al.,* 2008). Geothermal springs are usually mineralised to a greater or lesser extent, depending on the characteristics of the geological formations associated with the circulating groundwater (Todd, 1980). Odiyo and Makungo (2012) reported that geochemical dissolution of rock increases with temperature, hence more mineralisation of the geothermal springs as well as their isotopic compositions (Pang *et al.,* 2006). This also accounts for trace metals emanating from the

geothermal springs to the surrounding soils and vegetation. People have used water from geothermal springs for different purposes for thousands of years (Olivier *et al.,* 2011). Documentary and oral history reveal that geothermal springs were used for bathing, medicinal, religious, hygienic and social purposes across the world, for instance, India, Crete, Egypt, Turkey, Japan, Brazil and Canada (van Vuuren, 1990; Lund, 2000).

Previous studies on the geothermal springs in Limpopo Province have been on the Hydrogeology and water chemistry (water quality) of the springs (Kent, 1948; Oliver *et al.,* 2008, 2010, 2011). Olivier *et al*. (2008, 2011) reported significant changes in the water chemistry and the spring yield at some of the springs over a period of more than 50 years. Recently, Durowoju (2015) reported that geothermal spring waters have the potential to contaminate the surrounding soils with some trace metals, which are assumed to be due to rock-water interaction emanating from the deep aquifer. The study clearly showed that geothermal springs are used for domestic and irrigation purposes by neighbouring population. For example, the Tshipise Spring is located within the Honnet Nature Reserve (a popular holiday resort), which is located approximately 36 km from Musina. The spring water is used for irrigation of food crop (Siloam), flowers, grasses and Acacia trees (Tshipise). It also serves as the source of water for the pool at the resort (Tshipise Resort). Trace metals are transferred from the spring across the soil to the vegetation and can have adverse effects on humans when their concentrations are above the standard guidelines (SANS or WHO).

Hence, there is a need to increase the understanding of geothermal spring-soil-vegetation system. Therefore, this research focused on delineating deep groundwater flow systems using environmental isotopes, water chemistry and geochemical data, to ascertain the source of geothermal spring water and their impacts on the ecosystem and human health. The research was carried out in rural settlements within the Soutpansberg region, where the communities depend on spring water as a reliable alternative source of water coupled with indigenous knowledge with its curative ability (medicinal capability). The study, therefore, focused on the isotopic signatures and geochemical parameters of geothermal springs and the ecosystem and human health, thereby, elucidating on the environmental isotopes in the geothermal springs water, soil and vegetation within the study areas. In

addition, assessing the potential health risk of the trace metals from geothermal spring water and the surrounding soils within inhabitants. The study intends to increase the existing knowledge on geothermal springs; by focusing on the declination of the deep groundwater flow system of the geothermal springs, the age of the geothermal springs, soil water variation, photosynthetic pathway of the vegetation and trace metals potential health risks assessment of the inhabitants. This collective information will be useful for the general body of knowledge and not just the study areas of South Africa.

1.2 Problem statement

Studies across the world have found that geothermal water may contain toxic metals such as arsenic (As), chromium (Cr), cobalt (Co), lead (Pb), zinc (Zn) and mercury (Hg) (Manda and Suzuki, 2002; Romero *et al.,* 2003; Churchill and Clinkenbeard, 2005; Ochieng *et al*., 2007; Li *et al*., 2010), radio-active elements such as uranium (U), thorium (Th) and Radon (Rn) (Kempster *et al.,* 1997; Baradács *et al.,* 2001). These trace metals could pose negative health impacts such as cancers and other chronic diseases on the consumers (USEPA, 2009; WHO, 2011). Most of these geothermal springs are found in communities in which there is limited water availability, particularly in a developing country such as Kenya, Ethiopia, South Africa among others. The study areas (Mphephu, Sagole, Siloam and Tshipise) are rural settlements in Limpopo, South Africa where people have little or no scientific knowledge of the effects of toxic contaminants from the geothermal spring to the ecosystem. Thus, spring water is used for various domestic purposes, swimming and irrigation as indicated earlier, with no clear understanding of the potential health effects of major and trace metals. As mentioned earlier, several studies have been carried out on the physicochemical parameters of geothermal springs (Kent, 1949; Olivier *et al.,* 2008, 2011; Mamba *et al.,* 2008; Tekere *et al.,* 2012) with major and trace metal compositions studied. However, none has shown their impacts on the soil and vegetation, except the study by Durowoju *et al*. (2016a). The findings of the latter study showed that geothermal springs have the potential to contaminate the environmental media, especially the surrounding soil. Hence, there is a need to assess the potential human health risks they possess to the inhabitants (adults and children) in the study areas.

There is no detailed study on the environmental isotopic compositions (stable and radiogenic) of the geothermal springs in Limpopo province except unpublished study by Saeze and Rikhotso (2013); and none has elucidated on the isotopic compositions of the geothermal springs and their interconnectivity with the surrounding environmental media (soils and vegetation). Thus, there is a need to determine the isotopic compositions of the geothermal spring water in relation to their environmental media, as well as their interconnectivity. Variations of hydrogen ($\delta^{2}H$) and oxygen ($\delta^{18}O$) in rainfall forms primary background data for groundwater recharge investigations (Ingraham, 1998; Gupta and Deshpade, 2003; Gat, 2010; Kortelainen, 2009). Trace metal contamination was observed in the surrounding soil at Siloam (Durowoju *et al.,* 2016b) and there is need to assess the potential health risks of trace metals concentrations from geothermal spring water and surrounding soil. Although, studies by Oliveir *et al*. (2008, 2011) and Durowoju (2015) have determined the trace metals concentrations of the springs and their impacts on surrounding soils and vegetation, none has assessed the potential health risks. Hence, the trace metals concentrations were used to assess the potential health risks in adults and children within selected communities (where the geothermal springs were located). The study was aimed at enhancing and extending the existing knowledge of the geothermal systems, such that water resource management could be applied successfully in the respective areas within similar characteristics for the benefit of the local communities and society at large.

1.3 Motivation

Most geothermal springs in the world are used for electricity generation, greenhouse heating, balneological purposes, thermal tourism and heating of swimming pools (Tarcan and Gemici, 2003; Gemici, *et al.,* 2004). The ones found in the study areas are mainly used for recreation, domestic purposes and limited irrigation. There is a need to evaluate the characteristics of the geothermal springs in Siloam, Mphephu, Sagole and Tshipise to maximise their potential to enhance the development of the rural communities in which they are found. In addition, assessment of potential health risk associated with the trace metals from the geothermal springs and their surrounding soils in the selected communities where the springs are used for domestic purposes, recreation and/or limited

irrigation, is imperative. There is a need to provide information regarding the extent of the local and regional groundwater systems and their interactions with the environment by determining the isotopic compositions (δD, $\delta^{18}O$ and ^{13}C) of the geothermal springs, soil and vegetation, as well as their interconnectivity to expand the existing scientific knowledge. Studies have reported that δD, $\delta^{18}O$ and ^{13}C are ideal tracers of water system since they are incorporated in the water molecules and therefore their behaviour and variations reflect the origin, the hydrological and geochemical processes that affect natural water bodies (Gonfiantini, 1998; Fawzia and Mohamed, 2004; Ako *et al.,* 2010; Li *et al*., 2009). There is need to generate reliable dataset for proper isotopic information in the Province. Hence, short-term monitoring of rainfall (one hydrological cycle) was incorporated in this study to generate the local meteoric water line (LMWL), which is crucial in the evaluation of groundwater recharge.

Therefore, there is a need for study for better understanding and expansion of existing knowledge on the isotopic compositions from the rainwater, geothermal springs/boreholes, soils and vegetations as well as the interconnectivity among the environmental media to ascertain the source and processes; soil-water variation and photosynthetic pathway of the vegetation; to assess the possible potential health risks associated with trace metals on the inhabitants {children (0 – 14 years) and Adults (15 years above)}. This study gives an improved understanding of the environmental media around geothermal springs for sustainability and evaluation of potential health risks associated with trace metals, which is the motivation for this research.

1.4 Objectives of the study

1.4.1 Main objective

The main objective of this study is to elucidate on the isotopic signatures and trace metals concentrations from the geothermal springs to the surrounding soils and vegetation within the Soutpansberg region (Mphephu, Sagole, Siloam and Tshipise), Limpopo Province, South Africa. The study further evaluates the potential health risks associated with trace metals from the geothermal springs and surroundings soils.

1.4.2 Specific objectives

The specific objectives include:

1) To assess the physicochemical, geochemical parameters and environmental isotopes ratios (δD, $\delta^{18}O$ and $\delta^{13}C$) in geothermal spring water, rainwater and boreholes within Soutpansberg region.
2) To evaluate the ages of the geothermal springs, using Carbon-14 (^{14}C) and Tritium (^{3}H) within the Soutpansberg region.
3) To assess the environmental isotopes ratios (δD and $\delta^{13}C$) in the surrounding soil and vegetation; and their interconnectivity with rainwater and geothermal spring water within Soutpansberg region.
4) To evaluate trace metals concentrations and potential human health risk of inhabitants (adults and children) from the geothermal spring water and surrounding soils within the Soutpansberg region.

1.5 Hypotheses

1) The studied geothermal springs and boreholes in the Soutpansberg region have similar physicochemical, geochemical and isotopic characteristics.
2) Geothermal springs within the Soutpansberg region have approximately the same ages.
3) Soils and vegetation surrounding geothermal springs and rainwater have similar stable isotopic compositions.
4) The concentrations of trace metals in geothermal springs and surrounding soils could pose potential health risks on the inhabitants of Siloam, Mphephu, Sagole and Tshipise.

1.6 Study Areas

Mphephu and Siloam, Sagole, and Tshipise springs are located in Makhado, Mutale and Musina municipalities, respectively, in Vhembe District, Limpopo Province, South Africa (Figure 1.1). Geothermal springs are located on the coordinate of 22° 36’ 05.48" S and 30° 10’ 23.01" E; 22° 53’ 09.66" S and 30° 12’ 40.36" E; 22°, 31’ 49.440" S and 30°, 39’ 7.128" E; 22° 54’ 26.280" S and 30° 10’ 35.582" E of the equator for Siloam, Tshipise, Sagole and Mphephu, respectively. The study areas fall under Quaternary catchments of the Nzhelele River catchment, which is in the northern region of Limpopo Province, South Africa (Makungo *et al.,* 2010). Brandl (1999) reported that Tshipise and Siloam

geothermal springs are drained in rocks by an intergranular and fractured aquifer, with borehole yields ranging between 0.1 L/s and 0.5 L/s. Sagole and Mphephu geothermal springs are drained in rocks by fractured aquifers, with borehole yields ranging from 0.5 L/s to 2 L/s (Brandl, 2002).

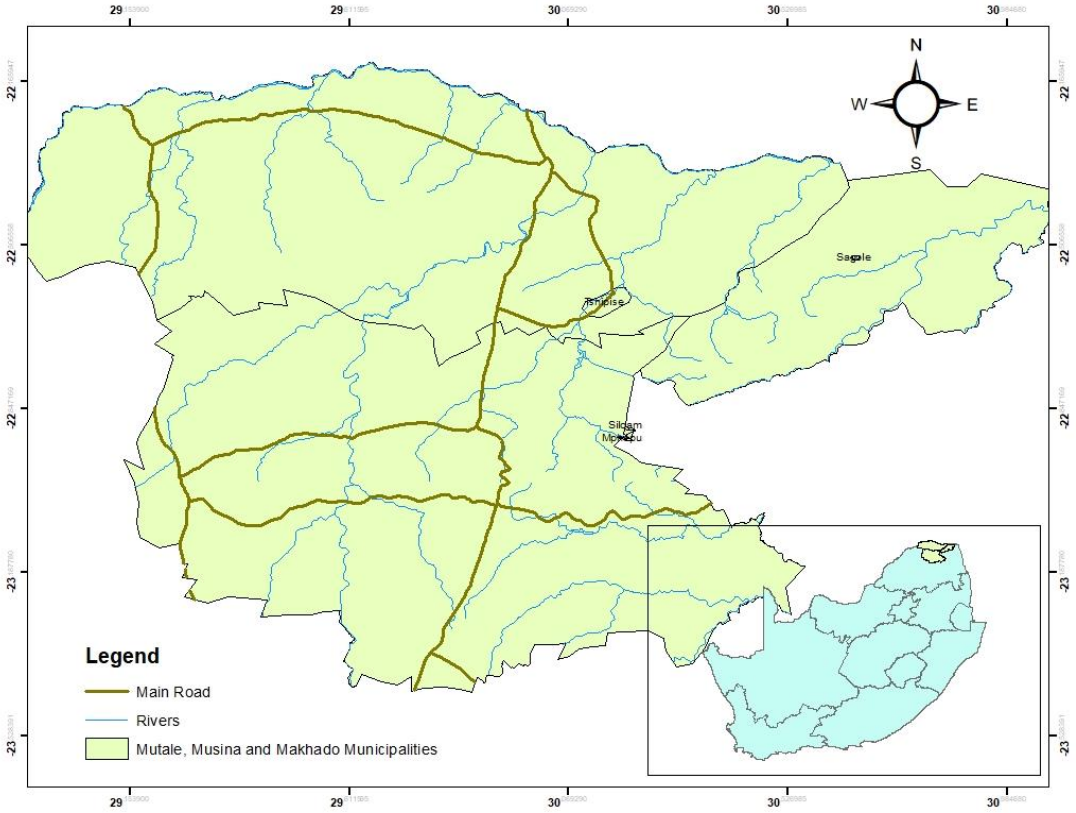

Figure 1.1: Study areas within the Vhembe District, Limpopo Province, South Africa.

1.6.1 Geology of study areas

The study areas are underlain by block-faulted Karoo Supergroup and Soutpansberg Supergroup rocks in the northern part of the Limpopo Province (Figure 1.2). These rocks have very low primary porosity, permeability and storage capacity, with limited groundwater flow (Brandl, 2002). Groundwater occurrence is mainly related to secondary hydrogeological features such as faults and joints, which present preferential pathways and thus enhance the potential for groundwater flow in the region. Mostly, the geology determines the extent to which the reaction with the host rock proceeds, depending on the chemical composition of the rock and the rate at which water passes through the rock.

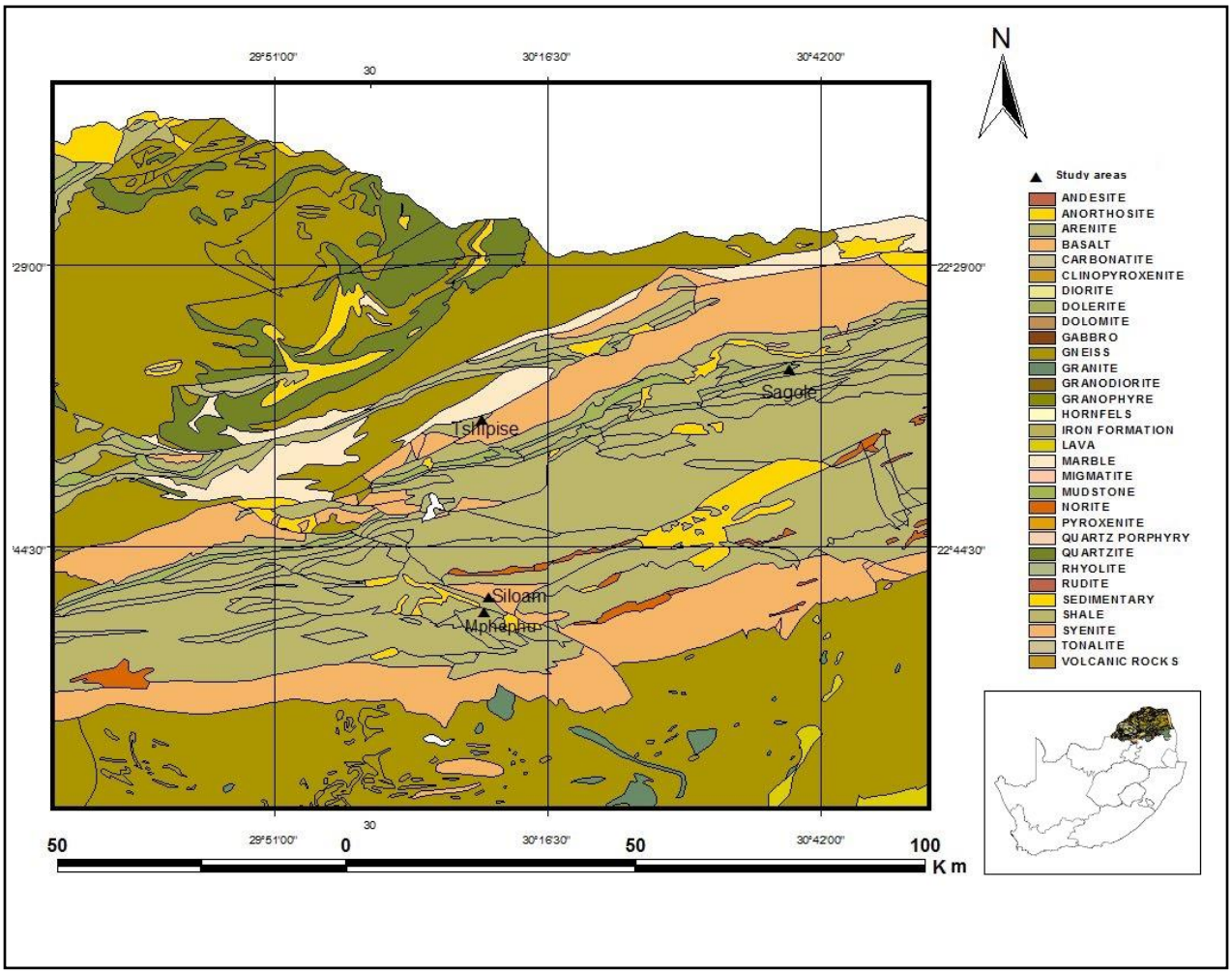

Figure 1.2: Geology map of study areas within Soutpansberg region.

Mphephu geothermal spring is underlain by Wyllie's Poort and Nzhelele Formations of the Soutpansberg Supergroup. These lithologies mainly comprise sandstone and quartzite. Mphephu geothermal spring is associated with the Nzhelele Fault (Brandl, 2002).

The Sagole geothermal spring is associated with the Klein Tshipise Fault, which lies in the contact zone between the Karoo and Soutpansberg Supergroups. To the South of the fault is the basalt of the Musekwa Member of the Nzhelele Formation and to the north of the fault are the sedimentary rocks of the Madzaringwe and Mikambeni Formations of the Karoo Supergroup. The Mikambeni Formation consists of mudstone, shale and laminated sandstone, whereas the Madzaringwe Formation comprises alternating

sandstone, siltstone and shale, with sporadically occurring coal seams (Johnson *et al.,* 2006).

The Siloam geothermal spring is found in the Nzhelele Valley in Siloam Village, which falls under, the youngest Formation of the Soutpansberg Group, the Sibasa Formation. It is dominated by basalt, which originated from the lava at the base of the Formation. Basalt is responsible for the more undulating topography to the south of the Soutpansberg (Brandl, 1986). There are dark-red shales and sandstones that are fine, thin-bedded sandstones. There is an interlayer of tuff, ignimbrite and chert and in places tuffaceous shale (Mundalamo, 2003). Various types of conglomerates are also available, such as argillaceous and arenaceous types. The mudstone and siltstone of Delvis Gully Member also exist (Mundalamo, 2003). Siloam village is characterised by fractured aquifers of sandstone where groundwater occurs.

Tshipise geothermal spring is underlain by basalt and minor andesite of the Letaba Formation of Lebombo Group and Karoo Supergroup. The Lebombo Group rests with the Tshipise member of the Clarence Formation, which comprises white to cream-coloured sandstones. These lithologies are intruded by Karoo dolerite dykes and sills, with strongly developed faults (Johnson *et al.,* 2006). Tshipise geothermal spring occurs at the intersection of two post-Permian faults in Upper Karoo, one of which is the Tshipise Fault (Olivier *et al.,* 2011).

1.6.2 Climate (Rainfall and Temperature)

The study areas (Mphephu, Sagole, Siloam and Tshipise) are categorised under the hot semi-arid region (Figure 1.3). It receives much of its rainfall during summer (November to February) (Figure 1.4), as the area is within the northward and southward oscillation of the inter-tropical convergence zone (ITCZ) and associated southerly monsoon winds. The study areas are characterised by high-temperature variations in different seasons of the year, with temperatures in the winter ranging from 16ºC to 22ºC, and in summer, from 22ºC to 40ºC (Makungo, 2008). The mean annual rainfall of Nzhelele ranges from 350-400 mm per annum (Makungo *et al*, 2010) (Figure 1.3). More than 80% of the rainfall occurs in the summer and only about 20% occur in the winter (DWAF, 2001).

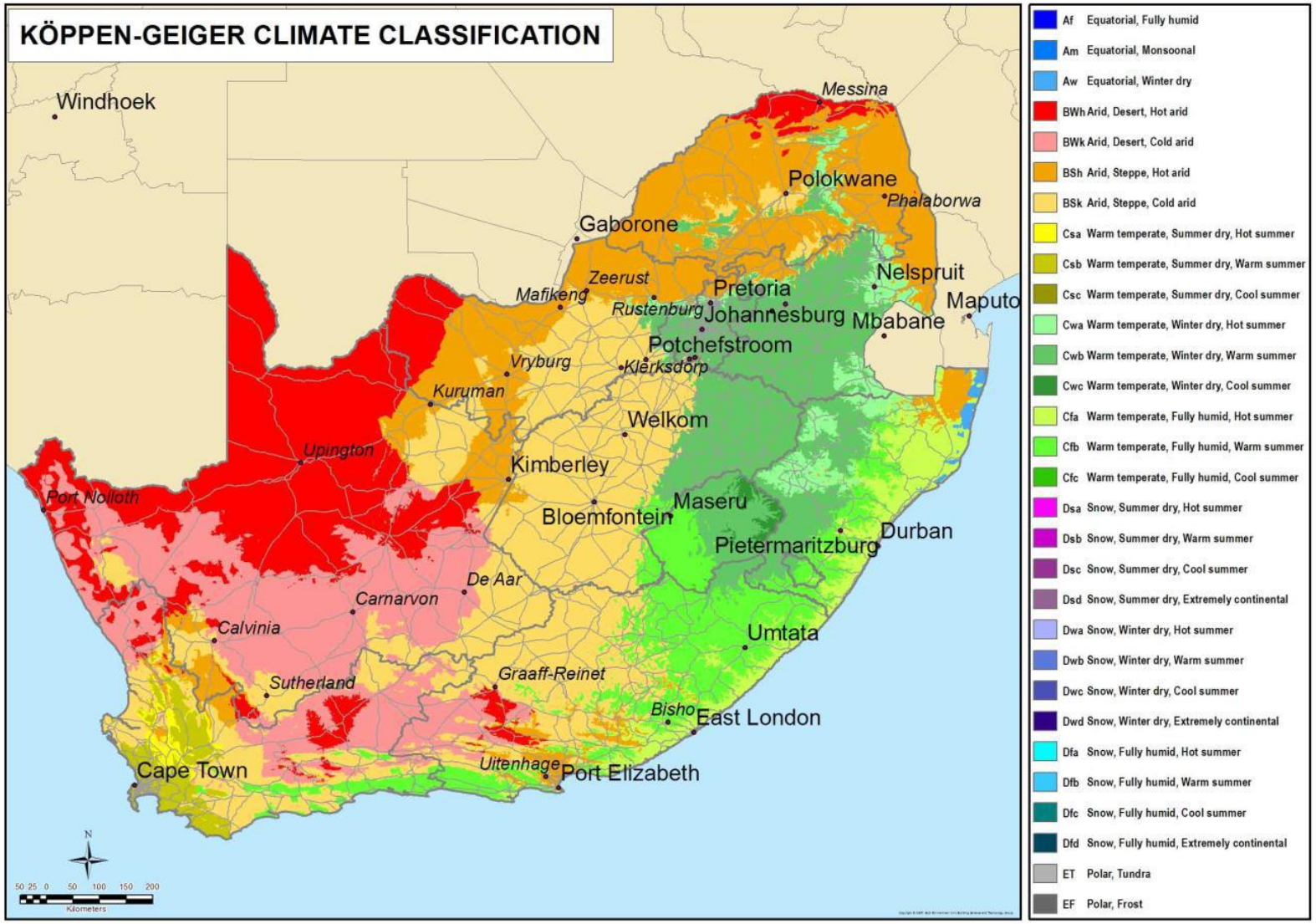

Figure 1.3: Koppen-Geiger climate classification of South Africa (Kottek *et al.,* 2006).

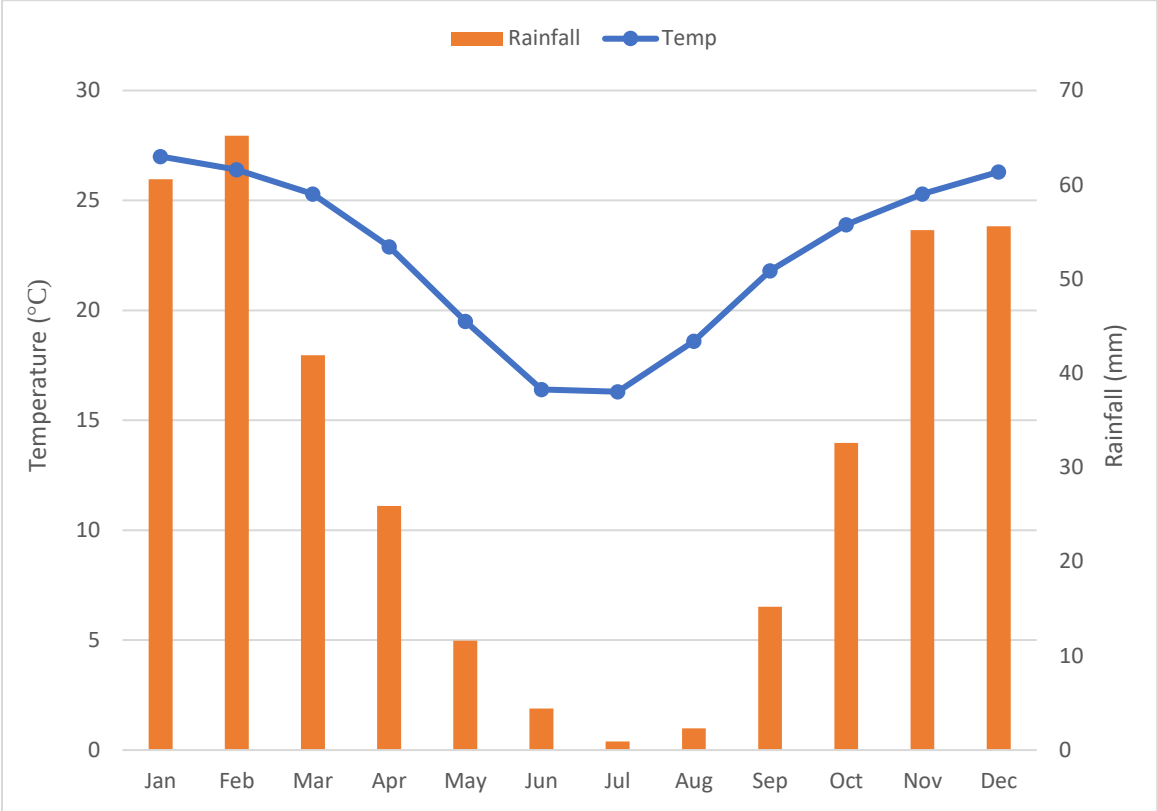

Figure 1.4: Average temperature and rainfall within the study areas (Nzhelele) over the past 100 years (1916 – 2016) (http://www.weatherbase.com).

1.6.3 Vegetation

Mucina and Rutherford (2006) map nine biomes in South Africa (Figure 1.5). The study areas fall within the Savanna biome in Limpopo Province. They are characterised by a grassy ground layer and a distinct upper layer of woody plants. Shrubveld is the upper layer vegetation near the ground, whereas, Bushveld is dense vegetation as Woodland (Mucina and Rutherford, 2006). Almost every major geological and soil type occurs within the biome (Low and Rebelo, 1996). The grass layer is dominated by C 4-type grasses, which are at an advantage where the growing season is hot, but where rainfall has a strong winter component, C 3-type grasses dominate (Low and Rebelo, 1996; Mucina and Rutherford, 2006). They lack sufficient rainfall, which prevents the upper layer from dominating, coupled with fires and grazing, which keep the grass layer dominant in biomes.

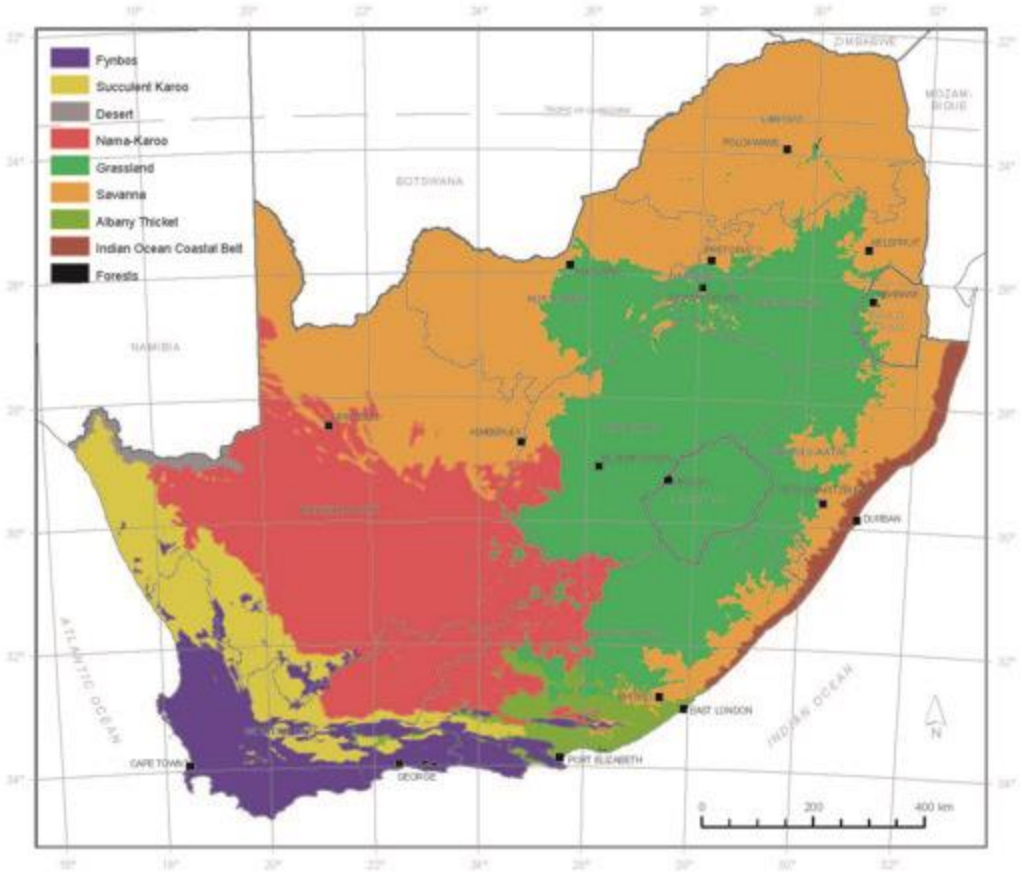

Figure 1.5: Vegetation map of South Africa (Mucina and Rutherford, 2006).

CHAPTER TWO

LITERATURE REVIEW

2.1 Preamble

This chapter presents a review of relevant literature for this research. It highlights South African geothermal springs, benefits, geology and chemistry of geothermal springs, potential health risk assessment of trace metals and the isotopic compositions (stable and radiogenic) of the geothermal springs, surrounding soils and vegetation.

2.2 Geothermal springs in South Africa

South African geothermal springs are associated with rainfall, faulting and shearing (Olivier *et al.,* 2010). They are usually situated in topographically low areas, with the surrounding elevated terrain, serving as the catchment area for rainfall that permeates downwards through fracture planes in the rocks into narrow conduits. The narrow conduits allow water to percolate to a deeper level where it is heated. The impermeable parts of faults, fractured zones or dykes restrict percolation of water and cause water to rise to the earth's surface (Kent, 1969). The mineral content of these geothermal springs is influenced by the rock through which the water percolates (Kent, 1969).

Olivier *et al*. (2011) reported the geothermal sources for some of these springs (sulfur springs, Tugela, and Windhoek) or geothermal boreholes and not naturally-occurring springs, whereas the geothermal source of other geothermal springs (Vetfontein, Paddysland, Stindal, and Makutsi) could not be located. Figure 2.1 shows the number of geothermal springs with some associated boreholes per province in South Africa. In South Africa, geothermal spring waters were initially used for domestic and irrigation purposes, and later developed as health resorts and tourism destinations (Hoole, 2001). South African geothermal springs extend into the distant past; for instance, the Khoi (Hottentots) used the geothermal spring at Caledon, calling it 'a fountain of life'. They believed that it could cure any type of illness and if the water was drunk, it made old men become 'active like the younger ones' (Boekstein, 1998). The geothermal spring at Montagu was also frequented by the Khoi and the San (Rindl, 1936).

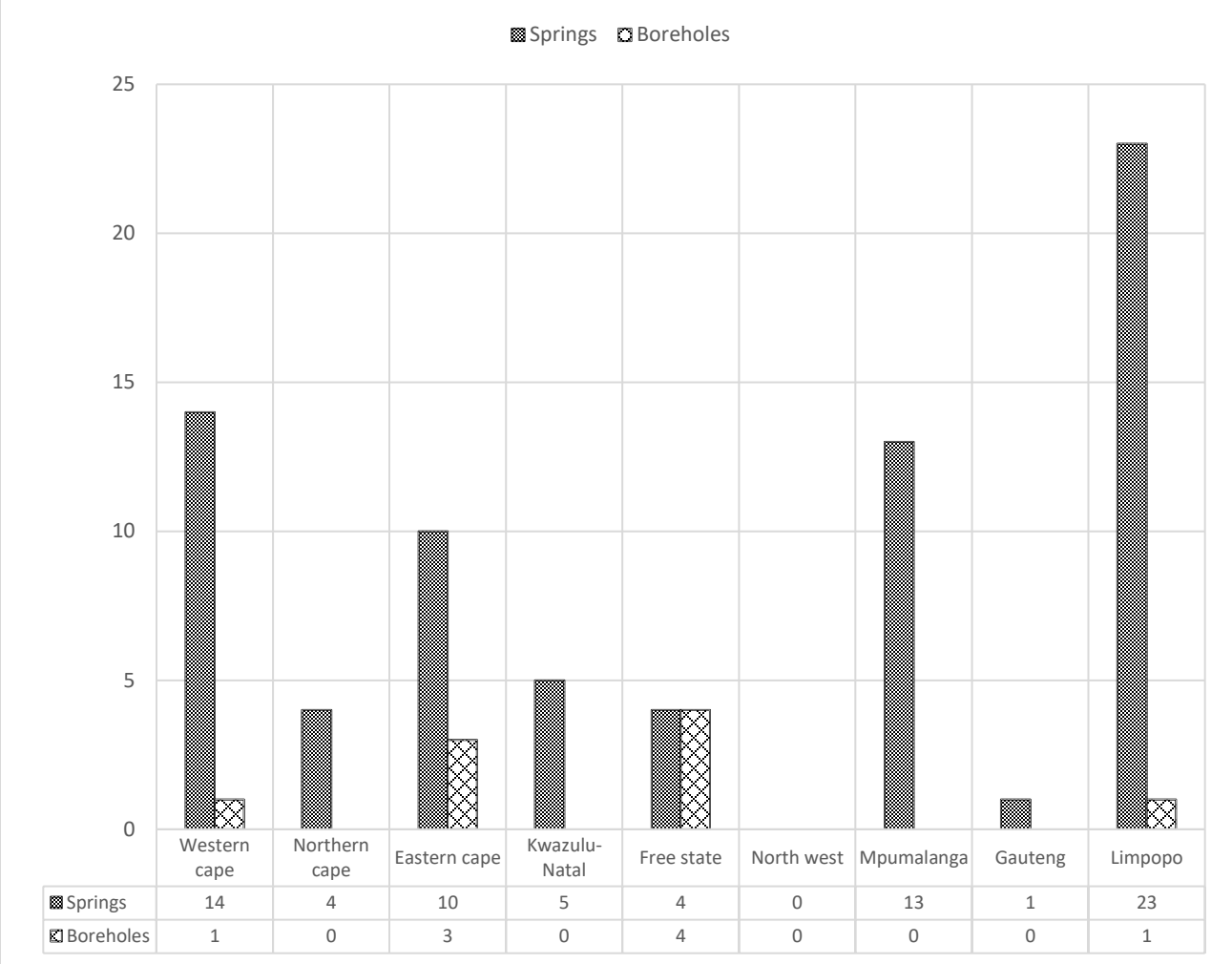

	Western cape	Northern cape	Eastern cape	Kwazulu-Natal	Free state	North west	Mpumalanga	Gauteng	Limpopo
Springs	14	4	10	5	4	0	13	1	23
Boreholes	1	0	3	0	4	0	0	0	1

Figure 2.1: Distribution of geothermal springs and geothermal boreholes per province in South Africa (Olivier *et al.,* 2008).

Early western settlers in what became known as the Western Cape Province, started visiting the geothermal springs in this part of the world in the late 1600s and early 1700s, predominantly for health reasons. It was believed that bathing in the geothermal water cured ailments such as rheumatism (Booyens, 1981). Geothermal springs in Limpopo at Letaba (Die Eiland) and Bela Bela (Warmbaths) were also used before the arrival of the first Europeans. Letaba (Die Eiland) geothermal spring was used by indigenous people to produce salt by “lixiviating the mud through which the water issued and evaporating the resultant solution over the open fire in clay pots” (Kent, 1942). The spring was also

used as a place where people would go and be cleansed as part of purification and spiritual harmonisation after battle (Ntsoane, 2001).

2.3 Benefits of geothermal springs

2.3.1 Religious and traditional benefits

Religious and traditional uses of geothermal springs have been an ancient practice across the world even before modern civilisation. For instance, the American Indians used geothermal springs for traditional rituals and as a neutral ground where different tribes could hunt, trade and bath and where warriors could travel and relax (Hoole, 2001). The Greeks usually attribute their religion to cleanliness. Therefore, they built their temples close to geothermal springs so that the water reticulation system could bring water to the holy place (Virk *et al.,* 1998). Africans were not exempted from these beliefs; geothermal springs found in the Gumara River in Ethiopia were discovered by Ethiopian saints; Qergos and Takla Haymanot. It was believed that Saint Qergos, while flying in the sky, was attacked by eagles and his bones fell to the ground, causing warm and healing water to rush out where they were dropped (Pankrust, 1990). Some of the sites have been declared heritage sites and are presently visited by both local and international tourists (Pankrust, 1990; Nguyen, 2007).

2.3.2 Medicinal benefits

Medicinal benefits and religious purposes of geothermal springs are interrelated and can be traced back to 2 500 years ago (La Moreaux and Tanner, 2001). Geothermal springs were believed to be a special kind of groundwater owing to its higher mineralisation as well as trace elements, dissolved gases, radioactivity or temperature (Wang and Xie, 2003). Different minerals and gases within the geothermal waters have proven to have different curative abilities. The use of carbolic water is thought to have significant medical importance, for circulatory and heart disorders (Skapare *et al.,* 2003). Sulphated water may heal hepatic insufficiency and problems with the accumulation of organic waste (Skapare *et al.,* 2003). Bicarbonated water may relieve gastrointestinal illness, hepatic insufficiency and gout (Skapare *et al.,* 2003). Sodium chlorinated water may cure a chronic infection of the mucous membrane (Lund, 2000; Skapare *et al.,* 2003).

Ancient Greeks and Roman prescribed drinking and bathing in geothermal springs for its therapeutic effects, especially for ailments such as jaundice and rheumatism (Hoole, 2001; Spicer and Nepgen, 2005). Chinese people used the Huang hot spring on the Shahe River for treatment of various ailments (La Moreaux and Tanner, 2001; Spicer and Nepgen, 2005). The Ethiopians used geothermal springs for the treatment of various diseases, such as skin diseases, leprosy and other contagious diseases (Pankurst, 1990). The ancient Egyptians are believed to have used geothermal baths for therapeutic purposes since 2000 BC. Many of these springs became known as sacred sites, and later evolved as healing centres (Spicer and Nepgen, 2005).

2.3.3 Agricultural benefits

Thermal springs have been used for irrigation purposes from time immemorial. Chinese people have used geothermal springs since the time of the Jin Dynasty (AD 265-420) (La Moreaux and Tanner, 2001). During this period, the Cunzhou City geothermal spring in the Hunan province was used to irrigate rice paddies so that they could grow rice, even during the winter season (La Moreaux and Tanner, 2001).

The European Commission (1999) reported that 25% of the direct heat produced by geothermal springs is used for agricultural purposes, which can be subdivided into the following activities:

a) Agricultural crop drying
b) Aquaculture
c) Mushroom farming
d) Heating greenhouses and irrigation

The agricultural uses of the geothermal spring depend on the surface temperature of the spring, which have been summarised in Table 2.1 below.

Table 2.1: Temperatures required for various agricultural activities

Temperature in °C	Agricultural uses
20 – 25	Soil heating
35 – 95	Heating greenhouses
35 – 95	Food processing
20 – 40	Aquaculture
35 – 50	Biogas processing
45 – 65	Mushroom cultivation
65 – 95	Drying fruits and vegetables
50 – 70	Pasteurisation
60 – 85	Beet sugar extraction
70 – 100	Blanching and cooking
110 – 125	Sugar pulp drying

Source: Popovski and Vasilevska, 2003

Geothermal springs can be classified as low temperature (less than 90°C), moderate temperature (90°C -150°C) and high temperature (greater than 150°C) (Geo-Heat Centre, 2005). South African geothermal springs can thus be classified as low temperature geothermal resources and can be used for activities that require temperatures below 70 °C (European Commission (EC), 1999; Geo-Heat Centre, 2005) (as indicated in Table 2.1). There is real potential for some of these geothermal resources to be used to dry locally produced fruits and vegetables, mushrooms and flowers. Siloam and Tshipise springs are in rural areas and utilising these resources would benefit the rural communities and improve the socioeconomic status of the rural population.

2.3.4 Tourism and recreation benefits

Tourism is one of the catalysts responsible for the development of many geothermal springs into spas or resorts, and many spas are changing their focus to recapture the essence of a true spa's contribution to health and well-being. Currently, about 15 million Europeans immerse themselves daily in geothermal spring waters (Hoole, 2001; Spicer and Nepgen, 2005). Forty-eight countries (e.g China, Canada, USA, Kenya, Brazil among others) used geothermal springs as resorts in the year 2000 (Lund and Freeston, 2001).

These countries do not include those which did not submit data to the Geothermal World Conference of 2000, such as South Africa, Malaysia, Ethiopia, Mozambique and Zambia, though it is known that they do have geothermal springs and spas for recreational use (Lund and Freeston, 2001). Tshibalo (2011) reported that thirty-one (31) out of eighty-three (83) known South African geothermal springs are used for recreation and tourism purposes. Recreational and tourism facilities and activities in South African geothermal spring resorts include the followings: exercise areas, rest areas, restaurants, ladies' bars, shops, solariums, camping facilities, conference facilities, cocktail lounges, picnic sites, golf courses, tennis and squash courts, volleyball, snooker and pool, bowls, heated and cold swimming pools, hot mineral pools, jacuzzis, paddle boats, caravan and camping, game drives, birdwatching, and horse riding (Tshibalo, 2011).

2.4 Geology of the Soutpansberg Group

The Soutpansberg Group overlies the eastern part of the Limpopo Mobile Belt, as well as the Palala Shear Zone and parts of the Kaapvaal Craton (Johnson *et al.,* 2006). This Belt formed between two major crustal blocks, namely, the Kaapvaal Craton in the south and the Limpopo Mobile Belt in the north (Brandl, 1986). Deposition started with basaltic lava, followed by sedimentary rocks. Then, there was an erosional period, in which a pink massive quartzite covering a much larger area than the original rift was deposited.

Until the deposition of the Karoo rocks, the Soutpansberg rocks formed a flat featureless landscape. Only after sedimentation had ceased (about 150 million years ago), was the area strongly block-faulted and then uniformly tilted to the north (Johnson *et al.,* 2006). Today the landscape that is seen is formed from the erosion during the last ± 60 million years (Cheney *et al.,* 1990). The pink resistant quartzite was instrumental in shaping the present morphology. The Soutpansberg rocks which developed in a half-graben, subsided along a main border fault, situated most probably some 10–20 km south of the present Soutpansberg mountainous area (van Eeden *et al.,* 1955).

The rocks of the Soutpansberg Group occupy a wedge-shaped, mountainous area, which stretches from the Kruger National Park in the east, where it is at its widest, to the Blouberg in the west, where they wedge out against a fault on the northern side (Johnson *et al.,* 2006). The strike of rock beds is east-west, and the dip is moderate to steep to the

north. The group is classified into seven formations and they are affected by several faults of various geological ages. These faults have probably had a considerable influence on the processes of sedimentation as well as the associated igneous activity. The trough in which the Soutpansberg Group has been deposited represents an ancient fault trough with a long-life span, similar to an aulacogen (Jansen, 1975).

Eruptive activity within the basin was centred mainly on Sibasa, with smaller centres near Nzhelele Dam and the Blouberg (Johnson *et al.,* 2006). However, the absence of marine sediments in this trough, as would be expected in the aulacogen, and the feeding of sediments into this trough from the north, and not parallel to its length, as would be required for an aulocogen, testifies against what was carried out by Jansen (1975). Thus, the Soutpansberg trough is viewed as a yoked intracratonic or near-cratonic environment to the Limpopo Mobile Belt (Johnson *et al.,* 2006).

2.4.1 Stratigraphy of the Soutpansberg Group

The Soutpansberg rocks rest unconformably on gneisses of the Limpopo Mobile Belt and Bandelierkop Complex. Along the eastern and most of the northern margin, the Soutpansberg outcrops are unconformably overlain by or technically juxtaposed against rocks of the Karoo SuperGroup (Johnson *et al.,* 2006). The contact relationship between the Soutpansberg and Waterberg Groups' rocks is a tectonic one, though the latter rocks are believed to be younger (Johnson *et al.,* 2006). The Soutpansberg Group is best developed in the eastern part, where the maximum preserved thickness is about 5000 m (Cheney *et al.,* 1990). The Soutpansberg Group comprises a volcano-sedimentary succession which is subdivided into seven formations (Figure 2.2); Tshifefe, Sibasa, Fundudzi, Wylie's Poort, Nzhelele, Stayt and Mabiligwe (Brandl, 2002; Johnson *et al.,* 2006).

2.4.1.1 Tshifhefhe Formation

The basal discontinuous Tshifhefhe Formation is only a few meters thick, and made up of strongly epidotised clastic sediments, including shale, greywacke and conglomerate (Brandl, 2002).

2.4.1.2 Sibasa Formation

The Sibasa Formation is dominantly a volcanic succession, with rare discontinuous intercalations of clastic sediments, having a maximum thickness of about 3000 m. The volcanic succession comprises basalts, which were sub-aerially extruded and minor pyroclastic rocks. The basalts are amygdaloidal, massive and generally epidotised. The clastic sediments which include quartzite, shale and minor conglomerate, can reach locally a maximum thickness of 400 m. A radiometric age of 1749 ± 104 Ma was obtained (Johnson *et al.,* 2006).

2.4.1.3 Fundudzi Formation

The overlying Fundudzi Formation is developed only in the eastern Soutpansberg and wedges out towards the west. It is up to 1 900 m thick and consists mainly of arenaceous and argillaceous sediments with a few thin pyroclastic horizons. Near the top of the succession up to four, about 50 m thick layers of epidotised basaltic lava are intercalated with the sediments (Brandl, 2002).

2.4.1.4 Nzhelele Formation

This is the uppermost unit which consists of 400 m thick volcanic assemblages (Musekwa Member) at the base, followed by red argillaceous and then by arenaceous sediments. The maximum preserved thickness is of the order of 1 000 m. The volcanic rock consists of basaltic lava and several thin, though consistent horizons of pyroclastic rocks, one of which is copper-bearing (Brandl, 2002).

2.4.1.5 Stayt and Mabiligwe Formations

There is a predominantly volcanic series of rocks, with accompanying sedimentary succession. The series rests on the floor of rocks belonging to the Beit Bridge Complex but its roof is not well-established (Johnson *et al.,* 2006). The rocks are nearly horizontally disposed and consist of basal conglomerate, followed by considerable thickness of lava. The latter is followed by reddish, brown and purple shale, with pale-coloured quartzite, in which pebble beds are intercalated at the top (Cheney *et al.,* 1990). The thickness of the Formation varies between 1700 and 1800 m, and it is regarded as correlative of Sibasa Formation, on the strength of a radiometric age of 1769 ± 34 Ma (Barton, 1979).

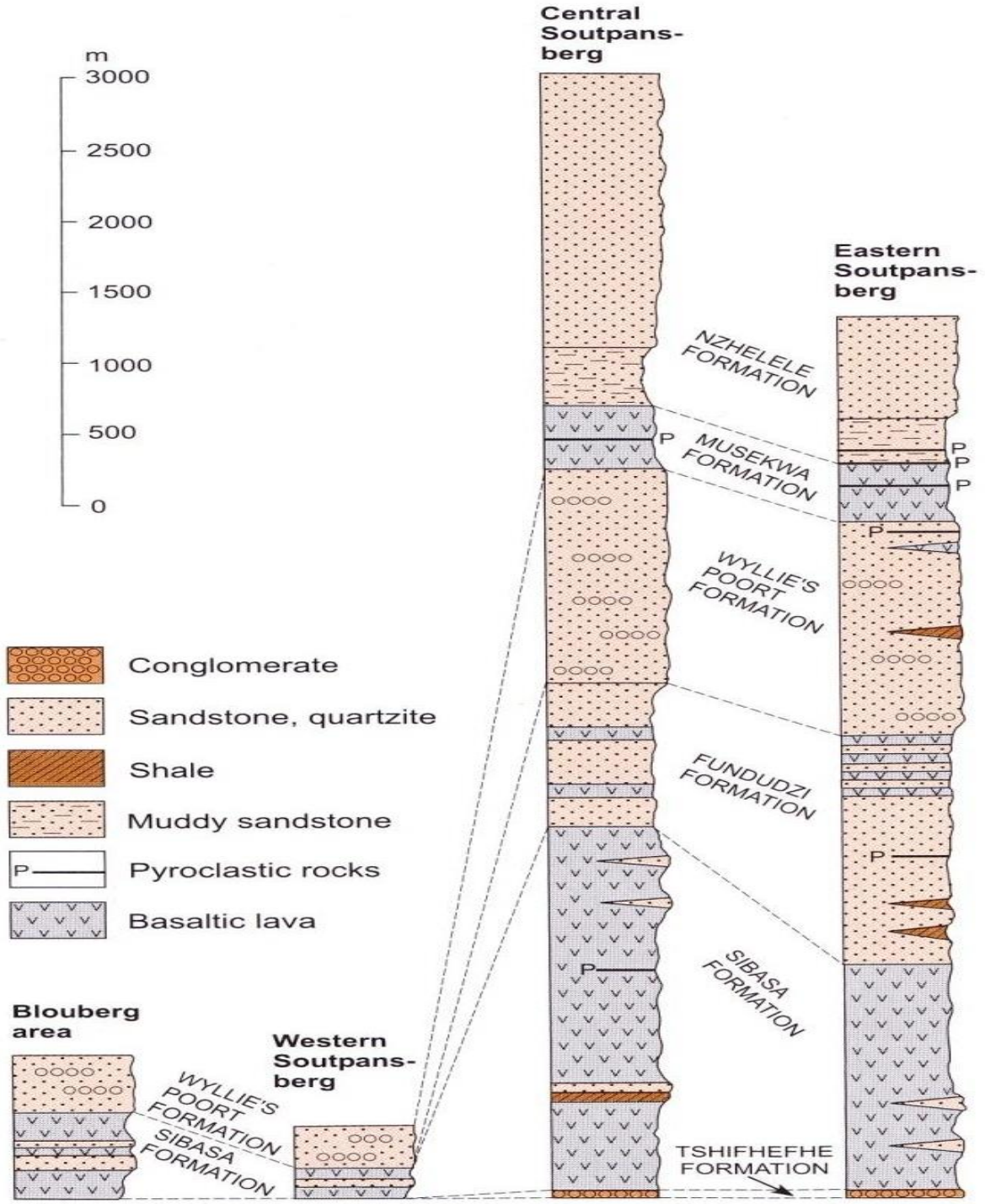

Figure 2.2: Stratigraphy of the Soutpansberg Group in the western, central and eastern Soutpansberg areas, as well as the Blouberg area (Barker *et al.,* 2006).

2.4.2 Structural Settings

The Soutpansberg strata shows a 30º dipping towards the north-northwest direction, with pronounced extensional faults categorised as the dominant East-North-East to West South West and the less-dominant North West to North West North (Figure 2.3) (Barker, 1979; Brandl, 1986, 2002). The dominant ENE trending fault was believed to be old and started occurring as far back as the formation of Soutpansberg strata. The Soutpansberg strata, though foliated, are not regionally strongly fractured but are often found locally fractured (Brandl, 2002). There is a heavy presence of fault planes intruded diabase dykes and shale-quartzite interface intruded sill (Brandl, 1986). Due to the nature of the geological formation in the area of study, groundwater is stored and transmitted through fractures and faults (Brandl, 1986).

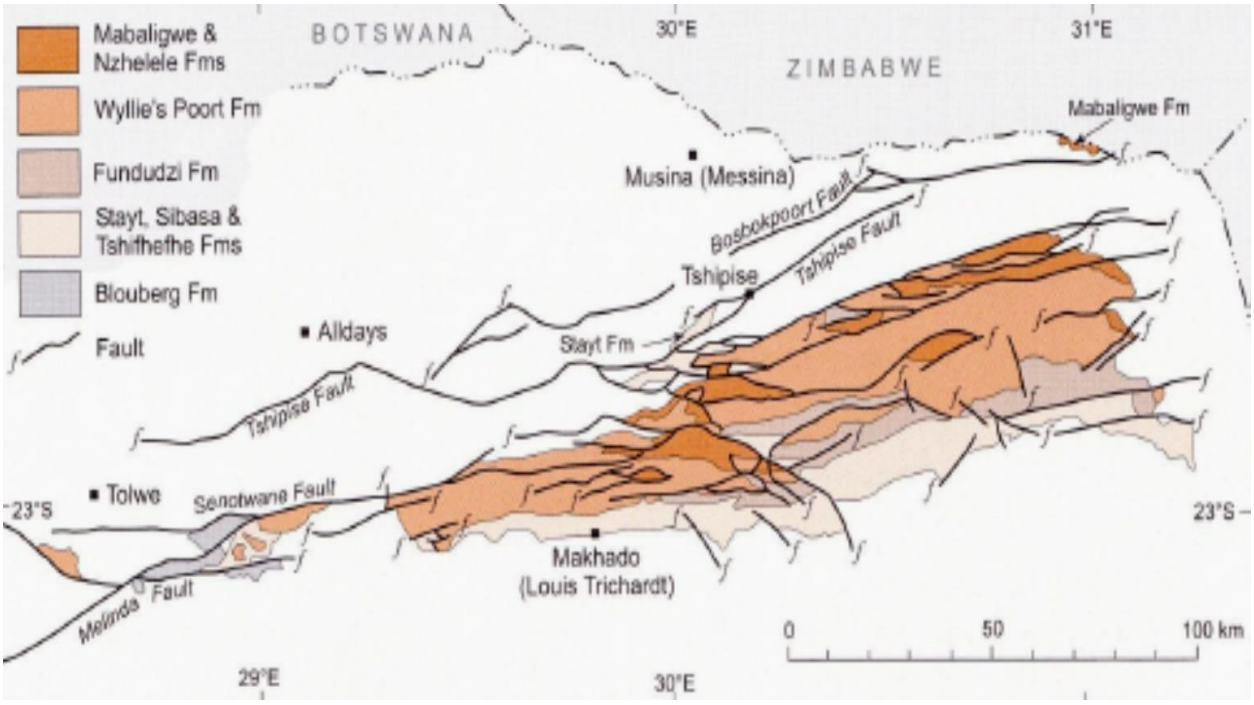

Figure 2.3: Distribution of the formations in the Soutpansberg Group as well as the Blouberg Formation (Barker *et al.,* 2006).

2.5 Physicochemical and geochemical characteristics of geothermal springs

2.5.1 pH

Geothermal springs that are characterised by low pH levels (acidic) are unlikely to be utilised as this adversely affects the survival of living organisms around them. As a result

of this, acidic springs are unlikely to be used for domestic, recreational and agricultural purposes (New Mexico Environment Department, 2002).

Low pHs of the springs might be attributed to the dissolution of carbonic rocks from weathering processes of the parent rocks, which the springs flow through (Zhou *et al.,* 2006). Metals tend to dissolve more in lower water pH and this could have health implication when deleterious heavy metals like lead and cadmium are washed into the spring via runoff (Zhou *et al.,* 2006). Low values of alkalinity, which ought to have served as a buffer to the spring against sudden changes in pH might also be responsible for generally low pH, especially during acid precipitation. Currently, most resorts or spas operate at thermal springs that are alkaline. The water suitable for swimming and bathing normally ranges between 6.5 and 8.3 in terms of its pH level because water below this level is likely to cause eye irritation (Hoole, 2001).

Some geothermal springs in the same geographic region show different water characteristics. The various springs probably originate from different depths and thus reflect variations in the geological structure within the area. The low water pH could lead to corrosion (Nordberg *et al.,* 1985).

2.5.2 Electrical Conductivity and Total Dissolved Solids

Electrical Conductivity (EC) is a measure of the capacity of water to conduct electrical current and is directly related to the concentrations of salts dissolved in water, and therefore the total dissolved solids (TDS). Salts dissolve into either positively charged or negatively charged ions, which conduct electricity (Hayashi, 2008). The World Health Organization (2003) describes TDS as “the inorganic salts and small amounts of organic matter present in solution”. The principal constituents are usually calcium, magnesium, sodium, potassium (cations) and carbonate, hydrogen carbonate, chloride, sulphate and nitrate (anions). If the electrical conductivity of water is high this indicates a high concentration of ions which then determines if the water is potable or not (Bruvold and Ongerth, 1969).

The electrical conductivity of water depends on the water temperature: the higher the temperature, the higher the electrical conductivity would be (Cassidy *et al.,* 2001). The electrical conductivity of water increases by 2-3% to an increase of 1 degree Celsius of

water temperature (Press and Siever,1986). Electrical conductivity is an indicator of total dissolved substances (TDS) and is based on the presence of ions (Hayashi, 2008). In a geothermal spring, high temperature implies high electrical conductivity values, which are indications of dissolved minerals in water (Olivier *et al.,* 2011). Most South African thermal springs have TDS concentrations in the region of 250-4000 mg/L and thus belong to classes A and B, which can be classified as slightly, or highly mineralised waters as seen in Table 2.2 below (Bond, 1946). A commonly used classification system for thermal springs is that devised by Bond in 1946. He divided thermal spring waters into five categories as shown in Table 2.2:

Table 2.2: Classification of thermal spring water in South Africa

Class	Water	Chemical Composition
A	Highly mineralised chloride-sulphate waters	*TDS > 1 000 mg/L; Cl^- > 270 g/Kg; SO_4 ≥ 50 g/kg
B	Slightly saline chloride waters	TDS 300 – 500 mg/L; Cl^- > 270 g/Kg; SO_4 ≤ 3 g/Kg
C	Temporary hard carbonate waters	TDS < 800 mg/L; pH > 7.6
D	Alkaline sodium carbonate water	TDS < 1 000 mg/L; Na_2CO_3 or $NaHCO_3$ > 150 mg/L No permanent hardness
E	“Pure” waters	TDS < 150 mg/L; pH < 7.1

*TDS-total dissolved solids

Source: Bond, 1946

2.5.3 Major cations

Sodium (Na)

Sodium is a cation in common salt found in groundwater, which can impart a salty taste at concentrations of over 250 mg/L (Gray, 2008). It can contribute to hypertension and high levels of sodium in drinking water should be noted by users on low sodium diets. A slight taste may be apparent above 100 mg/L (Johnson and Scherer, 2009). The

concentrations of sodium in Siloam, Tshipise, Sagole and Mphephu springs were 66.24,156.31, 65.15 and 44.37 mg/L, respectively (Olivier *et al.,* 2010).

Potassium (K)

Potassium is a cation in common salt found in groundwater, which is essential in the human diet. Excessive amounts in drinking water may have a laxative effect on humans. Acceptable concentration in drinking water can range from 0 to 8 mg/L (Johnson and Scherer, 2009). Previous study by Olivier *et al*. (2010), shows that the concentrations of potassium in Siloam, Tshipise, Sagole and Mphephu springs were 2.82, 4.25, 1.01 and 1.14 mg/L, respectively.

Calcium (Ca) and magnesium (Mg)

Calcium is a naturally occurring metal essential for human diet and is common in groundwater. Calcium concentration alone is not of major concern, but with magnesium, they are the main contributors to the hardness of water (Gray, 2008). Maximum limits have not been established for calcium. However, magnesium concentrations above 125 mg/L may cause diarrhea in some people (Johnson and Scherer, 2009). Previous work on Siloam, Tshipise, Sagole and Mphephu springs show that the concentrations of calcium are 1.40, 5.58, 1.31 and 13.73 mg/L and the concentrations of magnesium are 1.30, 0.17, 0.07 and 11.25 mg/L, respectively (Olivier *et al.,* 2010).

2.5.4 Major anions

Chloride (Cl^-)

Chloride is commonly found in groundwater. High concentrations of chloride ions can cause water to have a salty taste, corrode hot water plumbing systems and have a laxative effect on some people (Gray, 2008). A concentration below 200 mg/L has no undesirable health effects because the World Health Organization (2003) and European Union (1998) recommend 250 mg/L. The chloride concentrations at Siloam, Tshipise, Sagole and Mphephu geothermal springs are 44.35, 168.97, 47.85 and 39.38 mg/L, respectively, which are suitable for drinking without further treatment (Johnson & Scherer, 2009; Olivier *et al.,* 2010).

Fluoride (F^-)

Fluoride is a non-metal which occurs naturally in groundwater. It promotes dental health at concentrations of between 0.7 and 1.5 mg/L (Gray, 2008). At concentrations above 1.5 mg/L, dental fluorosis (brownish staining of the teeth) may occur (SABS, 1999; WHO, 2000). Previous studies show fluoride concentrations at Siloam, Tshipise, Sagole and Mphephu springs were 6.11, 5.63, 1.01 and 3.16 mg/L, respectively, which are above the South African guidelines for drinking water (SANS, 2015) except for Sagole. Since the concentrations do not fall within the recommended range for drinking water, geothermal water at Siloam, Tshipise and Mphephu are not suitable for drinking with regards to this mineral element.

Sulphate (SO_4^{2-})

Sulphate is a constituent of a common salt found in groundwater, which can impart a salty taste. Drinking water with high quantities of sulphate can result in diarrhea (Gray, 2008). With concentrations, less than or equal to 200 mg/L of sulphate, no adverse health effects are anticipated (Johnson and Scherer, 2009). The concentrations of sulphate in Siloam, Tshipise, Sagole and Mphephu springs were 9.26, 53.17, 18.20 and 9.26 mg/L, respectively (Olivier *et al.,* 2010), contributing to no adverse health effect.

Nitrate (NO_3^-)

Nitrate is a very soluble anion and is dissolved by rainwater and percolates deeper into the soil where it enters the groundwater by direct percolation. This makes nitrate the commonest chemical contaminant of groundwater (Spalding and Exner, 1993). WHO (2000) has set a standard of nitrate in drinking water at 10 mg/L; thus, Siloam, Tshipise, Sagole and Mphephu springs water are within the standard, having 0.00, 0.61, 0.00 and 2.12 mg/L, respectively (Olivier *et al.,* 2010). The inclusion in the primary regulations is to protect against methemoglobinemia in infants under the age of 6 months (Gray, 2008).

2.5.5 Trace metals

Arsenic (As)

Arsenic (As) is a semi-metallic element that occurs in a wide variety of minerals, mainly as As_2O_3, and can be recovered from processing of ores containing mostly copper, lead, zinc, silver and gold. It is also present in the ashes from coal combustion. Arsenic exhibits

fairly complex chemistry and can be present in several oxidation states (-III, 0, III, V) (Smith *et al.,* 1995). A high concentration of arsenic in drinking water can cause cancer, nausea, vomiting, diarrhea and decreased production of red and white blood cells, and damage to blood vessels. The guideline value for drinking water is 0.01 mg/L (WHO, 2008; SABS, 1999). Olivier *et al*. (2010) shows that the concentrations of arsenic in Siloam, Tshipise, Sagole and Mphephu springs water were 0.27, 0.14, 2.88 and 0.43 µg/L, respectively. These are below compliance standards and hence there is no potential to cause health problems, unless accumulation occurs over a long time.

Barium (Ba)

Barium is a metallic element belonging to the alkaline earths. It is present as a trace element in both igneous and sedimentary rocks. Its guideline value in drinking water is 0.7 mg/L (WHO, 2008). There is no evidence that barium is carcinogenic (causing cancer) or mutagenic (causing changes in genetic mutation). The greatest concern to humans is its potential to cause hypertension (WHO, 2008). At Siloam, Tshipise, Sagole and Mphephu springs, the concentrations of barium were 4.22, 13.63, 5.14 and 51.90 µg/L, respectively (Olivier *et al.,* 2010). Thus, it has no potential to cause hypertension, unless accumulation takes place in a long time.

Beryllium (Be)

Beryllium is a metallic element which does not degrade nor, can it be degraded. It occurs naturally in drinking water. Be is not likely to be found in natural water above trace levels as a result of the insolubility of oxides and hydroxides at the normal pH range (WHO, 2009). The primary concern with beryllium exposure is the lung disease caused by inhaling beryllium, and intestinal lesions. According to the United States Environmental Protection Agency (EPA), MCL of beryllium is 4 µg/L (New Hampshire Department of Environmental Services, 2007). Be was undetected in the study carried out by Olivier *et al*. (2010).

Cadmium (Cd)

Cadmium is a rare natural element which is widely distributed in the earth's crust in very small amounts (Water UK, 2001). It is a soft, bluish-white metal. Its guideline value is 0.005 mg/L (EU, 1998) and 0.003 mg/L (WHO, 2008). When people breathe in cadmium,

it can severely damage the lungs and may even cause death. Utilisation of cadmium by animals via eating or drinking could sometimes lead to high blood-pressure, liver disease and nerve or brain damage (Gray, 2008). A maximum acceptable concentration of 0.005 mg/L (5 µg/L) for cadmium in drinking water has been established on the basis of health considerations (Jarup *et al.,* 1998). Olivier *et al*. (2010) shows the concentrations of cadmium at Siloam, Tshipise, Sagole and Mphephu are 0.00, 0.02, 0.01 and 0.00 µg/L, respectively. Thus, cadmium concentrations in springs in the study area have no potential to cause negative health problems, unless it accumulates over along period.

Chromium (Cr)

Chromium is a metal found in natural deposits as ores containing other elements. Chromate and dichromate also adsorb on soil surfaces, especially iron and aluminium oxides. Cr (III) is the dominant form of chromium at low pH (<4). Cr^{3+} forms solution complexes with ammonia, hydroxide, chloride, fluoride, cyanide, sulphate and soluble organic ligands. Cr (VI) is the most toxic form of chromium and is also more mobile. Cr (III) mobility is decreased by adsorption to clays and oxide minerals below pH 5 and low solubility above pH 5 due to the formation of $Cr(OH)_3(s)$ (Chrotowski *et al.,* 1991). Chromium mobility depends on sorption characteristics of the soil, including clay content, iron oxide content and the amount of organic matter present. Chromium can be transported by surface runoff to surface waters in its soluble or precipitated form. Soluble and un-adsorbed chromium complexes can leach from soil into groundwater. The leachability of Cr (VI) increases as soil pH increases and most chromium released into natural waters is particle associated (Smith *et al.,* 1995).

The guideline values for drinking water are 0.05 mg/L (WHO, 2008) and 0.1 mg/L (SABS, 1999). Chromium has the potential to cause the following health effects from long-term exposure at levels above MCL set by EPA: damage to the liver, kidney, circulatory system, nerve tissues and skin irritation. Olivier *et al*. (2010) found the concentrations of chromium in Siloam, Tshipise, Sagole and Mphephu springs water as 0.97, 0.70, 0.49 and 1.20 µg/L, respectively. This means that the chromium concentrations in the springs in the study area may not cause negative health effects unless they accumulate above the recommended safe levels.

Cobalt (Co)

Cobalt is an element that occurs naturally in the environment in air, water, soil, rocks, plants and animals. Co is widely dispersed in the environment and humans may be exposed to it by breathing air, drinking water and eating food that contain cobalt (George, 2003). Body contact with soil or water that contain cobalt may also enhance exposure. Exposure to cobalt may cause weight loss, dermatitis, and respiratory hypersensitivity. International Agency for Research on Cancer (IARC) has listed cobalt and cobalt compounds within group 2B (agents which are possibly carcinogenic to humans). Previous study by Olivier *et al*. (2010) shows that the concentrations of cobalt in Siloam, Tshipise, Sagole and Mphephu springs water were 0.05, 0.01, 0.01 and 0.00 µg/L, respectively. Surface water and groundwater concentrations of stable cobalt are low ranging from 1 to 10 µg/l (WHO, 2006a). This means that the cobalt concentrations in the springs have no potential to cause adverse health problems, unless it accumulates over a long period.

Copper (Cu)

Copper is a reddish metal that occurs naturally in rocks, soil, water, sediment and air. Copper and its compounds are widely distributed in nature, and this element is found frequently in surface water and in some ground waters (Alloway and Ayres, 1997). Copper is an essential and beneficial element in human metabolism and is generally considered non-toxic except at high doses (WHO, 2008) and the guideline value is 1 mg/L (WHO, 2008). The acute lethal dose for adults lies between 4 and 400 mg of copper (II) ion per kg of body weight, based on data from accidental ingestion and suicide cases (Agarwal *et al.,* 1990). Individuals ingesting large doses of copper end up with gastrointestinal bleeding, haematuria, intravascular haemolysis, methaemoglobinaemia, hepatocellular toxicity, acute renal failure and oliguria (Agarwal *et al.,* 1990). At lower doses, copper ions can cause symptoms typical of food poisoning (headache, nausea, vomiting and diarrhea). Olivier *et al*. (2010) shows the concentrations of copper for all the springs studied as 0.00 µg/L, which implies no negative potential health effects.

Lead (Pb)

Lead is a metal found in natural deposits as ores containing other elements. It is generally used in household plumbing materials. Lead released to groundwater, surface water and land is usually in the form of elemental lead, lead oxides and hydroxides, and lead metal oxyanion complexes (Smith *et al.,* 1995). Most lead that is released to the environment is retained in the soil. The primary processes influencing the fate of lead in soil include adsorption, ion exchange, precipitation, and complexation with absorbed organic matter. These processes limit the amount of lead that can be transported into the surface water or groundwater. The relatively volatile organo-lead compound tetra-methyl lead may form in anaerobic sediments as a result of alkylation by microorganisms (Smith *et al.,* 1995). The amount of dissolved lead in surface water and groundwater depends on pH and the concentration of dissolved salts and the types of mineral surfaces present. The U.S Environmental Protection Agency (EPA) has set the MCL of water at 0 mg/L because it believes the level of protection would not cause health problems (USEPA, 2009). Exposure at levels above the MCL has the potential to cause strokes, kidney disease and cancer. The South Africa drinking water guideline values are 0.02 mg/L (SABS, 1999) and 0.01 mg/L (WHO, 2008). Olivier *et al*. (2010) shows the concentrations of lead in Siloam, Tshipise, Sagole and Mphephu springs water as 0.05, 0.08, 0.12 and 0.16 µg/L, respectively. This implies that Pb has no potential to cause negative health effects in the springs studied, unless it accumulates over a long period.

Manganese (Mn)

Manganese is a naturally occurring metal, important in the human diet. Mn is reactive when pure and as a powder, will burn in oxygen; it reacts with water (its rust like iron) and dissolves in dilute acids (Lenntech, 1998-2009). According to Johnson and Scherer (2009), a high concentration of manganese does not appear to cause a health hazard. However, manganese concentration greater than 0.05 mg/L can cause brown and black stains on laundry, plumbing fixtures and sinks. The guideline values for drinking water are 0.05 mg/L (Kempster *et al.,* 1997) and 0.1 mg/L (SABS, 1999). Olivier *et al*. (2010) showed the concentrations of manganese in Siloam, Tshipise, Sagole and Mphephu springs water were 0.75, 0.00, 0.20 and 0.00 µg/L, respectively, which are low with no negative effects unless they accumulate over a long time.

Mercury (Hg)

Mercury is a liquid metal found in natural deposits as ores containing other elements (APEC, 2010). Mercury is a toxic element, with particularly damaging effects on the brain and central nervous system. It serves no beneficial physiological function in man. The main toxicological effects of mercury include neurological damage, paralysis, blindness, and chromosome breakage (Alloway and Ayres, 1997). Mercury concentrations above the guideline value can cause kidney damage in humans and animals. The maximum acceptable concentration of mercury is set at 1 µg/L (WHO, 2008) which was adopted by the EC in the drinking water directive, while the USEPA MCL has been set at 2 µg/L. Surface water and groundwater are generally well below this level. Olivier *et al*. (2010) found mercury concentrations at Siloam, Tshipise, Sagole and Mphephu as 0.53, 0.33, 0.00 and 0.23 µg/L, respectively. These are below the acceptable standards and cannot cause negative health effects unless they accumulate over a long period.

Molybdenum (Mo)

Molybdenum is a silvery white metal which can be attacked slowly by acids. It is a valuable alloying agent, but toxicity does occur at >100 ng/kg of body weight resulting in diarrhoea, anaemia and elevated uric acid in the blood (Gray, 2008). It is an essential element in plant nutrition. Some plants can have up to 500 ppm of the metal when they grow in alkaline soil and the recommended daily intake of the mineral is 75 µg as a food supplement (Lenntech, 1998-2009). Doses larger than 200 µg may cause kidney problems and copper deficiencies. WHO (2008) guideline value is 70 µg/L, while the National Health and Medical Research Council (NHMRC) (2004) of Australia set the guideline value at 0.05 mg/L. Molybdenum concentrations were 2.23, 1.41, 1.06 and 0.91 µg/L at Siloam, Tshipise, Sagole and Mphephu, respectively (Olivier *et al.,* 2010). These values are below the standards with minimal or no negative health effects.

Nickel (Ni)

Nickel is a silvery white, hard, malleable and ductile metal. It occurs in very low levels in the environment, especially in drinking water (<10%) (Gray, 2008). It is generally used as an ingredient in the steel and other metal products. It may be found in slate, sandstone, clay minerals and basalt. It is a dietary requirement for many organisms. Nickel

concentrations in plants are 1 µg/g (Gray, 2008) and concentrations of nickel higher than 50 µg/g can be toxic (EU, 1998). The human body contains about 10 mg of nickel (Gray, 2008). The guideline value for drinking water is 0.02 mg/L (WHO, 2003) and 0.15 mg/L (SABS, 1999). Olivier *et al*. (2010) shows that nickel concentrations in Siloam, Tshipise, Sagole and Mphephu springs water are 0.00, 37.19, 0.00 and 0.00 µg/L, respectively. The concentration of Ni in Tshipise is above the recommended WHO (2003) standard for drinking water but less than the SABS (1999) standard. It may not be detrimental to human health unless it accumulates over a long time.

Selenium (Se)

Selenium is a non-metallic chemical element found in natural deposits as ores containing other elements (Smith *et al.,* 1995). The major use of selenium is as an alloying additive in the metallurgical industry to improve the properties of copper, lead and steel. The toxic effects of long-term selenium exposure in humans are manifested in nails, hair and liver. In drinking water, health-based guidelines values for drinking water are 0.01 mg/L (WHO, 2003) and 0.02 mg/L (SABS, 1999). The use of selenium's antioxidant and curative properties as a dietary supplement has shown a positive effect on the following health problems: AIDS, arthritis, asthma, cancer, cardiovascular diseases, reproduction, thyroid and viral infections (George, 2003). Olivier *et al*. (2010) show that selenium concentrations in Siloam, Tshipise, Sagole and Mphephu springs water are 0.72, 2.35, 0.20 and 0.00 µg/L, respectively. These concentrataions are lower than the compliance standards and hence no negative health impacts are envisaged except for long term exposure to cumulative values.

Zinc (Zn)

Zinc is a trace element that is essential for human health and is one of the most mobile heavy metals in surface waters and groundwater because it is present as soluble compounds at neutral and acidic pH values (Gray, 2008). When people absorb too little zinc they can experience loss of appetite, decreased sense of taste and smell, slow wound healing and skin sores. Zinc shortages can even cause birth defects. Very high levels of zinc can damage the pancreas and disturb the protein metabolism, and cause arteriosclerosis (Smith *et al.,* 1995). The maximum allowable concentration and the

permissible concentration of zinc in drinking water are 10 and 5 mg/L respectively, according to international organisation for standardisation (ISO, 1986). Olivier *et al*. (2010) shows that zinc concentrations at Siloam, Tshipise, Sagole and Mphephu are 3.46, 2.48, 205 and 1.95 µg/L, respectively, compared to the WHO standard of 3000 µg/L (WHO, 2003). This implies that Zn has no potential to cause negative health effect in the springs studied, unless it accumulates over a long period

2.6 Chemistry of geothermal springs

Temperature plays a major role in the chemical composition of geothermal spring waters and the depth at which the water is emanating from (Hartnady and Jones, 2007). The temperature of groundwater provides insight into the subsurface geological processes that generate and transport heat (Witcher, 2002). The classification of springs may also influence usage of the spring, but generally they are classified by surface temperature (Subtavewung *et al.,* 2005) as follows; < 20°C (cold spring), 20 – 29°C (hypothermal/tepid spring), 30 – 50°C (thermal/hot spring), above 50°C (Scalding/hyperthermia spring).

Different chemical reactions occur within geothermal waters, which are mostly associated with the interactions between water and rocks in deep aquifers. Within the waters, many other reactions occur, and these typically involve anions and/or metal cations/trace elements (Hodder, 2005). As the rainwater falls in the recharge area, it first passes down through leaves, soil and other debris on the surface. The living animals in the debris and soil give off carbon dioxide, which is dissolved in the water and forms a weak carbonic acid (equations. 2.1 and 2.2).

$$H_2O + CO_2 \rightleftharpoons H_2CO_3 \quad \text{2.1}$$

$$H^+_{(aq)} + HCO_3^-{}_{(aq)} \rightleftharpoons H_2CO_{3\,(aq)} \quad \text{2.2}$$

This acidic water then moves further down in the earth, through the different layers of chert, including the thick layers of novaculite. The novaculite and chert include the skeletons and spicules of Radiolarians and graptolites, which are made of calcium. This calcium, along with the rock, exists in a form called calcium carbonate ($CaCO_3$). As the water passes through the chert formations, it dissolves some of the calcium carbonate (Olivier *et al.,* 2010). The carbonic acid in the water reacts with the calcium carbonate to form soluble calcium bicarbonate (equations 2.3 and 2.4).

$$H_2CO_3 + CaCO_3 \rightleftharpoons Ca(HCO_3)_2 \quad \text{.....2.3}$$

$$H^+_{(aq)} + HCO_3^-{}_{(aq)} + Ca^{2+}_{(aq)} + CO_3^{2-}{}_{(aq)} \rightleftharpoons Ca(HCO_3)_{2\,(aq)} \quad \text{.....2.4}$$

In this process, the carbonic acid is partially neutralised, and the solution gradually becomes more alkaline. Calcium bicarbonate only exists as a solution. As this solution moves deeper into the earth, it heats up and dissolves some silica from the surrounding rock layers (Tarcan and Gemici, 2003). The underground heat helps to make the calcium bicarbonate solution (water) more buoyant, and the broad cracks and faults across the face of the geothermal spring provide this solution an escape route to the surface. When the solution Ca $(HCO_3)_2$ reaches the surface, the dissolved carbon dioxide (CO_2) quickly escapes as shown in equations 2.5 and 2.6:

$$2Ca(HCO_3)_2 \rightleftharpoons 2CaCO_3 + 2H_2O + 2CO_2 \quad \text{.....2.5}$$

$$2Ca(HCO_3)_{2\,(aq)} \rightleftharpoons 2Ca^{2+}_{(aq)} + 2CO_3^{2-}{}_{(aq)} + 2H_20_{(l)} + 2CO_{2\,(g)} \quad \text{.....2.6}$$

It is important to note that calcium carbonate is formed from the release of carbon dioxide, not from the change in temperature from rising to the surface (Tarcan and Gemici, 2003). Calcium carbonate is actually more soluble in cold water. The water remains in the aquifer for a sufficiently long time (hundreds to thousands of years) and the reactions are sufficiently slow for them to be used to calculate the temperature of the water. In effect, the ratios of the concentrations of the liberated cations (Ca^{2+}, Na^+, K^+) are temperature dependent. The solubility of silica is also temperature dependent, but this equilibrium is attained rather more rapidly than the dissolution of other silicate minerals (eqns. 2.7 and 2.8) (Tarcan and Gemici, 2003; Hodder, 2005).

$$2H_4SiO_4\,(aq) \rightleftharpoons 4H_2O + 2SiO_2 \quad \text{.....2.7}$$

Dissolved silica Quartz siliceous sinter

$$Si(OH)_{4\,(aq)} + 4\,OH^-_{(aq)} \rightleftharpoons 4H_2O_{(L)} + 2SiO_{2\,(L)} \quad \text{.....2.8}$$

These reactions (eqns. 2.7 and 2.8) can be used as a geothermometer too. Any difference in temperatures obtained from the two geo-thermometers is related to the sampling of the water relative to the deep aquifer: waters that have moved away from the aquifer are likely to have lower temperatures derived from silica concentrations than temperatures derived from concentrations of Na^+, K^+ and Ca^{2+}. As the water rises to the surface it cools, and silica and other minerals are precipitated. Hence, it helps "cap" the aquifer, and prolong the geothermal system's existence. Water that does reach the surface through faults and

fractures will cool further and produce the sinter mounds and terraces that are typical around geysers and hot springs (Tarcan and Gemici, 2003; Hodder, 2005).

Hydrogen sulphide and other gases, including hydrogen chloride are dissolved in geothermal water that originates from the magma. Thus, chloride ion in geothermal waters can be at high concentrations. Both hydrogen sulphide ions (HS^-) and chloride ions (Cl^-) can form complexes with trace elements, as shown in eqn. 2.9 below:

$$M^{2+}(aq) + nX^-(aq) \rightarrow M(X)_n^{2-n}(aq) \quad \text{.....2.9}$$

Where, X^- are anions such as Cl^-, SO_4^{2-}, HCO_3^{2-}, HS^- among others; M - trace metals.

Some of these trace elements may have been expelled from the magmas as gaseous sulfides and halides; others may have entered the geothermal water through their reactions with aquifer rocks (Hodder, 2005).

2.6.1 Water geothermometers

Water geothermometer is used for prediction of subsurface temperatures in the exploration of geothermal resources. Geothermometer provides valuable insight of the nature of geothermal system, taking into account mineral – solute reactions at equilibrium (Karingithi, 2009). Various methods have been developed by using, for example, Na-K ratio, K-Mg ratio, Na-Li ratio, Na-K-Ca-Mg, CH_4/C_2H_6 ratio, concentrations of SiO_2, CO_2, H_2S, H_2 and CH_4 among others. Each of these methods has their limitations and strengths. The water types (Na-Cl/ Na-HCO_3) play a significant role is the selection of the appropriate method. Hence, Na-K geothermometer was used to predict the reservoir temperature of the geothermal springs and hot boreholes. The following rules were used to constrain the data and informs the decision of the specific geothermometer method used (Fournier, 1979; Giggenbach, 1991; Karingithi, 2009):

- Use for waters indicating reservoir temperatures >100
- Use if the waters contain low Ca; i.e. the value of (log ($Ca^{1/2}$/Na) + 2.06) is negative
- Use for near neutral/slightly alkaline pH.

The response of the Sodium/Potassium (Na/K) ratio, decreasing with increasing fluid temperature, is based on temperature dependent cation exchange reaction between albite and K feldspar (Orthoclase):

$$NaAlSiO_3O_8 + K^+ \rightarrow KAlSi_3O_8 + Na^+ \quad \text{.....2.10}$$

Albite Orthoclase

The equilibrium constant, K for equation 2.10 is:

$$K(eq) = \frac{[KAlSi3O8][Na+]}{[NaAlSiO3O8][K+]} \quad \text{.....2.11}$$

If activities of the solid reactants are assumed to be in unity and the activity of dissolved species is almost equal to their molar concentrations, the equation will be reduced to:

$$K(eq) = \frac{[Na+]}{[K+]} \quad \text{.....2.12}$$

2.7 Health risk assessment of trace metals

Health impact assessment can be defined as the estimation of the effects of a specified action on the health of a defined population (Scott-Samuel, 1998, 2005). According to USEPA (2001, 2004), human health risk assessment is the process to estimate the nature and probability of adverse health effects in humans who may be exposed to chemicals in contaminated environmental media, now or in the future. The risk assessment process is made up of four basic steps: hazard identification, exposure assessment, toxicity (dose-response) assessment, and risk characterisation (Figure 2.4).

Hazard Identification involves determining whether exposure to a stressor can cause an increase in the incidence of specific adverse health effects (cancer, birth defects) (Asare-Donkor *et al.,* 2016). It is also used to determine whether the adverse health effect is likely to occur in humans. In the case of chemical stressors such as trace metals (TM), the process examines the available scientific data for a given chemical (or group of chemicals) and develops a weight of evidence to characterise the link between the negative effects and the chemical agent. Exposure to a stressor may generate many different adverse effects in a human such as diseases, formation of tumors, reproductive defects, death, among others (USEPA, 1992a, 2002, 2008). One of the major components is evaluating the weight of evidence regarding a chemical potential to cause adverse human health effects.

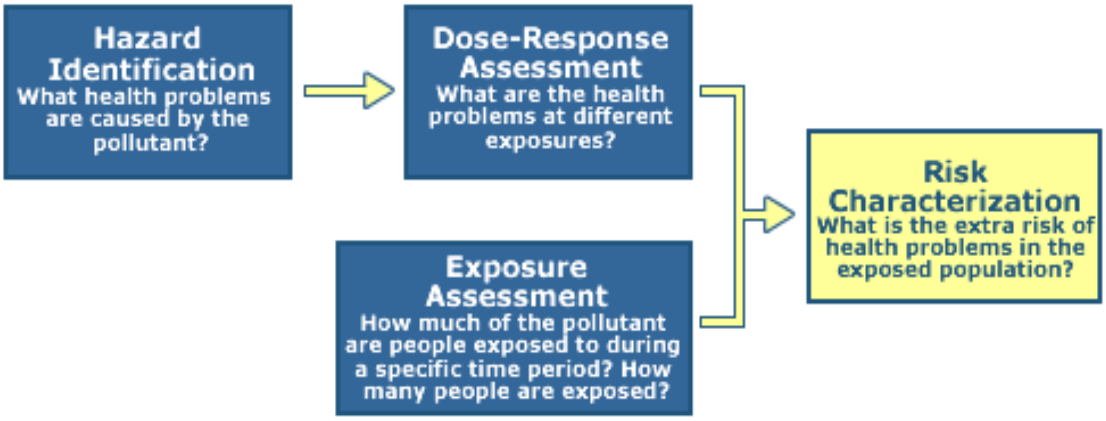

Figure 2.4: Four step risk assessment process (USEPA, 2001).

Dose-Response is the resulting biological response in an organ or organism expressed as a function of a series of doses. It further describes how the likelihood and severity of adverse health effects (the responses) are related to the amount and condition of exposure to an agent (the dose provided). Generally, an increase in dose, increases the measured response. Therefore, at low doses there may be no response and at some level of dose the responses begin to occur in a small fraction of the study population or at a low probability rate. Here are some of the factors that shape the dose-response relationship; agent (e.g. trace metal), the kind of response (e.g. cancer) and the experimental subject (human or animal) (USEPA, 1991, 2001; Asare-Donkor *et al.,* 2016).

Exposure assessment is the process of measuring or estimating the magnitude, frequency, and duration of human exposure to an agent in the environment or estimating future exposures for an agent that has not yet been released (USEPA, 1992a). An exposure assessment includes some discussion of the size, nature, and types of human populations exposed to the agent, as well as discussion of the uncertainties in the above information (USEPA, 1992a, 2001). Exposure can be measured directly, but more commonly is estimated indirectly through consideration of measured concentrations in the environment, consideration of models of chemical transport and fate in the environment and estimates of human intake over time. Exposure assessment considers

both the exposure pathway (ingestion, dermal and inhalation) and the exposure route (means of entry of the agent into the body) (USEPA, 1992a; Chrostowki, 1994).

Risk characterisation is the integration of the information on the hazard exposure and dose-response to provide an estimate of the likelihood that any identified adverse effect will occur in the exposed people (Chrostowki, 1994). It conveys the risk assessor's judgment as to the nature and presence or absence of risks, along with information about how the risk was assessed, where assumptions and uncertainties still exist, and where policy choices will need to be made. Risk characterisation takes place in both human health risk assessments and ecological risk assessments (USEPA, 1999).

2.8 Stable isotopes of Carbon, Hydrogen and Oxygen

2.8.1 Stable Carbon Isotopes

Carbon has two stable isotopes, which are ^{12}C and ^{13}C. Their abundances are 98.9% and 1.1%, respectively, so that the $^{13}C/^{12}C$ ratio is about 0.011 (IAEA, 2001). Most carbon in basalts is in the form of CO_2, which has limited solubility in basaltic liquids. As a result, basaltic magma begins to exsolve CO_2 before they erupt. Thus, virtually every basaltic magma, including those that erupted at mid-ocean ridges, has lost some carbon, and sub-areal basaltic magma have lost virtually all carbon (Staddon, 2004). Figure 2.5 presents a broad survey of natural abundances of various compounds consisting of, at the low-^{13}C end bacterial methane (marsh-gas), and at the high end the bicarbonate fraction of groundwater under special conditions. In the carbonic acid system variations, up to 30‰ are normally observed (IAEA, 2001). Wider variations occur in systems in which carbon oxidation or reduction reactions take place, such as the CO_2 (carbonate) - CH_4 (methane) or the CO_2 - $(CH_2O)_x$ (carbohydrate) systems (IAEA, 2001).

Isotopes of carbon and their interactions make an important contribution, often together with the water chemistry. In nature equilibrium carbon isotope effects, occur specifically between the phases CO_2 - H_2O - H_2CO_3 - $CaCO_3$. The values for the fractions involved only depend on temperature and are obtained from laboratory experiments. The kinetic fractionation of specific interest occurs during carbon dioxide assimilation, i.e. the CO_2 uptake by plants. The relatively large fractionation (up to about −18‰) is comparable to

the effect observed during absorption of CO_2 by an alkaline solution (White, 2015). By international agreement, Pee Dee Belemnite (PDB) was used as the primary carbon reference (standard) material.

$$\delta^{13}C_{NBS20\,/\,PDB} = -1.06‰ \quad \text{.....2.13}$$

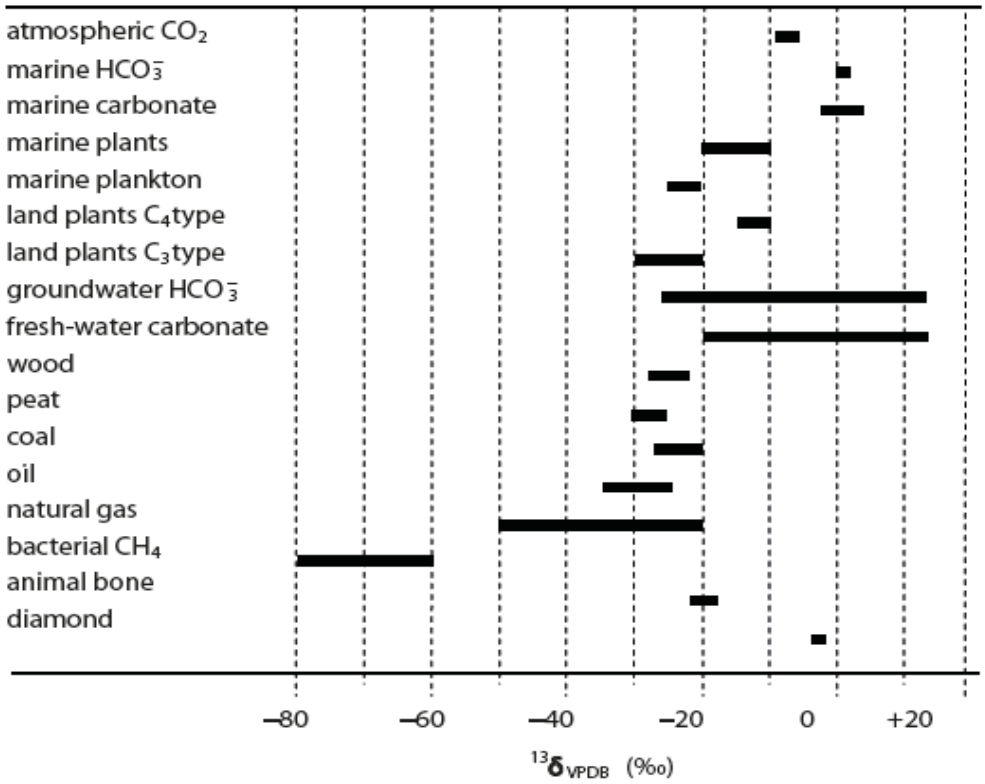

Figure 2.5: General view of $^{13}C/^{12}C$ variations in natural compounds (IAEA, 2001).

Based on this comparison, in 1983, an International Atomic Energy Agency (IAEA) panel adopted this new standard to define the new VPDB (Vienna PDB) scale as:

$$\delta^{13}C_{NBS19\,/\,VPDB} = +1.95‰ \quad \text{.....2.14}$$

Soil CO_2 is important in establishing the dissolved inorganic carbon content of groundwater. After dissolution of this CO_2 the infiltrating rainwater can dissolve the soil limestone (Figure 2.6):

$$CO_2 + H_2O + CaCO_3 \rightleftharpoons Ca^{2+} + 2HCO_3^- \quad \text{.....2.15}$$

Because limestone generally is of marine origin ($\delta^{13}C \approx +1‰$), this process results in $\delta^{13}C$ of the dissolved bicarbonate of about −11 to −12‰ (in temperate climates) (IAEA, 2001). In soil, the HCO_3^- first formed exchanges with the often-present excess of gaseous CO_2, ultimately resulting in $\delta^{13}C$ (HCO_3^-) = $\delta^{13}C$ (soil CO_2) + $^{13}\varepsilon_{b/g} \approx -25‰ + 9‰ = -16‰$ (White, 2015). Consequently, $\delta^{13}C$ (HCO_3^-) values in the range of −11 to −12‰ are observed in soil water as well as in fresh surface water such as rivers and lakes (IAEA, 2001; Staddon, 2004). In surface water, such as lakes ^{13}C enrichment of dissolved inorganic carbon (DIC) can be caused by isotope exchange with atmospheric CO_2 ($^{13}\delta \approx -7.5‰$), ultimately resulting in values of $\delta^{13}C + {}^{13}\varepsilon_{b/g} = -7.5‰ + 9‰ = +1.5‰$, identical to oceanic values (IAEA, 2001). Consequently, freshwater carbonate minerals may have "marine" $\delta^{13}C$ values. In these cases, the marine character of the carbonate is to be determined by $\delta^{18}O$. In addition to HCO_3^-, natural waters contain variable concentrations of CO_2 with the effect that the $\delta^{13}C$ value of DIC is lower than that of the bicarbonate fraction alone: in groundwater (Seki *et al.,* 2010; White, 2015), and in streams and river waters derived from groundwater (Figure 2.6), the $\delta^{13}C$ (DIC) values are generally in the range of −11 to −16‰ (White, 2015).

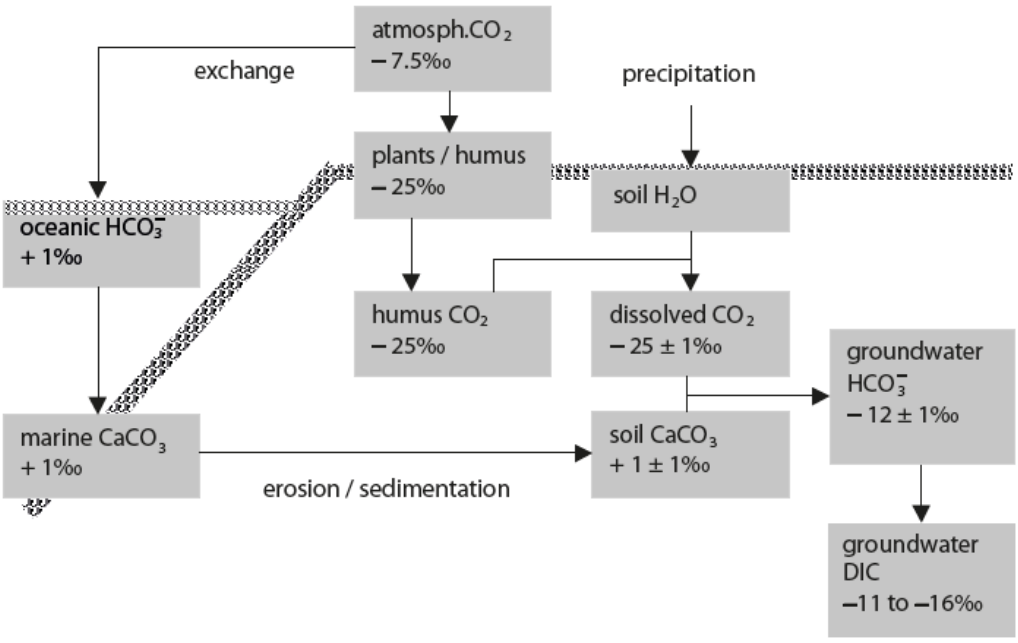

Figure 2.6: Schematic representation of the formation of dissolved inorganic carbon in groundwater from soil carbonate and soil CO_2 (White, 2015).

Plant carbon has a lower ^{13}C content than the atmospheric CO_2 from which it was formed. The fractionation which occurs during CO_2 uptake and photosynthesis depends on the type of plant and the climatic and ecological conditions. The dominant modes of photosynthesis give rise to strongly differing degrees of fractionation (IAEA, 2001; White, 2015). The Hatch-Slack photosynthetic pathway (C4) results in $\delta^{13}C$ figures between −10 to −15‰ and is primarily represented by certain grains and desert grasses (sugar reed, corn) (Scholl *et al.,* 2002). Generally, in temperate climates, plants employ the Calvin mechanism (C3), producing $\delta^{13}C$ values in the range of −26 ± 3‰ (Scholl *et al.,* 2002). A third type of metabolism, Crassulacean Acid Metabolism (CAM) produces a large spread of $\delta^{13}C$ values around −17‰ (Deines, 1980). The CO_2 content of the soil atmosphere can be in orders of magnitudes larger than that of the free atmosphere. The additional CO_2 is formed in the soil by the decay of plant remains and root respiration, and consequently has $\delta^{13}C$ values centring around −25‰ in temperate climates where Calvin plants dominate (Deines, 1980).

2.7.2 Stable Oxygen Isotopes

Oxygen has three stable isotopes, ^{16}O, ^{17}O and ^{18}O, with abundances of 99.76, 0.035 and 0.2%, respectively (IAEA, 2001; Mook, 2006). The observation of ^{17}O concentrations provides little information on the hydrological cycle in the strict sense above, which can be gained from the more abundant and, consequently, most accurately measurable ^{18}O variations. Therefore, the focus of attention here is on the $^{18}O/^{16}O$ ratio (≈ 0.0020). Values of $\delta^{18}O$ show natural variations within a range of almost 100‰ (Mook, 2006). ^{18}O is often enriched in (saline) lakes subjected to a high degree of evaporation, while high-altitude and cold climate precipitation, especially in the Antarctic, is low in ^{18}O (Figure 2.7) (White, 2015). Generally, in the hydrological cycle in temperate climates, $^{18}\delta$ does not exceed 30‰ (Mook, 2006; White, 2015).

Originally $^{18}O/^{16}O$ of an arbitrary water sample was (indirectly, via a local laboratory reference sample) compared to that of average seawater, the Standard Mean Ocean Water (SMOW). This SMOW in reality never existed. Measurements on water samples from all oceans by IAEA (2001) were averaged and referred to a truly existing reference

sample, NBS1, that time available at the US National Bureau of Standards (NBS). In this way the isotope water standard, SMOW, became indirectly defined by Craig (1961) as:

$$\delta^{18}O_{NBS1\,/\,SMOW} = -7.\,94‰ \quad \text{.....2.16}$$

The IAEA Section of Isotope Hydrology, in Vienna, Austria and the US National Institute of Standards and Technology (NIST, the former NBS) now have available for distribution batches of well-preserved standard mean ocean water for use as a standard for ^{18}O as well as for ^{2}H. This standard material, VSMOW, prepared by Craig (1961) to equal the former SMOW as closely as possible both for $\delta^{18}O$ and $\delta^{2}H$, had been decided by an IAEA panel in 1976 to replace the original SMOW in fixing the zero point of the $\delta^{18}O$ scale. All water samples are to be referred to this standard. From an extensive laboratory inter-comparison, it became clear that the difference between the early SMOW and the present VSMOW is very small (IAEA, 1977), probably:

$$\delta^{18}O_{SMOW\,/\,VSMOW} = +0.05‰ \quad \text{..... 2.17}$$

At present two standard materials are available for reporting $\delta^{18}O$ values, one for water samples, and one for carbonates. This situation arises from the practical fact that neither the isotope measurements on water nor those on carbonates are performed on the original material itself, but are made on gaseous CO_2 reacted with or derived from the sample. The laboratory analysis of $^{18}O/^{16}O$ in water is performed by equilibrating a water sample with CO_2 of known isotopic composition at 25°C, followed by mass spectrometric analysis of this equilibrated CO_2 (Mook and de Vries, 2001; White, 2015).

The transformation of atmospheric water vapour to precipitation depends on so many climatological and local factors, thus the $\delta^{18}O$ variations in precipitation over the globe are very large. Generally, the more negative $\delta^{18}O$, the further the rain is removed from the main source of the vapour in equatorial regions. In the Arctic and Antarctic, $\delta^{18}O$ of ice can be as low as –50‰.

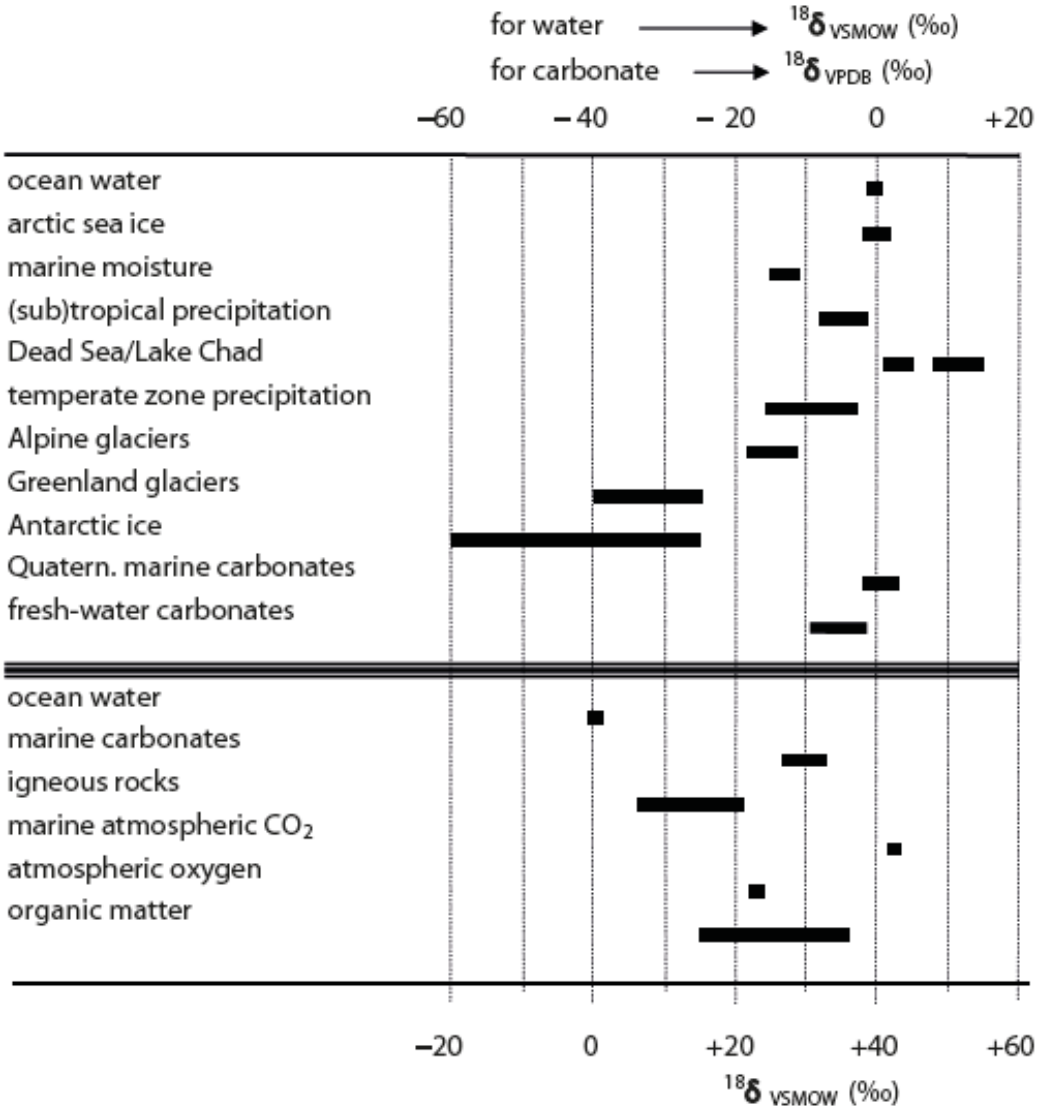

Figure 2.7: Variations of $^{18}O/^{16}O$ in natural compounds (IAEA, 2001).

The following effects cause regional and temporal variations on $\delta^{18}O$ of precipitation (IAEA, 2001; Mook, 2006):

a) Latitudinal effect, with lower $\delta^{18}O$ values at increasing latitude.
b) Continental effect, with more negative $\delta^{18}O$ values for precipitation the more inland.
c) Altitude effect, with decreasing $\delta^{18}O$ in precipitation at higher altitude.
d) Seasonal effect (in regions with temperate climate), with more negative $\delta^{18}O$ values during winter.

e) Amount effect, with more negative $\delta^{18}O$ values in rain during heavy storms.

2.7.3 Stable hydrogen isotopes

Hydrogen consists of two stable isotopes, ^{1}H and ^{2}H (D or Deuterium), with an abundance of about 99.985 and 0.015% and an isotope ratio $^{2}H/^{1}H \approx 0.00015$ (IAEA, 2001; Mook, 2006). Hydrogen, which is primarily present as water, but also as H_2, H_2S and CH_4, can be lost from magmas during degassing (Mook and de Vries, 2001; Mook, 2006). However, basaltic larva which erupts beneath a kilometer or more of ocean retain most of their dissolved water. Thus, mid-ocean ridge basalts and basaltic larva which erupt on seamounts are important sources of information of the abundance and isotopic composition of hydrogen in the mantle (Mook and de Vries, 2001; White, 2015). This isotope ratio has a natural variation of about 250‰, higher than the $\delta^{13}C$ and $\delta^{18}O$ variations, because of the relatively large mass differences between the isotopes. As with ^{18}O, high ^{2}H, concentrations are observed in strongly evaporated surface waters, while low ^{2}H contents are found in polar ice (Figure 2.8) (IAEA, 2001).

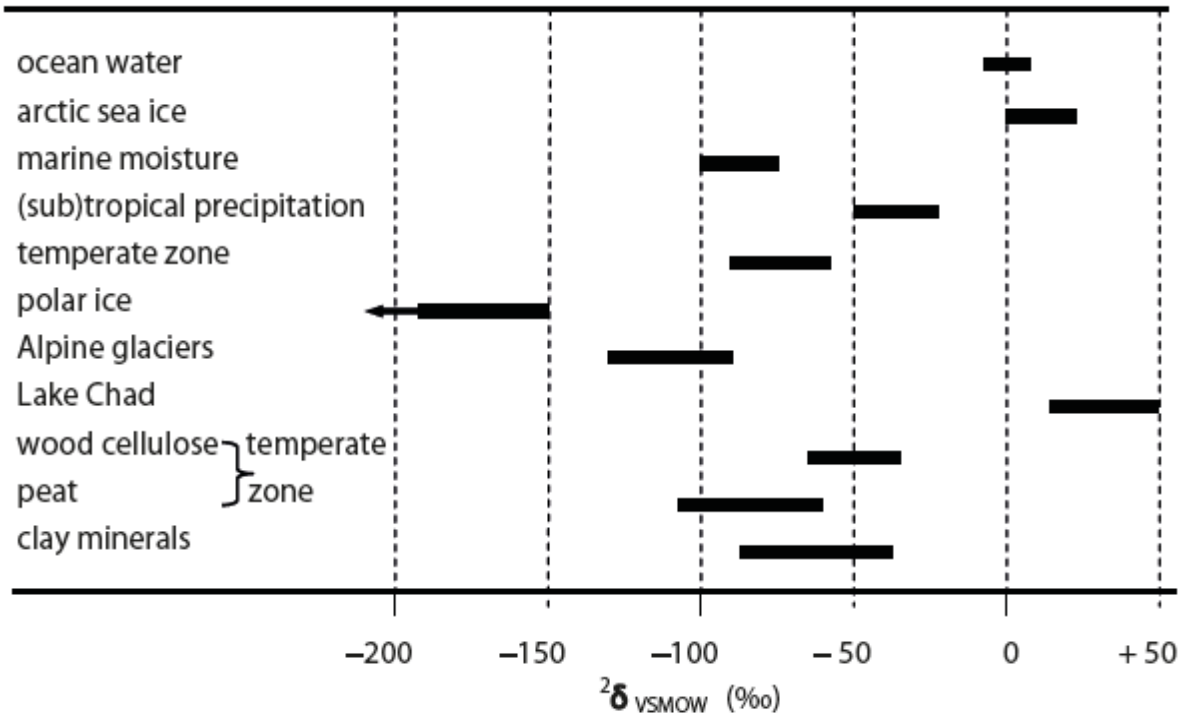

Figure 2.8: Variations of $^{2}H/^{1}H$ in natural compounds (IAEA, 2001).

VSMOW is the standard for $^{2}H/^{1}H$ as it is for $^{18}O/^{16}O$ ratios. The IAEA (2001) reported values for the absolute $^{2}H/^{1}H$ ratio of VSMOW and standard light Antarctic precipitation (SLAP) are reported to be $(155.76 \pm 0.07) \times 10^{-6}$ and $(89.02 \pm 0.05) \times 10^{-6}$; $(155.75 \pm 0.08) \times 10^{-6}$ and $(89.12 \pm 0.07) \times 10^{-6}$; and $(155.60 \pm 0.12) \times 10^{-6}$ and $(88.88 \pm 0.18) \times 10^{-6}$, respectively (White, 2015). The average $\delta^{2}H$ value of the secondary standard SLAP on the VSMOW scale consequently is −428.2 ± 0.1‰. Based on these data the $\delta^{2}H$ value has been defined as:

$$\delta^{2}H_{SLAP\ /\ VSMOW} = -428.0‰ \quad \text{.....2.17}$$

No significant difference in $\delta^{2}H$ has been detected between the original SMOW standard and VSMOW (IAEA, 2001). Henceforth, all $\delta^{2}H$ values will be reported relative to VSMOW. The relationship found between the $\delta^{2}H$ and $\delta^{18}O$ values of precipitation from various parts of the world is given in equation 2.17 (Craig, 1961; Dansgaard, 1964).

$$\delta^{2}H = 8\ \delta^{18}O + 10‰ \quad \text{.....2.18}$$

This relation, shown in Figure 2.9, has become known as the Global Meteoric Water Line (GMWL) and is characterised by a slope of 8 and a certain intercept with the ^{2}H axis (referring to the $\delta^{2}H$ value at $\delta^{18}O = 0‰$). The general equation of the meteoric water line (MWL) is:

$$\delta^{2}H = s \times \delta^{18}O + d \quad \text{.....2.19}$$

Where the slope (s = 8), as explained by the ratio between the equilibrium isotope fractions of hydrogen and oxygen for the rain condensation process, d is referred to as the deuterium excess (d-excess), the intercept of the line with the $\delta^{2}H$ axis. In several regions of the world, as well as during certain periods of the year and even certain storms, the $\delta^{2}H$ value is different from 10‰, depending on the humidity and temperature conditions in the evaporation region (IAEA, 2001; Mook and de Vries, 2001). The isotopic composition of water vapour over sea water with $\delta^{2}H = \delta^{18}O = 0‰$ vs VSMOW is somewhat lighter than would follow from isotopic equilibrium with the water: the evaporation is a non-equilibrium (partly kinetic) process. However, from the observed vapour composition onward the vapour and precipitation remain in isotopic equilibrium, because the formation of precipitation is likely to occur from saturated vapour (i.e. vapour

in physical equilibrium with water). Consequently, the $\delta^{18}O$ and $\delta^{2}H$ values both move along the meteoric water line (IAEA, 2001; Mook and de Vries, 2001).

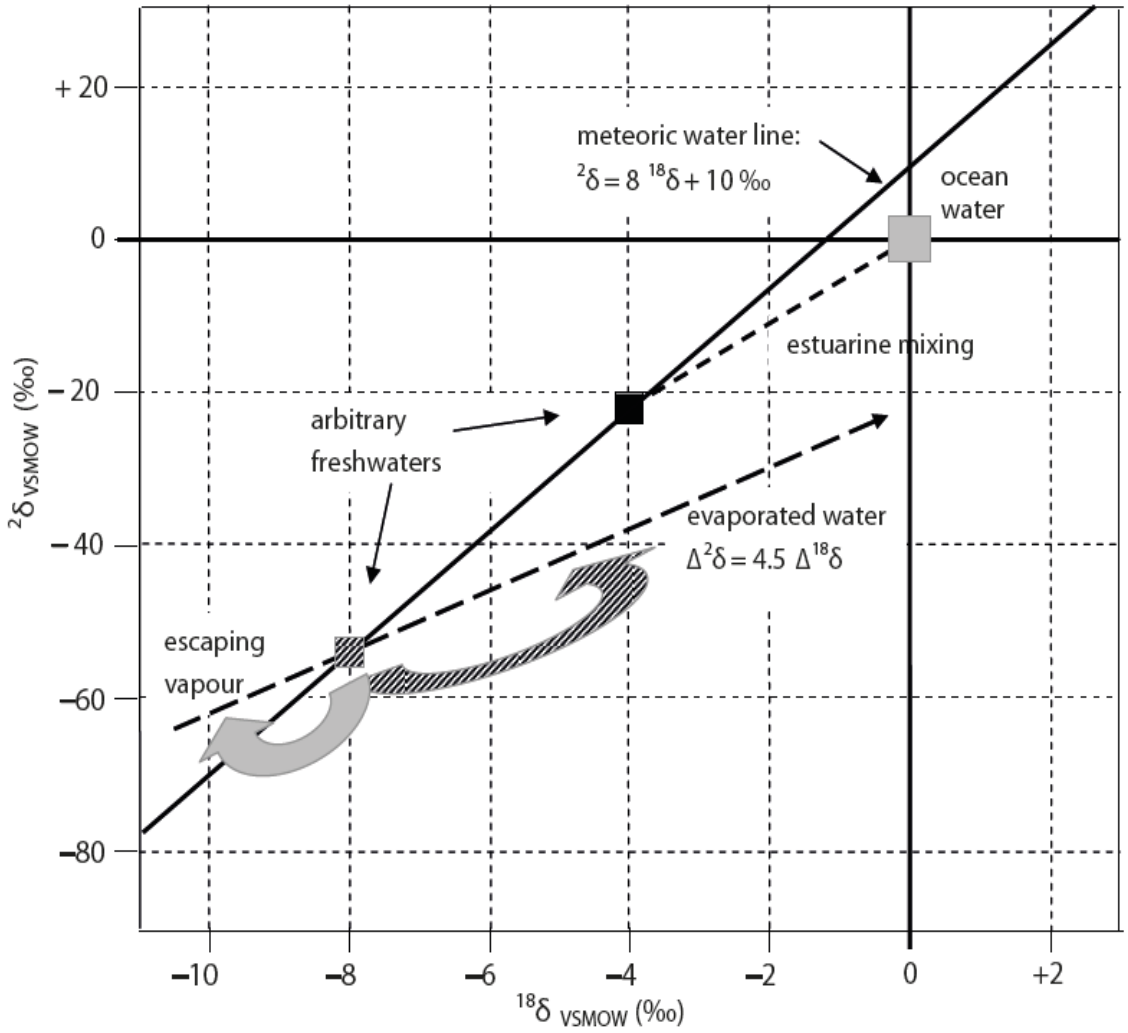

Figure 2.9: Relation between $\delta^{18}O$ and $\delta^{2}H$ for evaporating surface water (IAEA, 2001).

2.8 Radioactive isotopes of Carbon and Hydrogen

2.8.1 Radioactive carbon isotope

The natural occurrence of the radioactive carbon isotope, ^{14}C or radiocarbon, was first recognised by (IAEA, 2001). It is naturally formed in the transitional region between the stratosphere and troposphere about 12 km above the earth's surface through the nuclear reaction:

$$^{14}N + n \rightarrow {}^{14}C + p \quad \ldots\ldots 2.20$$

Where ^{14}N - atmospheric nitrogen, n – thermal neutron, p – proton.

The thermal neutrons required are produced by reactions between very high-energy primary cosmic ray protons and molecules of the atmosphere. The ^{14}C thus formed very soon oxidises to ^{14}CO, and ultimately to $^{14}CO_2$ which mixes with the inactive atmospheric CO_2 (Figure 2.10) (White, 2015). Through exchanges with oceanic dissolved carbon (primarily bicarbonate), most $^{14}CO_2$ molecules enter the oceans and living marine organisms. Some are also assimilated by land plants, so that all living organisms, vegetables as well as animals, contain ^{14}C in concentrations about equal to those of atmospheric CO_2. ^{14}C decays according to:

$$^{14}C \rightarrow {}^{14}N + ß^{-} \ldots\ldots 2.21$$

With a maximum $ß^-$ energy of 156 keV and a half-life of 5730 ± 40 years (Godwin, 1962).

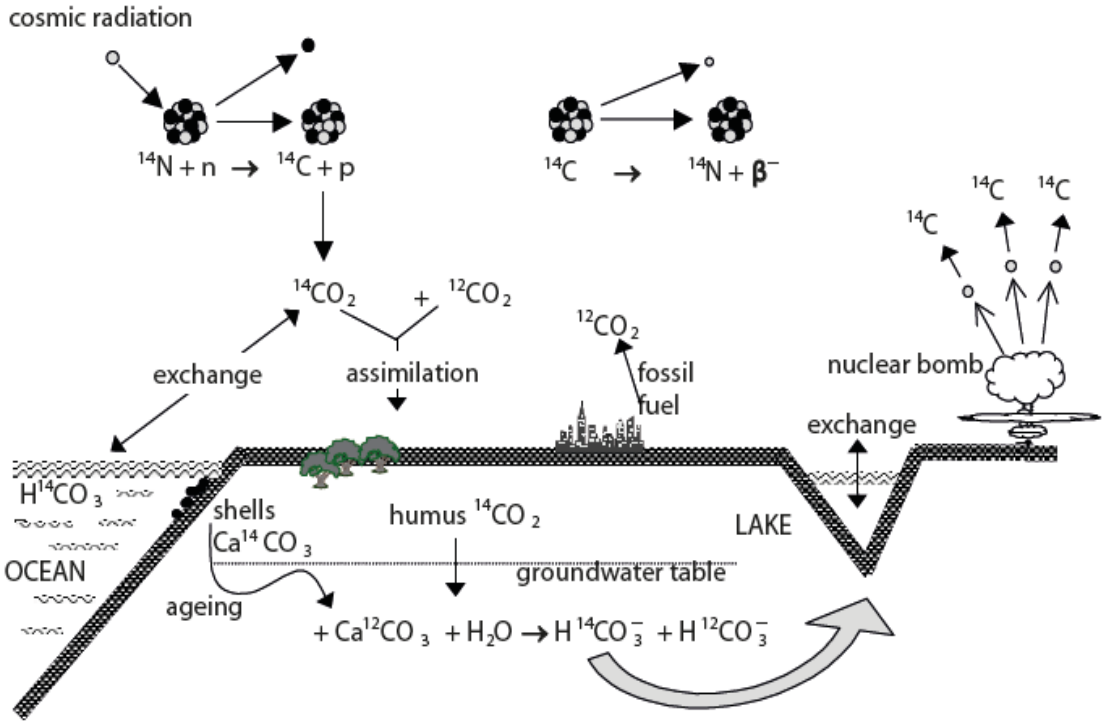

Figure 2.10: Origin and distribution of ^{14}C in nature (White, 2015).

The production and distribution of ^{14}C in nature occur through a series of chemical and biological processes which have become stationary throughout much of geologic time. Therefore, the concentration of ^{14}C in the atmosphere, oceans and biosphere reached a steady-state value which has been almost constant during a geological period which is long, compared to the life span of a ^{14}C nucleus (Staddon, 2004; Ehleringer *et al.,* 2005). This natural concentration, $^{14}C/C$, is of the order of 10^{-12}, which is equivalent to a specific activity of about 0.25 Bq/gC (disintegrations per second per gram of carbon).

Through the processes of erosion and re-sedimentation, fossil carbonate is generally part of terrestrial soils. Here it may be dissolved by the action of soil-CO_2, which is contained by the infiltrating rain water. In this way, the dissolved inorganic carbon in groundwater also contains ^{14}C (IAEA, 2001). The longer the carbonate in groundwater, thus without ^{14}C (^{14}a = 0%) — generally, but not always — the bicarbonate resulting from the reaction (eqn. 2.14) will have a ^{14}C content that is one half that of the CO_2 (^{14}a = 50%).

Isotopic exchange with soil CO_2 or atmospheric CO_2 leads to higher ^{14}C concentrations of the inorganic carbon fraction of recent groundwater, in combination with respectively decreased or increased $^{13}\delta$. This increases the level of ^{14}C in atmospheric CO_2 since 1963, and can lead to ^{14}C contents in soil organic matter and soil CO_2, which even the natural atmospheric value (IAEA, 1977; Staddon, 2004).

2.8.2 Radioactive hydrogen isotope

The radioactive isotope of hydrogen, ^{3}H (tritium or T), originates from a nuclear reaction between atmospheric nitrogen and thermal neutrons (IAEA, 2001):

$$^{14}N + n \rightarrow {}^{12}C + {}^{3}H \quad \text{.....2.22}$$

The ^{3}H thus formed enters the hydrologic cycle after oxidation to $^{1}H^{3}HO$ (Figure 2.11). According to a recent re-evaluation (IAEA, 2001), a preferable value is 4500 ± 8 days (approximately 12.32 years).

Owing to the nuclear reaction in eqn. 2.20 has a lower probability than the reaction in eqn. 2.22, the residence time of ^{3}H in the atmosphere is much smaller than that of ^{14}C, and the natural ^{3}H concentration in the air is much smaller than that of ^{14}C. Therefore, natural ^{3}H abundances are either presented as specific activities in Bq per litre of water or in Tritium

Units (TU), the latter is equivalent to a concentration of $^{3}H/^{1}H = 10^{-18}$ (1 TU = 3.19 pCi/L = 0.118 Bq/L) (White, 2015).

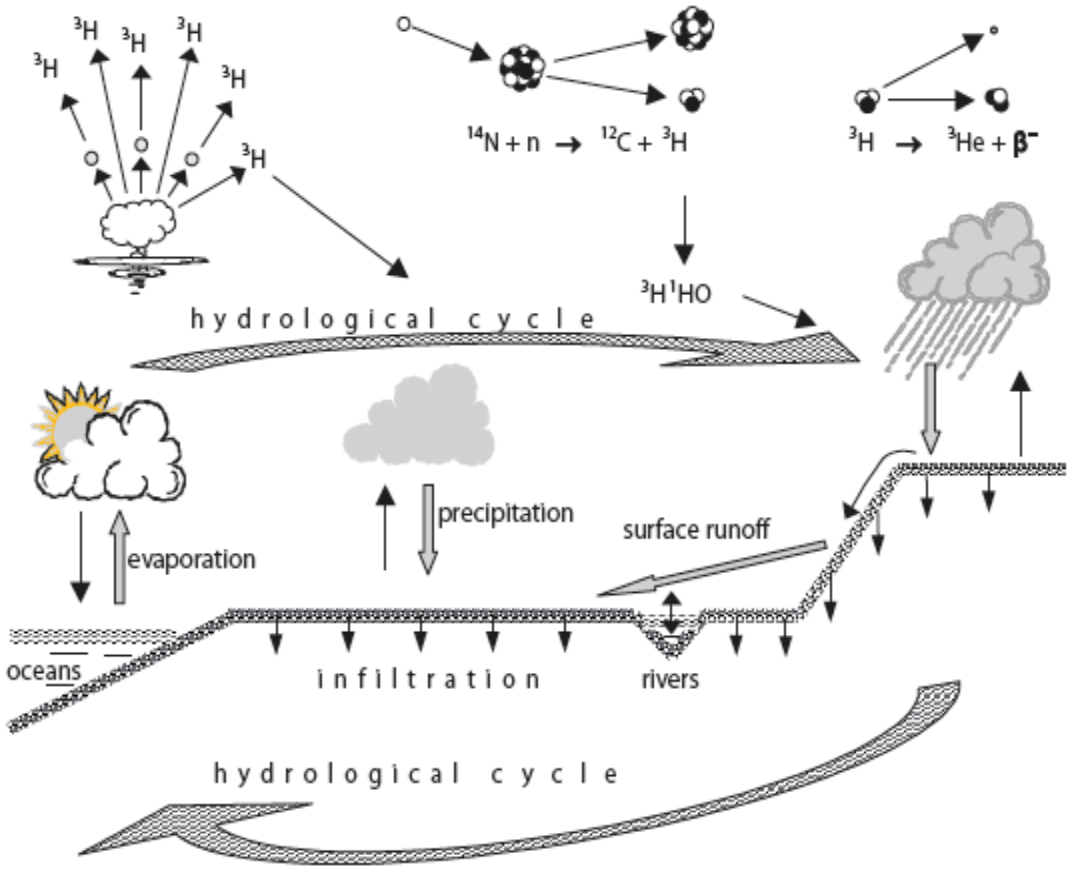

Figure 2.11: Origin and distribution of ^{3}H in nature (White, 2015).

Under undisturbed natural conditions the ^{3}H concentration in precipitation is probably about 5 TU, which is equivalent to a specific activity of about 0.6 Bq/L. A large part of the ^{3}H (as well as ^{14}C) produced by the nuclear explosions is injected into the stratosphere and returns to the troposphere each year during spring and early summer (Mook, 2006). This causes seasonal variation in both ^{3}H and ^{14}C, more pronounced in the former, because the residence time of H_2O to which ^{3}H is coupled with the atmosphere is very small (in the order of weeks). The probability of contamination of young groundwater by bomb ^{3}H prevents the water to be simply dated by measuring the degree of ^{3}H decay. Nevertheless, ^{3}H data can often be used to determine dates ante quem or post quem

(Mook, 2006). For instance, water with $^{3}H < 5$ TU must have a mean residence time of more than 40 years; water having $^{3}H > 20$ TU must date from after 1961 (IAEA, 1977).

2.9 Groundwater Dating

Dating groundwater determines the age of groundwater; that is, the time elapsed since the water became groundwater, in other words, from the time it infiltrates the soil as precipitation or any other type of surface water (rivers, lakes) (Mook, 2006). Numerous methods exist for age dating groundwater, including chlorine-36 (^{36}Cl), krypton-85 (^{85}Kr), carbon-14 (^{14}C), chlorofluorocarbon (CFC), tritium (^{3}H) among others (Fontes, 1992). For this study, carbon-14 (^{14}C) and tritium (^{3}H) are the proposed methods and therefore discussed below. Although, the main challenge is the unknown isotopic values at the initial time of infiltration for ^{3}H and ^{14}C, the combination of ^{14}C and ^{3}H in groundwater will simply measure the age of groundwater, i.e. the period of time elapsed since the infiltration of the water. Hence, ^{14}C and ^{3}H together certainly offer the possibility to set limits to absolute ages rather than the apparent ages, especially in combination with hydrogeological and hydrochemical evidence.

2.9.1 Radiocarbon (^{14}C)

Radiocarbon dating of groundwater gives indication to when the water was taken out of contact with the atmosphere; that is, when it went underground. However, there are uncertainties regarding the calculation of the percentage of carbonate species that originated from living plants in the aquifer outcrop and the atmosphere, as opposed to that added by ancient carbonaceous deposits in the aquifer matrix (Mook, 2006; Moran, 2007). For this reason, radiocarbon dating of groundwater is most useful when repeated sampling occurs. In this case, obtaining absolute ages with their attendant uncertainties are not the primary numbers used in site interpretations (Fontes, 1992). The uncorrected apparent ages are the primary numbers; they are used to compare with other apparent ages in the study. This largely obviates the correction uncertainty. In all cases, the most useful data comes from these comparisons and not from absolute ages. Hence, the uncorrected apparent ages can be interpreted as maximum ages; that is, the real age of the groundwater is equal to or less than the apparent age. By extracting the carbonates of the water for radiocarbon dating, the measurements can provide information on the

recharge of underground deposits as well as flow directions and rates. This is valid for samples from 10 years old to 40,000 years old (Mook, 2006).

The basic radiocarbon age determination, calculation is as follows:

$$t = - 8035 \ln (\delta^{14}C_{final} / \delta^{14}C_{initial}) \quad \text{.....2.23}$$

Where, t = the radiocarbon age of the sample; 8035 = the decay constant of radiocarbon, i.e., the half-life divided by ln 2. A half-life of 5568 years for carbon 14 is used, as per international convention; ln = the natural logarithm; $\delta^{14}C_{final}$ = the measured net radiocarbon content of the sample; $\delta^{14}C_{initial}$ = the net radiocarbon content of the modern standard.

The results of radiocarbon dating of ground water are presented as three items:

- The “apparent age” gives the simple measurement age of the groundwater, from the above formula, before the carbon dilution correction would be applied. The apparent age is used as the reference value in sequential sampling studies because the carbon dilution correction is in only one direction, making the age younger, the apparent or reference age should be taken as a maximum age of the groundwater sample.
- The carbon-13 value is used for the estimation of the carbon dilution factor, leading to a corrected age or “best estimate age.”
- The “best estimate age” is the age obtained after the carbon dilution correction. It should not be used for further calculations or quantitative interpretations since the veracity of the carbon dilution correction cannot be verified. The best estimate age is only intended to present easily visualised results. The apparent age is the best reference and is used for all comparative studies (Mook, 2006; Moran, 2007).

2.9.2 Tritium (^3H)

Tritium concentrations are measured in tritium units (TU) where 1 TU is defined as the presence of one tritium in 10^{18} atoms of hydrogen (H) (Mook, 2006). In the earth, small amounts of natural tritium are produced by alpha decay of lithium-7 (Mook, 2006). Natural atmospheric tritium is also generated by secondary neutron cosmic ray bombardment of nitrogen, which then decays to carbon-12 and tritium (eqn. 21). Tritium atoms then combine with oxygen, forming water that subsequently falls as precipitation. Prior to

atmospheric nuclear bomb testing in the 1950s, tritium natural average concentrations ranged from approximately 2 to 8 TU. Approximately 1.13 x 10^9 TU were added in the northern hemisphere from atmospheric nuclear bomb testing with the largest tritium concentrations peaking in 1963 (Mook and de Vries, 2001). Since the cessation of atmospheric nuclear tests, tritium concentrations have dropped to between 12 and 15 TU, although small contributions from nuclear power plants occur (Mook, 2006). This is because most tritium is disseminated in the environment as water, it enters the hydrologic cycle as precipitation and eventually becomes concentrated at levels detectable in groundwater (Moran, 2007).

Groundwater tritium concentrations reflect atmospheric tritium levels when the water was last in contact with the atmosphere, tritium can be used to date groundwater recharge. Given that TU values vary both spatially and temporally, it is important to establish the closest precipitation measurement point to provide a reference to estimate groundwater recharge and travel times (Mook, 2006). Groundwater age estimation using tritium only provides semi-quantitative, “ball park” values:

- <0.8 TU indicates sub modern water (prior to 1950s)
- 0.8 to 4 TU indicates a mix of sub modern and modern water
- 5 to 15 TU indicates modern water (<5 to 10 years)
- 15 to 30 TU indicates some bomb tritium (Clark and Fritz, 1997)

In the period of three half-lives (1963 to 2000), tritium concentrations have been reduced by a factor of 8 (Mook, 2006; Moran, 2007). With no further atmospheric nuclear weapons testing, tritium will continue to drop to near natural background levels. Therefore, usage of tritium for the age dating groundwater recharge will soon be obsolete (Moran, 2007). Several studies such as IAEA, 2011; Abiye, 2013; Labasque *et al*., 2014; Visser *et al*., 2014, 2016 and Duvert *et al*., 2016 still find the relevance/usefulness in the use of titium particularly for deep groundwater despite its limitation. It is however advisable to use tritium together with any other dating method for better result.

2.9.3 Tritium-Helium-3 (^{3}He) Method

Tritium decays to ^{3}He by beta particle emission and knowing this decay rate allows for a more accurate shallow groundwater recharge age. T/^{3}He ratios are useful for

groundwater ages ranging from several months to about 30 years (but no further out than about 50 years) (Mook, 2006). T/^{3}He ratios have an accuracy of one to three years (Clark and Fritz, 1997). Groundwater ages can be estimated using the following equation:

Groundwater Age (in years) = –17.8ln (1+ $^{3}He_{trit}/^{3}H$) ……2.24

Where:

- $^{3}He_{trit}$ = component of ^{3}He from the decay of tritium corrected for other ^{3}He sources such as the Earth's atmosphere, small contributions from spontaneous fission of lithium-6, and from uranium and thorium decay.
- ^{3}H = tritium concentration in TU.

^{3}He is also present within the mantle, in the ratio of 200 to 300 parts of ^{3}He to a million parts of ^{4}He, ratios of ^{3}He/^{4}He more than atmospheric concentrations are indicative of a contribution of ^{3}He from the mantle (Moran, 2007). This commonly occurs in geothermal areas and crystalline crustal sources dominated by ^{4}He, which is produced by the decay of radioactive elements in the crust and mantle (Mook, 2006). Therefore, in terrains other than alluvial terrain, terrigenic-produced helium may give anomalous results (Moran, 2007).

2.10 Reviews on applications of isotopic compositions in ecosystem

Craig (1963) presented evidence from many geothermal areas that show that thermal waters undergo a progressive ^{18}O-enrichment with respect to the GMWL, as a result of water-rock oxygen exchange, and that δD value remain relatively constant throughout this process. Qin *et al*. (2005) showed that the stable isotopic compositions of the Xi'an geothermal waters are of meteoric origin. Comparison of the δ^{2}H values of geothermal waters with those of cold groundwaters shows that:

- Deuterium is about 10–20‰ more depleted in geothermal waters than cold ground water, showing distinct differences in the recharge area. The geothermal waters are recharged from a higher elevation in the Qinling Mountains; and
- Both the geothermal and shallow waters show an oxygen shift with similar δ^{2}H values, suggesting a common source and area of recharge, but also that the waters have travelled for different distances (Qin *et al.,* 2005).

A significant oxygen isotope shift, as compared to cold groundwater, could be a result of several processes, including oxygen-18 exchange between water and calcite or silicate minerals, or cooling of much deeper geothermal waters that have already undergone strong ^{18}O exchange at higher temperatures (Qin *et al.,* 2005). This may reflect the hydraulic isolation between the shallow and deep geothermal aquifers caused by the presence of aquitards (Tao, 1995). Water in deeper aquifers probably have longer residence times, higher temperatures and lower flow rates than shallow groundwaters. In addition, the stable isotope values for geothermal waters are different from those of the karstic groundwaters, indicating that the geothermal system is not recharged by water from the surrounding mountain (Qin *et al.,* 2005). Giggenbach (1992) showed a positive shift in both $\delta^{18}O$ and δD with respect to the local meteoric composition in several thermal areas, ascribed to mixing of local meteoric and andesitic (magmatic) waters.

Abiye *et al*. (2011) outlined that environmental isotopes of oxygen and hydrogen such as $\delta^{18}O$, $\delta^{2}H$ and ^{3}H have been widely used to gain some insight into the subsurface flow and recharge condition in the complex hydrogeological setting of the Johannesburg area. Their study's objective was to spatially characterise the impact of mining operation on groundwater quality which targeted to follow its hydrogeochemical footprint in different aquifer systems in the Johannesburg-Pretoria area. They concluded that environmental isotope signals for the acid mine decant showed an average value of -5.6‰ for $\delta^{18}O$, -22.0‰ for $\delta^{2}H$, and 1.8 T.U. for ^{3}H, which implies that the water is discharged from deep circulating groundwater from wider hydrogeological basin or mixing of different water recharged at different times/seasons.

Another study in the Lake Nyos catchment Northwest Cameroon was carried out (Kamtchueng *et al*., 2015). This research was aimed at using multi-environmental tracers (isotopes of oxygen and deuterium, tritium, sulphur fluoride (SF), and chlorine (Cl)) to determine the origin, apparent age and recharge mechanism of shallow groundwater in the Lake Nyos catchment. The equilibration method for oxygen-18 and the chromium reduction method for hydrogen was used to analyse isotope ratios for the samples.

A comprehensive study by Pang *et al*. (2006) on the isotopic composition (^{2}H, ^{18}O, ^{13}C and ^{3}H) of geothermal water and local groundwater in East Asia and Pacific region such

as China, India, Indonesia, Korea, Malaysia, Pakistan, Philippines and Thailand showed the following different types of geothermal water:

- Mixing of meteoric and Andesitic magmatic waters;
- Mixing of meteoric with sea water;
- Meteoric water heated by deep circulation;
- Mixing of a hotter and a colder component of meteoric water during Accent.

The differences in isotopic compositions of geothermal water and local groundwater show that although waters are of meteoric origin, the recharge area of the geothermal water can be different from that of the local groundwater (Pang *et al.,* 2006). In case of Mae Hong Son area in Thailand, the recharge area of the geothermal water is estimated to be 200 m higher than that of the local groundwater. Hence, this implies that there are different recharge sources and circulation pathways.

Fry (2006) showed that the assessment of isotopic compositions in the biosphere allows characterisation and quantification of the bio-geochemical cycles and exploration of the food webs. Isotopic compositions of animals and plants are, however, also affected by the isotopic compositions of the nutrients and organic compounds forming the base of their food web (Gustafson *et al.,* 2007). Isotopic signatures reflect the extent and source of the nutrient contributions, pathways, marine or freshwater origins or through different sources of nutrient pollution (Gustafson *et al.,* 2007). Consequently, isotopic compositions of biological communities can vary with space and time. Most recently, the use of stable hydrogen isotope analyses (δD) to link organisms to broad geographic origin in North America was based on large scale isotopic contours of growing-season average δD value in precipitation. This was extremely useful in tracking the migration and movement of a wide number of animals from insects to birds and mammals (Hobson, 1999).

The stable isotope composition of marine food webs tends to be more enriched with several elements compared with terrestrial C_3 or freshwater biomes. Deuterium and ^{18}O are other stable isotopes that are typically more enriched in marine versus terrestrial systems (Schaffner and Swart 1991; Hobson, 1999) but their use in tracing sources of animal nutrition has been relatively limited due to analytical considerations. In terrestrial systems, the most important isotopic differentiation used to trace animal diets and origins

is that related to stable carbon isotopic fractionation associated with plant photosynthetic pathways responsible for distinct isotopic differences between C_3 and C_4, or Crassulacean acid metabolism (CAM) plants (Hobson, 1999). Within both terrestrial and marine biomes, the occurrence of point source pollutants or other anthropogenic sources of elements in food webs with distinct isotopic signatures offers another potential means of tracing feeding origin of organisms (Macko and Ostrom, 1994).

Studies by Merwe van der *et al*. (1990) and Vogel *et al*. (1990) aimed to develop a technique to fingerprint the source of ivory based on the expected differences among populations in their relative dependence on C_4 grasses, their use of arid regions, and their occurrence in areas of differing surficial geology. In contrast to grazers of C_4 grasses, woodland elephants consume primarily C_3 plants and have more negative $d^{13}C$ signatures. Those elephants feeding in dense tropical forests where plant-respired CO_2 can be recycled back into plants under the canopy (Merwe van der and Medina, 1989) showed even more negative $d^{13}C$ values (Merwe van der *et al.,* 1990).

CHAPTER THREE

METHODOLOGY

3.1 Preamble

This chapter presents the methods used in this research. It covers methods used during field sampling, sample preparation techniques, analytical methods, and methods used for data analysis and interpretation. This is a quantitative study which shows the relationship between the isotopic compositions of geothermal spring water, soil and vegetation. The study also investigates the trace metals availability in geothermal water, soil and vegetation and their potential health risks on the community members. The rainwater was sampled for a period of 12 months, which was used to generate the local meteoric line of the area. Data were collected in standard procedures and measured numerically for appropriate statistical analyses and interpretation.

3.2 Sampling

Sampling was carried out for a period of 12 months to accommodate two major seasons in the study areas. It was done once a month (thrice per season), specifically winter (dry) and summer (wet) seasons, to establish the seasonal effect on the parameters (Yahaya *et al.,* 2009). The geothermal spring water, rainwater, boreholes, surrounding soils and vegetation were sampled following the standard procedures and ensuring appropriate quality control. The geothermal spring waters were sampled for both physical and geochemical analyses which also included isotopic analyses. The rainwater samples were collected on a monthly basis for one hydrological year. At Siloam, the geothermal spring was sampled for a season because it dried up even till to date. In addition, four boreholes were sampled at Siloam (two of which were hot boreholes and others were tepid boreholes). Also, community tapwater was sampled from Siloam and Tshipise, which serves as control. The surrounding soil was sampled at depths of 10 cm, 30 cm and 50 cm for isotopic and trace metals analyses except for Siloam and Mphephu, where two points (10 and 30 cm) were used due to the rocky soil. Three surrounding plants were sampled at the study sites which included: Amarula tree (*Sclerocarya birrea*), Guava tree (*Psidium guajava*) and Mango tree (*Mangifera indica*) at Siloam; Acacia tree (*Acacia robusta*), Fig tree (*Ficus sycomorus*) and Amarula tree (*Sclerocarya birrea*) at Mphephu;

Amarula tree (*Sclerocarya birrea*), Lowveld mangosteen (*Garcinia livingstonei*) and Leadwood tree (*Combretum imberbe*) at Sagole; Sausage tree (*Kigelia Africana*), Amarula tree (*Sclerocarya birrea*) and Acacia tree (*Acacia robusta*) at Tshipise (Figure 3.1). Amarula is available in all the four study sites within the Soutpansberg region.

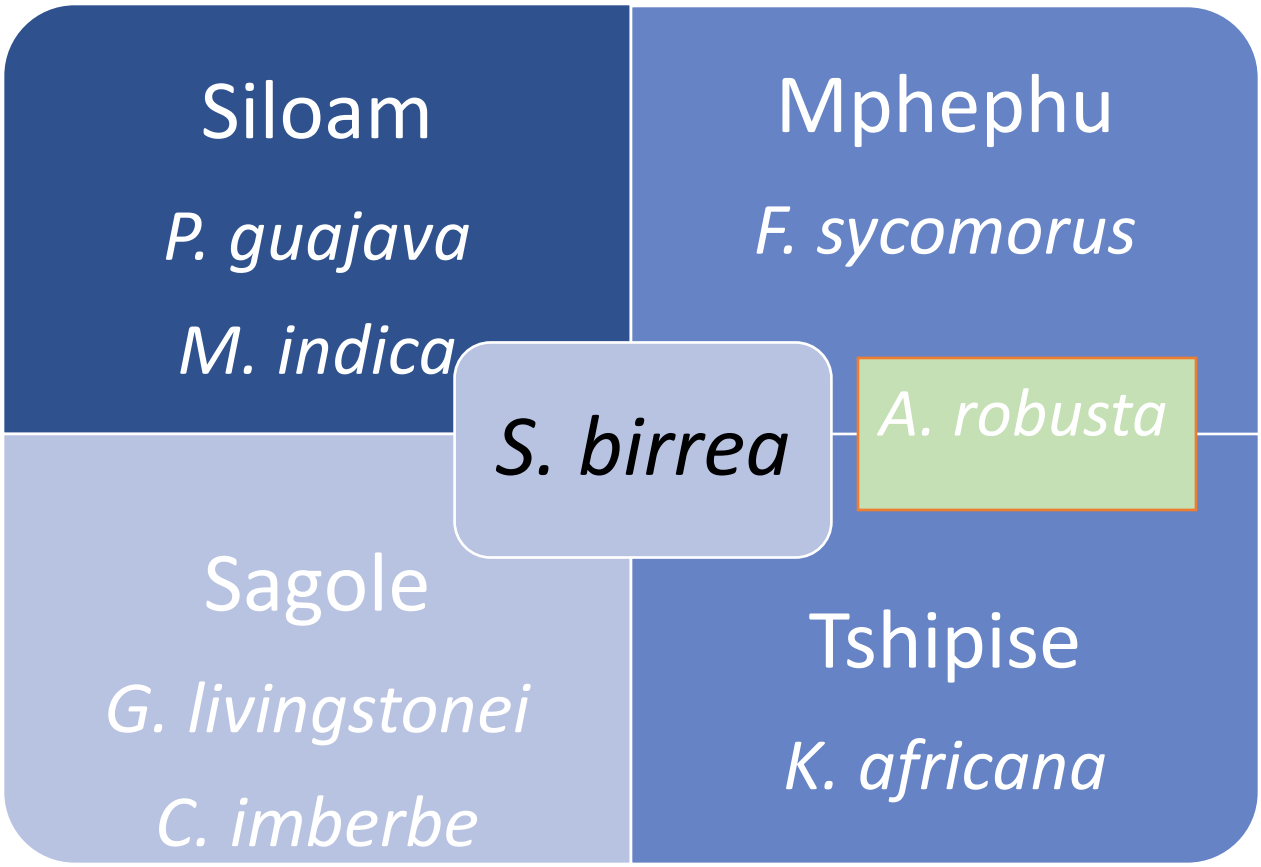

Figure 3.1: Selected indigenous plants within Soutpansberg region.

From each tree, three different parts were sampled: inner core (C), barks (B) and leaves (L). The root part of these plants was not sampled because permission was not given by the authority, hence, core (inner part) was sampled after getting the permission. Table 3.1 shows the number of samples collected for the study. Quality assurance/quality control (QA/QC) of field samples is incorporated into geothermal spring water, soil and vegetation sampling investigations to enhance sample integrity, increase the confidence of analytical data, and to prevent reporting values caused by contamination. Field blanks and splits were ensured for water samples, as well as rinse blanks and splits for soil samples and extract splits for the plant samples.

Table 3.1: Summary of samples and geographic coordinates of the sites

Study sites	Coordinates	Latitude (m)	Type of samples	No of samples per		
				trip	season	Total sample
Siloam	22° 52’ 58.80" S	835	Geothermal water	3	06	06
	30° 10’ 59.99" E		Surface soil (3 points)	3	06	06
			Sclerocarya birrea (C, B, L)	1	03	03
			Psidium guajava (C, B, L)	1	03	03
			Mangifera indica (C, B, L)	1	03	03
Mphephu	22° 54’ 26.28" S	890	Geothermal water	3	06	12
	30° 10’ 35.58" E		Surface soil	3	06	12
			Acacia robusta (C, B, L)	3	06	12
			Ficus sycomorus (C, B, L)	3	06	12
			Sclerocarya birrea (C, B, L)	3	06	12
Sagole	22°, 31’ 49.44" S	450	Geothermal water	3	06	12
	30°, 39’ 07.13" E		Surface soil	3	06	12
			Sclerocarya birrea (C, B, L)	3	06	12
			Garcinia livingstonei (C, B, L)	3	06	12
			Combretum imberbe (C, B, L)	3	06	12
Tshipise	22° 36’ 31.32" S	520	Geothermal water	3	06	12
	30° 10’ 20.71" E		Surface soil	3	06	12
			Kigelia Africana (C, B, L)	3	06	12
			Sclerocarya birrea (C, B, L)	3	06	12
			Acacia robusta (C, B, L)	3	06	12
UNIVEN	22° 58’ 40.12” S		Rainwater	1	12	12
	30° 27’ 04.25” E					
Total samples					123	213

Note C- core (inner part of the tree), B- bark and L- leaves

3.2.1. Water sampling

Geothermal spring water samples were collected from Mphephu, Sagole, Siloam and Tshipise springs, respectively, according to Mook and de Vries (2001). Water samples for stable isotope analysis were collected in glass bottles with poly-seal caps (caps with

conical plastic insert). In order to minimise the level evaporation and ion exchange as well as altering the sample's isotopic composition, oil was added to the samples. The glass bottles were rinsed properly with the spring water to avoid cross contamination.

Geothermal spring water samples for chemical analysis were obtained through random sampling, which involved taking water from every part of the spring with a plastic cup (Figure 3.2) (Harvey, 2000). The water samples were collected in 2 L plastic containers before transporting them to the laboratory for sample pre-treatment. The geothermal water samples were allowed to cool before pre-treatment and preservation in the laboratory.

The water sample codes are SGW and SGS; TSW and TSS; MPW and MPS in winter and summer for Sagole, Tshipise and Mphephu geothermal springs, respectively. Whereas at Siloam village, there is SAW – geothermal springs, SH1 and SH2 for thermal boreholes, BH1 and BH2 for tepid boreholes and SCC – community treated tap water. Also, TTP represents treated water from municipality at Tshipise.

Figure 3.2: Sampling the geothermal springs at Mphephu (A) and Sagole (B).

Rainwater samples were collected from May 2016 to April 2017 at the University of Venda, Thohoyandou (event based) (Table 3.2). ME01 to ME04 and ME12 were collected from May to August 2016 and April 2017 (winter/dry) while ME05 to ME11 were collected from September 2016 to March 2017 (summer/wet). The samples were collected by

attaching a funnel to a high-density polyethylene bottle and kept in an open place for direct collection of rainwater and immediately after the rain the bottle was unscrewed from the funnel and sealed with a plastic cone cap (Muhammad and Sadiq, 2014).

Table 3.2: Rainwater sample code and month collected

Sample Code	Month collected	Date	Year
ME01	May	26, 27	2016
ME02	June	22, 23	2016
ME03	July	07, 10	2016
ME04	August	16,17, 27	2016
ME05	September	10, 11	2016
ME06	October	22, 24	2016
ME07	November	13, 14	2016
ME08	December	05, 14	2016
ME09	January	28	2017
ME10	February	17	2017
ME11	March	03	2017
ME12	April	06, 07	2017

3.2.2 Soil sampling

Soil samples for chemical analysis were taken from the topsoil of depth 0-15 cm with an auger (Figure 3.3) and were put in a polypropylene sampling bag (Pleysier, 1995). All soil samples were then transported to the laboratory before sample pre-treatment.

Soil samples for isotopic analyses were collected from different depths simultaneously (10, 30 and 50 cm below the soil surface), by inserting a soil corer horizontally after digging open face soil pit to avoid any potential evaporation occurring where the soil was exposed. The soils were rapidly sealed in the glass vails (Martin-Gomez *et al.,* 2015) and the samples were placed on dry ice in the field before transporting them to the laboratory.

The soil sample codes are TSS, SGS, MPS and SMS for Tshipise, Sagole, Mphephu and Siloam, respectively. Although, seasonal variations of the composition were observed; 'W' stands for winter and 'S' stands for summer.

Figure 3.3: Sampling the surrounding soil of the geothermal spring at Tshipise.

3.2.3 Vegetation sampling

The simple random sampling procedure was adopted for plant sampling (Pleysier, 1995). The inner part of the tree (core) was taken from different species in the study areas using an increment borer (Goldsmith *et al.,* 2011). Core samples give a true reflection of stored water from other sources or time period (Goldsmith *et al.,* 2011). The samples were placed into an airtight plastic bag and conveyed to the laboratory. The leaves and bark were also sampled and placed in a tight plastic bag.

Vegetation sampling (core, leaves and barks) for chemical analyses were taken from the surrounding of geothermal spring sites in the study areas. The barks and leaves of the plants were sampled owing to their ability to accumulate trace metals from the soil (Pyle *et al.,* 1996 and Robinson *et al.,* 2008). The leaf samples were hand picked (Figure 3.4), and a representative sample was achieved by taking several sample units randomly and

combining them to form a composite sample. The bark samples were collected using a knife and core samples were collected using an increment borer. All plant samples were stored in polypropylene bags and transported to the laboratory before sample pretreatment.

Figure 3.4: Sampling the surrounding vegetation (A – Mango and B – Guava trees) of the geothermal springs at Siloam.

3.3 Sample Pre-treatment

3.3.1 Water samples

Rain and geothermal wate and borehole samples were preserved by adding mineral oil which serves as a barrier against evaporation. Mineral oil density is less than water, so the water sinks below the protective oil layer (Scholl *et al.,* 2002). The samples were kept in the refrigerator until extraction and analyses.

The water samples were not filtered, but they were acidified with (1:1) HNO_3 to pH <2 (normally, 2 ml of (1:1) acid per liter of water sample) (USEPA, 2004b). Preservation can be done at the point of collection, however, to avoid hazards of strong acids in the field, transport restrictions, and possible contamination, samples were transported to the laboratory after collection and were preserved using acid upon receipt in the laboratory. After, acidification, the samples were mixed, held for 16 hours, and then verified to have

a pH < 2 just prior to withdrawing an aliquot for processing or direct analysis. All water samples (rainwater, geothermal water and borehole) were kept at 4°C in the refrigerator at University of Venda (univen) until further analyses.

3.3.2 Soil and Vegetation samples

The samples (soils and vegetation) were held in airtight plastic container and were air dried in oven. The samples were ground to powder, then packed ready for analysis (Goldsmith *et al.,* 2011). All the samples were kept in cupboard at room temperature at univen awaiting further analyses.

The pre-treatment of soil samples was carried out according to SR ISO 11466:1999. The soil samples were air-dried by breaking down aggregates, spreading the soil on a polythene sheet at 25°C. The dried soil samples were ground and sieved through 100 µm sieves, then kept in sealed plastic bags (Figure 3.5) until analyses were conducted.

Figure 3.5: Packed soil and vegetation samples ready for analysis.

The pre-treatment of plant samples (core, barks and leaves) was carried out according to SR ISO 11466:1999. The core, bark and leaf samples were intensely rinsed with tap water

and ultrapure water, to eliminate soil and dust from the core, barks and leaves. Then, the samples were oven dried at 40°C, ground and then sieved through the 100 µm sieve. The samples were kept in sealed plastic bags until analyses were conducted.

3.4 Experimental Analyses

3.4.1 Digestion process

The water samples were not digested because they were acidified during the sample pre-treatment as recommended by USEPA (2004b). Samples were further diluted depending on the analyses to be carried out. For ICP-OES analysis (Major cations), there was no further dilution while there was 10 times dilution for ICP-MS analysis (15 trace elements).

The soil samples were digested using a microwave digestion system (SR ISO 11466: 1999) (Figure 3.6). Approximately 1.0 g of pre-treated samples were digested with 9 mL HNO_3 and 1 mL H_2O_2. The solutions were allowed to stay overnight at room temperature and then, placed in the microwave for 30 minutes, followed by cooling. The solutions were diluted to 50 mL with distilled water.

Figure 3.6: Microwave digester (A) and extracts after digestion process (B) at Agricultural Research Council (ARC) laboratory.

The vegetation samples (core, bark and leaves) were digested using Hot Block Method (NIOSH, 2003) (Figure 3.7). A total of 0.5 g ground samples was weighed and 14 mL of 16 M HNO_3 added. The solution was allowed to stay overnight at room temperature and then, was placed on the block digestion system at initial temperature of 80°C for 30 minutes, which was then increased at intervals of 10°C up to 120°C (Figure 3.7). Three to four drops of H_2O_2 were added and shaken for a few minutes, then allowed to cool for 20 minutes. Then, the solution was made up to 100 mL with de-ionised water and filtered with 15 mm size filter paper for ICP-MS analysis.

Figure 3.7: Block digestion set up (A) and the extracts (B) at the Agricultural Research Council (ARC) laboratory.

3.4.2 Saturated soil paste extraction

The saturated soil paste analysis was carried out according to Garltey (2011). The weight of the empty dish was noted and approximately 250 g of dried, sieved soil sample was added. Distilled water was added to the soil in the dish while stirring with a spatula. After thorough mixing, the samples were allowed to stand for 2 hours and checked for saturation (when the total voids were filled up with water) as recommended by Garltey

(2011). The saturated paste was transferred to a Buchner funnel with a 9-cm filter paper. A vacuum was applied, and the saturated paste extract was collected in a 250-mL vacuum flask (Figure 3.8). The extracts were analysed for pH, EC and TDS.

Figure 3.8: Water soluble extraction set up for soils at Agricultural Research Council (ARC) laboratory.

3.4.3 Temperature, pH, EC and TDS analyses

The measurements of the pH, temperature, EC and TDS of the water samples were carried out using Multimeter (Multi 340i/SET, USA) at the laboratory. The temperature, EC and TDS of the geothermal spring water were measured *in situ* (Figure 3.9).

The water extracts obtained from the soil samples were analysed for the pH, EC and TDS following Garltey (2011) procedure. The extracts from soil were further filtered using a 0.45 µm membrane type filter. After calibration of the instrument, the saturated paste extract from the soil samples were analysed for pH, EC and TDS using a Mantech tritrasip autotitrator. All the samples were measured in triplicate and the mean values were estimated per season.

Figure 3.9: Measuring the physical parameters at Tshipise geothermal spring.

3.4.4 Major anions, cations and trace metals concentrations analyses

Water samples (non-acidified) were filtered with a 0.45 µm filter paper before taking a subsample for major cation and anion analyses. The EC value obtained was an indicator for indicating if further dilution was necessary. An EC value above 500 µS/cm requires 5 times dilution and above 1000 µS/cm requires 10 times dilution. The subsamples were poured into the auto sampler vials and analysed using IC (Dionex Model DX 500) (Figure 3.10) (USEPA, 1993). The measurements were carried out in triplicate and averaged to obtain a mean value to ensure quality measure.

The geothermal springs and boreholes samples (acidified) were analysed for trace metals using ICP-MS with a dilution factor of 10 (Figure 3.11) (USEPA, 2004b). The mass spectrometry for lowest, medium and highest mass numbers were obtained. All the measurements were carried out in triplicate and then averaged to obtain a mean value. The digested samples of the soils and vegetation were analysed for trace metals using ICP-MS after the background check up of the equipment (calibration) (USEPA, 2004b). All the measurements were carried out in triplicate to obtain a mean value for quality control.

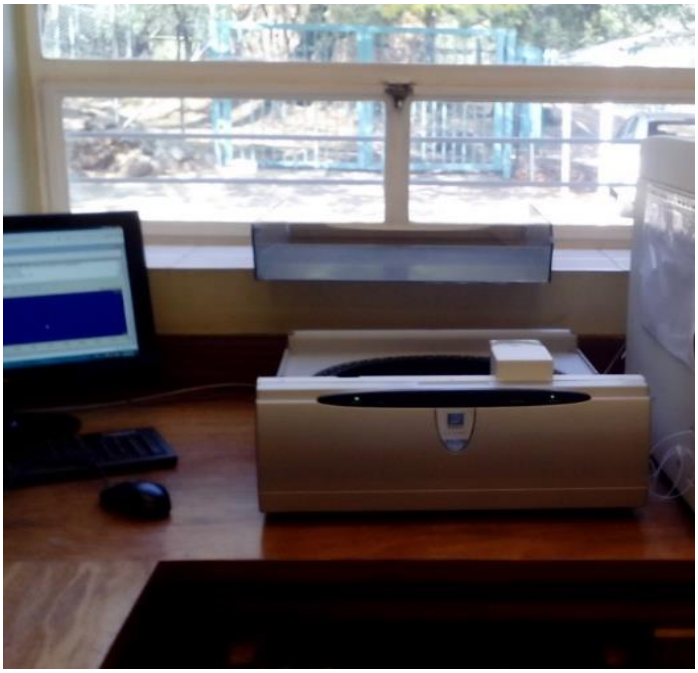

Figure 3.10: Ion chromatography (IC) for major anions and cations analyses at Agricultural Research Council (ARC) laboratory.

Figure 3.11: Inductively Coupled Plasma-Mass Spectrometer (ICP-MS) for trace metals analyses at ARC laboratory.

3.4.5 Estimation of reservoir temperature

The following empirical formulae were used to calculate the reservoir temperature (water geothermometers) of the geothermal system;

$$T\ (°C) = \frac{933}{0.993 + log\ (\frac{Na}{K})} - 273.15 \qquad \text{(Arnorsson } et\ al.,\ \text{1983)}$$

$$T\ (°C) = \frac{1217}{1.438 + log\ (\frac{Na}{K})} - 273.15 \qquad \text{(Fournier, 1979)}$$

$$T\ (°C) = \frac{1390}{1.75 + log\ (\frac{Na}{K})} - 273.15 \qquad \text{(Giggenbach, 1988)}$$

The mean data for Na and K were extracted from the results obtained from the major cations in section 3.4.4 to estimate the reservoir temperature of the geothermal springs and thermal boreholes.

3.4.6 Stable Isotopic analyses

Stable isotope analyses of the samples (rainwater, geothermal spring water and other boreholes water) were performed using a Thermo Delta V mass spectrometer connected to a Gasbench at Environmental Isotope Group (EIG) iThemba Laboratories Gauteng, Johannesburg, South Africa (Figure 3.12). The water samples were equilibrated along with Platinum catalyst (Pt) in preparation for measurement (Dolnikowski, 1995). The standard side of the dual inlet system was connected to a tank of reference hydrogen (δD) and reference carbon dioxide (CO_2). The equilibration time of the water samples with hydrogen gas was 40 minutes; whereas carbon dioxide gas was equilibrated with water samples in about twenty hours (20 hrs). Laboratory standards, calibrated against international reference materials, were analysed with each batch of the samples.

Conventionally, the isotope ratios of $^{2}H/^{1}H$ and $^{18}O/^{16}O$ in the water samples were expressed as per mil (‰) deviation relative to the Standard Mean Ocean Water (SMOW) as follows:

$$\delta\ (‰) = \frac{R_{sample} - R_{smow}}{R_{smow}} \times 1000 \quad \ldots\ldots\ldots\ldots\ldots\ldots\ldots\ldots\ldots\ldots\ldots\ldots\ldots\ldots\ 3.1$$

where R represents the ratio of heavy to light isotopes (D/H or $^{18}O/^{16}O$) in the sample and standard, respectively. The oxygen and hydrogen isotopic ratios were henceforth

expressed individually as $\delta^{18}O$ and δD, respectively, or collectively as δ values. Total analytical precisions were estimated at 0.2 ‰ for $\delta^{18}O$ and 0.8‰ for δD. Deuterium excess (d-excess) was calculated from the following equation (Dansgaard, 1964):

$$d = \delta D - 8 \times \delta^{16}O \quad \ldots\ldots 3.2$$

For $\delta^{13}C$ analyses of solid samples (soils and vegetation), approximately 40 - 60 mg of powdered samples were weighed and 60% of vanadium Penta-oxide (V_2O_5) was added. The sample was packed in the tin capsules (8 x 5 mm) pressed standard weight in the tray (Figure 3.13). The prepared samples were combusted in an elemental analyser and the CO_2 peak was injected into a continuous flow isotope ratio mass spectrometer (IRMS) (Gustafson *et al.,* 2007). For all methods, isotope ratios are expressed in per mil (‰) as in equation 3.1. Three calibration standards were used to adjust the delta values relative to V-SMOW and PeeDee Limestone.

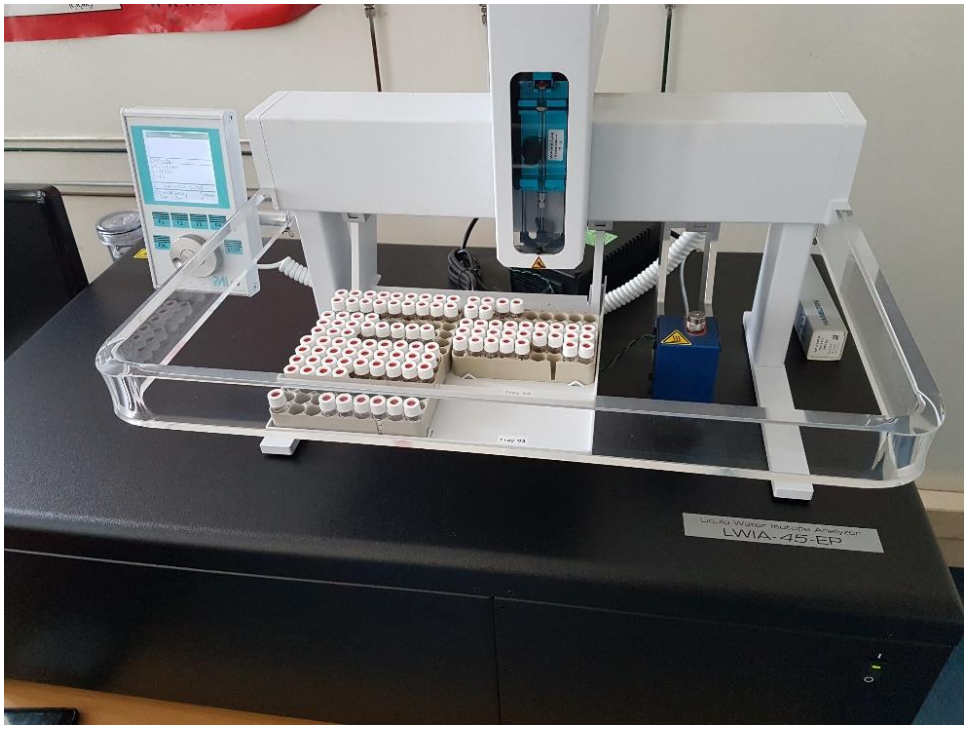

Figure 3.12: Running the samples on the Liquid Water Isotope Analyzer (LWIA-45-EP) for δD and $\delta^{18}O$ composition at iThemba laboratory.

Figure 3.13: Sample preparation of the soil and vegetation at iThemba laboratory.

3.4.6 Pyrolysis of the solid samples

Approximately 0.3 mg of the solid samples (soils, vegetation) were weighed in silver capsules (4 x 6 mm) and mixed with 60% V_2O_5. The solid samples were dropped with the auto sampler into the reaction tube (Figure 3.14). The samples were pyrolysed in the presence of reactive carbon and the gaseous pyrolysis products which are separated on a gas chromatography column. The column separates the major species H_2 and CO (CO_2 is not produced at temperatures above 1300°C) (Koziet, 1997). The pyrolysis products were transported by the carrier gas and separated in the GC-column into distinct H_2 and CO peaks. The infrastructure, made of a ConFloII interface with open split, 2 different reference gases, and He dilution, was applied to transfer the products into a delta plus an XL mass spectrometer. The pressure in the ion source is 2 x 10^{-6} mbar. The ion currents of masses m/z 2 and 3 to measure hydrogen isotopes and m/z 28 to 30 for the determination of oxygen isotopes were recorded by the ISODAT software and the results were calculated relative to H_2 and CO reference gases, respectively. Results of cellulose

measurements demonstrate the measurement of two isotope values, i.e. δD and $\delta^{18}O$ from pyrolysis experiments.

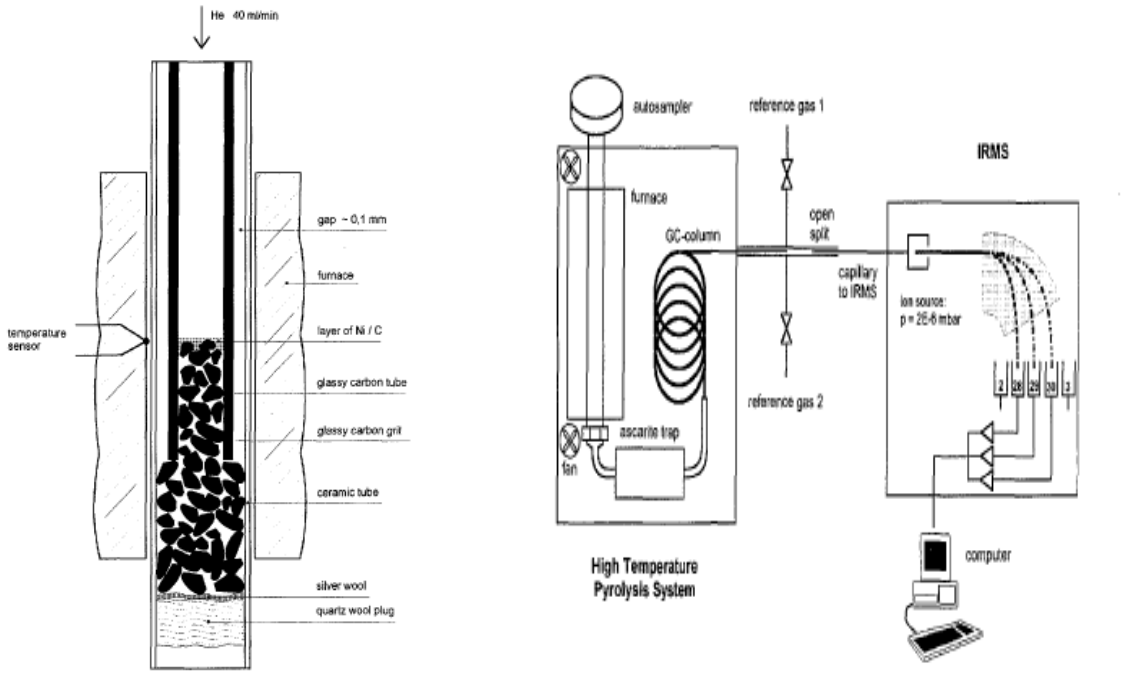

Figure 3.14: Schematic diagram of the HTP-reactor; HTP-Elemental Analyzer, ConFlo II-Split and IRMS at iThemba laboratory.

3.4.7 Tritium analysis (^3H)

The samples were distilled and subsequently enriched by electrolysis (Figure 3.15). The electrolysis cells consist of two concentric metal tubes, which are insulated from each other. 500 ml of the water sample, having first been distilled and containing sodium hydroxide, was introduced into the cell. A direct current of some 10–20 ampere was then passed through the cell, which was cooled because of the heat generation. After five days, the electrolyte volume was reduced to about 20 ml. The volume reduction of about 25 times produced a corresponding tritium enrichment factor of about 20. Samples of standard known tritium concentration (spikes) were run in one cell of each batch to check on the enrichment attained. Tritium concentrations were expressed as absolute concentrations, using tritium units (TU) and, no reference standard is required (Mekiso, 2011). For liquid scintillation counting samples were prepared by directly distilling the enriched water sample from the highly concentrated electrolyte. 10 ml of the distilled

water sample was mixed with 11 ml of Ultima Gold and placed in a vial in the analyser and counted for 2 to 3 cycles of 4 hours. Detection limit was 0.2 TU for enriched samples.

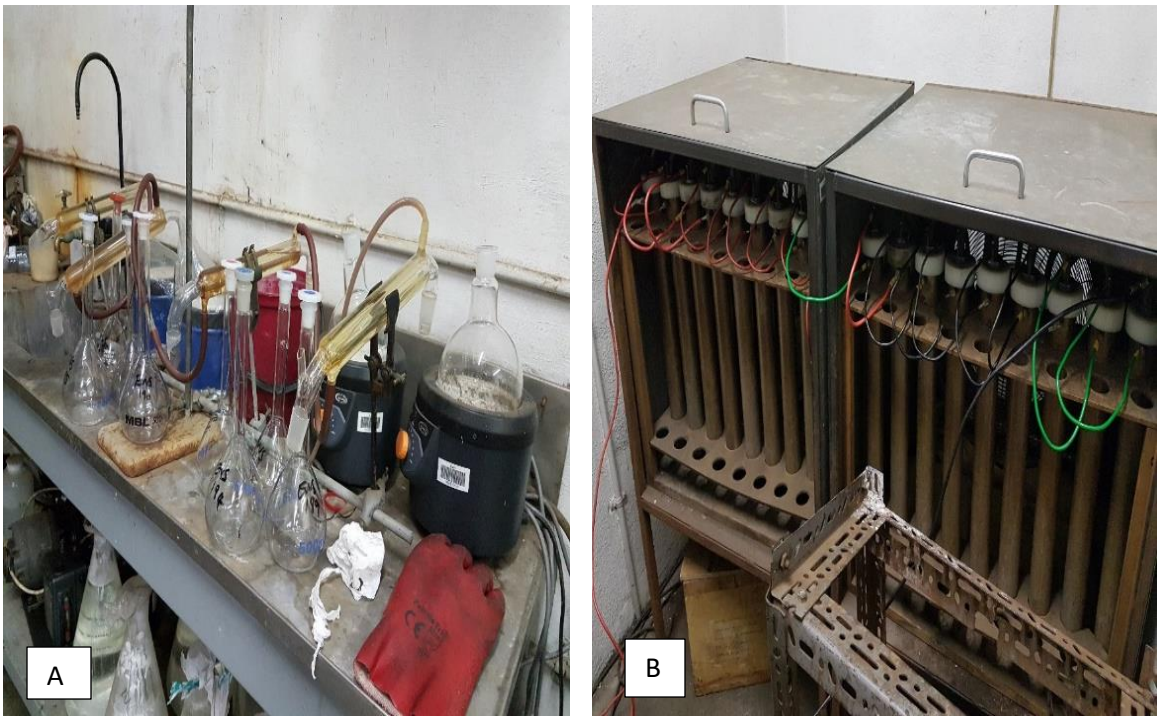

Figure 3.15: Distillation (A) and electrolytic processes (B) of the water samples for enrichment prior to analyses at iThemba laboratory.

3.4.8 Radiocarbon analysis (^{14}C)

CO_2 was generated by acidification of the field precipitates with phosphoric acid (H_3PO_4) (Figure 3.16). The CO_2 sample gas was transferred from the production/purification line into a 1-liter Pyrex flask, the pressure (610 mm Hg max.) was measured with a manometer and this measuring volume isolated. 10 ml of Carbosorb was pipetted into a standard 20 ml low-K glass counting vial that was attached to the system through a vacuum-tight, flexible connection. The air was removed by opening the vial briefly to roughing vacuum. The CO_2 sample was then transferred quantitatively from the measuring volume by freezing with liquid N_2 into a small trap which forms part of a low-volume (~60 ml) section of the system. The trap was pumped to high vacuum to remove residual non-condensable gas. The small volume section was isolated, the tap to the vial opened and the CO_2 allowed to sublimate whilst the vial was shaken by hand. The rate of CO_2 absorption usually balances its release from the trap through ambient (~25 °C)

warming, at pressures around 300-400 Torr. The rate was controlled when needed by slightly heating the trap or briefly cooling it with liquid N_2 (Enzenberger, 2015).

Uncooled, the rate of absorption under these conditions causes the temperature of the Carbosorb in the vial to rise to 70 °C. This does not seem to have any deleterious effect on the counting characteristics. However, the NH_4 released by the Carbosorb forms a gas "blanket" over its surface, through which the CO_2 must diffuse, the absorption rate dropping to near-zero at an equilibrium pressure of about 150 Torr. When the vial was kept cool in a water bath, the equilibrium pressure reduced to some 40 Torr, implying more complete CO_2 absorption, due to lower NH_4 pressures above the Carbosorb surface. The counting vial was removed from the vacuum system and 10 ml Permafluor®E+ was added. The vial was capped tightly, and the cocktail shaken well before counting. Because of a considerable overlap between the β pulse height spectrum of ^{14}C and the α spectrum of ^{222}Rn, samples for radiocarbon analysis needed to be stored for about three weeks to allow ^{222}Rn ($t_{1/2}$ = 3.85 days) to decay to below significant levels. The prepared sample cocktails were therefore placed immediately in the cooled and darkened sample changing chamber of a Hewlett Packard TriCarb liquid scintillation spectrometer. After the ^{222}Rn intensity had sufficiently declined, samples were counted four times at four hours duration of each count. The results were expressed in percent modern carbon (pMC).

Figure 3.16: ^{14}C extraction set-up (A) and the liquid scintillation analyser (B) at iThemba laboratory.

3.5 Potential Health risk assessment of trace metals

3.5.1 Assessment of potential health risk from geothermal springs

Common exposure pathways for water are the dermal absorption and ingestion routes (USEPA, 1989; Asare-Donker *et al.,* 2016). Hence, exposure dose to assess the human health risk was calculated using the following equations as adapted from the US EPA risk assessment guidance for Superfund (RAGS) methodology (USEPA, 1989; Asare-Donker *et al.,* 2016).

$$Exp_{ingestion} = \frac{Cwater X\ IR\ X\ EF\ X\ ED}{BW\ X\ AT} \quad \text{.....3.3}$$

$$Exp_{dermal} = \frac{(Cwater\ X\ SA\ X\ KP\ X\ ET\ X\ EF\ X\ ED\ X\ CF)}{BW\ X\ AT} \quad \text{.....3.4}$$

where, $Exp_{ingestion}$: exposure dose through ingestion of water (mg/kg/day); Exp_{dermal}: exposure dose through dermal absorption (mg/kg/day); C_{water}: average concentration of the estimated trace metals in water (µg/L); Kp: dermal permeability coefficient in water,

(cm/h), 0.001 for Cu, Mn, Fe and Cd, 0.0006 for Zn; 0.002 for Cr and 0.004 for Pb. Table 3.3 shows the different exposure parameters for health risk in children and adults.

Table 3.3: Exposure parameters used for the potential health risk assessment through different exposure pathways for water

Parameter	Unit	Child	Adult
Body weight (*BW*)	Kg	15	70
Exposure frequency (*EF*)	days/year	365	365
Exposure duration (*ED*)	Years	6	70
Ingestion rate (*IR*)	L/day	1.8	2.2
Skin surface area (*SA*)	cm^2	6,600	18,000
Dermal Absorption factor (*ABS*)	None	0.001	0.1
Particulate emission factor (*PEF*)	m^3/kg	1.3×10^9	1.3×10^9
Exposure time (ET)	hrs/day	1	0.58
Averaging Time (AT)	Days	365 x 6	365 x 70
Conversation factor (CF)	L/cm^3	0.001	0.001

Source: Asare-Donkor *et al.,* 2016; USEPA, 2009, WHO, 2006

Potential non-carcinogenic risks due to exposure of trace metals were determined by comparing the calculated contaminant exposures from each exposure route (ingestion and dermal) with the reference dose (RfD) (Table 3.5) using eqn. 3.5 to generate hazard quotient (HQ) toxicity potential of an individual via the two pathways using eqn. 3.6 (hazard index).

$$HQ_{\text{ing/dem}} = \frac{Exp_{ing/dem}}{\text{RfD}_{ing/dem}} \quad \text{.....3.5}$$

$$\text{HI} = \sum_{i=1}^{n} HQ_{\text{ing/dem}} \quad \text{.....3.6}$$

Chronic daily intake (CDI) of trace metals through ingestion was calculated using eqn. 3.7;

$$CDI = C_{water} \times \frac{IR}{BW} \quad \text{.....3.7}$$

Where C_{water}, IR and BW represent the concentrations of the trace metals in water, average daily intake of water and body weight, respectively. Carcinogenic risk (CR) through ingestion pathway was estimated using eqn. 3.8.

$$CR_{ing} = \frac{Exp_{ing}}{exP_{ing}} \quad \text{.....3.8}$$

Where exP is the carcinogenic slope factor presented in Table 3.5.

3.5.2 Assessment of health risk from surrounding soil

The mean trace metals concentrations were used to estimate intake at the different pathways using standard USEPA's exposure equations (USEPA, 1989; 2004a). Children and adults could be exposed to contaminants from soil via three different pathways that include oral intake ($Exp_{ingestion}$), inhalation intake ($Exp_{inhalation}$) and through skin exposure (Exp_{dermal}) (USEPA, 2004a). Based on this fact noncancer risk assessment in this study was estimated. For intake estimation via each exposure pathway, the following equations were used;

$$Exp_{ingestion} = \frac{C\ X\ IngR\ X\ EF\ X\ ED}{BW\ X\ AT}\ X\ 10^{-6} \quad \text{.....3.9}$$

where, C – concentration of a contaminant in soil (mg/kg), IngR – ingestion rate of soil (mg/day), EF – exposure frequency (days/year), ED – exposure duration (years), BW – average body weight (kg), AT – average time (days) = ED*365.

$$Exp_{inhalation} = \frac{C\ X\ InhR\ X\ EF\ X\ ED}{PEF\ X\ BW\ X\ AT} \quad \text{.....3.10}$$

where, InhR – inhalation rate (m^3/day), PEF – particle emission factor (m^3/kg)

$$Exp_{dermal} = \frac{C\ X\ SA\ X\ SAF\ X\ ABS\ X\ EF\ X\ ED}{BW\ X\ AT}\ X\ 10^{-6} \quad \text{.....3.11}$$

where, SA – surface area of the skin that contacts the soil (cm^2), SAF - skin adherence factor for soil (mg/cm^2), ABS – dermal absorption factor (chemical specific) = 0.001 (for all metals). After the three exposure pathways were calculated, hazard quotient (HQ) and

hazard index (HI) based on cancer/non-cancer toxic risk were calculated as follows (USEPA, 2004a):

$$HQ = \frac{Exp}{RfD} \quad \text{.....3.12}$$

$$HI_{ex}P = \sum HQexP \quad \text{.....3.13}$$

where, exP are Cancer Slope Factors for different exposure pathways, respectively. Reference dose (RfD) (mg/kg/day) is an estimated value of the daily exposure, maximum permissible risk, to the human population, including sensitive subgroups (children) during a lifetime. Tables 3.4 and 3.5 show the exposure parameters, reference doses and cancer slope factors used for the health risk assessment for standard residential exposure scenario through different exposure pathways.

Table 3.4: Exposure parameters used for the health risk assessment through different exposure pathways for soil

Parameter	Unit	Child	Adult
Body weight (*BW*)	Kg	15	70
Exposure frequency (*EF*)	days/year	350	350
Exposure duration (*ED*)	years	6	30
Ingestion rate (*IR*)	mg/day	200	100
Inhalation rate (*IRair*)	m^3/day	10	20
Skin surface area (*SA*)	cm^2	2100	5800
Soil adherence factor (*SAF*)	mg/cm^2	0.2	0.07
Dermal Absorption factor (*ABS*)	none	0.001	0.1
Particulate emission factor (*PEF*)	m^3/kg	1.3×10^9	1.3×10^9
Average time (*AT*)			
For carcinogens	days	365 × 70	365 × 70
For non-carcinogens		365 × ED	365 × ED

Source: Department of Environmental Affairs (DEA), 2010

Table 3.5: Reference doses (*RfD*) in (mg/kg/day) and Cancer Slope Factors (exP) for the different heavy metals

Heavy Metal	$RfD_{ingestion}$	RfD_{dermal}	$RfD_{Inhalation}$	$exP_{ingestion}$	exP_{dermal}	$exP_{Inhalation}$
As	3.00E-04	3.00E-04	3.00E-04	1.50E+00	1.50E+00	1.50E+00
Ba	2.00E-01	-	2.00E-01	-	-	-
Be	2.00E-04	-	2.00E-04	-	-	-
Cd	1.00E-03	1.00E-03	5.70E-05	6.30E+00	-	6.30E+00
Cr	3.00E−03	3.00E-03	3.00E−05	5.00E−01	-	4.10E+01
Co	2.00E-02	5.70E-06	5.70E-06	-	-	9.80E+00
Cu	3.70E-02	2.40E-02	3.70E-02	-	-	-
Hg	3.00E-04	3.00E-04	8.60E-05	-	-	-
Mn	2.40E-02	1.43E-03	2.40E-02	-	-	-
Ni	2.00E-02	5.60E-03	2.00E-02	-	-	-
Pb	3.50E−03	5.25E-04	3.50E-03	8.50E−03	-	4.20E−02
Sb	4.00E-04	-	4.00E-04	-	-	-
Se	5.00E-03	-	5.00E-03	-	-	-
V	5.04E-03	-	5.04E-03	-	-	-
Zn	3.00E-01	7.50E-02	3.00E-01	-	-	-

Source: DEA, 2010; USEPA, 1989 and 2004a

3.6 Data analyses

During the course of this research, many numerical data were generated, which were interpreted so as to achieve the research objectives (Saunders *et al.,* 2012). Data presentations were made using tables and graphs. The differences and trends; and correlation among the data were carried out statistically using ANOVA, correlation and regression analyses. Multivariate statistics such as principal component analysis (PCA) /factor analysis (FA) and hierarchical agglomerative analysis (HAA) were performed using Xlstat statistical software (Shan *et al.,* 2012). The PCA was used to establish major

variation and relationships among the different trace metals and hydrochemical parameters. Pearson's correlation coefficient was used to test the relationship between hydrochemical parameters and trace metals concentrations at α= 0.05 level of significance; and the control was used to ensure the validity of data obtained.

The carbon-14 results were corrected using NETPATH, which is inverse modelling that involves inverse geochemical modelling to assess the possible reaction and mixing processes that govern the geochemical evolution of groundwater. Radiocarbon age is corrected/adjusted from a more complete evaluation of the geochemical reactions (Figure 3.17)

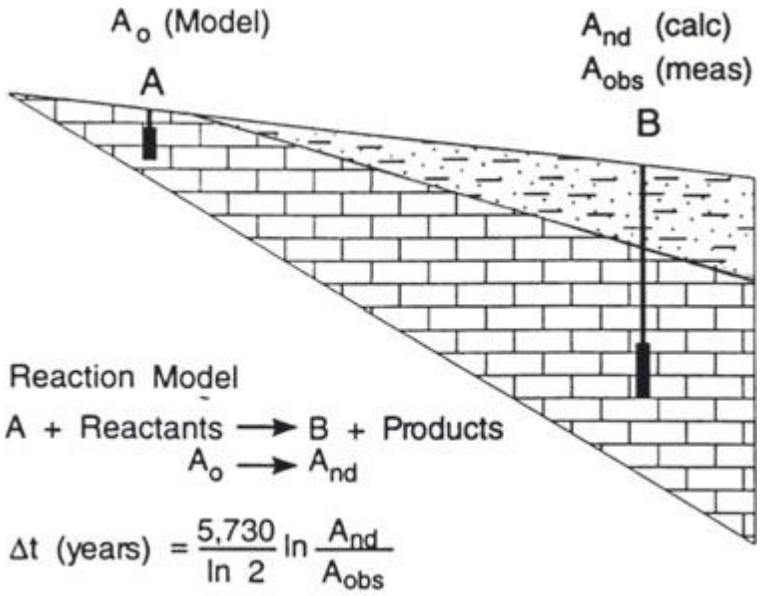

Figure 3.17: Conceptualisation of the generalised approach to radiocarbon dating of dissolved inorganic carbon (DIC) in NETPATH (El-kadi *et al*., 2010).

3.7 Ethical considerations

This research work involves the collection of samples from geothermal springs, soils and vegetation; where some of them are found in resort centers (Mphephu, Sagole and Tshipise) and the other is a private property (Siloam). Hence, there was need for permission to access the study sites for sampling. It was carried out through writing and meeting the management of the resorts and the owner of the property formally to access the sites for sampling. Some of the request letters are attached in the appendix. In

addition, the researcher maintained accuracy throughout the period and stages of this research. Also, the study does not require ethical clearance for the health component because the study focuses on the potential health risks from calculations without dealing directly with human subjects.

3.8 Summary

This chapter presented the different methods that were employed from field work to laboratory analyses and data analyses. This research was carried out by ensuring high quality and highest level of integrity, objectivity, discipline and trustworthiness. In addition, appropriate personal protective equipment was worn during the field work and in the laboratory.

CHAPTER FOUR

PHYSICOCHEMICAL, GEOCHEMICAL AND STABLE ISOTOPIC COMPOSITIONS (δD and $\delta^{18}O$) OF GEOTHERMAL SPRINGS, RAIN AND BOREHOLES WATER

4.1 Preamble

The objective of this chapter is to determine the physicochemical and geochemical parameters and the stable isotopic compositions for selected geothermal springs and boreholes within the study areas. In addition, the isotopic compositions of the rainwater were determined to generate the local meteoric line, which is a useful tool for indicating the source and water pathway within the locality (specific objective 1). This chapter elucidates on the relationship of the physicochemical and geochemical parameters, and the stable isotopic compositions of the geothermal springs, rainwater and boreholes to better understand the geothermal system and its geochemical processes. This chapter is based on the hypothesis 1 which states that "studied geothermal springs and boreholes in the Soutpansberg region have similar physicochemical, geochemical and isotopic characteristics".

4.2 Thermal characteristics of the geothermal springs and boreholes

The water temperature of springs in the study area ranges between 41.3°C and 68.9°C (Figure 4.1). Based on the above classification; Mphephu and Sagole springs, Siloam (SH1 and SH2) boreholes are thermal (hot) water with temperatures ranging between 41°C to 49°C. Siloam and Tshipise geothermal springs can be classified as scalding (hyperthermal) with temperature ranging between 53°C and 69°C. Figure 4.1 shows clearly the variations in the thermal property of the geothermal springs. Figure 4.1 indicates that there is no spatial correlation between the location of springs and their geothermal characteristics. Siloam, for instance, has a temperature of 67.7°C, while Mphephu, about 5 km away, has a temperature range of 41-43°C. The same applies to Tshipise and Sagole geothermal springs. This finding supports the literatures that

geothermal springs in close proximity to each other does not have same geothermal characteristics (Olivier *et al.,* 2010; Durowoju *et al.,* 2015).

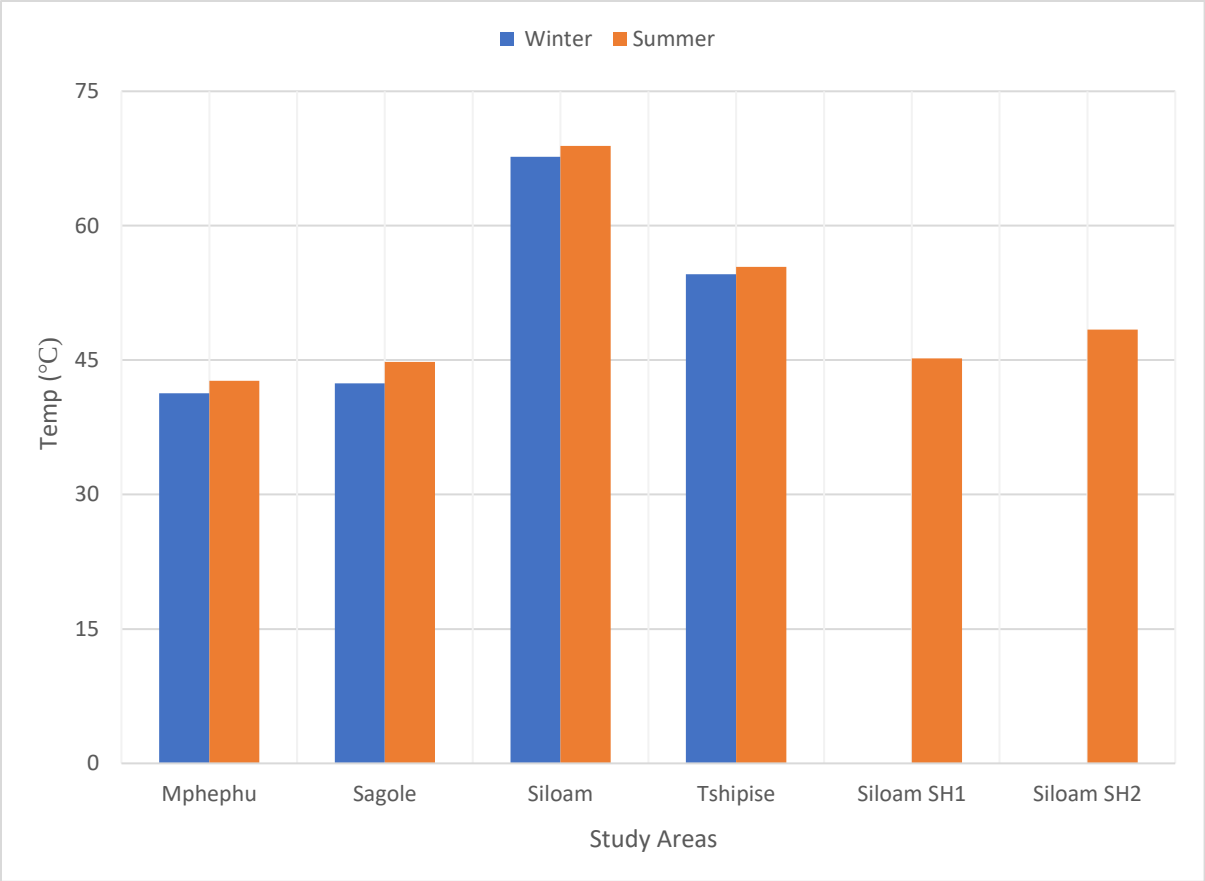

Figure 4.1: Mean temperatures of geothermal springs and boreholes within Soutpansberg during winter and summer.

These changes can be attributed to seasonal variation which leads to the fluctuation of the thermal property of the springs. During summer, there is high rainfall and more underground water (coupled with high flow rate), which is heated as a result of the geothermal gradient of 2°C - 3°C per 100 m (Press and Siever, 1986). This implies that geothermal spring water with high temperature emanates from a deeper source (1.6 to 2.8 km from the source in the studied geothermal springs and boreholes). From the calculated gradient, it was observed the geothermal springs were from deep sources. This results in high temperature in summer compared to winter. In all the sites, there is approximately 1°C difference in the thermal property of the geothermal spring in summer

compared to winter. These high temperatures in summer result in more transfer of moisture (evaporation and evapotranspiration) to the atmosphere until it reaches the dew point, hence there is potential to rain more intensely during this period.

The temperatures of the non-geothermal springs (BH1, BH2, SCC and TTP) were below 25°C (considered as tepid) and hence, not presented in Figure 4.1. The geothermal spring waters with lower temperatures are Na-Cl-HCO_3 type waters while the Na-Cl type waters are encountered in high temperature springs (Du *et al.,* 2008). Studies have shown that high water temperature increases vasodilatation in the veins of the skin, thereby accelerating the metabolic processes in the cells of the skin. This, however, improves capillary dilatation and blood circulation, oxygen supply is increased, and the metabolic processes are intensified in the skin and subcutaneous cells (Bjornsson, 2000; Skapare, 2001; Skapare *et al*. 2005). Hence, this is one of the therapeutic purposes of geothermal waters.

4.3 Hydrochemistry of the studied geothermal springs and boreholes

4.3.1 Physicochemical compositions of the groundwaters

Hydrochemical parameters of the geothermal springs, hot and tepid boreholes were used to understand the geochemical processes governing their formation; prediction of sub-surface temperature using chemical geo-thermometers; and assess suitability of the waters for domestic and irrigation purposes. Table 4.1 shows the results of the hydrochemical composition of the geothermal spring water, geothermal boreholes and non-geothermal spring water (tepid boreholes). The hydrochemical compositions of groundwater were not uniform but varied over a wide range. This implies that the groundwater compositions were heterogeneous in nature. This could be attributed to the underlying geology of the study areas (Olivier *et al.,* 2011).

Table 4.1: Statistical summary of Hydrochemical parameters of geothermal springs and boreholes within Soutpansberg

	SAGOLE		TSHIPISE			MPHEPHU		SILOAM					
Parameters	SGW	SGS	TSW	TSS	TTP	MPW	MPS	SAW	SH1	SH2	BH1	BH2	SCC
Temp (°C)	42.4±1.45	44.8±2.12	54.6±2.26	55.4±2.21	22.5±0.00	41.3±1.23	42.7±1.01	67.7±1.68	45.2±0.00	48.4±0.00	22.4±0.00	21.4±0.00	20.1±0.00
pH	8.82±0.95	7.98±0.22	8.46±0.22	8.47±0.21	8.17±0.00	8.05±0.02	8.15±0.07	9.39±0.06	8.86±0.01	9.19±0.00	8.17±0.01	8.10±0.01	7.17±0.02
SAR	33.88±546	19.20±15.48	25.75±0.98	25.45±1.29	0.82±0.01	2.07±0.06	2.18±0.06	7.39±0.04	17.25±0.02	19.04±0.01	4.65±0.01	10.75±0.01	0.28±0.01
EC (µS/cm)	330±0.00	347.33±16.17	746.67±5.77	745±7.07	290±0.02	335±7.07	365±21.21	340±2.07	630±0.01	330±0.00	690±0.01	730±0.01	90±0.02
TDS (mg/L)	133.13±1.85	196.70±122.43	377.48±5.36	390.61±7.63	82.99±0.01	124.38±1.41	120.84±1.19	215.18±9.25	305±0.01	130.12±0.1	296.45±0.1	423.07±0.1	10.78±0.10
Alkalinity (mg/L)	10.50±4.24	6.50±5.89	11.12±0.54	10.75±0.35	11.50±0.00	12.50±0.00	6.00±8.49	107.52±1.36	10±0.02	12±0.02	25.50±0.01	17.50±0.01	2±0.02
Na (mg/L)	64.20±1.84	57.13±11.98	157.67±4.51	154.50±4.95	18.30±0.01	42.50±1.27	42.35±1.06	78.77±7.54	118±0.00	62.70±0.01	124±0.03	170±0.01	1.69±0.01
K (mg/L)	1.98±0.01	2.04±0.05	4.55±0.06	4.84±0.05	2.08±0.00	2.06±0.04	2.11±0.01	2.61±0.06	2.73±0.02	2.21±0.1	5.15±0.01	4.67±0.02	1.06±0.01
Ca (mg/L)	0.29±0.11	4.27±6.61	2.84±0.07	2.79±0.10	18.90±0.00	12.20±0.00	11.90±0.28	5.69±0.05	3.53±0.00	0.81±0.01	27.80±0.02	12.80±0.01	0.76±0.01
Mg (mg/L)	0.00±0.00	3.47±6.00	0.00±0.00	0.00±0.00	11.50±0.01	10.50±0.00	10.35±0.07	1.04±0.08	0.00±0.00	0.00±0.00	15.80±0.01	3.72±0.01	1.17±0.2
F (mg/L)	0.77±0.15	2.60±1.71	5.01±0.63	5.98±0.08	0.15±0.01	2.69±0.01	4.16±2.48	6.51±0.08	4.55±0.01	4.95±0.01	4.02±0.01	3.92±0.01	0.00±0.00
NO_3 (mg/L)	0.99±0.36	1.71±0.85	2.13±1.80	5.85±1.48	0.35±0.00	3.02±0.40	6.25±3.23	0.60±0.03	0.17±0.01	1.31±0.01	3.22±0.01	83.95±0.01	0.64±0.01
Cl (mg/L)	41.34±0.30	81.15±75.10	151.86±0.28	156.67±0.02	20.20±0.02	33.90±0.06	98.82±86.34	24.11±0.77	153.3±0.00	38.90±0.01	80.14±0.1	103.23±0.0	3.73±0.01
SO_4 (mg/L)	16.95±0.54	27.89±27.23	45.81±2.15	51.78±0.42	4.11±00	9.21±0.03	21.14±18.31	8.99±0.06	16.45±0.01	10.55±0.01	17.56±0.01	25.88	0.48±0.01
PO_4 (mg/L)	0.92±0.82	13.09±21.49	1.38±1.22	2.14±1.46	0.43±0.00	1.28±0.74	22.6±30.96	0.42±0.06	1.15±0.02	1.52±0.01	3.29±0.02	4.59±0.01	0.17±0.01
CO_3 (mg/L)	1.50±2.12	0.00±0.00	0.58±0.50	0.60±0.42	0.00±0.00	0.00±0.00	0.00±0.00	16.13±0.41	1.80±0.01	2.40±0.01	0.00±0.00	2.70±0.00	0.00±0.00
HCO_3 (mg/L)	9.76±0.86	7.93±7.19	12.38±0.37	11.90±0.43	14.03±0.01	15.25±0.00	7.32±10.35	98.75±2.08	8.54±0.02	9.76±0.02	31.11±0.00	15.86±0.00	2.44±0.00

SGW-Sagole (Winter), SGS-Sagole (Summer), TSW-Tshipise (Winter), TSS-Tshipise (Summer), MPW-Mphephu (Winter), MPS-Mphephu (Summer), SAW-Siloam (geothermal spring), SH1- Siloam (Hot borehole), SH2- Siloam (Hot borehole), BH1- Siloam (tepid borehole), BH2-Siloam (tepid borehole), SCC-Siloam (Community tap water), TTP – Tshipise (Tshipise tap water).

Results showed that geothermal springs were more mineralised than geothermal boreholes and non-geothermal water (tepid boreholes). This could be attributed to the rock-water interaction at the deeper aquifer leading to more mineralisation (Todd, 1980; Durowoju *et al.,* 2016b). Interestingly, Siloam hot and tepid boreholes show similar variations in hydrochemical parameters with geothermal springs and this could be attributed to underlying geolology or aquifer connectivity. Non-geothermal water (SCC and TTP) falls within domestic water quality (DWAF, 1996; WHO, 2000) values for pH, sodium adsorption ration (SAR), electrical conductivity (EC) and total dissolved solids (TDS).

Generally, the measured pH values range from 7.17 to 9.39 which implies that the waters are alkaline in nature. Most of the groundwater pH falls within recommended South African National Guidelines for Domestic Water Quality (DWAF, 1996; SANS, 2015) values of 7-9 except for Siloam geothermal spring water (SAW) and Siloam hot borehole (SH2) having pHs of 9.39 and 9.19, respectively. The TDS values were generally less than 450 mg/l ranging from 10.8 to 423 mg/l for all the samples with a slight difference across seasons. Hence, the TDS values fall within the South African Guidelines for Domestic Water Quality (DWAF, 1996; SANS, 2015) value of 450 mg/L. Although, previous studies showed that the TDS value for Tshipise geothermal spring was higher than 450 mg/L (Olivier *et al.,* 2011; Durowoju *et al.,* 2018), this study recorded a lower value. This could be as a result of the decrease in water temperature of the spring in this present study (decreased from 58°C to 55.6°C).

The dominant ionic compositions found in the site waters are sodium (Na^+), bicarbonate (HCO_3^-), sulphate (SO_4^{2-}) and chloride (Cl^-) (Table 4.1). The concentration of sodium (Na^+), chloride (Cl^-) and sulphate (SO_4^{2-}) were highest in Tshipise (TSW and TSS) and Siloam (SH1, BH1 and BH2). At Siloam village, BH1 and BH2 (tepid water) were found to have higher Na^+ concentrations than SAW (geothermal spring); though, Na^+ concentrations in Siloam were generally high except for the community tap water (SCC) that is already treated from the municipality.

The high Na^+ concentrations probably originate from the dissolution of sodium-rich plagioclase feldspars (albite) in the sandstone and shale. The general order of dominant

cations is $Na^+ > Ca^{2+} > K^+ > Mg^{2+}$ and the sequence of the abundance of the anions are in this order: $Cl^- > SO_4^{2-} > HCO_3^- > F^- > NO_3^- > PO_4^{3-}$. These uneven distributions of the hydrochemical parameters play a vital role in understanding the processes governing the system as well as the suitable benefits of these springs, considering the fact that these geothermal springs are in the rural communities, where the community members see the springs as a viable source of water and they use it for various purposes including drinking, domestic, irrigation among others.

4.3.2 Water types

In order to understand the geochemical evolution of groundwater in the study areas, the samples were plotted on a Piper's diagram (Piper, 1944) and Durov's diagram (Durov, 1948) using Geochemist's Workbench version 11.0.7 (GWB 11) software. Piper diagram is a multifaceted plot wherein milliequivalents percentage concentrations of major cations (Ca^{2+}, Mg^{2+}, Na^+ and K^+) and anions (HCO_3^-, SO_4^{2-}, and Cl^-) were plotted in two triangular fields, which were then projected further into the central diamond field (Ravikumar *et al.,* 2015). In contrast, Durov diagram is a composite plot consisting of two ternary diagrams where the milliequivalents percentages of the cations of interest were plotted against those of anions of interest; sides form a central rectangular, binary plot of the total cation against total anion concentrations (Ravikumar *et al.,* 2015). Both diagrams were used in this study to understand hydrochemical processes involved along with the water type of the geothermal spring/ground water. Durov's plot was used to validate the water types and the process of formation.

The Piper's diagram revealed that most of the geothermal spring water and boreholes (80%) falls in Na-Cl water type except for Siloam geothermal spring (SAW - WT29 and WT30) which falls under Na-HCO_3 water type, and TTP (Tshipise tap water) and SCC (Siloam community tap water) fall under Ca-Mg-Cl (Figure 4.2). The findings of this study are in line with the recent findings by Durowoju *et al*. (2018) but differs from Olivier *et al*. (2011), which report $NaHCO_3$ and Na-Ca-HCO_3 water types for Sagole and Mphephu springs, respectively. This could be as a result of convergence outcomes obtained from both Piper plot and Durov plot, which corroborate each other and validate the present

findings. Also, small sample size collected (sampled in 2004 and 2010) by Olivier *et al*. (2011) as well as source rock interaction could be responsible for the difference obtained.

Na-Cl water type is dominated by Na^+ and Cl^-, derived from Na-Cl brines in winter and summer linked to the underlying geology emanating from gneissic rocks. Na-Cl and Na-HCO_3 water types showed a typical marine and deeper ancient groundwater influenced by ion exchange. The Na-HCO_3 water type from Siloam geothermal spring showed that the spring emanates from basaltic rocks. It is the most evolved of the waters and it derives its Na^+ from cation exchange of Ca^{2+} for Na^+ and K^+ as well as dissolution of rock mineral (plagioclase) (Lipfert *et al.,* 2004). TTP and SCC with Ca-Mg-Cl water type demonstrate the dominance of alkaline earths over alkali (Ca+Mg > Na+K) and strong acidic anions over weak acidic anions (Cl+SO_4 > HCO_3).

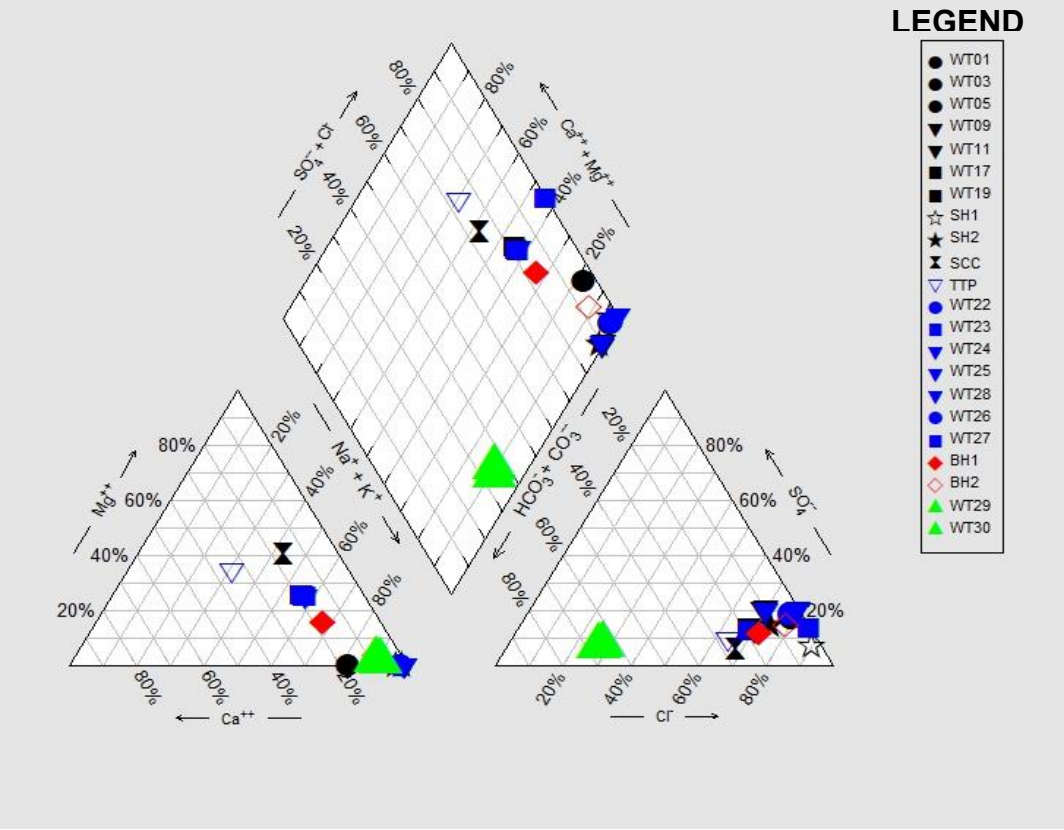

Figure 4.2: Piper diagram of geothermal springs and boreholes within the Soutpansberg region.

Durov's diagram corroborates with the finding from the Piper's diagram (Figure 4.3). Most of the geothermal spring/groundwater has Cl^- and Na^+ dominating and the water could result from the reverse ion exchange of Na-Cl waters. Hence making the water type Na-Cl as observed in the Piper diagram. As observed from Piper's diagram, Siloam geothermal spring (SAW) has Na-HCO_3 water type which is formed as a result of the reverse ion exchange of Na-Cl waters, making Cl^- a dominant anion and Na^+ a dominant cation making the water Na-HCO_3 (Durov's diagram). Na-HCO_3 could be formed as a result of ion exchange of $CaCO_3$ (carbonated rock) within the aquifier. The TTP and SCC have no dominant anion and cation which indicates that the water exhibits simple dissolution or mixing compared to the geothermal spring water and other boreholes.

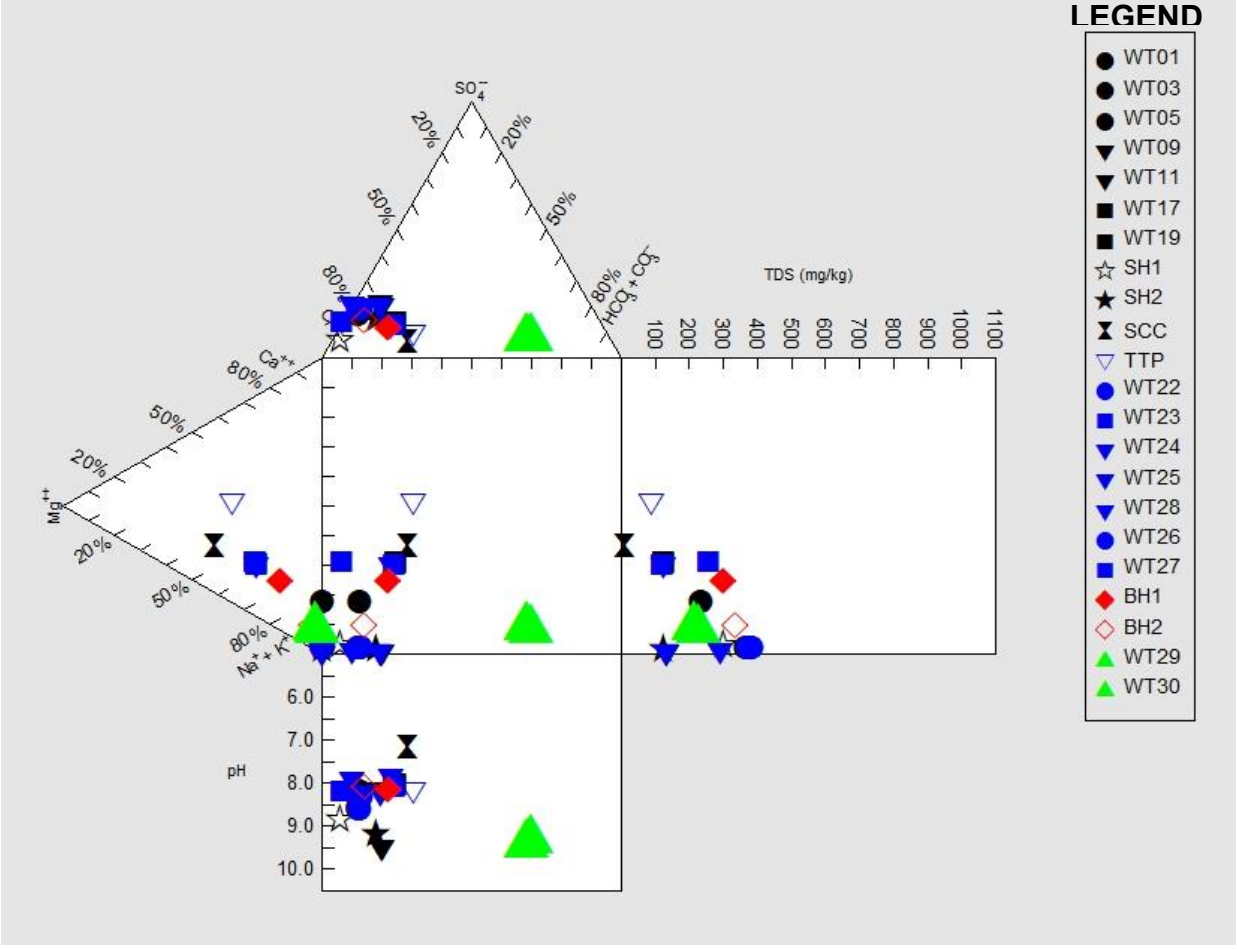

Figure 4.3: Durov diagram of geothermal springs and boreholes within Soutpansberg region.

Durov's diagram further explains the geochemical processes leading to the respective water type, hence, the advantage of the Durov's diagram over the Piper's diagram. The major water types are Na-Cl and Na-HCO_3 which are typical of marine and deep groundwaters influenced by the ion-exchange process. There is no variation in the water type with season for the studied geothermal spring and boreholes. The Na^+ and HCO_3^- ions were also present, making the water type fall under class C (temporary hard carbonate water) (Bond, 1946) as reported by Olivier *et al*. (2011). Hence, the presence of Na^+ in groundwater in the area is due to water-rock interaction as a result of oxidisation and evapotranspiration processes. These findings support the previous studies by Olivier *et al*. (2011) and Durowoju *et al*. (2018).

4.3.3 Water geothermometers

The mean data for Na and K were extracted from Table 4.1 and used to estimate the reservoir temperature of the geothermal springs and thermal boreholes using the empirical formulae stated in chapter three (section 3.4.5). Values obtained from this study were compared with literature around the world. The reservoir temperature of all the geothermal springs and boreholes within Soutpansberg regions were concentrated in the range between 80°C to 185°C from three Na-K geothermometer empirical formulae (Table 4.2). This finding is relatively satisfied with the normal geothermal regime of earth's continental crust (Doan *et al.,* 2014).

Outcomes from Arnorsson's empirical formula gives the least temperatures compared to that of Fournier and Giggenbach. The results obtained from Fournier and Giggenbach's empirical formulae were close within (±15°C) and hence, this study proposes the use of these formulae to complement one another. Fournier or Giggenbach's empirical formulae have been commonly employed from literature (Table 4.2) and were both adopted for reliable outcomes. Comparing findings from this study with literature (Table 4.2), Na-K thermometer gives reliable outcome ranging between 90°C to 180°C except for Bogaria S8 (230°C) and Rior (310°C). The high reservoir (aquifer) temperatures obtained from these springs were as a result of high calcium concentration in their composition, hence another geochemical thermometer should be employed (Ranjit, 1994; Karingithi and Wambugu, 2009; Karingithi, 2014). Dhansay *et al*. (2017) reported that the study areas

were among the listed zone for low-enthalpy geothermal energy resources (Figure 4.4), which this study supports. Hence, there is a possibility of generation of low-enthalpy geothermal energy within Soutpansberg region.

Table 4.2: Results of Na-K geothermometer from geothermal springs and hot boreholes

sites	Water temp (°C)	Na (mg/L)	K (mg/L)	Na-K(°C) Arnorsson	Na-K(°C) Fournier	Na-K(°C) Giggenbach	Source
SGW	42.4	64.20	1.98	99.45	139.53	153.10	Present study
SGS	44.8	57.13	2.04	109.23	148.69	161.63	
TSW	54.6	157.67	4.55	95.33	135.65	149.47	
TSS	55.4	154.50	4.84	100.50	140.51	154.02	
MPW	41.3	42.50	2.06	131.10	168.91	180.36	
MPS	42.7	42.35	2.11	133.21	170.85	182.14	
SAW	67.7	78.77	2.61	104.13	143.92	157.19	
SH1	45.2	118.00	2.73	81.74	122.75	137.36	
SH2	48.4	62.70	2.21	108.28	147.81	160.82	
Rior	33	310	4	-	310	-	Nepal[a]
Surai Khola	37	123	3.9	-	100	-	
Sadha Khola	69	300	12	-	115	-	
Rgapur	42	-	-	-	-	154	India[b]
Unahavie	71	-	-	-	-	145	
Ganshipuri	52	-	-	-	-	149	
Bogaria S12	86	1240	37	-	151	-	Kenya[c]
Bogaria S14	45	110	15	-	145	-	
Bogaria S8	39	13	01	-	230	-	

[a] Ranjit (1994); [b]Sarolkar (2005); [c]Karingithi and Wambugu (2009).

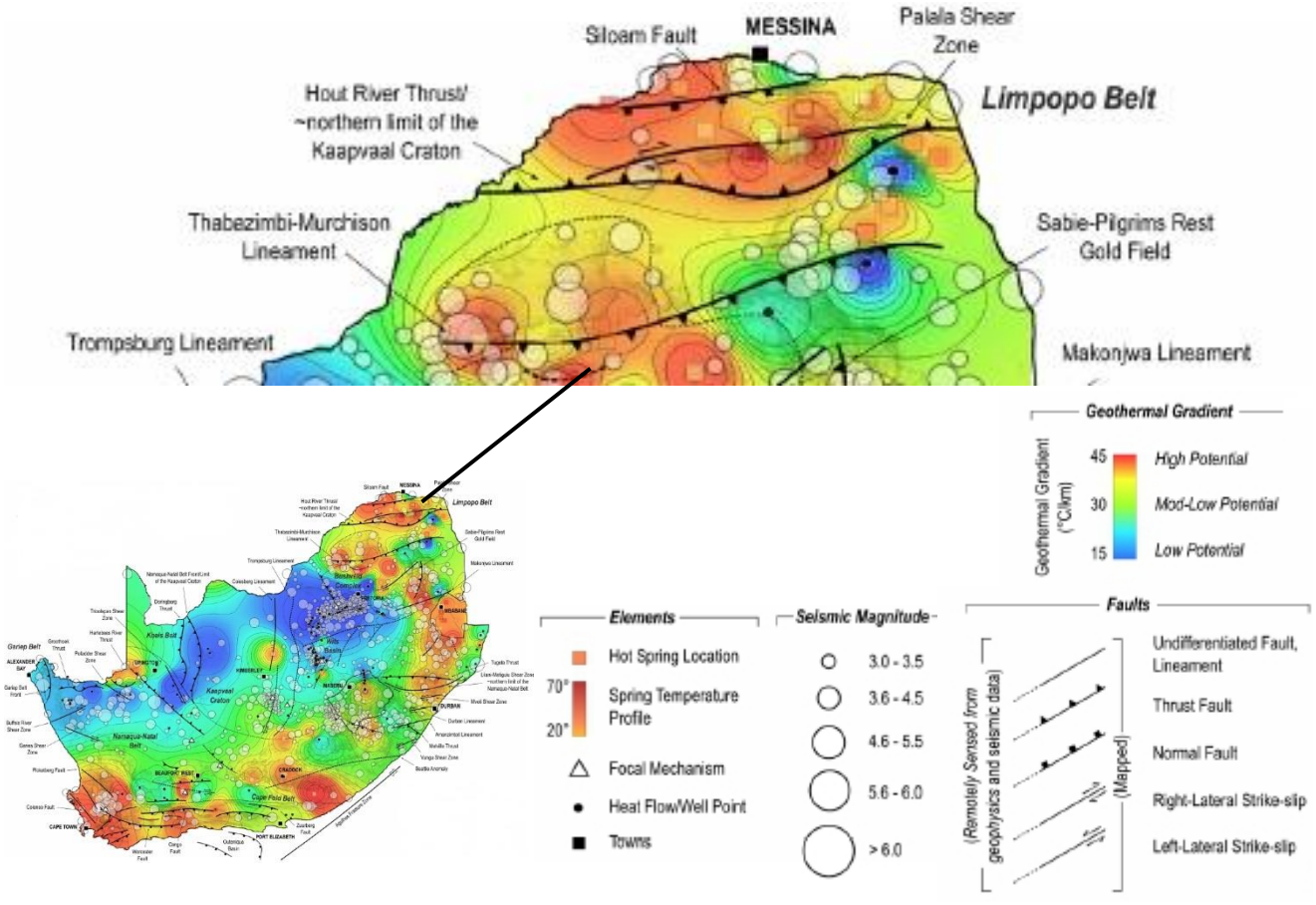

Figure 4.4: Modified graphical overview of South African Map including tectonics contacts and structures, seismic activity and earthquake focal mechanism and geothermal springs (Dhansay *et al.,* 2017).

The waters of the geothermal springs and boreholes within the Soutpansberg region are nearly in equilibrium with common hydrothermal alteration minerals. Information about water types and geothermometer of the springs and boreholes combined inferred that ratio of Na-K is dominated by percolation resulting to Na-Cl waters after partial or mixed equilibrium in large reservoirs. Hence, most of the geothermal springs/boreholes' waters are mature (Giggenenbach, 1991; Chandrasekharam and Bundschuh, 2008) except for Na-HCO_3 water at Siloam, which is peripheral. Since most of the geothermal springs and borehole sources were characterised with high chlorine from the Na-Cl water type, they are affected by geothermal water mixed with salty water (possibly brine from the underlying geology of Soutpansberg Mountain), which is not native water. Na-HCO_3-Cl water indicate water rising from the periphery of hot granitic source or hydrogeochemical evolution (Siloam).

4.3.4 Geochemical processes controlling groundwater chemistry

The geochemical processes controlling the geothermal spring chemistry were demonstrated by Gibbs (1970). Gibbs plot provides vital information on the mechanisms (precipitation, rock-water interaction or evaporation) controlling groundwater system by plotting the EC against Na/(Na+Ca) and Cl/(Cl+HCO_3). Figure 4.5 shows that all the geothermal springs/boreholes were plotted in rock-water interaction zone, as reported by Durowoju *et al*. (2018) for Siloam and Tshipise springs. Thus, it shows that the groundwater chemistry in the studied areas is controlled mainly by rock-water interaction processes caused by the chemical weathering of the rock-forming minerals. Hence, this implies that weathering of aquifer material is the dominant process controlling the chemistry of the springs resulting in chemical budget of this water (Aghazadeh and Mogaddam, 2010). Along the path of groundwater movement from recharge to discharge areas, several chemical reactions take place with the solid phase. These chemical reactions vary temporally and spatially, depending on the chemical nature of the initial water, geological formations and residence time (Aghazadeh and Mogaddam, 2010).

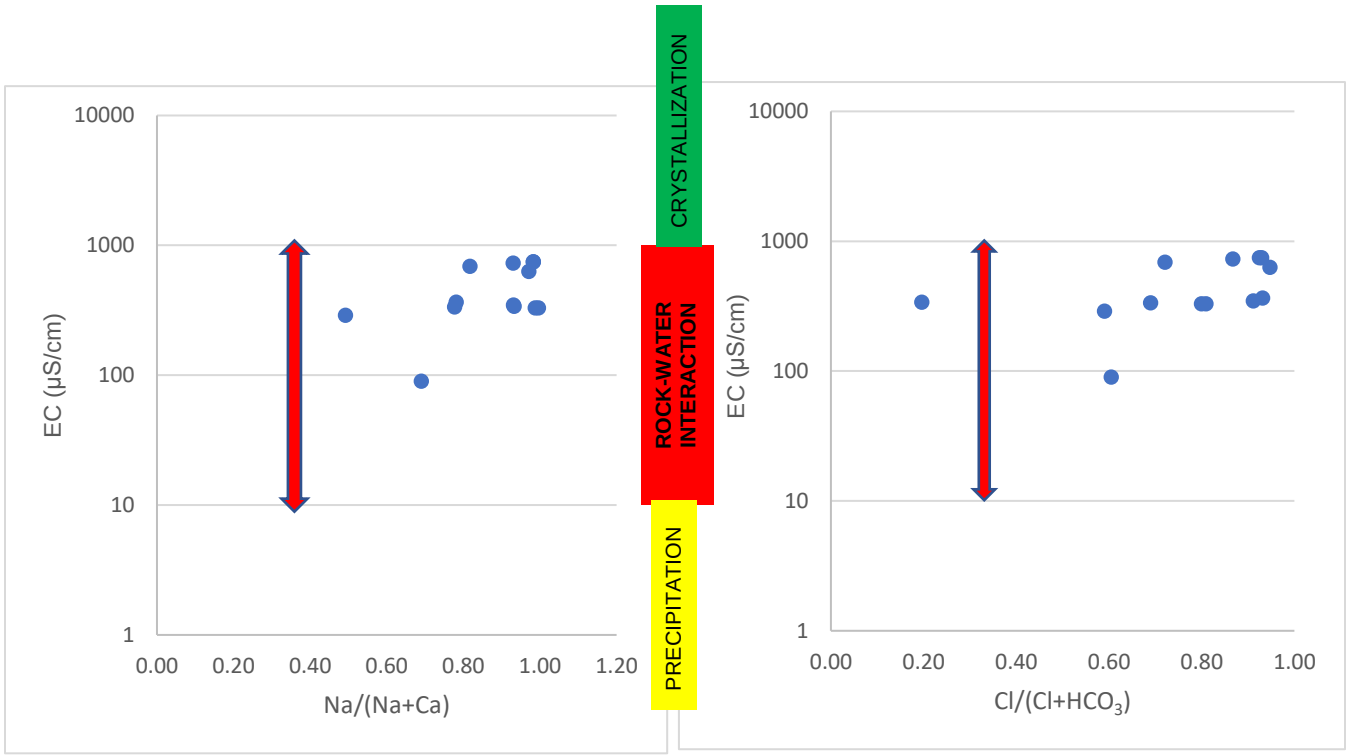

Figure 4.5: Mechanisms controlling chemistry of the geothermal springs and boreholes-Gibbs plot of samples in blue shaded circles.

Datta and Tyagi (1996) and Lakshmanan *et al*. (2003) revealed that the plot of (Ca + Mg) against (HCO_3+SO_4) is also another tool to determine geochemical processes. It shows the distribution of geothermal water and borehole water between silicate and carbonate weathering processes that is used to assess the effects of the carbonate and sulfate mineral dissolution in the system (Figure 4.6), by distinguishing between carbonate and silicate weathering controlling factors. The water samples are distributed below and above the 1:1 line, which shows they are in the field of silicate or carbonate weathering, respectively (Figure 4.6). This contradicts findings from Durowoju *et al*. (2018), which reported that Siloam and Tshipise geothermal springs fall in silicate weathering zone. This could possibly be as a result of the sample size and instability of the rock-water interaction leading these chemical weathering (Lakshmanan *et al.,* 2003). Those groundwater samples that fall above the 1:1 line resulted from the effect of reverse ion change in the system which indicate carbonate weathering processes (Figure 4.6) which support the Gibb's diagram.

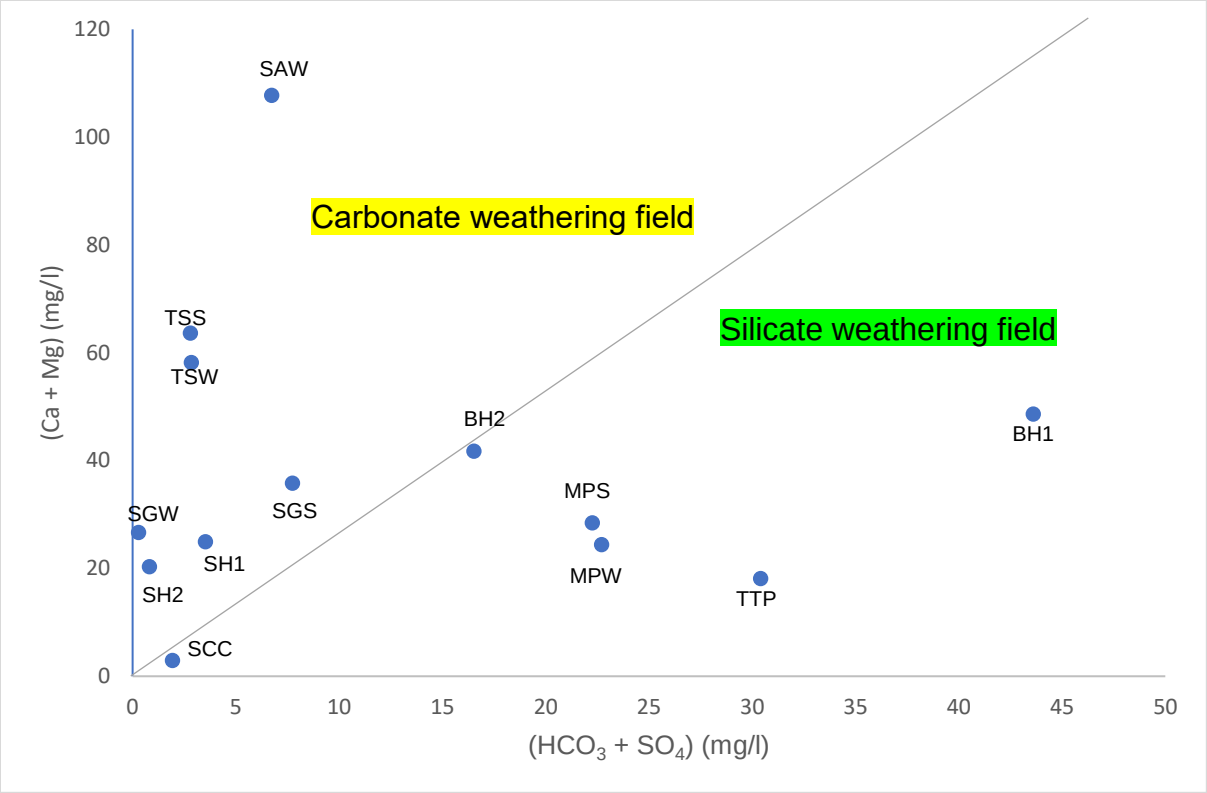

Figure 4.6: Plot (Ca+Mg) vs (HCO_3+SO_4) for the geothermal springs/boreholes' samples within the Soutpansberg region. ● Samples of geothermal springs//boreholes.

Samples that fall above the 1:1 line mostly include geothermal springs, except for Mphephu (MPW and MPS) (Figure 4.6). All the tepid water (BH1, BH2, SCC and TTP) and Mphephu geothermal water fall below 1:1 line, which indicates silicate weathering. This further shows the contributions of the cation exchange, and carbonate and sulfate minerals dissolutions. There is the possibility that hot boreholes (SH1 and SH2) at Siloam share the same geochemical processes with the geothermal spring (SAW) suggesting interconnectivity between the two aquifers. Therefore, ion exchange processes between groundwater and the aquifer materials are relatively high. Hence, this shows that the plot of (Ca + Mg) against (HCO_3+SO_4) is in good agreement with Gibb's diagram.

The chloro-alkaline indices (CAI 1, 2) indicate the possible ion exchange reaction between groundwater and the host environment as suggested by Schoeller, (1977). Chloro-alkaline indices used in the evaluation of base exchange are calculated using equations 4.4 and 4.5 and results are presented in Table 4.3 and Figure 4.7.

$$CAI\text{-}1 = Cl - (Na + K)/Cl \quad \text{.....4.4}$$

$$CAI\text{-}2 = Cl - (Na + K) / (SO_4 + HCO_3 + NO_3) \quad \text{..... 4.5}$$

Table 4.3: CAIs for geothermal springs and boreholes within the Soutpansberg region and comparison with results of other studies

Sites		CAI-1	CAI-2
Sagole	SGW	-0.6	-0.85
	SGS	0.27	0.59
Tshipise	TSW	-0.07	-0.17
	TSS	-0.02	-0.04
	TTP	-0.01	-0.01
Mphephu	MPW	-0.31	-0.39
	MPS	0.55	1.57
Siloam	SAW	-2.38	-0.46
	SH1	0.21	1.21
	SH2	-0.67	-1.08
	BH1	-0.61	-0.94
	BH2	-0.69	-0.56
	SCC	0.26	0.28
Northeastern, Nigeria	GW	0.22 – 0.95	0.008 – 021[a]
Tamil Nadu, India	GW	0.29 – 1.22	0.05 – 0.85[b]
Andhra Pradesh, South India	GW	-4.4 – 0.30	-0.56 – 0.27[c]
Yinchuan, China	GW	-0.45 - 0.89	-0.35 – 0.56[d]
Northwestern, China	GW	-2.2 - -0.04	-1.48 – -0.08[e]

[a]Ishaku *et al*., 2011; [b] KrishnaKumar *et al*., 2014; [c] Nagaraju *et al*., 2014:
[d]Wu *et al*., 2015; [e]Liu *et al*., 2015.

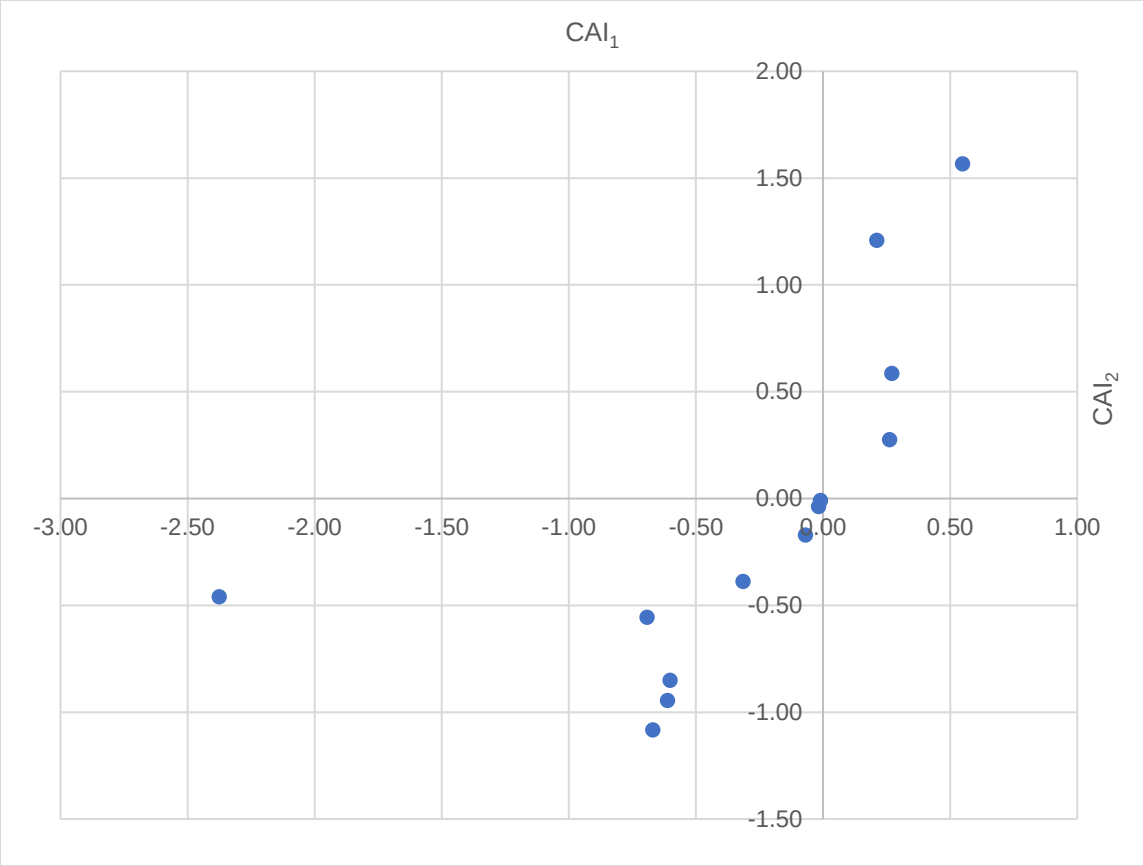

Figure 4.7: A plot of CAI_1 against CAI_2 of the groundwaters within Soutpansberg region.

CAI-1 varied from -2.38 to 0.55 and CAI-2 ranged from -1.08 to 1.57, which were negative in most samples (80%) suggesting the presence of base-exchange processes (Table 4.3, Figure 4.7). The direct exchange occurred when the indices are positive, meaning that there is ion exchange of Na and K from the water with Mg^{2+} and Ca^{2+} in the rock and vice versa (Durowoju *et al.,* 2018).

Ca^{2+} and Mg^{2+} exchange with Na^{+} sorbed on the exchangeable sites on the aquifer minerals, resulting in the decrease of Ca^{2+} and Mg^{2+} and increase of Na^{+} in the groundwater by reverse ion exchange (Schoeller, 1977; Glover *et al.,* 2012). This confirms that Ca^{2+}, Mg^{2+} and Na^{+} concentrations are interrelated through reverse ion exchange. Similar results were obtained in Northwestern China, which indicates cation–anion exchange (chloro-alkaline disequilibrium) (Liu *et al*., 2015). This study indeed clearly shows that Na^{+} and K^{+} are released by the Ca^{2+} and Mg^{2+} exchange, which a common form of cation exchange in the study areas. The remaining 20% of samples,

which had positive CAIs, indicated direct exchange of Ca^{2+} and Mg^{2+} from the aquifer matrix with Na^{+} and K^{+} from the groundwater (Figure 4.7). Similar results with positive CAIs were obtained from studies in Northeastern, Nigeria and Tamil Nadu, India. This explains the fact that alkaline earth elements were abundant. Studies from Yinchuan, China and South India showed both positive and negative CAIs (Table 4.3), which were similar to the results obtained from this study with more negative CAIs. This shows that the cation exchange is one of the major contributors to higher concentrations of Na^{+} in the groundwater.

Table 4.4 presents the correlation between the physicochemical and geochemical data in the studied areas. This is achieved by calculating the Pearson correlation coefficients with unevenly distributed data (Locsey and Cox, 2003). A strong relationship exists between pH, alkalinity, F^{-}, CO_3^{2-} and HCO_3^{-}; which implies that the waters are more alkaline. High F^{-} concentrations are associated with alkaline medium, hence, this explains the presence of high F^{-} content in the studied groundwater/spring water. There are strong positive correlations between total dissolved solids (TDS) and cations such as Na^{+} and K^{+}; anions such as F^{-}, Cl^{-}, NO_3^{-} and SO_4^{2-}. Temperature shows a weak correlation with SAR, EC, TDS, Alkanity, Na^{+}, K^{+}, Cl^{-}, SO_4^{2-} and HCO_3^{-} ($R^2 < 0.5$); and a strong correlation with pH, F^{-} and CO_3^{2-} ($R^2 > 0.5$). This implies that temperature favours the dissolution of soluble solid in water (Odiyo and Makungo, 2012). Also, temperature shows a strong negative correlation with Ca^{2+} and Mg^{2+}, which implies that increase in the water temperature leads to decrease in concentrations of Ca^{2+} and Mg^{2+} in water. Again, this accounts for lower concentrations of Ca^{2+} and Mg^{2+} in the studied groundwater/spring water.

Fluoride shows very strong positive correlations with Na^{+} and K^{+} but weak negative correlations with Ca^{2+} and Mg^{2+}. This also justifies the presence of high F^{-} content in the boreholes and geothermal spring water since the most dominant cation is sodium (Durowoju *et al.,* 2015). There are also strong correlations between Na^{+} and other anions such as Cl^{-} and $SO4^{2-}$. This further justifies the fact that Na-Cl water type is mostly the dominant water type in the studied geothermal water and boreholes. As explained earlier, this water type is characteristic of deep groundwater that is influenced by ion exchange processes.

Table 4.4: Pearson correlation matrix of correlation among physicochemical variables in geothermal water and boreholes

	Temp	pH	SAR	EC	TDS	Alkalinity	Na	K	Ca	Mg	F	NO_3	Cl	SO_4	PO_4	CO_3	HCO_3
Temp	1.00																
pH	**0.71**	1.00															
SAR	0.49	0.47	1.00														
EC	0.13	0.21	0.38	1.00													
TDS	0.22	0.25	0.42	**0.96**	1.00												
Alkalinity	0.48	**0.55**	-0.15	-0.04	0.10	1.00											
Na	0.22	0.29	0.47	**0.96**	**0.99**	0.09	1.00										
K	0.03	0.13	0.25	**0.94**	**0.90**	0.08	**0.91**	1.00									
Ca	***-0.54***	-0.25	***-0.60***	0.22	0.08	0.06	0.05	0.36	1.00								
Mg	***-0.52***	-0.37	***-0.68***	-0.04	-0.20	-0.08	-0.23	0.09	**0.93**	1.00							
F	**0.69**	**0.61**	0.23	**0.61**	**0.66**	0.48	**0.66**	**0.57**	-0.09	-0.24	1.00						
NO_3	-0.37	-0.16	-0.06	0.40	**0.50**	-0.03	0.49	0.42	0.19	-0.01	0.09	1.00					
Cl	0.29	0.13	0.47	**0.85**	**0.82**	-0.25	**0.79**	**0.67**	-0.09	-0.22	**0.57**	0.19	1.00				
SO_4	0.40	0.09	**0.62**	**0.76**	**0.77**	-0.19	**0.75**	**0.70**	-0.19	-0.29	**0.52**	0.17	**0.84**	1.00			
PO_4	0.02	-0.23	-0.17	-0.06	-0.09	-0.22	-0.14	-0.12	0.14	0.30	0.08	0.07	0.21	0.18	1.00		
CO_3	**0.55**	**0.62**	-0.05	-0.09	0.08	**0.96**	0.07	-0.03	-0.16	-0.30	0.48	0.02	-0.24	-0.20	-0.22	1.00	
HCO_3	0.45	**0.52**	-0.19	-0.02	0.11	**1.00**	0.09	0.12	0.14	0.00	0.47	-0.05	-0.25	-0.18	-0.21	**0.93**	1.00

Values in bold are different from 0 with a significance level alpha=0.05

The plot of Na^+ against Cl^- is used to establish the role of evaporation for higher concentration of Na in groundwater (Figure 4.8). Gurdak *et al*. (2007) reported that the influence of semi-arid climate as intercalation in the soil zone enhances active evaporation in the study area. This implies that there is loss of groundwater quantity during summer by the action of evaporation resulting in an increase in salt concentration in groundwater.

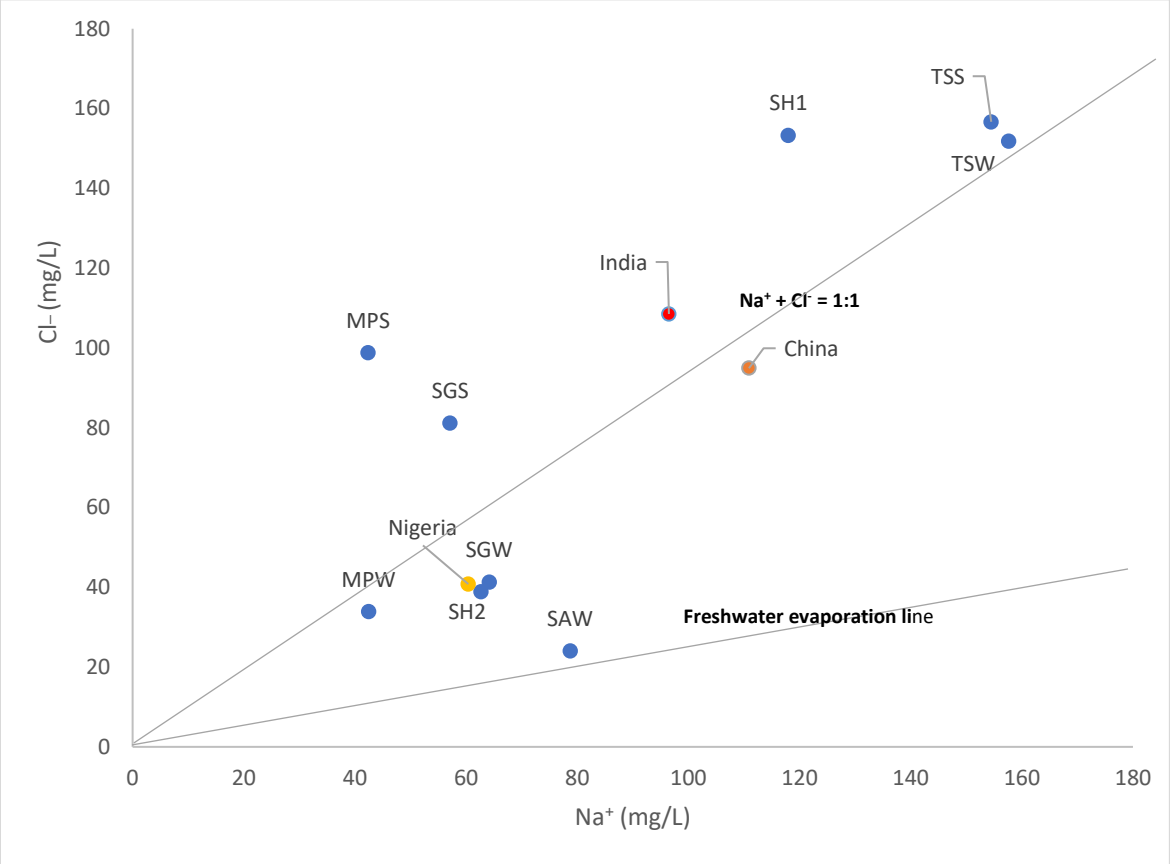

Figure 4.8: Relation between Na^+ and Cl^- in the geothermal springs within the Soutpansberg region and around the world.

Groundwater data from around the world (96.5, 60.4 and 110.9 mg/L for Na; 108.5, 40.8 and 94.9 mg/L for Cl in Tamil-Nadu, India (Krishna Kumar *et al*., 2014); Northeastern, Nigeria (Ishaku *et al*., 2011); and Northwestern, China (Wu *et al*., 2015) respectively were incorporated in Figure 4.8. All groundwater samples plotted above the freshwater evaporation line (Figure 4.8). This indicates that evaporation is one of the processes, controlling the geochemistry of geothermal springs (Gurdak *et al.,* 2007).

4.4 Evaluation of geothermal springs and boreholes water quality for drinking, domestic and irrigation purposes

4.4.1 Suitability for drinking and domestic purposes

Geothermal springs water is found in some rural communities, where it serves as an alternate source of domestic water. The community uses spring water for drinking and domestic purposes without proper understanding of its composition and potential health effect. Hence, there is need for sustainability and maintenance of the quality of geothermal spring water for drinking as it is one of the targets of the Sustainable Development Goals (SDGs), (2016). Water quality is assessed in comparison with national and international accepted permissible drinking limits (WHO, 2006).

Results were obtained to ascertain the suitability of the geothermal water/groundwater in the studied areas for drinking and domestic purposes based on the South African National Standards (SANS, 2015) and World Health Organisation (WHO) (WHO, 2006; 2011) standards (Table 4.5). Although, pH values have no effect on human health, it remains a crucial parameter because it affects other chemical constituents of water. Most of the geothermal water/groundwater falls within the recommended permissible drinking water limit of pH except for Siloam geothermal spring (SAW) and Siloam hot borehole (SH2) water. The following hydrochemical parameters in all geothermal water/groundwater fall within guidelines recommended by the WHO and SANS for drinking water; EC, TDS, Ca^{2+}, Mg^{2+}, Na^{+}, K^{+}, Cl^{-}, SO_4^{2-} and HCO_3^{-}. Whereas, fluoride concentrations were higher than the recommended guidelines except in Sagole geothermal spring (SGW – 0.77 mg/l), Siloam tap water (SCC – 0.00 mg/l) and Tshipise tap water (TTP – 0.15 mg/l). SCC and TTP are both treated tap water, hence they contain little or no fluoride. Also, the NO_3^{-} concentration in all the samples were within the permissible limit for drinking water except for BH 2. This could be attributed to anthropogenic factors (proximity to the pit latrine, application of fertilizer among others) within the vicinity of the borehole (Odiyo and makungo, 2018).

Generally, the geothermal water/groundwater is not fit for drinking due to high fluoride content (Odiyo and Makungo, 2012), except for the treated water such as water from SCC and TTP. This study also confirms previous findings from Olivier *et al*. (2011) and

Durowoju (2015) that the geothermal spring water is not fit for drinking purposes until the quality is evaluated and where necessary treated to compliance. Generally, the utilisation of the geothermal springs across the world is solely dependent on the chemical compositions. Hence, this study recommends that the geothermal springs within the Soutpansberg region should be used for direct heating in refrigeration, green-housing, spa, therapeutic uses, aquaculture, sericulture, concrete curing and coal washing. They could also be used for drinking and cooking if the fluorides and nitrates are managed where there are high non-compliance concentrations of either of the two or both (Odiyo and Makungo, 2018).

Table 4.5: Geothermal water and boreholes water quality within Soutpansberg and compliance to SANS (2015) and WHO (2011) drinking water standards

Parameters	WHO Limit	SANS Limit	Sample ranges	Remarks of samples that fall within the guideline
pH	6.5 – 8.5	6 - 9	7.17 – 9.39	ALL except SAW and SH2
EC (µS/cm)	750	750	90 – 746.7	ALL
TDS (mg/L)	500	450	10.78 – 423.07	ALL
TH (mg/L)	100	NS	0.73 – 134.28	ALL except BH1 which is moderately hard
Ca (mg/L)	75	NS	0.29 – 27.80	ALL
Mg (mg/L)	30	NS	0.00 – 15.80	ALL
Na (mg/L)	200	<200	1.69 – 170.00	ALL
K (mg/L)	100	50	1.06 - 5.15	ALL
F (mg/L)	1.5	≤1.5	0.00 – 6.51	NONE except SGW, SCC and TTP
Cl (mg/L)	250	<300	3.73 -156.67	ALL
NO_3 (mg/L)	10	<11	0.17 – 83.95	ALL except BH2
SO_4 (mg/L)	250	<500	0.48 – 51.78	ALL
HCO_3 (mg/L)	200	NS	2.44 – 98.75	ALL

NS – Not Stipulated, TH - Total Hardness

The hardness of water is attributed to the presence of alkaline earth metals, that is Ca^{2+} and Mg^{2+}, and they are very important property of water for domestic uses. Although, hardness has no known adverse effect on human health, it has an adverse effect on aesthetic property of the water, due to the unpleasant taste. Hardness has the following

effects: prevents formation of lather with soap, increases the boiling point of water and causes encrustation in water supply distribution system (Ako, 2011). Durvey *et al*. (1991) reported that long term consumption of extremely hard water might lead to an increased incidence of urolithiasis, anencephaly, perinatal mortality, cancer and cardiovascular disorder. In addition, high range of total hardness (TH) in water may cause corrosion in the pipe when certain heavy metals are present (Garg *et al.,* 2009). Hardness of water is usually expressed as total hardness and is calculated by equation 4.6 (Todd, 1980):

$$TH = 2.5\,Ca + 4.1\,Mg \quad \text{.....4.6}$$

Where TH: total hardness as $CaCO_3$ in mg/l, Ca: Ca^{2+} concentration in mg/l, Mg: Mg^{2+} concentration in mg/l.

In this study, most of the water is classified to be soft except for BH1 that has moderately hard water (Table 4.5). Studies have shown that there is a link between TH and cardiovascular diseases. For instance, Dissanayake *et al*. (1992) reported a negative correlation between TH and leukemia and other cardiovascular disease in Siri-Lanka. Perkin *et al*. (2016) reported hard water as an environmental trigger for eczema in children. Hence, soft waters are recommended because they can be helpful towards avoiding the irritation and improving certain health problems. Therefore, the hardness of these geothermal springs and boreholes were within the WHO recommendations except for BH1, which is moderately hard. Hence, they are suitable for domestic purposes due to their softness (based on these findings).

4.4.2 Irrigation purposes

The suitability of the geothermal water and boreholes for irrigation purposes is measured by several parameters. Tables 4.1 and 4.6 show these parameters; electrical conductivity (EC), sodium adsorption ratio (SAR), residual sodium carbonate (RSC), percentage sodium (SP), Kelly's ratio (KR), permeability index (PI) and Wilcox (US salinity) classification indices. Salinity is one of the major negative environmental impacts leading to loss of production, which is associated with irrigation. Salinity greatly affects crop germination and yield and can render the soil infertile. Hence, the need to assess the water quality for irrigation purposes. For example, low quality irrigation waters could be suitable for sandy soil but hazardous to clayey soil and vice versa. Richards (1954)

classified SAR and EC values for irrigation water into four categories: low (EC ≤ 250 µS/cm, SAR < 10), medium (EC = 250 - 750 µS/cm, SAR= 10 - 18), high (EC = 750 – 2,250 µS/cm, SAR= 18 - 26) and very high (EC = 2,250 – 5, 000 µS/cm, SAR > 26). Ako (2011) reported that excessive solutes in irrigation water constitute a problem in semi-arid areas where water losses through evaporation is high. In this study, the geothermal water and borehole has EC values ranging from (90 – 746.67 µS/cm) and thus have low to medium salinity which make them suitable for irrigation. Sodium percentage (SP) is a good parameter to assess the suitability of water for irrigation (Wilcox, 1958). High SP in soil causes impairment of tilth, dispersion and low permeability of soil. SP in geothermal water/groundwater was calculated using equation 4.7;

$$SP = (Na + K) / (Ca + Mg + Na + K) * 100 \quad \text{.....4.7}$$

Table 4.6: Index methods for groundwater suitability

SITES	CODES	RSC	PI	KR	SP
Sagole	SGW	10.97	104.39	221.38	99.56
	SGS	0.19	92.41	7.38	88.43
Tshipise	TSW	10.12	100.42	55.52	98.28
	TSS	9.71	100.42	55.38	98.28
	TTP	-16.37	45.27	0.6	40.13
Mphephu	MPW	-7.45	71.17	1.87	66.25
	MPS	14.93	69.75	1.9	66.65
Siloam	SAW	108.15	103.75	11.7	92.36
	SH1	6.81	99.5	33.43	97.16
	SH2	11.35	103.64	77.41	98.77
	BH1	-12.49	77.31	2.84	74.76
	BH2	2.4	93.28	10.29	91.36
	SCC	0.51	89.84	0.88	58.76

RSC - Residual sodium carbonate, PI - Permeability index, KR - Kelly's ratio, SP - Sodium percentage.

Pair (1983) reported that water with SP greater than 60% may result in sodium accumulations that will cause a breakdown in the soil's physical properties hence, not suitable for irrigation. This implies that all the samples from the study areas are not suitable for irrigation (> 60%) (Table 4.6) except for SCC and TTP, which are treated water. The sodium hazard is often expressed as SAR and is plotted against the conductance in a Wilcox diagram (Figure 4.9).

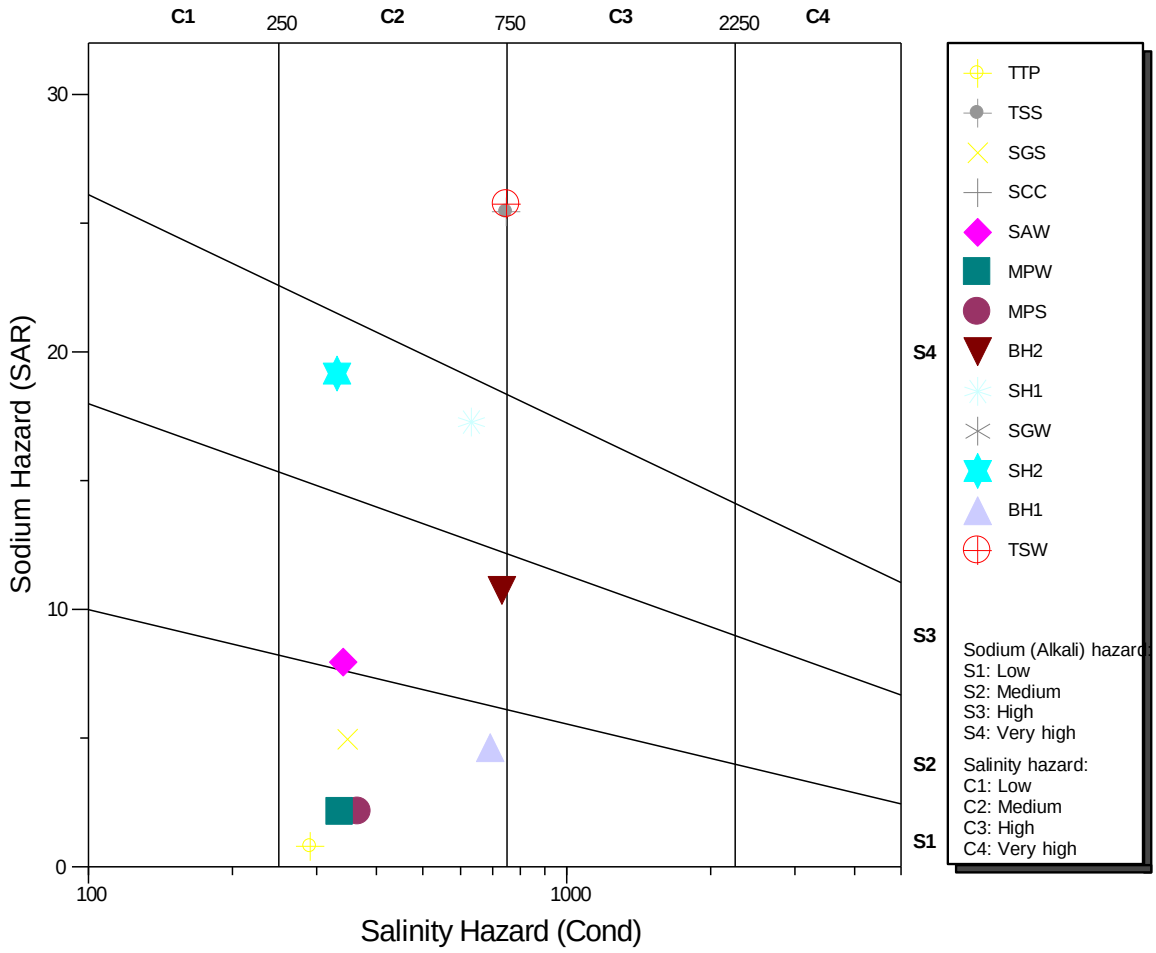

Figure 4.9: Wilcox (US salinity) diagram of geothermal spring water and boreholes samples for winter and summer from the study areas.

Most of the geothermal water and boreholes are in C2S1 (medium salinity and low alkalinity) and C2S2 (medium salinity and medium alkalinity) fields which are suitable for irrigation. Siloam hot boreholes (SH1 and SH2) fall in C2S3 (medium salinity and high

alkalinity) and Tshipise geothermal water (TSW and TSS) falls in (medium salinity and very high alkalinity), which implies that they are suitable for irrigation. Generally, groundwater is of typical quality with possible exception. For example, similar studies in Andhra Pradesh (South India) and Yinchuan (China) showed that the majority of the groundwater samples possess high salinity with low sodium (C3–S1) which is not suitable for irrigations (Nagaraju *et al.,* 2014; Wu *et al.,* 2015).

The water quality diminishes when the total carbonate levels exceed the amount of Ca^{2+} and Mg^{2+}. Hence, the residual sodium carbonate (RSC) index is calculated by equation 4.8 (Eaton 1950);

$$RSC = (CO_3^{2-} + HCO_3^-) – (Ca^{2+} + Mg^{2+}) \text{ ……..……4.8}$$

The classification of irrigation water according to the RSC values is such that waters containing more than 2.5 meq/l of RSC are not suitable for irrigation, while those having 1 to 2.5 meq/l are marginal and those from 0 –1 meq/l are good for irrigation (Eaton, 1950). Based on this classification, some of the water samples are not suitable for irrigation except for SGS, TTP, MPW, SCC and BH1 that are good for irrigation. The permeability index (PI) values also indicate the suitability of groundwater for irrigation and it is defined as follows (Equation 4.9):

$$PI=100*([Na^+] +\sqrt{} [HCO_{3-}])/([Na^+] + [Ca^{2+}] + [Mg^{2+}] \text{ …….....4.9}$$

The World Health Organisation (WHO) (WHO, 1989) uses a criterion for assessing the suitability of water for irrigation based on PI. PI is classified under class I (>75%), class II (25-75%) and class III (<25%) orders, with class I and II good for irrigation. According to the PI values (Table 4.5), the geotherma/borehole water can be designated as class I and II and this implies that the water is good for irrigation (Doneen, 1964; Aastri, 1994). Since there is little or no difference in the PI per season for different sites, the groundwater has no permeability and infiltration problems.

Kelly's ratio (KR) is computed by equation 4.10:

$$KR= Na^+ / (Ca^{2+} + Mg^{2+}) \text{ ……..……4.10}$$

The concentration of Na^+ measured against Ca^{2+} and Mg^{2+} is known as the Kelly's ratio (KR), based on which the quality of irrigation water can be assessed (Kelly, 1946). Kelly's

ratio of water is categorised into suitable if KR is <1, marginal when KR is 1-2 and unsuitable if KR is >2 (Kelly, 1946). According to the classification, most of the geothermal water/groundwater were not suitable for irrigation except for TTP and SCC (Good), and MPW and MPS (Marginal). This corroborates with the sodium percentage (SP), which depicted that most of the samples in the studied sites are not suitable water for irrigation.

From the various indices employed in this study; SAR, RSC, PI and EC showed that geothermal springs and for RSC, quite a number of geothermal springs and boreholes were suitable for irrigation purposes except for KR and SP for which most geothermal springs/boreholes were not suitable for irrigation. According to Wilcox (US salinity) classification, the springs are suitable for irrigation. Hence, it can be concluded that the geothermal springs should be used for irrigation.

4.5 Isotopic composition of rainwater, geothermal springs and boreholes

4.5.1 Isotopic compositions of the rainwater

Table 4.7 shows the isotopic composition of rainwater occurrences between May 2016 and April 2017 at the University of Venda, Thohoyandou. According to the International Atomic Energy Agency (IAEA) (IAEA-WMO 2015), warm regions are characterised by more enriched isotopic values (+ve) of ^{2}H and ^{18}O; while cooler regions are characterised by more depleted isotopic values (-ve). The study area falls under the hot semi-arid region of the country and it is expected to have more enriched isotopic values of ^{2}H and ^{18}O in the rainwater samples, but seasonal effect is observed in the study. Figure 4.10 shows that the area has most of its rainfall from November 2016 to February 2017 which constitute part of the summer when samples (ME06 – ME011) were collected and the isotopic values were more depleted (Figure 4.10; Table 4.7). Whereas more enriched isotopic values were obtained from May to October 2016 (ME01 – ME05) and April 2017 (ME12). This could be due to amount effect, i.e., the lesser the volume of rainfall, the higher the $\delta^{18}O$ or δD content (Dansgaard, 1964; Coplen *et al.,* 2000) (Figure 4.10). This proves that there is a strong negative correlation between the rainfall amount and isotopic composition (δD or $\delta^{18}O$). The amount effect which is a characteristic of tropical low-latitude precipitation, has also been observed in other studies such as in Cameroon

(Njitchoua *et al.,* 1999; Kuitcha *et al.,* 2012; Wirmvem *et al.,* 2014), Nigeria (Mbonu and Travi, 1994), Niger (Taupin *et al.,* 2000; Risi *et al.,* 2008), Ghana (Adomako *et al.,* 2015), Ethiopia (Kebede and Travi, 2012; Kebede, 2013), Costa Rica (Sanchez-Murillo *et al.,* 2013) and India (Rai *et al.,* 2013).

Table 4.7: Stable isotopic compositions of contemporary rainwater in Thohoyandou

Sample Code	δD (‰)	$\delta^{18}O$ (‰)	d - excess (‰)
ME01	16.0	-0.48	19.81
ME02	22.1	1.94	6.58
ME03	15.2	-0.74	21.09
ME04	1.3	-1.81	15.78
ME05	18.0	3.07	-6.60
ME06	-49.6	-7.22	8.14
ME07	-76.3	-10.78	9.93
ME08	-4.2	-2.18	13.25
ME09	-41.9	-6.75	12.03
ME10	-15.9	-3.89	15.22
ME11	-24.5	-5.19	17.06
ME12	22.7	1.61	9.77
Mean Value (s)	-9.8	-2.7	11.8

The rainwater samples collected from the area of study (event rainfall) showed a wide range of stable isotopes compositions (Table 4.7). The δD values of the rainfall varied from -76.3 ‰ to +22.7 ‰ (SMOW) with a weighted mean of – 9.8 ‰ and $\delta^{18}O$ values ranged from -10.78 ‰ to +3.07 ‰ (SMOW) with a weighted mean of -2.7 ‰ (n=12). This shows the degree of evapotranspiration in the study area. The d-excess values varied widely from -6.60 to 21.09 ‰ with a mean d-excess value of 11.8 ‰. As shown in Table 4.7, the annual mean d-excess value in rainwater was above 10 ‰ of the ocean moisture (Dansgaard, 1964), which is the primary source of most rainfall, although, transpired moisture can be an important moisture source for many terrestrial regions (Brubaker *et*

al., 1993). Hence, this implies that high values (>10 ‰) suggest an additional source of moisture, such as moisture recycling among others (Wirmvem *et al.,* 2016).

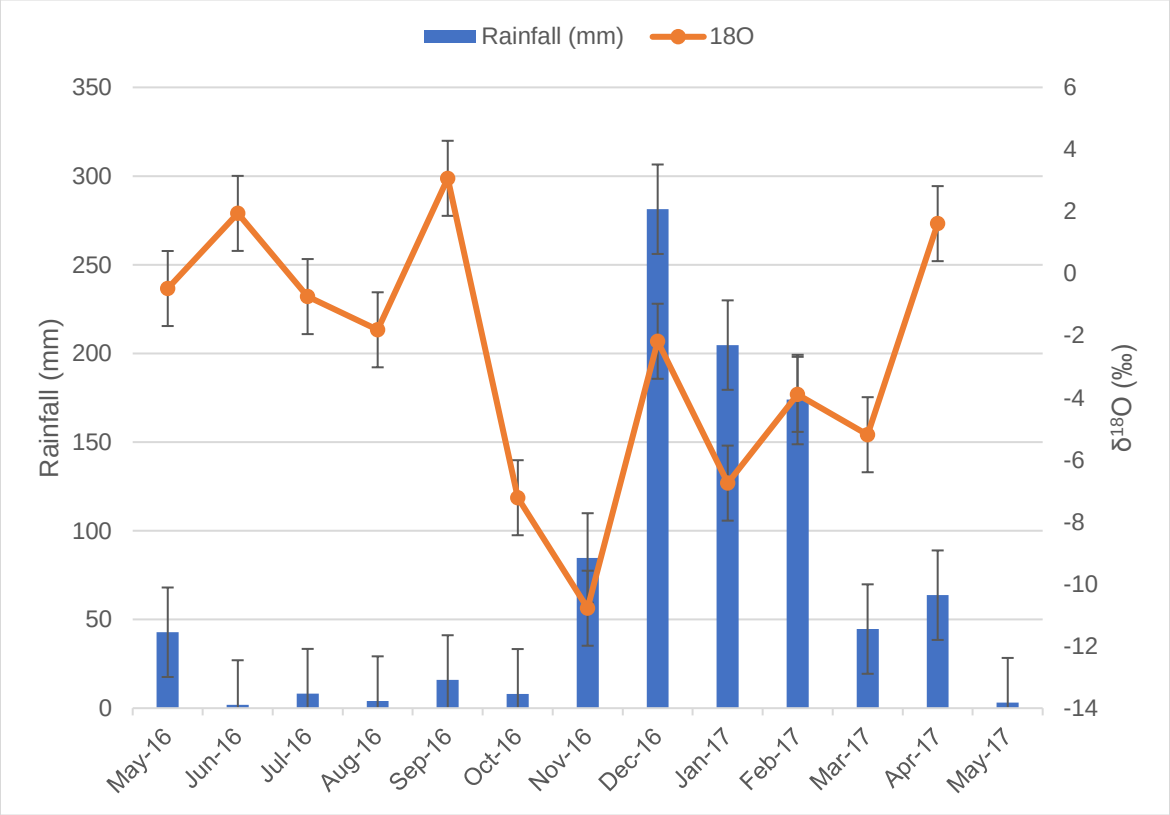

Figure 4.10: Variation of $\delta^{18}O$ as a function of the monthly rainfall from May 2016 to May 2017 in Thohoyandou.

It should be noted that the weather and climate differ from place to place with variations in rainfall, temperature, wind, which contribute to the shift in the local meteoric water line (LMWL) compared to the GMWL (Figure 4.11). From the study, the amount effect yielded isotopically light rainfall and hence it seems that the weather is responsible for determining where in the meteoric water line the data falls on. On the other hand, the meteoric water line also shifts from a point to an outlier position below/above the GMW line, by kinetic effects associated with evaporation (Gat, 1996; Rai *et al.,* 2013; Sanchez *et al.,* 2013 and Wirmvem *et al.,* 2016). This accounts for the slight differences in the LMW lines for Cape Town, Pretoria and Thohoyandou (Figure 4.12).

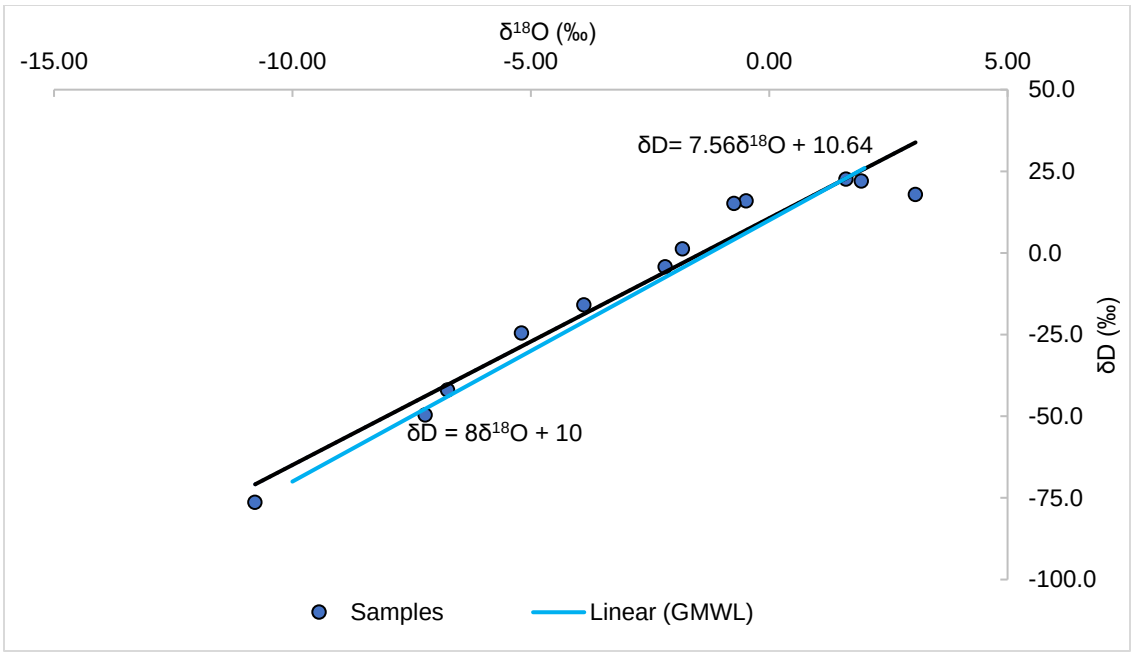

Figure 4.11: Conventional $\delta^{18}O$–δD relationships of rainwater from May 2016 to May 2017 at Thohoyandou.

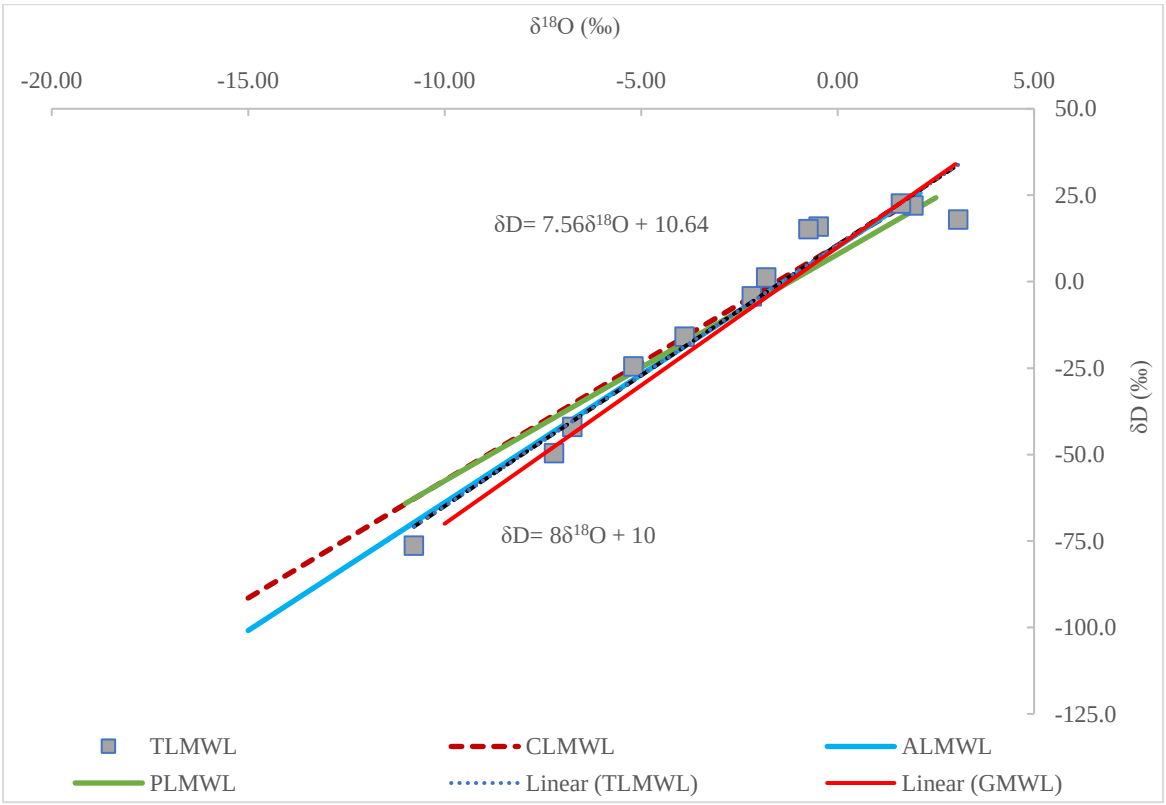

Figure 4.12: The relationships show the Thohoyandou local meteoric water line (TLMWL) in comparison with the Global meteoric line (GMWL), Africa local meteoric water line (ALMWL), Cape Town local meteoric line (CLMWL) and Pretoria local meteoric water line (PLMWL).

The observed wide ranged d-values of rainwater in one hydrological year resulting in variations in the stable isotopes composition of rainwater, could be caused by the seasonality (basically winter and summer). The distinctive variations in rainfall occurrence for isotopic signatures offer a tool to determine the timing of groundwater recharge within Soutpansberg Group. Most of the rainfall occurs during the summer season, hence there is evidence of depleted values with heavy rainfall, but enriched values are associated with low rainfall (Figure 4.10) (Wirmvem *et al.,* 2016). The observed heavy and depleted $\delta^{18}O$ values in the rainwater within the period (Figure 4.10) could possibly be associated with the higher vertical velocity of ascending air masses and smaller effect of exchange between atmospheric air leading to more rain out fractionation effect (Joseph *et al.,* 1992). Meanwhile, enriched isotopic values at the edges of the rainy season are likely due to large exchange with atmospheric vapour, and partial evaporation of the rain drops during rainfall (Taupin *et al.,* 2000; Gat, 2010; Rai *et al.,* 2013).

The $\delta^{18}O$–δD plot of the one-hydrological year data gave the regression line that represents the local meteoric water line for Thohoyandou (TLMWL):

$$\delta D = 7.56\delta^{18}O + 10.64 \quad \text{.....4.11}$$

Equation 4.11 shows nearly similar slope to the GMWL of Craig (1961) but relatively high d-intercept (Figure 4.11). This implies that the process of rain formation in Thohoyandou within the Soutpansberg Group, Limpopo Province occurs in equilibrium conditions with minor evaporation effect when raining. The slightly high d-excess value is an indication that the rainwater is formed from the water vapour evaporation near the land surface that is, either by re-condensation of the evaporated rainfall or evaporation of surface waters (Russel and Johnson, 2006). The slope also suggests that the raindrops were not notably affected by evaporation effect (Dansgaard, 1964; Craig, 1961; Rozanski *et al.,* 1993) including small and enriched rain event from May to August of 2016 with high d-excess values (Table 4.7).

The stable isotopic composition (δD and $\delta^{18}O$) of the rainwater samples for Thohoyandou was compared to the Global Meteoric Water Line (GMWL) ($\delta D = 8\delta^{18}O + 10$; Craig, 1961), Africa local meteoric water line (ALMWL) ($\delta D = 7.4\delta^{18}O + 10.1$; Cohen *et al.,* 1997), Cape Town local meteoric water line (CLMWL) ($\delta D = 6.8\delta^{18}O + 10.5$; Harris *et al.,* 1999) and

Pretoria local meteoric water line (PLMWL) ($\delta D = 6.55\delta^{18}O + 7.9$; Abiye, 2011) (Figure 4.12). Slight differences in the d-intercept of the meteoric lines (10 for GMWL; 10.1 for ALMWL; 10.5 for CLMWL; 7.9 for PLMWL and 10.64 for TLMWL) may be attributed to changing conditions at the source of atmospheric moisture (Gonfiantini *et al* 2001) and local climatic effects such as re-evaporation (Taupin *et al.,* 2000; Salati *et al.,* 1979 and Lui *et al.,* 2014). From the ALMWL, it can be deduced that the rain formation in Africa occurs under equilibrium with minor evaporation effect during rain drop. A study by Joseph *et al*. (1992) reported that there was no continental effect (distance from the coast effect) in Africa, which was supported by studies from Cameroon, Nigeria, Ethiopia and Kenya (Kebede and Travi, 2012; Kebede, 2013; Muhammad and Sadiq, 2014; Wirmvem *et al.,* 2016). The lack of evidence of the continental effect on stable isotopes ratios of rainwater is also evident in Thohoyandou.

The climatic and geographic factors play a vital role in differentiating the LMW lines from the GMW line. For instance, Cape Town gets most of its rainfall in winter compared to Thohoyandou that gets its rainfall in summer. The generated local meteoric water line (TLMWL) is useful in assessing the origin and mechanism of groundwater recharge in the locality. Recharge value can be obtained by integrating rainfall value with the stable isotope values (D and ^{18}O). Integrated recharge values are calculated by multiplying the $\delta^{18}O$ and δD values recorded for each month, by the fraction of rainfall that fell in that month, the fraction being calculated as a rainfall fraction of all the months collected (Diamond, 1997).

Salati *et al*. (1979) explained that during evaporation, high d-excess value is obtained when there is an increase in the evaporated moisture, such that precipitation from such moisture decreases in residual moisture. In this study, about 60% of the samples had d-excess values greater 10‰ (Table 4.7). The d-excess value is useful for the determination of the relative contributions of inland moisture and oceanic moisture to groundwater recharge as well as the conditions of recharge. Also, the depletion effect has been called the "continental effect" and results in lighter stable isotope ratios when moving away from the ocean and into the continent. The higher d-intercept further reflects a possibility of an additional supply of recycled regional moisture across the region. This implies that the continental effect is not affected by inland moisture from vegetation and other water

bodies in the region. The generated TLMWL was used in the interpretation of the source and geochemical processes of groundwater within the region.

4.5.2 Isotopic compositions of geothermal springs and boreholes

The utilisation of stable isotopes is vital in the assessment of water resources, especially in groundwater when water infiltrates and reflects the underlying isotopic composition of the recharging rainwater. The generated local meteoric water line will be useful in the proper understanding of the geothermal springs and boreholes within the studied areas. Generally, groundwater holds its isotopic signature except there is blending or dilution with waters with various isotopic compositions or heat up at about 60 – 80 °C (Gat and Gonfaintini, 1981). The summarised data for δD and $\delta^{18}O$ values for the investigated geothermal springs water and boreholes are presented in Table 4.8. The observed values vary from -5.73 to -4.98 ‰ for $\delta^{18}O$ and -33.5 to -33.2 ‰ for δD at Tshipise geothermal spring; -5.82 to -5.08 ‰ for $\delta^{18}O$ and -30.7 to -30.4 ‰ for δD at the Sagole geothermal spring; -4.82 to -4.92 ‰ for $\delta^{18}O$ and -26.1 to -24.6 ‰ for δD at Mphephu geothermal spring for both winter and summer seasons, respectively. At Siloam, the geothermal spring has - 5.41 ‰ for $\delta^{18}O$ and -27.4 ‰ for δD; thermal borehole has - 5.30 ‰ for $\delta^{18}O$ and -27.3 ‰ for δD; tepid borehole has - 5.30 ‰ for $\delta^{18}O$ and -28.8 ‰ for δD and the community tap water from the municipality has – 4.20 ‰ for $\delta^{18}O$ and -11.0 ‰ for δD. Also, at Tshipise the treated tapwater has – 2.16 ‰ for $\delta^{18}O$ and -11.8 ‰ for δD.

δD and $\delta^{18}O$ values were plotted to groundwater samples and gives a clear understanding of the origin and recharge processes (Figure 4.13). It was observed that the geothermal springs at Tshipise, Sagole and Mphephu were more depleted in winter as compared to summer season. This could be attributed to the paleoclimatic effect which makes groundwater isotopically depleted with respect to modern waters (Kebede, 2013). This is indicative of a colder climate in winter season compared to summer season. Although, most of the rainfall within Soutpansberg occurred during summer, the groundwaters were more depleted in winter than summer (also showing seasonal effect). Hence, there is no amount effect observed, but the temperature effect leading to evaporation resulting to slightly higher values of $\delta^{18}O$ and δD in summer was observed. The isotopic signatures

of the groundwaters were more depleted in winter than in summer which negates the amount effect.

Table 4.8: Mean values of $\delta^{18}O$ and δD for the geothermal waters and boreholes with other parameters

Sites	$\delta^{18}O$ (‰)	δD (‰)	TEMP (°C)	EC (µS/cm)	Cl (mg/l)
TSW	-5.73	-33.5	54.6	746.67	151.86
TSS	-4.98	-33.2	55.4	745	156.67
SGW	-5.82	-30.7	42.4	330	41.34
SGS	-5.08	-30.4	44.8	347.33	81.15
MPW	-4.92	-26.1	41.3	335	33.9
MPS	-4.82	-24.6	42.7	365	98.82
SAW	-5.41	-27.4	67.7	340	24.11
SH 1&2	-5.3	-27.4	46.3	480	96.1
BH 1&2	-5.3	-28.8	21.9	710	91.63
TTP	-2.16	-11.8	22.5	290	20.2
SCC	-4.2	-11	20.1	90	3.73

Figure 4.13 on isotopic data differentiates between the three possible types of origin of geothermal water, i.e. magmatic, oceanic and meteoric. Ranges of $\delta^{18}O$ and δD of all the geothermal water samples are -5.7 to -4.8 ‰ and –33.5 to -24.6 ‰ respectively (Table 4.8). These data showed no presence of any significant amount of magmatic water, which generally has $\delta^{18}O$: +6 to +9 ‰ and δD: -40 to -80 ‰ (Pearson and Rightmire, 1980; Giggenbach, 1992). The possibility of oceanic origin of these waters is ruled out because $\delta^{18}O$ and δD are not approximately 0‰ (Craig, 1961). The isotopic compositions of groundwater were significantly lighter than those of modern rainwater, indicating that such

groundwater could possibly originate from seepage of meteoric water in the past during colder climates (Yeh and Lee, 2018). Hence, the origin of these waters is possibly meteoric. The isotopic ranges of the geothermal springs/groundwater are relatively reflective of rainwater signature (δD = -9.8‰ and $\delta^{18}O$ = -2.7‰). This indicates that the groundwater came from precipitation that took place in the high mountain of the Soutpansberg mountain range. Most groundwater samples might have derived from the infiltration of local precipitation, with significant contribution of another type of water in the deeper part of the aquifer.

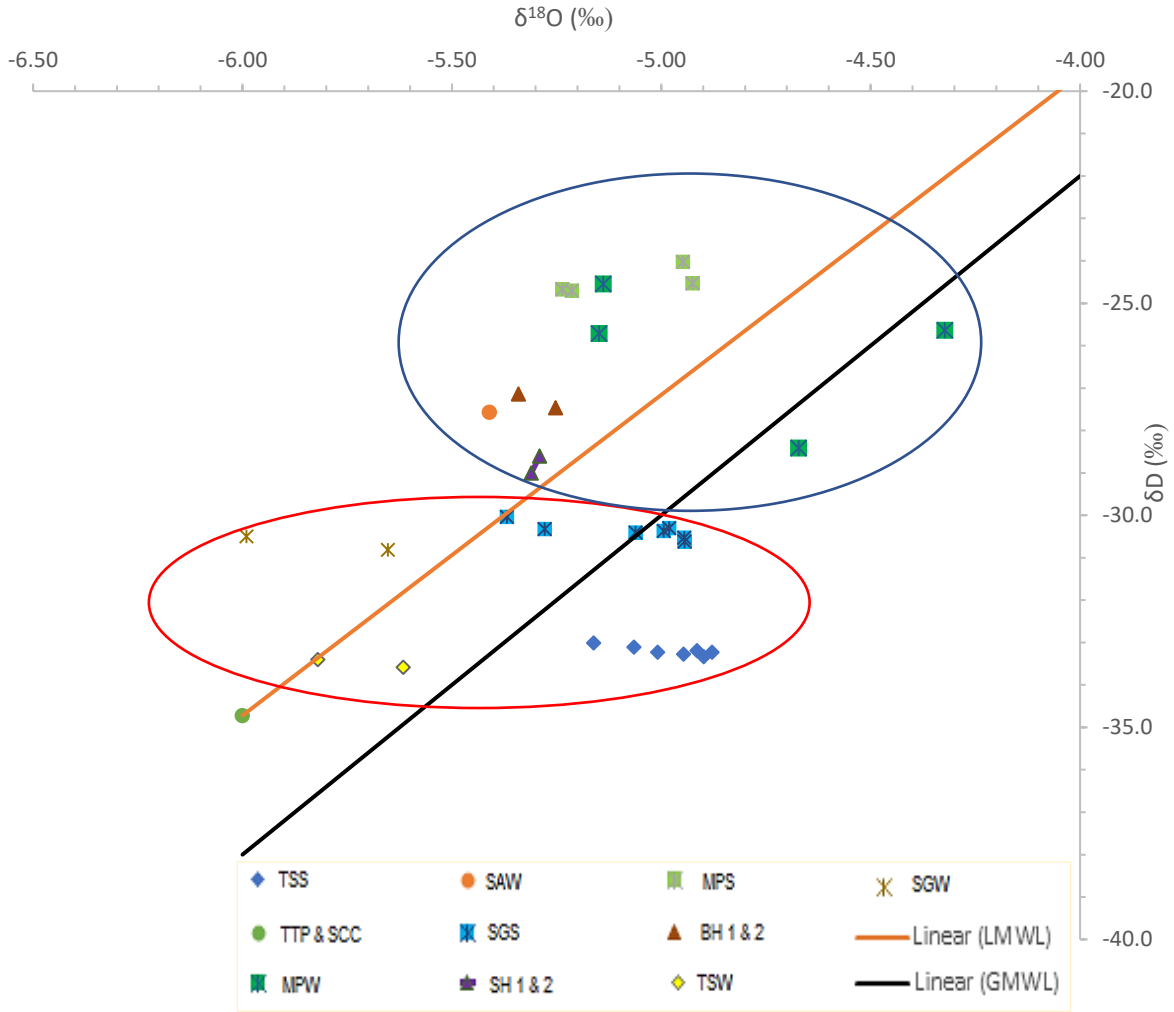

Figure 4.13: Variation of δD and $\delta^{18}O$ values of the geothermal springs and boreholes within Soutpansberg region.

The convectional δD against $\delta^{18}O$ diagram shows that the geothermal springs and various boreholes plot close to the local meteoric water line (LMWL) (Figure 4.13), giving an indication of meteoric origin, which implies that rainfall is the fundamental source of these groundwaters (Figure 4.14). However, some of the samples (TSW, TSS, SGS) fall below the LMWL, which implies that they were mainly subjected to evaporation before or during their underground transit (Gat, 2010). These could be achieved by local processes such as selective infiltration, direct percolation through the faults, degree of differentiation both on land surface and in the unsaturated (vadose) zone and mixing mechanism from surface water and irrigation processes (Ako *et al.,* 2011). Figure 4.14 shows the conceptual model for the studied groundwater within Soutpansberg.

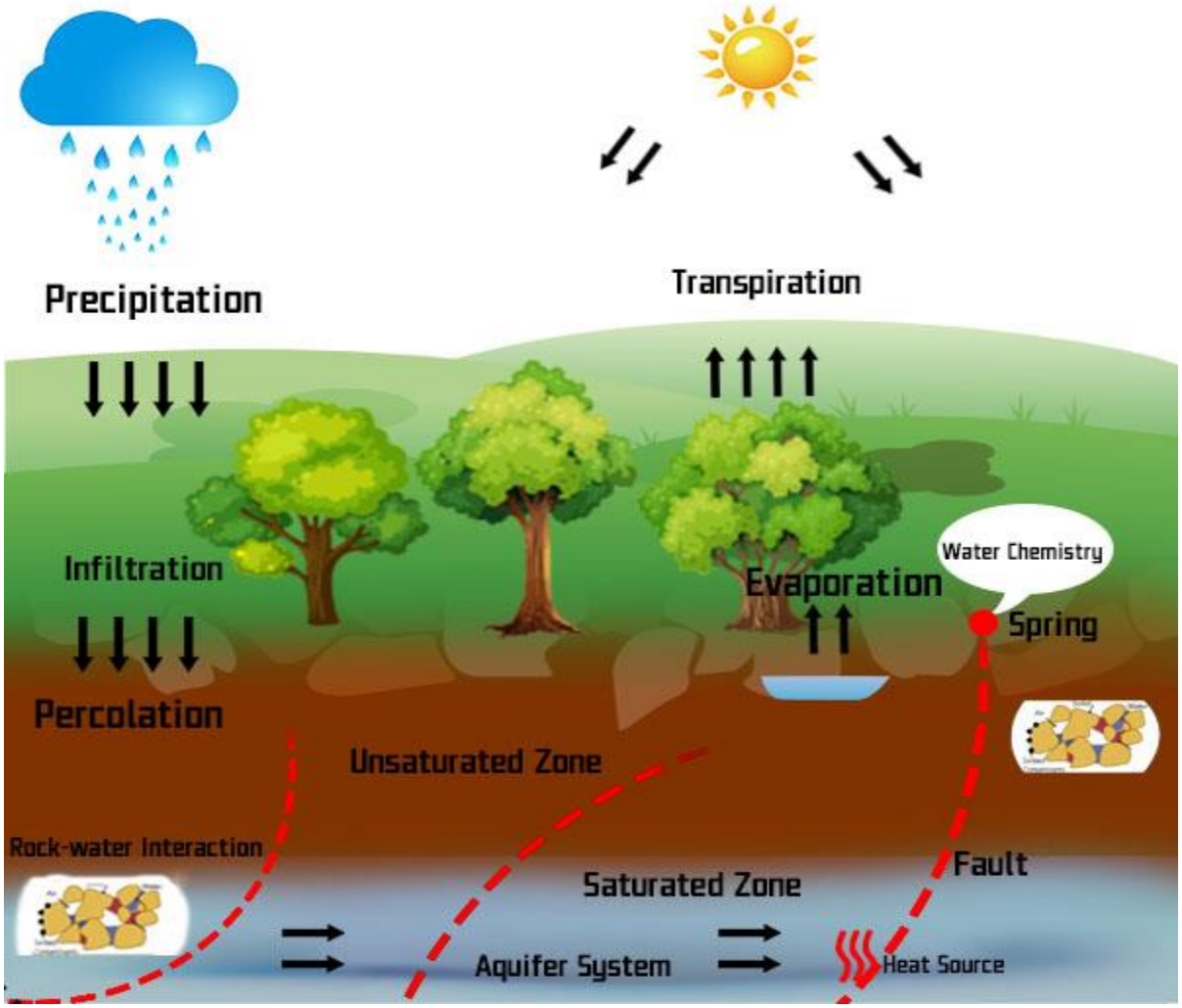

Figure 4.14: Conceptual model of the studied groundwater within Soutpansberg

Other samples plotted above the LMWL, which indicate the average isotopic composition of rainwater resulting from relatively aquifer-mixed system. This is mostly experienced in winter, during which there is a low amount of rainfall. Hence, there is mixing of water from rainwater and other water bodies (rivers and lakes) in the aquifer. The aquifer system of the studied geothermal springs are weathered and fractured, there is possibly direct infiltration through faults and shearing and could conserve the isotopic composition of the original rain. Hence, the groundwaters would not be affected by isotopic fractionation, which makes it distinct from rainwater resulting to a depletion of heavy isotopes due to Rayleigh fractionation processes.

The different types of groundwater were classified into two groups according to their isotopic composition; Group 1 (Sagole and Tshipise with altitude of 450 m and 520 m, respectively) and Group 2 (Siloam and Mphephu with altitude of 835 m and 890 m, respectively). Group 1 are more isotopically depleted in δD values than Group 2, this could be attributed to the altitude (More depletion at high altitude compared to lower altitude). Interestingly, Siloam geothermal spring and hot borehole have a very similar isotopic composition, suggesting that they are either derived from the same aquifer or from two different aquifers which are connected through a minor fault. Isotopic signatures from treated tap waters (SCC and TTP) are more enriched than the groundwaters (geothermal springs and boreholes). At Siloam, both hot and tepid boreholes (SH and BH) have $\delta^{18}O$ value of -5.30 ‰ and the treated borehole (SCC) has -4.20 ‰, which implies that there was a 1.10 ‰ increment in $\delta^{18}O$ during the treatment process. Likewise, Tshipise geothermal spring had an average $\delta^{18}O$ value of -5.35 ‰ and -2.16 ‰ for treated borehole (TTP). This means that there was a 3.19 ‰ increment in $\delta^{18}O$ during the treatment process. Hence, the water treatment process increases the $\delta^{18}O$ value (enrichment) of the water.

The study infers that the geothermal spring waters are from a deep aquifer with more depleted isotopic signatures (light isotopic composition) while borehole water are from the shallow aquifer with more enriched isotopic signature (heavier isotopic composition). Except for hot borehole (shallow aquifer) which has a similar isotopic signature with the geothermal spring (deep aquifer) at Siloam, for which it can be inferred that there is either

direct interconnectivity between the two aquifers (shallow and deep) systems through the fault at Siloam or they are from the same aquifer. This can be attributed to the geological formations and climatic factors of the area.

Fontes (1980) reported that evaporation from open water and dissociation of rock minerals are the most common isotopic differentiation processes that affect the relationship between δD and $\delta^{18}O$. Owing to the high-water temperature (geothermal spring water), δD is generally not affected by reaction with aquifer materials at low temperature. Hence, δD – values were plotted against the EC and Temperature (Figure 4.15). There were negative correlations between δD – EC (R^2 > 0.5) and δD – Temperature (R^2 < 0.5). This implies that the higher the EC and Temperature of groundwater, the more isotopically depleted are the signatures. This corroborates with the previous findings that treated water are more isotopically enriched compared with the geothermal water and hot boreholes.

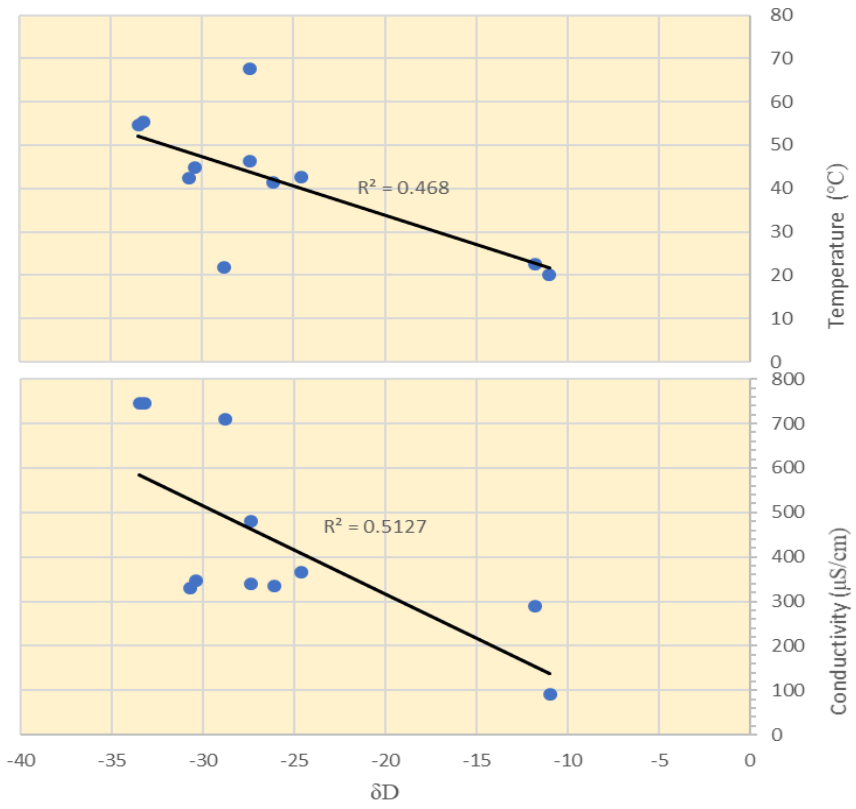

Figure 4.15: Relationship between δD with temperature and electrical conductivity of geothermal springs/boreholes within the Soutpansberg region.

This relationship has also proven that the depletion of isotopic signatures and active rock-water interaction of the aquifer is more profound in geothermal springs/hot boreholes compared to ordinary groundwater (tepid boreholes). Evaporation plays a vital role in the dissolution of salts in water as a function of its composition and atmospheric humidity among others. The significance of evaporation and dissolution of minerals can be seen on a $\delta^{18}O$ – Cl^- diagram (Figure 4.16). The diagram shows that there is a weak correlation between $\delta^{18}O$ and Cl^-. This implies that the deviation from LMWL is caused by an evaporative enrichment of the signatures of the groundwater on the surface before groundwater recharge. This means that there is intense recycling of groundwater used for irrigation purposes within Soutpansberg, hence evaporation can contribute to the concentration of salts in its groundwater (Ako *et al*., 2011). Therefore, surface evaporation before recharge contributes to groundwater salinisation in the studied areas. This further affirms that there is evaporation, particularly on the surface water bodies which also contributes to the groundwater recharge. Hence, there is need to assess the surrounding surface water bodies to determine which of them is contributing to groundwater recharge in specific areas.

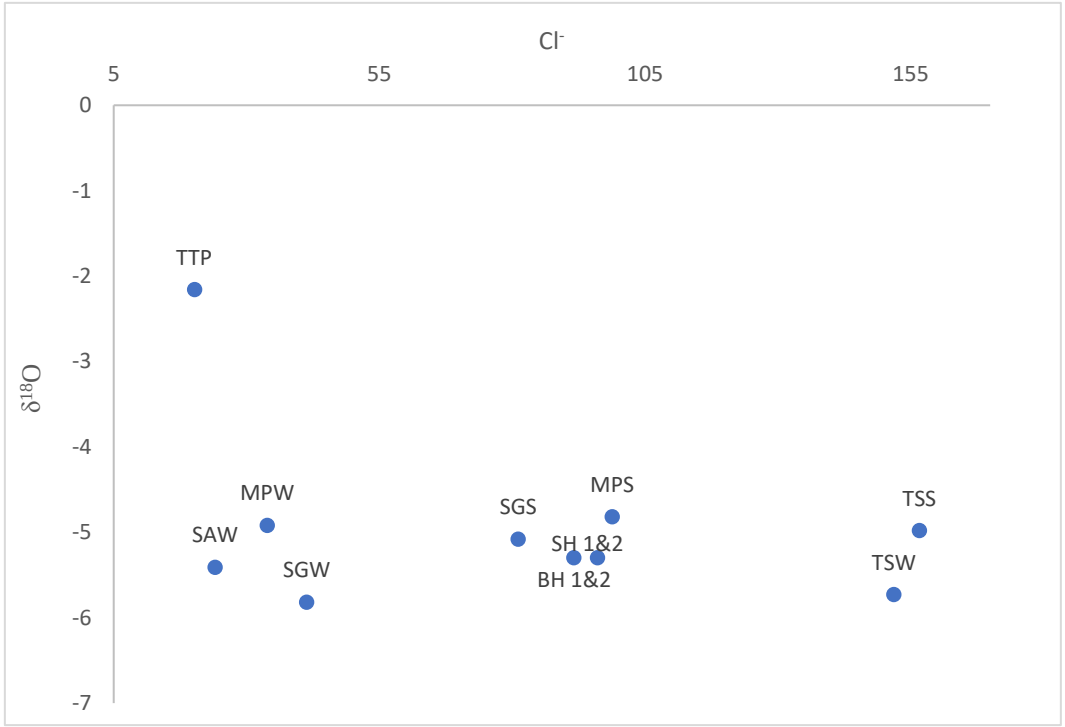

Figure 4.16: Plot of $\delta^{18}O$ against Cl^- of the geothermal water and boreholes within Soutpansberg region.

4.5 Synopsis

The objective of this chapter was to determine the physicochemical, geochemical parameters and stable isotopic compositions in the selected geothermal springs and other boreholes within the study areas (Specific Objective 1). The following results were obtained:

- Generally, the studied geothermal springs and boreholes were classified according to their temperature as hot and scalding; except for tepid bore holes (treated water). The temperature plays a significant role in the geochemical processes governing the geothermal springs and boreholes.
- Piper diagram revealed that most of the geothermal spring water and borehole (80%) falls in Na-Cl water type except for Siloam geothermal spring (SAW - WT29 and WT30) with Na-HCO_3 water type and TTP (Tshipise tapwater) and SCC (Siloam community tap water) with Ca-Mg-Cl. Durov's diagram corroborates and substantiate more on findings from the Piper's diagram; generally the major water types are Na-Cl and Na-HCO_3 which are typical of marine and deeper groundwaters, influenced by ion-exchange process. Cl^- and Na^+ are the most dominated ions, and the water could result from the reverse ion exchange of Na-Cl waters. Hence making the water type Na-Cl as observed in the Piper diagram. Siloam geothermal spring (SAW) has Na-HCO_3 water type which is formed as a result of the reverse ion exchange of Na-Cl waters, making Cl dominant anion and Na dominant cation resulting to Na-HCO_3 water type. The reservoir temperature of all the geothermal springs within Soutpansberg in ranged dbetween 95°C to 185°C. Most of the geothermal spring waters are mature except for Siloam geothermal spring water that is peripheral.
- The Gibb's plot indicates that the groundwater chemistry in the studied areas is mainly controlled by rock-water interaction process leading to chemical weathering of rock-forming minerals. Plot of (Ca + Mg) against (HCO_3+SO_4) showed that most of the geothermal springs, except for Mphephu (MPW and MPS) indicate carbonate weathering processes which supported the Gibb's diagram. All tepid waters (BH1, BH2, SCC and TSS) and Mphephu geothermal water fall below 1:1

line which indicates silicate weathering. This further shows the contributions of the cation exchange and carbonate and sulfate minerals dissolutions.

- Generally, the geothermal spring waters and boreholes are not fit for drinking due to high fluoride content, except for the treated water such as water from SCC and TTP. But these waters could be used for direct heating in refrigeration, green-housing, spa, therapeutic uses, aquaculture, sericulture, concrete curing and coal washing. Various indices such as SP, SAR, RSC, PI, KR and EC were used to evaluate groundwater quality for irrigation. Majority of the indices such as SAR, RSC, PI, and EC showed similar results except for KR and SP, implying that the geothermal spring water and boreholes fall under excellent to good category in both seasons. According to Wilcox (US salinity) diagram, all geothermal water and boreholes samples were suitable for irrigation purposes.
- The δD values of rainwater varied from -76.3 to +22.7 ‰ (SMOW) with a weighted mean of – 9.8 ‰ and $\delta^{18}O$ values ranged from -10.78 to +3.07 ‰ (SMOW) with a weighted mean of -2.7 ‰ (n=12). The amount and seasonal effects were profound in the rainwater samples leading to more depleted signatures in summer compared to winter. Rain formation processes at Thohoyandou occurred under isotopic equilibrium conditions with minor evaporation effect during the precipitation, as reflected by the slope of the local meteoric water line of $\delta D = 7.56\delta^{18}O + 10.64$. The slightly higher d-intercept value above the GMWL (10 ‰) reflects a possibility of an additional supply of recycled moisture across the regions. This implies that there is no continental effect, but inland moisture from various water bodies and vegetation. The slightly high d-excess value is an indication that the rainwater is formed from the water vapour evaporation near the land surface that is, either by re-condensation of the evaporated rainfall or evaporation of surface waters.
- The δD and $\delta^{18}O$ values of the geothermal spring water and boreholes confirm that the waters are of meteoric origin, which implies that rainfall is the fundamental component of these groundwaters. That is, the groundwater was derived from the infiltration of local precipitation, with significant contribution of another type of water in the deeper part of the aquifer (sea water). That is, there is mixing of meteoric water with sea water. The stable isotope ratios depict that the geothermal springs

at Sagole and Tshipise (Group 1) and Siloam and Mphephu (Group 2) have similar geochemical processes leading to similar isotopic composition. This could be attributed to attitude effects. The stable isotopic compositions of the geothermal spring waters and boreholes also show that evaporation and rock-water interactions are the main processes that control groundwater chemistry in the study areas. The isotopic signatures further confirm that there is an interconnectivity between the hot boreholes and geothermal spring at Siloam through minor faults that connect the shallow aquifer of hot boreholes and the deep aquifer of the geothermal spring.

CHAPTER FIVE

RADIOGENIC DATING OF THE GEOTHERMAL SPRINGS USING CARBON-14 (^{14}C) AND TRITIUM (^{3}H)

5.1 Preamble

This chapter presents results and discusses ages of the geothermal springs as well as the residence time from the source. This chapter focuses on reporting results on the use of radiogenic isotopes (^{14}C and ^{3}H) to ascertain the residence time from the source of groundwater recharge (Specific objective 2). This chapter further substantiates the previous findings from chapter 4 and draws conclusion on the source and the residence time of the water in the aquifer system. This chapter is based on Hypothesis 2, which states that "Geothermal springs within Soutpansberg have approximately the same ages".

5.2 Tritium content of the geothermal springs and boreholes

Tritium concentrations in groundwater studies give qualitative information on the recharge time to the aquifer system or residence time. The presence of higher tritium concentrations in groundwater samples than that produced by cosmic radiations itself indicates that some of the water was recharged after 1952 (Last hydrogen bomb testing) (Clark and Fritz, 1997). The interpretation of the tritium concentrations of the geothermal springs and boreholes were based on Clark and Fritz's classification (Clark and Fritz, 1997). Furthermore, the presence of tritium in groundwater samples at concentrations greater than 1 TU indicates that the groundwater was recharged after the start of atmospheric testing of thermonuclear weapons. Atmospheric tritium from weapons testing continues to decay, and tritium concentrations in recent and current rainfall are still distinguishable from tritium concentrations in groundwater recharged prior to the period of bomb testing (Zouari *et al.,* 2003). The measured tritium concentrations of the geothermal springs and boreholes are shown in Table 5.1. The tritium values range from 0.4 to 1.4 TU, which implies that the water falls on "submodern" (recharged before 1952) and "mixture of the submodern and modern" (recharged before 1952 and after 1952) (Clark and Fritz, 1997). This variation of the tritium concentrations in the aquifer indicates two types of water:

a) Old (submodern) deep water circulating with less or no influence by the modern recharge (deep aquifer) and;
b) Water near the surface made of modern recharge (shallow aquifer).

Table 5.1: Mean tritium concentrations of geothermal springs within Soutpansberg region and comparison with results of other studies

Sample Code	Tritium (TU)	Age classification by Clark and Fritz, 1997
TSW	0.6±0.2	Submodern
TSS	1.4±0.2	Mix (Submodern and modern)
SAW	0.8±0.2	Mix (Submodern and modern)
SGW	0.4±0.2	Submodern
SGS	0.8±0.2	Mix (Submodern and modern)
MPW	0.6±0.2	Submodern
MPS	0.9±0.2	Mix (Submodern and modern)
Springs and boreholes (Mohlapitsi Wetland, South Africa)[a]	0.6 – 1.9	Submodern - Mix (Submodern and modern)
Karst Springs (India)[b]	13.19 – 16.65	Modern
Groundwater (Karnataka, India)[c]	1.95 – 11.35	Mix (Submodern and modern) - Modern
Groundwater (Kitsap county, Washington, USA)[d]	5.3 – 17	Modern
Groundwater (deep aquifer) (Kitsap county, Washington, USA)[d]	<0.1 – 0.4	Submodern

[a] Mekiso *et al.,* 2015; [b]Nadeem and Jeelani, 2016; [c]Ravikumar and Somashekar, 2011; [d]Cox, 2003

This study shows the existence of two water types that is groundwaters recharged by present day meteoric water (rainwater) with a higher tritium concentration in the summer (wet) and older groundwater in deeper parts of the aquifer system with lower tritium concentrations. In summer, evidence of modern rainfall was profound in the study in all the geothermal springs, resulting to a mixture of submodern and modern waters. From the studies such as Makiso *et al*. (2015); Nadeem and Jeelani (2016); Ravikumar and Somashekar (2011); Cox (2003); the waters range from modern, mix (Submodern and modern) and submodern, which depend on water sources. From Table 5.1, thermal springs and deep groundwaters (Karnataka, India and Washington, USA) were submodern and mix (Submodern and modern), which conforms with findings from this study. This implies that deep groundwaters have a long residence time from low tritium values.

Generally, geothermal springs within Soutpansberg are submodern (old water from deep aquifer) with modern rainfall infiltration in the summer resulting to a mixture of modern and submodern. The lower tritium concentrations in the study areas are consistent with previous studies which have shown that tritium concentrations in the southern hemisphere are approximately a tenth of that of the northern hemisphere (Kendall and McDonnell, 1998; Kebede, 2013). This is because most of the tritium was released in the northern hemisphere and transferred from the stratosphere to the troposphere preferentially at high latitudes (Kendall and McDonnell, 1998; Kebede, 2013). Also, more washout and dilution effect of the tritium concentration is a result of the higher proportion of the ocean surface in the southern hemisphere and the high vapour pressure in equatorial regions (Kebede, 2013). Again, the tritium concentrations show seasonal variation in the geothermal springs waters; the waters were recharged pre-1952 (Submodern) in the winter and a mixture of the submodern and modern water (recharge pre-1952 and post-1952) in summer (Figure 5.1). Submodern waters have less or no influence of the present-day rainfall, which accounts for low tritium values. This finding supports the general observation that groundwater recharge occurs after heavy rainfall and without significant evapotranspiration of the vegetation (Gonfiantini *et al.,* 1998; Clark and Fritz, 1997; Mook, 1980; Truesdell and Hulston, 1980).

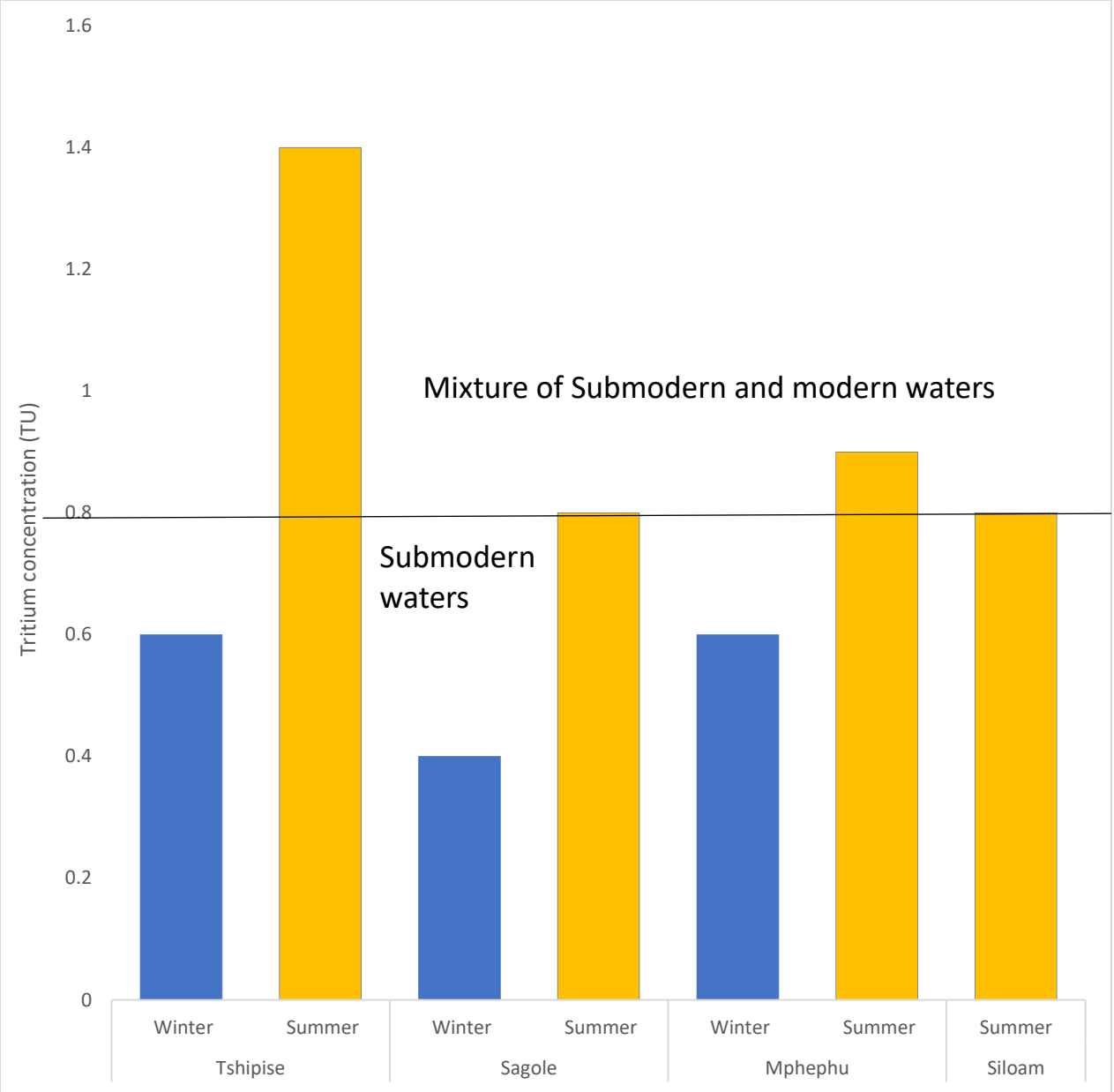

Figure 5.1: Seasonal variations of the tritium concentration in the geothermal springs within Soutpansberg. Straight line was adopted from Clark and Fritz's classification to differentiate the two types of water present in the study sites.

As earlier mentioned, most of the rainfall in the study area occurs in summer (October to February), hence, this accounts for the higher tritium values in summer compared to that obtained in winter (Figure 5.1; Table 5.1). Also, there are limited infiltration processes, resulting in relatively low tritium values in winter season compared to summer. Therefore, the water has a longer residence time in the aquifer system in winter compared to summer

when there is a mixture of modern and old waters with less retention time in the aquifer system. This implies that the input of new water (modern rainfall) from the rainfall event causes the groundwater system to rejuvenate.

However, the tritium concentration has been used in this study as a guide to differentiate between old (older than 50 years) waters and waters with contribution of recent rainfall (modern; less than 50 years). It can be inferred that most of the geothermal springs within Soutpansberg were submodern with significant contribution of modern rainfall in the summer leading to higher tritium values. The contour analysis showed the spatial distribution of tritium concentration in geothermal springs within Soutpansberg (Figures 5.2 and 5.3). On comparing these results with standard ^{3}H values given by Clark *et al*. (1997) and Zouari *et al*. (2003), it is evident that the majority of the samples were pre-modern (submodern) with a mixture of modern rainfall at a specific period (summer). In other words, groundwaters get recharged with modern rainfalls and have short circulation time in the ground (that is the origin is meteoric with short travel time). Contour analysis shows that Siloam and Mphephu geothermal springs are recharged at higher altitude compared to Sagole and Tshipise geothermal springs at lower altitude. This conforms with the results obtained from δD and $\delta^{18}O$ values of the geothermal springs (Chapter 4).

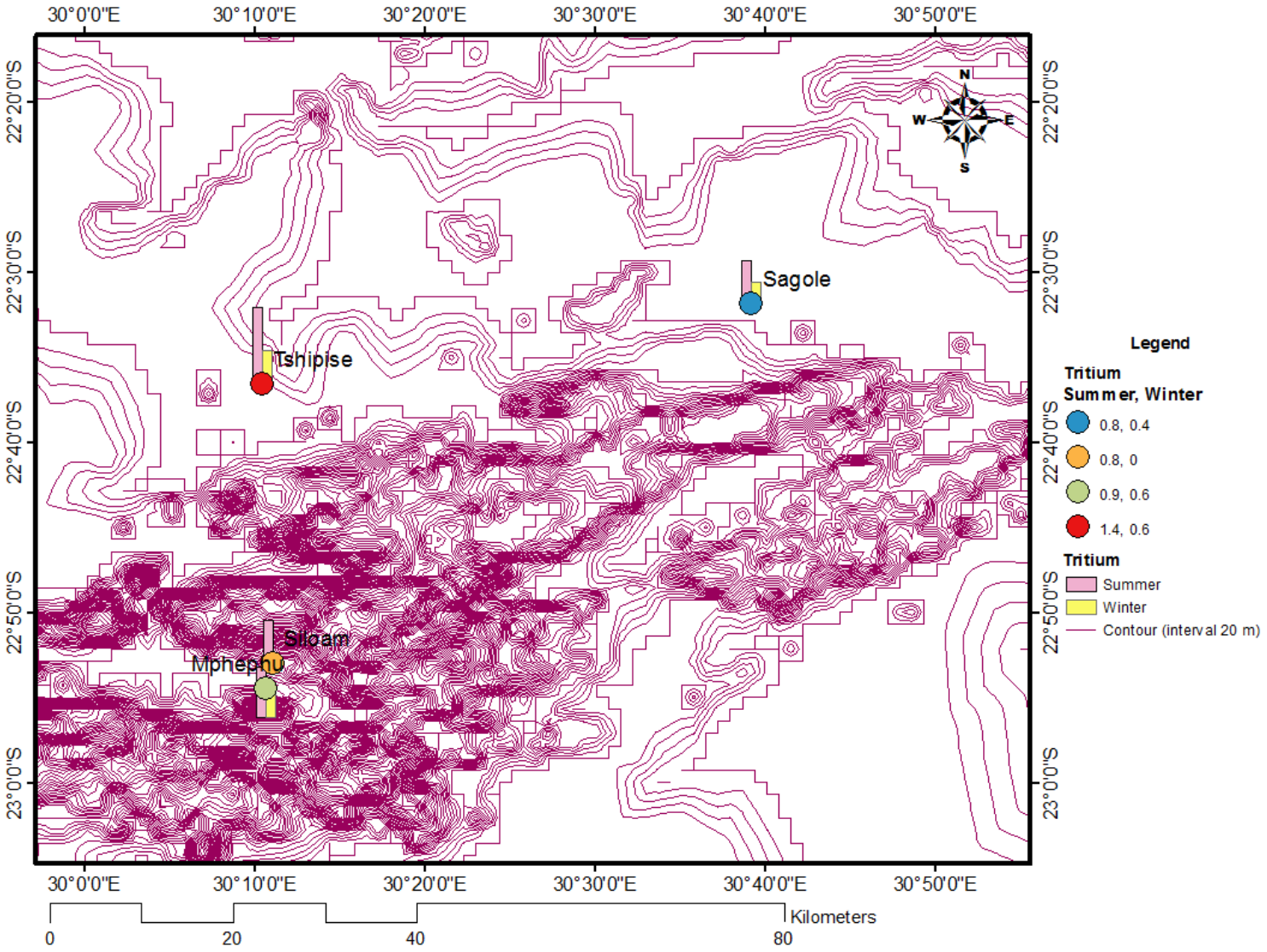

Figure 5.2: Spatial distribution of tritium content in geothermal springs within Soutpansberg region.

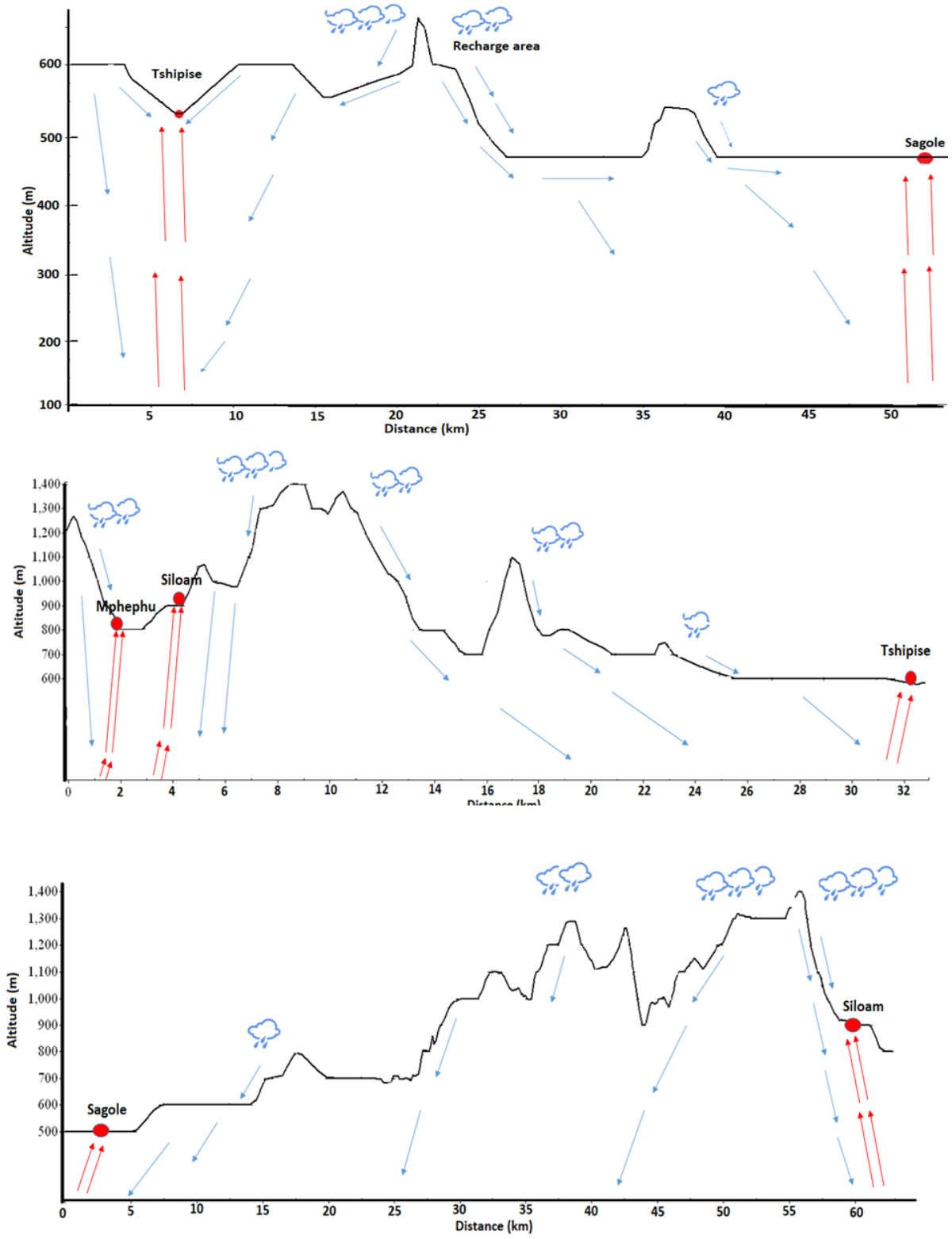

Figure 5.3: Conceptual model of the groundwater recharge with respect to altitude within Soutpansberg

5.2 Stable and radioactive carbon isotope geochemistry

Carbon source and the influence of CO_2 content are significantly useful in the determination of the variation in the amount of $\delta^{13}C$ in groundwater. The $\delta^{13}C$ in CO_2 dissolved in groundwater are attributed to two main sources: inorganic and organic origins (Truesdall and Hulston, 1980). Studies such as Deines (1970), Kyser (1986) and Sheppard (1986) have shown that $\delta^{13}C$ in CO_2 dissolved in groundwater from inorganic sources are mantle derived carbon, which ranges from -8 to -1‰; CO_2 derived from marine limestone with $\delta^{13}C$ values close to 0‰, whereas; $\delta^{13}C$ in crustal CO_2 have values from -70 to 15‰ (Ohmoto and Tye, 1979). For organic sources, CO_2 can be due to decay of organic matter and have mean $\delta^{13}C$ values between -26 to -22‰. The Calvin photosynthetic pathway or C_3 plants derive carbon with $\delta^{13}C$ range of -24 to -38‰ (Vogel, 1993), while the Hatch-Slack photosynthetic pathway or C_4 plants have slightly higher $\delta^{13}C$ between -17 and -9‰ (Deines, 1980). The latter type of vegetation is characteristic of area with warm and dry conditions (Vogel, 1978 and Scott and Vogel, 2000) and the former vegetation type reflects species that are typical for areas with moisture availability and relatively cool conditions. The third category of plants is the Crassulacean Acid Metabolism (CAM) plant type, which uses both C_3 and C_4 photosynthesis pathways. These vegetation types have $\delta^{13}C$ values in between C_3 and C_4 plants. These plant types differ in their photosynthetic pathway (Clark and Fritz, 1997), the $\delta^{13}C$ signature associated with each of the cases is, in most of the cases, used to identify the sources of carbon and the processes occurring underground (Gonfiantini *et al.*, 1998).

The study areas ^{13}C were determined on dissolved inorganic carbon (DIC) and the results varied between -9.36 to -17.38‰ (Table 5.2). Thus, these results suggest that the source of carbon in the area is the soil induced by Hatch-Slack photosynthetic pathway or C_4 plants. Hence, there is the possibility that the following isotopic fractionation processes occurred after groundwater recharge;

(i) Weathering of silicate minerals that does not change the $\delta^{13}C$ content which possibly affect alkalinity (Mook, 1980; Fritz and Mozeto, 1981);

(ii) Dissolution and precipitation of carbonate rocks or minerals, including dolomite, which has $\delta^{13}C$ concentration close to 0‰. These processes promote the isotope exchange between DIC and the aquifer matrix and result in ^{13}C enrichment and ^{14}C depletion in DIC (Pearson and Hanshaw, 1970, Clark and Fritz, 1997). This defines the local type of vegetation, pH and system conditions (Clark and Frtiz, 1997); and

(iii) Transport of CO_2 gas from soil atmosphere and oxidation of organic matter with introduction of light carbon (Grossman *et al.,* 1989; Liu *et al.,* 2009).

Table 5.2: Mean carbon isotopes and radiogenic carbon of the geothermal springs within the Soutpansberg region and comparison with results of other studies

Sample Code	^{13}C DIC (‰)	^{14}C (pmC)	Radiogenic age (BP)	Observed Age
TSW	-9.07	41.2±2.2	6900 - 7800	Submodern
TSS	-16.23	45.2±1.7	6250 - 6900	Submodern
SAW	-9.36	72.0±1.9	2500 - 2950	Modern/Submodern
SGW	-13.24	44.4±1.7	6400 - 7050	Submodern
SGS	-15.76	49.8±1.8	5450 - 6050	Submodern
MPW	-16.45	66.5±1.9	3150 - 3600	Modern/Submodern
MPS	-17.38	70.7±1.9	2650 - 3100	Modern/Submodern
Deep groundwater USA[a]	-4.7 - -20.3	51 - 72	2120 - 1510	Modern/Submodern
Springs (Alberta) Canada[b]	-13.5 - -13.9	51.3 - 56.5	2402 - 1558	Modern/Submodern
Thermal springs Jordan[c]	-9.4 - -13.5	2.9 – 4.8	21,860 -20,659	Submodern

*BP- Before Present; [a]Cox, 2003; [b]Lemay, 2002; [c]Al-Saudi and Yaseen, 2017.

The ^{14}C concentration was used to determine the age of the geothermal springs applying the decay law with no correction method. ^{14}C is not part of the water molecule, hence its activity is distorted with chemical reaction between the aquifer material and dissolved constituent in the water that occurs during and after infiltration. Carbon dioxide enters groundwater during/after recharge; water is in contact with the atmosphere, occurring mostly in the unsaturated zone where the gas concentration of $^{14}CO_2$ is substantially increased by root respiration and microbial oxidation of organic matter (Liu *et al.,* 2009). Generally low, ^{14}C concentration depicts that water is relatively "old", or it may be interpreted as a mixture of relatively "young" and 'old" water. Hence, ^{14}C concentration from the studied geothermal springs corroborate with tritium age. Studied geothermal springs are classified into Submodern (old water) and a mixture of modern/submodern (mixture of young and old water). From literature such as Cox (2003); Lemay (2002); Al-Saudi and Yaseen (2017); it can be deduced that most deep groundwaters and the springs were submodern and mixture of submodern and modern waters, which corroborate with the tritium age of the studied geothermal springs. The radiocarbon age was at least 1000 years Before Present (BP), which supports the present findings from this study. Thermal springs from Jordan (Syria) were very old (submodern) (Table 5.2) compared to other springs (studied springs inclusive) because Jordan springs were from volcanic origin with long residence time in the aquifer system. Although, the radiocarbon age (apparent age) still need to be corrected to obtain appropriate/best estimated age of the springs.

In Figure 5.4, the ^{14}C activity against ^{13}C diagram shows a decreasing ^{14}C activity to increase in ^{13}C concentration. This shows the possible existence of an isotopic fractionation between the dissolved inorganic carbon (DIC) and the aquifer material (Group 1). That is, there is an inverse relationship between the ^{14}C activity and ^{13}C in the studied geothermal springs. However, Siloam geothermal spring showed exception which seems to depict different geochemical process from the other geothermal springs (Group 2). This implies that the decrease of ^{14}C activity is not accompanied by any change of ^{13}C concentration. This finding further supports the fact that there are two geochemical distinctions leading to the two water types among the geothermal springs (Na-Cl and Na-HCO_3) from Durov and Piper's diagrams (chapter 4). Similar variations were observed in

^{14}C concentrations in the contour analysis (Figure 5.5), where the seasonality effect was profound. There was a higher radiocarbon age in the winter compared to summer. This could be attributed to the more rainfall occurrence in the summer leading to mixing of the waters with short residence times compared to winter when there is limited or no rainfall.

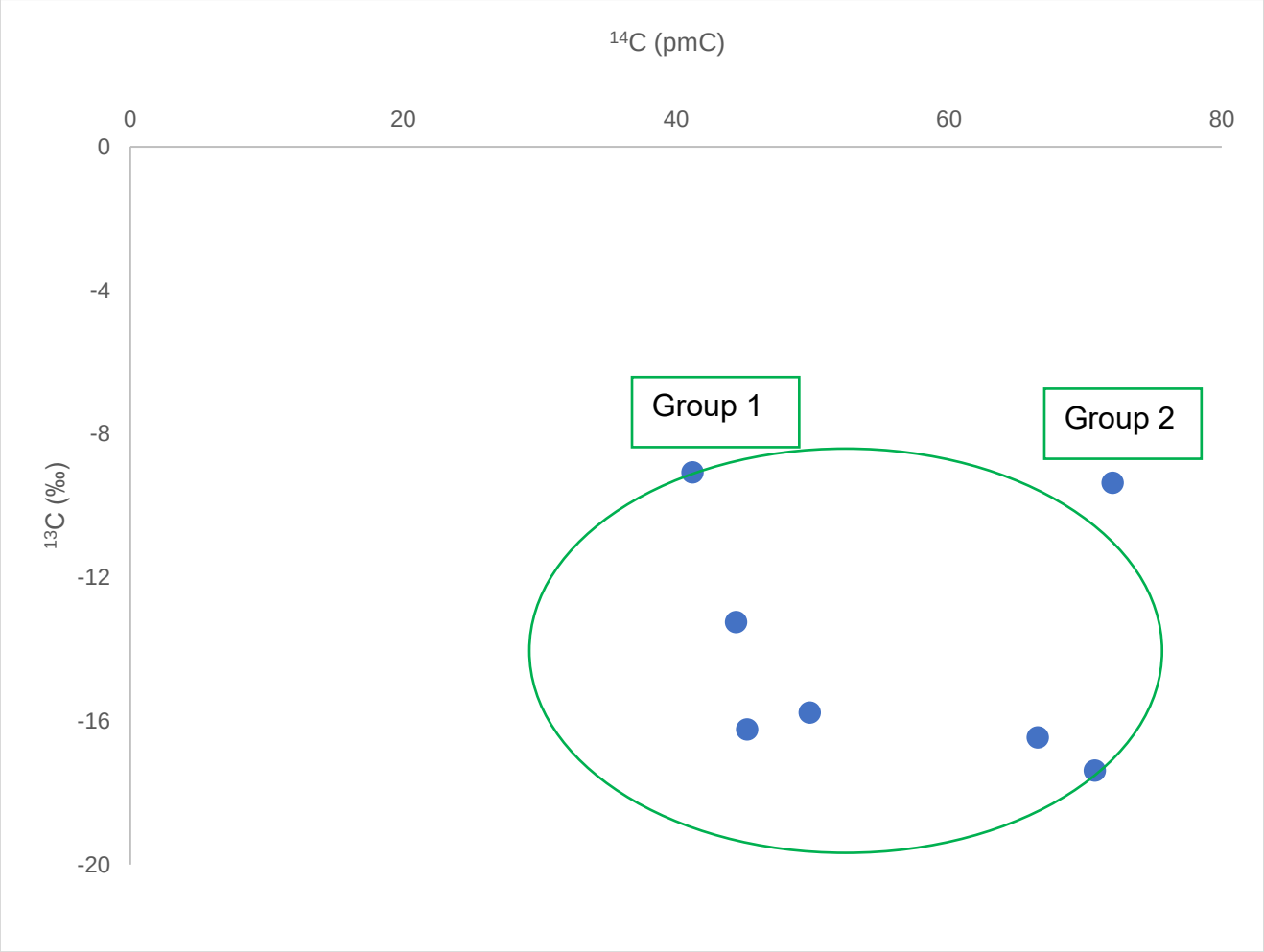

Figure 5.4: Relationship ^{14}C activity vs $\delta^{13}C$ concentrations of geothermal springs within Soutpansberg region.

The contribution of carbon from different sources can sometimes be estimated from $^{13}C/^{12}C$ ratio measurements and chemical constituents (Drever, 1997) so that corrections can be made to arrive at better and more reliable isotopic based ages. Hence, this is the most difficult aspect in using ^{14}C for dating groundwater. This study incorporates the DIC and geochemical parameters for springs to estimate a more reliable radiocarbon age.

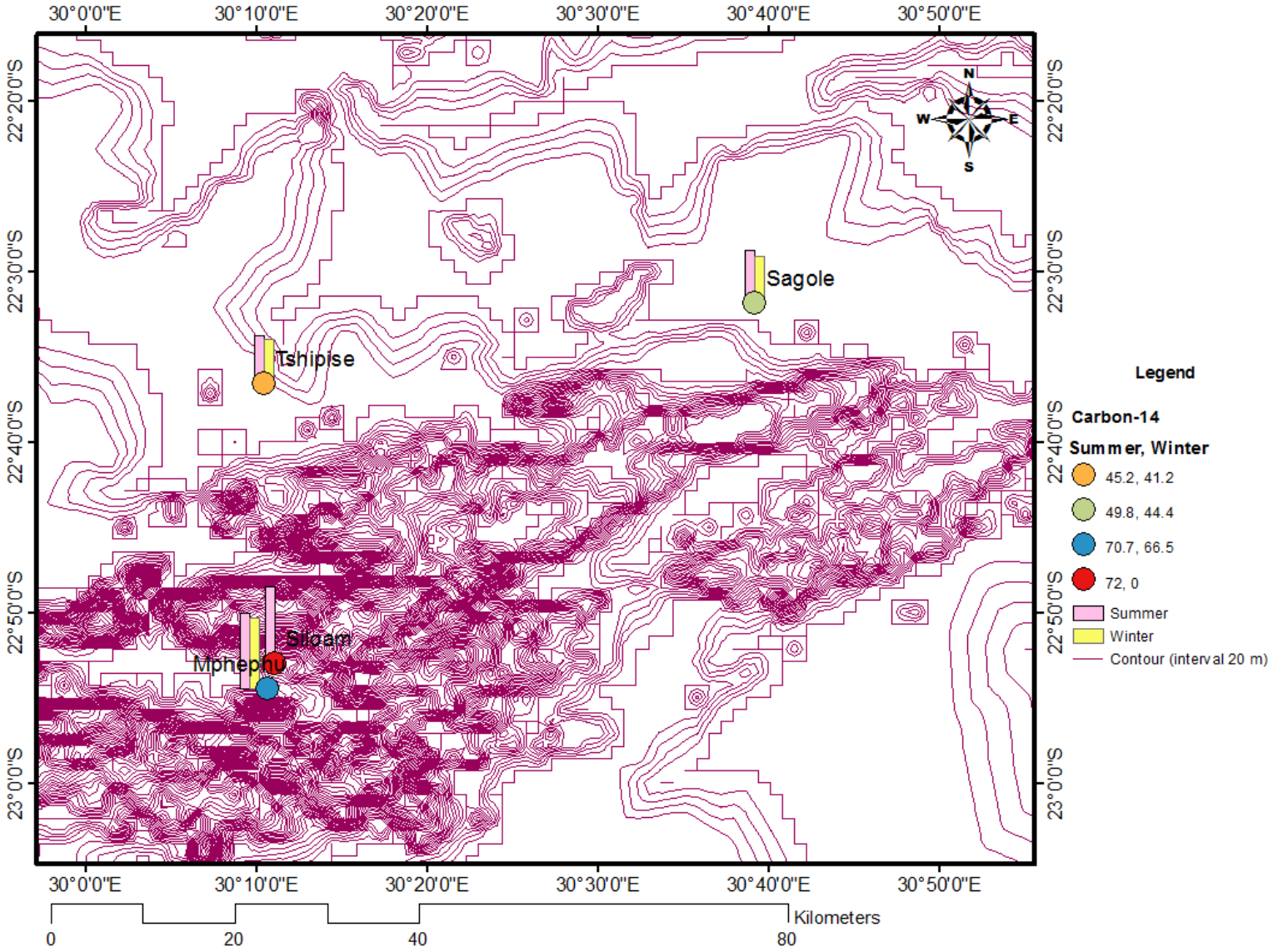

Figure 5.5: Spatial distribution of ^{14}C concentrations of geothermal springs within Soutpansberg region.

A better interpretation of ^{14}C measurements in groundwater dating can be deduced if the knowledge of the flow of water, sources of DIC in the water, hydrogeological and geochemical measurements are known as reported by Talma *et al*. (1997), Elliot *et al.* (1999), Buckau *et al.* (2000), Plummer and Sprinkle, (2001), Zongyu *et al.* (2003). However, knowledge of the flow of water and hydrogeological measurements are the delimitations of this study. An additional source of dissolved carbon is derived from the oxidation of organic carbon. The ^{13}C concentrations play a very vital role in the radiocarbon dating of groundwater.

The initial ^{14}C estimation of the actual groundwater age is highly significant to determine the extent to which the heavier carbon has reduced the relative ^{14}C concentration of the groundwater (Table 5.2). Thus, to overcome the complexity of the isotopic modification in groundwater dating using radiocarbon, several correction methods have been developed, including computer intensive simulation models which vary in parameters, processes and configurations (Ingerson and Pearson, 1964; Pearson and White, 1967; Pearson and Hanshaw, 1970; Tamers 1975; Gonfiantini, 1988; Clark and Fritz, 1997). An inverse modelling is highly needed to constrain the range of possible simulations and optimise the parameter values (given configurations and processes chosen for a system). Hence, Inverse modelling involve inverse geochemical modelling with NETPATH to assess the possible reaction and mixing processes that govern the geochemical evolution of the groundwater. These methods are considered the most important chemical processes affecting carbon isotopes in groundwater.

The statistical correction model (Vogel, 1970), proposes 85±5‰ for the initial ^{14}C activity. The chemical mixing approach takes into consideration the dissolution of sedimentary carbonates by primary recharge DIC (Ingerson and Pearson, 1964; Pearson and White, 1967; Pearson and Hanshaw, 1970; Tamers 1975; Gonfiantini, 1988; Clark and Fritz, 1997). This method relies on the ^{13}C concentration differences between the recharge areas and the dilution of DIC from carbonate rocks in the aquifer. Hence, most of these models are incorporated in the USGS Computer code NETPATH (Plummer *et al.,* 1994), which was employed in this study (Figures 5.6 and 5.7). The decision on which correction

model to use in any particular situation is dependent on the knowledge of the climatic condition and soil type; hydrological and geochemical composition of the system.

Initial Carbon-14, A0, (percent modern)
for Total Dissolved Carbon

	Model	Initial well	Age
1	Original Data	72.00	0.00
2	Mass Balance	91.71	2000.61
3	Vogel	85.00	1372.14
4	Tamers	50.04	-3008.13
5	Ingerson and Pearson	25.44	-8600.15
6	Mook	13.68	-13730.51
7	Fontes and Garnier	22.34	-9673.25
8	Eichinger	17.89	-11512.95
9	User-defined	100.00	2715.63
10	Revised F&G gas ex	16.91	-11974.59
11	Revised F&G solid ex	21.18	-10116.64

Figure 5.6: Result of carbon-14 correction models from NETPATH at Siloam

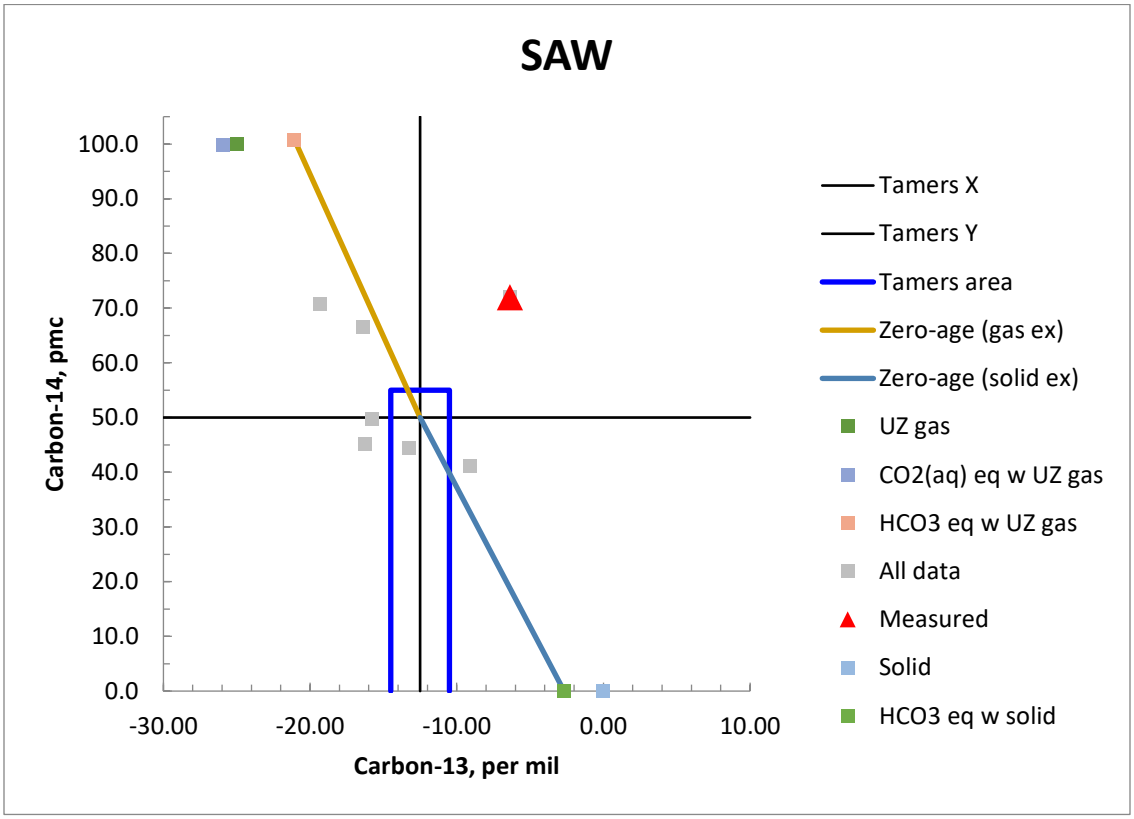

Figure 5.7: Plot of carbon-14 against carbon-13 from NETPATH at Siloam

Most of the correction models underestimate the geothermal spring age compared with the apparent age, except for the Mass balance model (Table 5.4). The Mass Balance model uses extensive water chemistry and isotopic data to identify the main reactions affecting the chemical evolution of the groundwater (Plummer *et al*., 2004). It provides the most complete analysis of all the models and, therefore, tends to produce the best estimates for the geothermal spring ages. The mass balance model has higher values compared to the apparent ages except for Siloam (SAW). As earlier mentioned, the DIC does not really affect the geothermal water at Siloam (Group 2) (Figure 5.2). This accounts for the negative value with all the models except for Vogel model (Table 5.3). This implies that the ^{14}C content decrease does not have an influence on the $\delta^{13}C$ of DIC, hence, calculation of the groundwater age needs only the application of radioactive decay equation. This is true because the mass balance model does not overestimate the age of Siloam geothermal spring.

Other models such as Tamers, Ingerson and Pearson, Mook, Fontes and Garnier, Eichinger, Revised F&G gas exchange and Revised F&G solid exchange models were in close agreement which are marginally lower compared to the apparent age (Table 5.4; Figure 5.8). This could be as a result of dissolution mixing reaction based on the isotopic balance and isotopic exchange with solid or gas (Tamers, 1967; Ingerson and Pearson, 1964, Fontes and Garnier, 1979; Fontes, 1992; Eichinger, 1983). The Vogel model gave results which closely approaches the uncorrected age (apparent age). This model uses the empirical estimation to account for mixing and exchange processes (Vogel and Ehhalt, 1963), hence this model appears to give a reasonable result which is close to estimated apparent ages in this study compared to other models. The limitation of the Vogel's model is that it is only useful for soil, waters and shallow groundwaters in temperate climates (Vogel and Ehhalt, 1963). Hence, this model is not appropriate for deep groundwaters.

A study from Australia recommended Tamer and Ingerson & Pearson models as the most preferable due to their climatic condition (sub-humid and semi-arid) (Eglinton and Eglinton, 2008), which is similar to the study area climate. The results obtained from the Tamer model in this study contradict the previous findings. The values obtained were

inconsistent and not coherent in terms of seasonality. Hence, there is a wide disparity in the values obtained per season compared to the apparent ages (Table 5.3). This could be as a result of dissolution-mixing reaction based on the chemical balance and does not take into account any isotopic exchange reactions (Tamers, 1967). Ingerson and Pearson model accounts for isotopic exchange reaction, hence, it gives a better result compared to Tamer's model. Some of the geothermal springs gave negative ages, indicating the presence of anthropogenic ^{14}C. This implies that there is possible potential contamination of geothermal springs by surface runoff (Gallagher *et al.,* 2000).

Table 5.3: Correction models for radiocarbon dating of groundwater within the Soutpansberg region.

Models	SGW	SGS	MPW	MPS	TSW	TSS	SAW
Carbon-13	-13.24	-15.76	-16.45	-17.38	-9.07	-16.23	-6.36
Carbon-14	44.4	49.8	66.5	70.7	41.2	45.2	72
Apparent age (BP)	**6700**	**5750**	**3350**	**2850**	**7350**	**6550**	**2700**
Mass Balance (BP)	12933.71	8156.69	0.00	0.00	19983.71	18227.38	2004.56
Vogel (BP)	5368.46	4419.65	2029.04	1522.76	5986.81	5220.83	1372.14
Tamers (BP)	1005.22	186.05	-2225.39	-2762.26	1650.51	884.32	-3008.06
Ingerson & Pearson (BP)	1457.39	1948.9	740.15	727.08	3698.21	2993.01	-8600.15
Mook (BP)	1645.61	3038.39	3384.97	3135.04	7528.38	4036.61	-13730.51
Fontes and Garnier (BP)	1607.16	2452.23	1686.33	1645.79	4679.17	3464.6	-9673.27
Eichinger (BP)	1155.2	1851.72	759.55	809.94	3715.39	3017.64	-11513.03
Revised F&G gas exchange (BP)	1787.91	3134.26	1555.15	3310.35	-4922.43	4139.42	-11995.1
Revised F&G solid exchange (BP)	1203.75	1844.6	-196.86	813.16	-2086.23	3056.77	-10123.82

*__BP__- Before Present

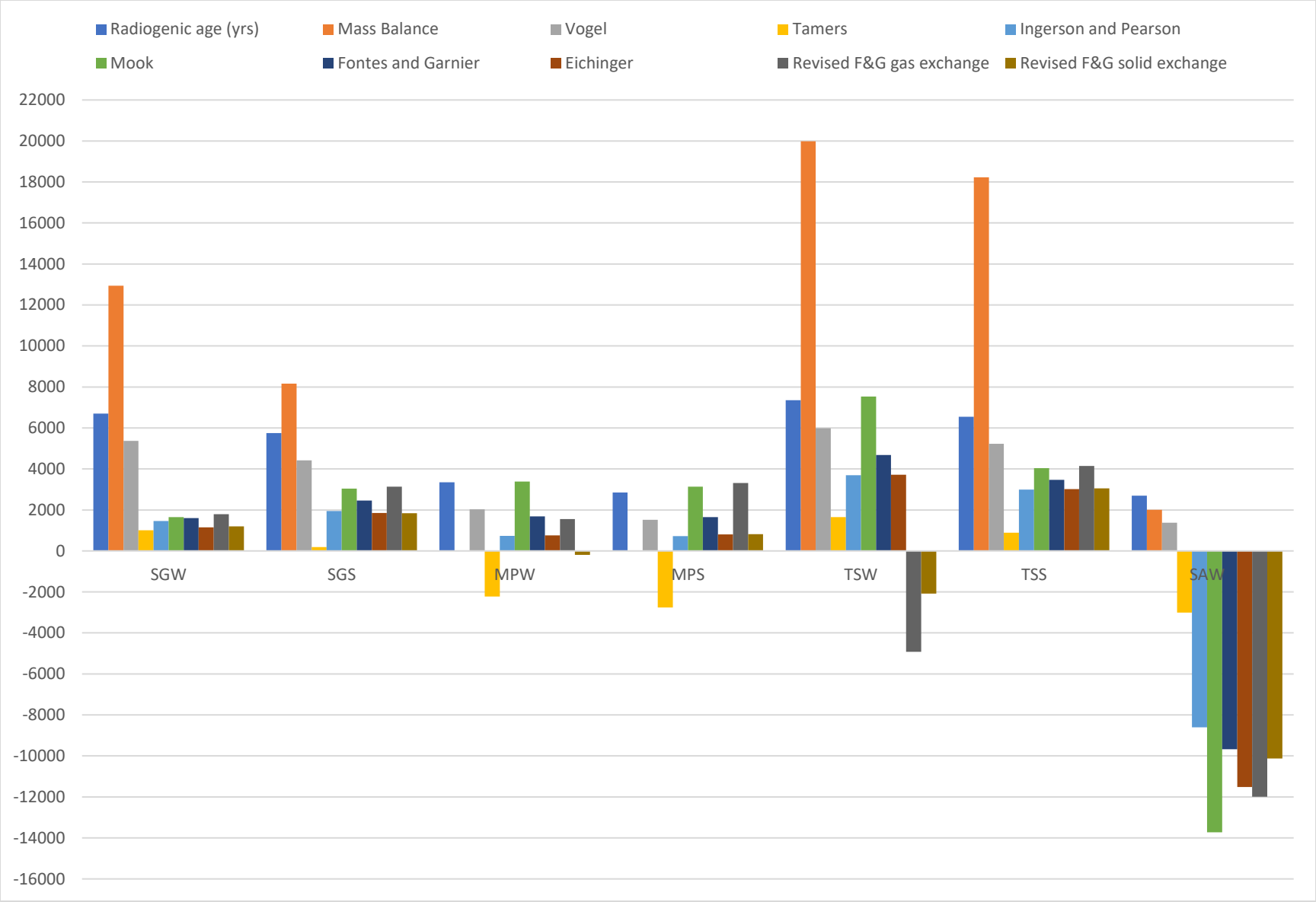

Figure 5.8: Comparison of the apparent ages with the various correction models.

Mook, Fontes and Garnier, and Eichinger models were in good agreement with the outcomes obtained from Ingerson and Pearson model. These three models have the advantage of using Tamer's reaction and isotopic exchange with either gas phase or solid phase, which in turn gives a better result compared to Tamer's model (Mook, 1980; Fontes and Garnier, 1979; Eichinger, 1983). Hence, there is a need to constrain the correction model results with tritium relative ages of the geothermal springs and come up with the most appropriate model.

Clark and Fritz (1997) suggest that the best approach is to collect as much field data as possible, including samples from the recharge area, and compare results with various models. In comparison of the various correction models with the obtained value for ^{14}C concentrations, the Vogel model result was in good agreement with the uncorrected age (Figure 5.7). Although, the study has shown that Vogel model gave good results close to the apparent age, but its limitation as explained earlier makes it not appropriate for radiocarbon dating of the groundwater in Group 1 (Figure 5.4). In the Group 1, an increase of $\delta^{13}C$ with decreasing ^{14}C content (Figure 5.4) could be explained by a partial mixing between biogenic CO_2 and carbonate matrix. For this group, corrections of the activities are required in order to determine the initial activity (Ao). Therefore, Mook, Fontes and Garnier, Eichinger and Ingerson and Pearson models could represent fairly the geothermal springs water age of this group, considering the hydrochemical parameters of springs. The water types (NaCl and $NaHCO_3$) of the geothermal springs have impacts on the ^{14}C content of the water. As earlier mentioned, Group 2 (SAW) is not affected by DIC, hence the mass balance model is most appropriate for such a case since other models gave negative values.

Figure 5.9 shows that all the geothermal springs within Soutpansbergs are mixed waters (old groundwater) that is a mixture of modern and submordern water. Combination of ^{3}H and ^{14}C values for the springs give more reliable outcomes of the retention time of the geothermal springs.

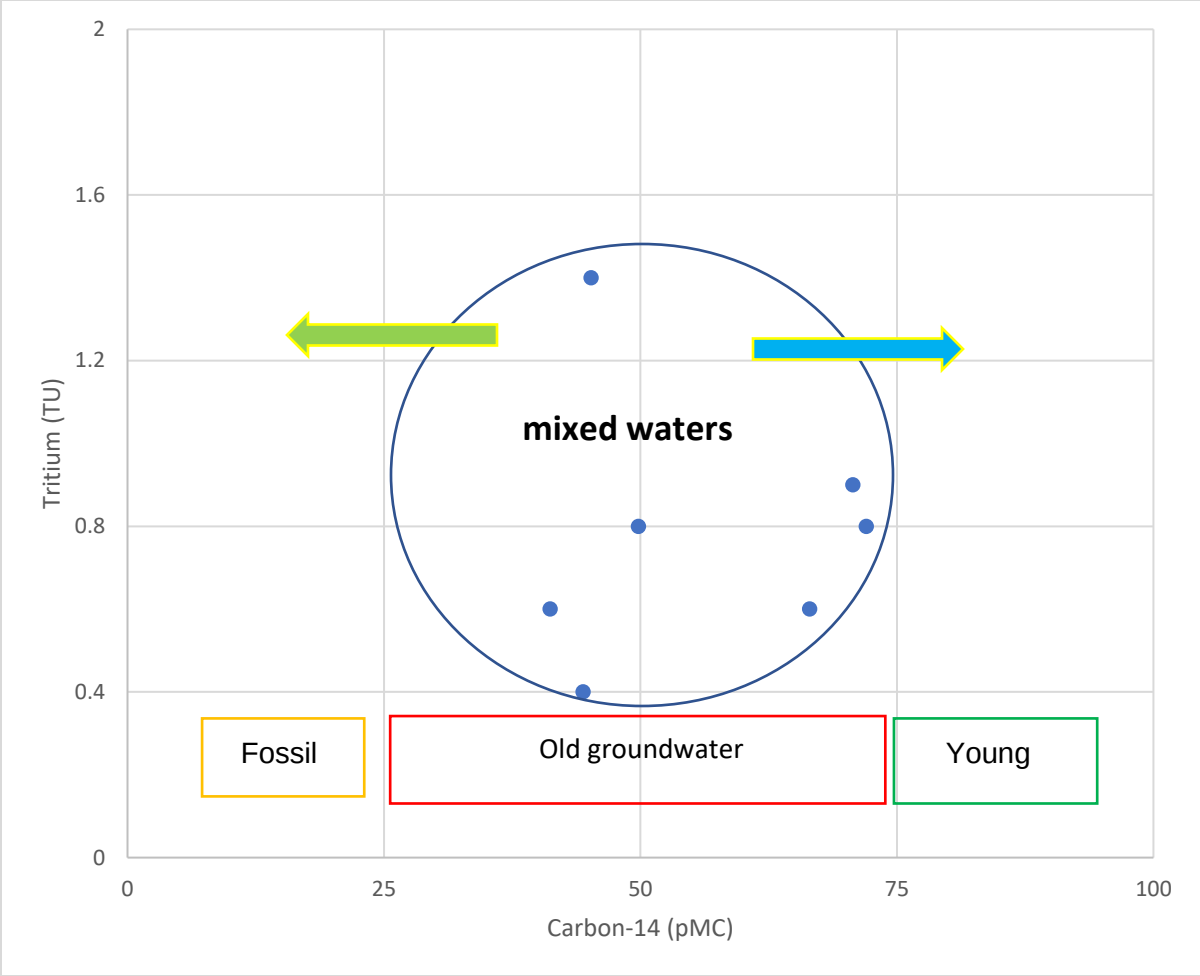

Figure 5.8: Plot of Tritium (TU) againt Carbon-14 (pmC) of the geothermal springs within Soutpansberg.

The ^{14}C - correction models were subjected to Two-ways ANOVA to ascertain if there are any significant differences in their outputs. Table 5.4 shows clearly that there was a significant difference in the output from an individual correction model used ($P < 0.05$). This implies that the output obtained from each model were either due to dissolution of mixing reaction based on chemical balance or isotopic balance. Then, the accuracy of each model was constrained with relative tritium age earlier obtained.

Table 5.4: Two ways ANOVA without replication for ^{14}C - correction models

Source of Variation	*SS*	*df*	*MS*	*F*	*P-value*	*F critical*
Study sites	9.08E+08	6.00	1.51E+08	13.46	**2.89E-09**	2.27
Carbon-14 correction models	6.05E+08	9.00	6.72E+07	5.97	**9.14E-06**	2.06
Error	6.07E+08	54.00	1.12E+07			
Total	2.12E+09	69.00				

Generally, most of the ^{14}C correcting models further support that the geothermal spring age is older in winter compared to summer. This implies that there is a high retention time in winter than summer within the aquifer system. As explained earlier, there is limited rainfall in winter, hence resulting in limited infiltration processes and older water (submodern water). Comparing the tritium age with the various carbon-14 correction models (Table 5.5), Ingersion and Pearson, Fontes and Garnier and Eichinger models would be considered most appropriate. The result obtained was in good agreement with the tritium result and is supported by studies from Australia (Eglinton and Eglinton, 2008; Sachse *et al.,* 2012). Geothermal springs within the Soutpansberg region are submodern and a mixture of submodern and modern waters based on relative tritium age. Although, the Vogel model result is closer to the apparent ages of the geothermal springs, but with respect to tritium age in this study, the model would not be appropriate. In addition to Australia study, this study recommends the use of Ingerson and Pearson, Eichinger and Fontes and Garnier correction models for radiocarbon dating of groundwater in semi-arid region (Table 5.5).

Table 5.5: Tritium age against various correction models of carbon-14 age based on performance outcome.

Sites	^{3}H-age	Tamer	Ingerson and Pearson	Mook	Fontes and Garnier	Eichinger	Revised F&G gas exchange	Revised F&G solid exchange
TSW	*	**	*	*	*	*	-	**
TSS	**	**	**	*	**	**	*	**
SAW	**	-	-	-	-	-	-	-
SGW	*	**	**	**	**	**	**	**
SGS	**	***	**	*	**	**	**	**
MPW	*	-	**	*	**	**	**	-
MPS	**	-	**	*	**	**	**	**

*Submodern age

**Mixture of Submodern and Modern age

***Modern age

5.3 Synopsis

The objective of the study was to report results and discussion on the ages of geothermal springs with respect to season within the Soutpansberg region using Tritium and carbon-14 (Specific Objective 2). The following results were obtained:

- The geothermal springs have higher tritium values in summer compared to winter season. This implies that the geothermal springs were recharged before 1952 (submodern) for winter and recharged before and after 1952 (Mixture of modern and submodern) for the summer season. This is an indication that the present rainfall contributes more to the geothermal spring recharge, particularly in summer compared to winter.

- Radiocarbon values of the geothermal spring range from 2700 BP to 7350 BP (where the BP- Before Present, which is 1950) without correction. The radiocarbon further confirms the longer residence time in the aquifer in winter compared to summer, where there is a mixture of modern and submodern water for recharge.
- Some geothermal springs after the correction models gave negative ages, indicating the presence of anthropogenic ^{14}C. There were significant differences in the outputs from different correction models employed in this study. From several carbon-14 correction models deployed in this study, Vogel model which is an empirical model showed a good result with respect to the uncorrected radiocarbon age (apparent age). Incorporating the tritium age, Ingerson and Pearson, Eichinger and Fontes and Garnier correction models were the most appropriate models for radiocarbon correction of groundwater in this semi-arid region.

CHAPTER SIX

STABLE ISOTOPES RATIOS (HYDROGEN AND CARBON) IN THE SURROUNDING SOIL AND VEGETATION

6.1 Preamble

The objective of this chapter was to determine the stable isotope compositions (hydrogen and carbon) in the surrounding soils and vegetation within the study areas. This chapter explores the isotopic compositions of the surrounding soil at different depths with respect to the seasons; different parts of the vegetation; and their interconnectivity (Specific Objective 3). Stable isotopic compositions were used to understand the water movement and the vegetation pathway mechanism within the environment. This chapter establishes relationship between the stable isotopic compositions and soil depths. This chapter is based on hypothesis 3, which states "that soils and vegetation surrounding geothermal spring have similar stable isotopic compositions".

6.2 Stable Isotopic compositions (Hydrogen and Carbon) in surrounding soils

The mean values for δD and $\delta^{13}C/^{12}C$ in soils are presented in Table 6.1 with % carbon content. δD values increase with depth at all sites such that the topsoil has the least concentrations (Figures 6.1 and 6.2). This implies that there is a reduction in depletion rate with the soil depth. Studies have shown that the δD of soil-water, partially reflects the isotopic composition of precipitation, which is correlated with the mean annual temperature (Zimmerman *et al.,* 1967; Estep and Hoering, 1980; Estep and Dabrowski 1980; Sternberg, 1989). Note that the δD value for local rainfall within the study areas ranges from -76.3 to 21.7‰ (Chapter four), whereas that for soil-water ranges from -135.70 to -29.08 ‰ (Table 6.1). Hence, this reflects the composition of the local rainfall in the soil-water, although, more isotopically depleted than rainwater. This is as a result of the isotopic fractionation within the soil zone (Eglinton and Eglinton, 2008). The difference in the composition of δD in both seasons further confirms the relationship between soil-water and rainwater composition. The composition of δD was higher in summer compared to winter and this could be attributed to the more rainfall events during summer. Although, the δD values for winter were more depleted compared to summer,

this is an indication that there is mixing action between rainwater and soil water, making the δD values less depleted in summer (Eglinton and Eglinton, 2008; Sachse *et al.,* 2012).

Table 6.1: Mean isotopic composition (δD and $\delta^{13}C$) in surrounding soils of the geothermal springs within the Soutpansberg region.

		δD (‰)		$\delta^{13}C$ (‰)		%C	
Sites	Depth (cm)	Winter	Summer	Winter	Summer	Winter	Summer
Tshipise	10	-103.51	-44.44	-17.96	-16.17	0.52	1.43
	20	-98.37	-40.77	-16.07	-18.29	0.30	0.84
	30	-78.12	-39.27	-16.68	-21.97	0.37	1.19
	40	-87.89	-32.01	-16.16	-23.64	0.37	1.08
	50	-73.96	-31.24	-16.84	-24.72	0.40	0.99
Sagole	10	-135.70	-67.30	-19.88	-19.17	0.45	1.24
	20	-131.20	-58.23	-20.89	-19.54	0.31	0.45
	30	-123.90	-55.98	-21.59	-22.35	0.15	0.21
	40	-120.20	-56.62	-24.15	-22.42	0.09	0.16
	50	-109.80	-43.70	-23.51	-23.04	0.09	0.11
Mphephu	10	-94.40	-42.91	-18.05	-20.87	1.24	2.66
	20	-79.40	-34.39	-19.19	-18.27	0.85	1.14
	30	-62.30	-29.08	-18.15	-18.84	0.46	1.45
Siloam	10	-90.70	-	-14.79	-	1.41	-
	20	-87.10	-	-15.72	-	1.13	-
	30	-84.20	-	-17.67	-	0.46	-

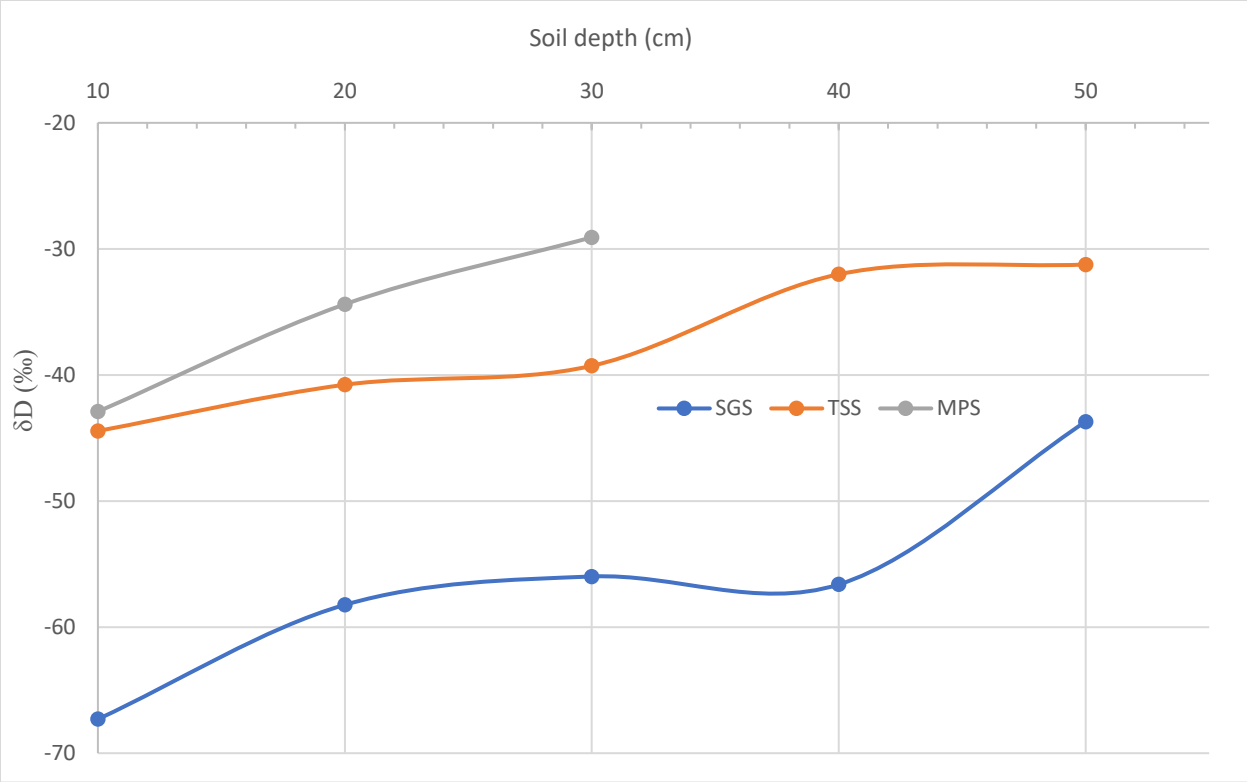

Figure 6.1: Plot of the soil depth against δD at Sagole, Tshipise and Mphephu in summer.

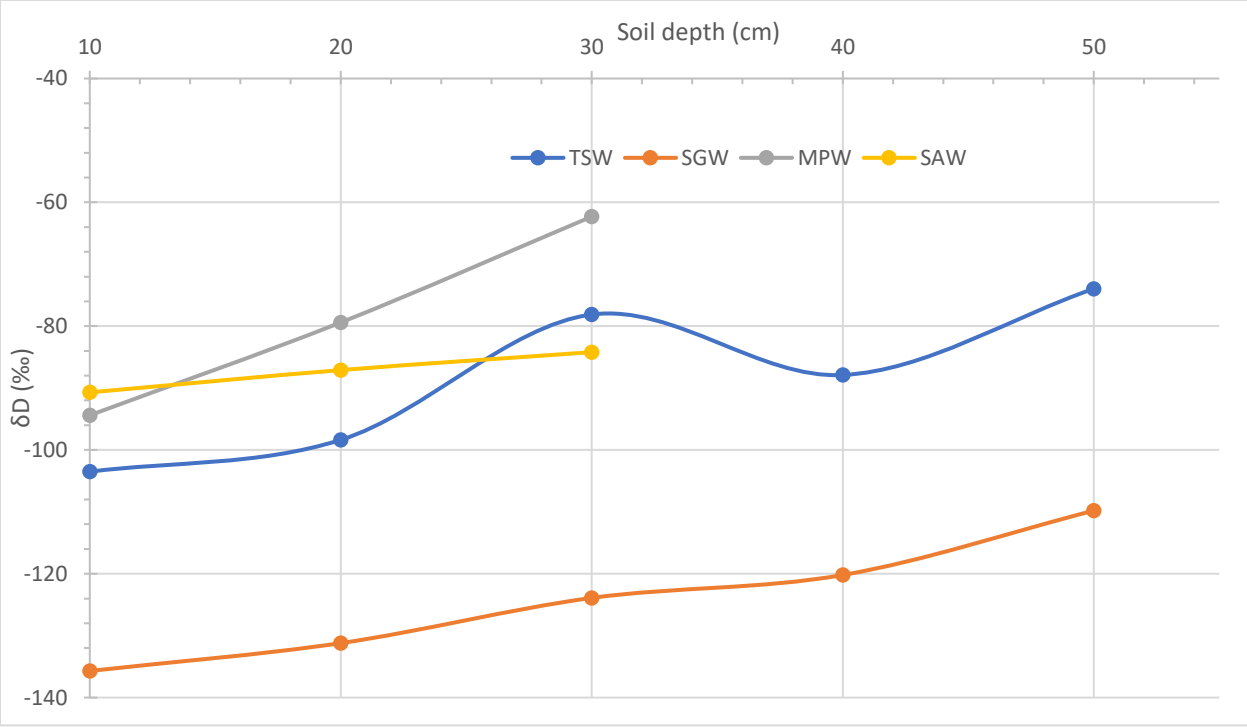

Figure 6.2: Plot of the soil depth against δD at Siloam, Sagole, Tshipise and Mphephu in winter.

The observed variations in δD values were statistically significant in both seasons ($P < 0.05$) (Table 6.2). This means that there is significant difference in the δD compositions in both seasons for all the studied sites. This indicates that the observed variations in compositions of δD is as a result of isotopic fractionation and further confirms the seasonal effect of the soil-water at the studied sites.

Table 6.2: ANOVA for δD values in both seasons

Source of Variation	SS	df	MS	F	P-value	F critical
Between Groups	20333.58	1	20333.58	63.63496	1.42E-08	4.210008
Within Groups	8627.438	27	319.5348			
Total	28961.02	28				

The composition of $\delta^{13}C/^{12}C$ in soil-water ranges from -24.15 to -14.79‰ (Table 6.1), which is a reflection of Crassulacean Acid Metabolism (CAM) (mix of C3 and C4 photosynthetic cycles) with a stronger C4 trend (Figure 6.3). $\delta^{13}C$ values for C3 plants range from -22‰ to -38‰, whereas the values for C4 plants range from -9‰ to -21‰ resulting in distinct values between C3 and C4 plant tissues (Raven *et al.,* 1981; Tieszen and Archer, 1990; O'Leary, 1993). This study shows that the source of carbon in the areas is soil induced by Hatch-Slack photosynthetic pathway as obtained from $\delta^{13}C$ of geothermal spring/borehole water. The CAM is similar to C4 photosynthesis based on their metabolism having both C3 and C4 cycles of CO_2 fixation and reduction. Owing to the nature of CAM photosynthesis, C3 and C4 cycles occur both spatially in different parts of the same cell (Moore *et al.,* 2003) and temporally, that is, C4 cycle at night and C3 cycle during daytime. This accounts for a few of the samples falling under either C3 or C4 photosynthetic soil (Figure 6.3) rather than CAM. Hence, this study shows that there is a good relationship between the $\delta^{13}C$ of soil-water and geothermal/borehole water (Chapter 5) within the study areas. Studies have shown that semi-arid areas have mostly CAM plants, which this study supports (Staddon, 2004; Ehleringer *et al.,* 2005). This shows that there is a good relationship between the $\delta^{13}C$ of soil-water and geothermal/borehole water.

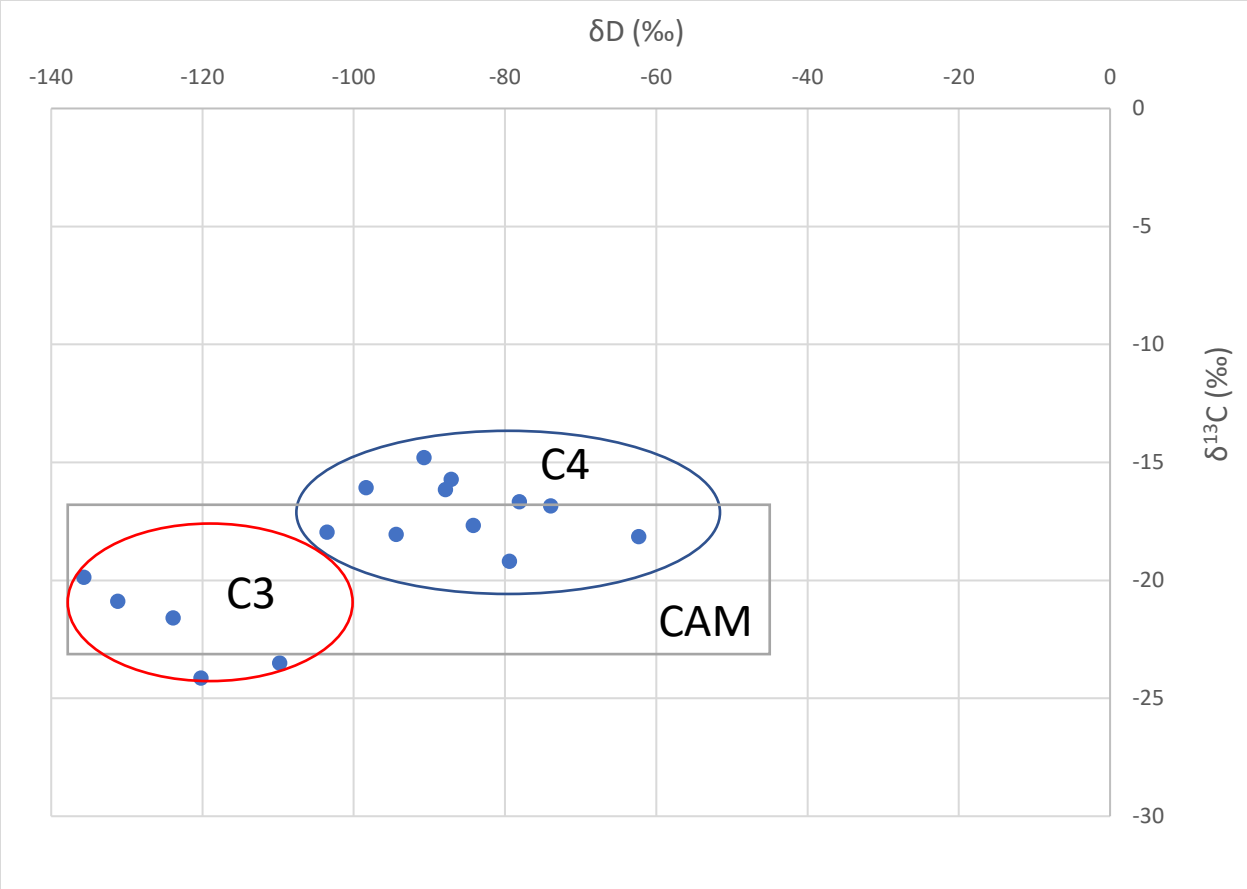

Figure 6.3: Plot of δD against $\delta^{13}C$ showing the vegetation type within the Soutpansberg region.

The trend of $\delta^{13}C$ variations is similar across the four sites with predominantly CAM soil except for a few depths with C3 and C4 soils. Contrastingly, the composition of $\delta^{13}C$ in soil-water decreases with depth (Figures 6.4 and 6.5), making the topsoil to have the highest concentration (heavier) than the soil at deeper depths. This is because more carbon in soil carbonates is from soil gas (vegetation, respiration, atmosphere) and not from the parent material that soil is found on (Schmidt and Gleixner, 2005). At deeper depths, most carbon is digested by microbes and released into the soil as CO_2, leaving little remaining carbon (lighter) in deeper depth soils (Ehleringer *et al.,* 1993; Lajtha and Michener, 1994; Schmidt and Gleixner, 2005). Hence, this accounts for the reduction of $\delta^{13}C$ with depth of the soil. A similar trend was found in the %carbon content of the soil-water for both seasons (Figure 6.6), the % carbon decreased with the depth of the soil.

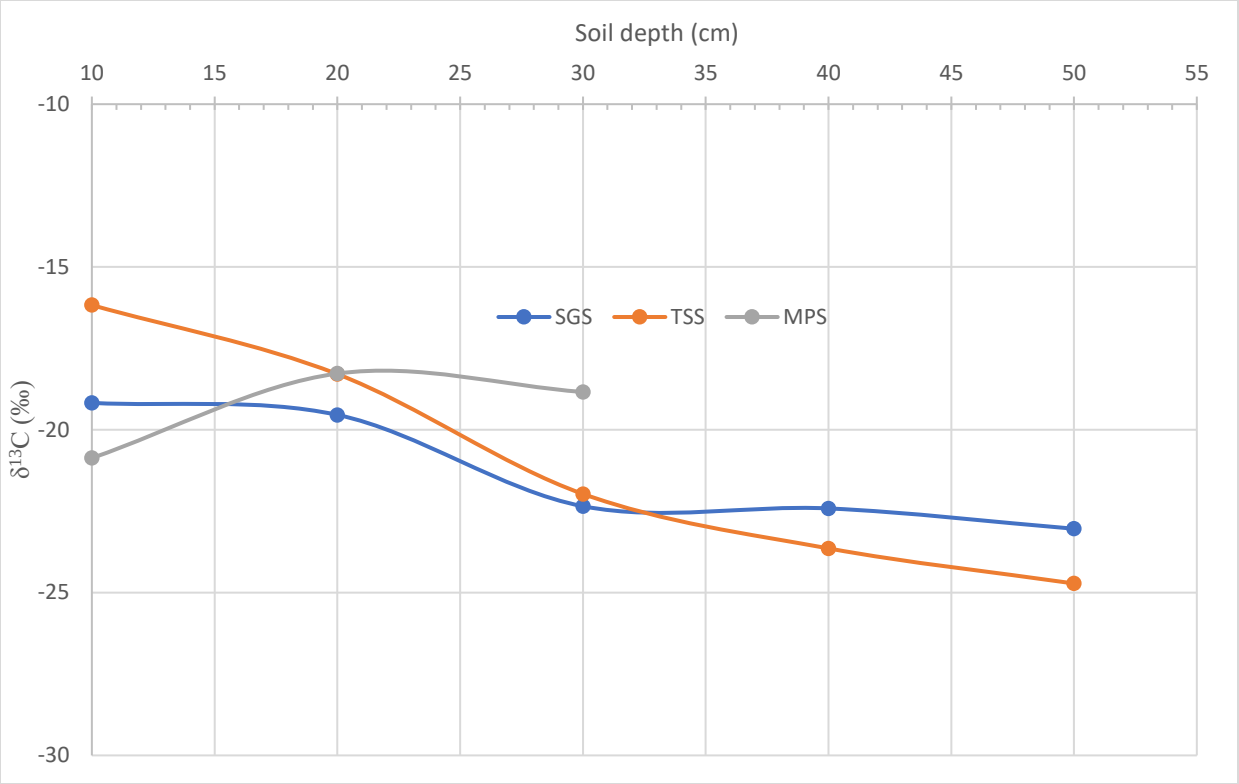

Figure 6.4: Plot of the soil depth against $\delta^{13}C$ at Sagole, Tshipise and Mphephu in summer.

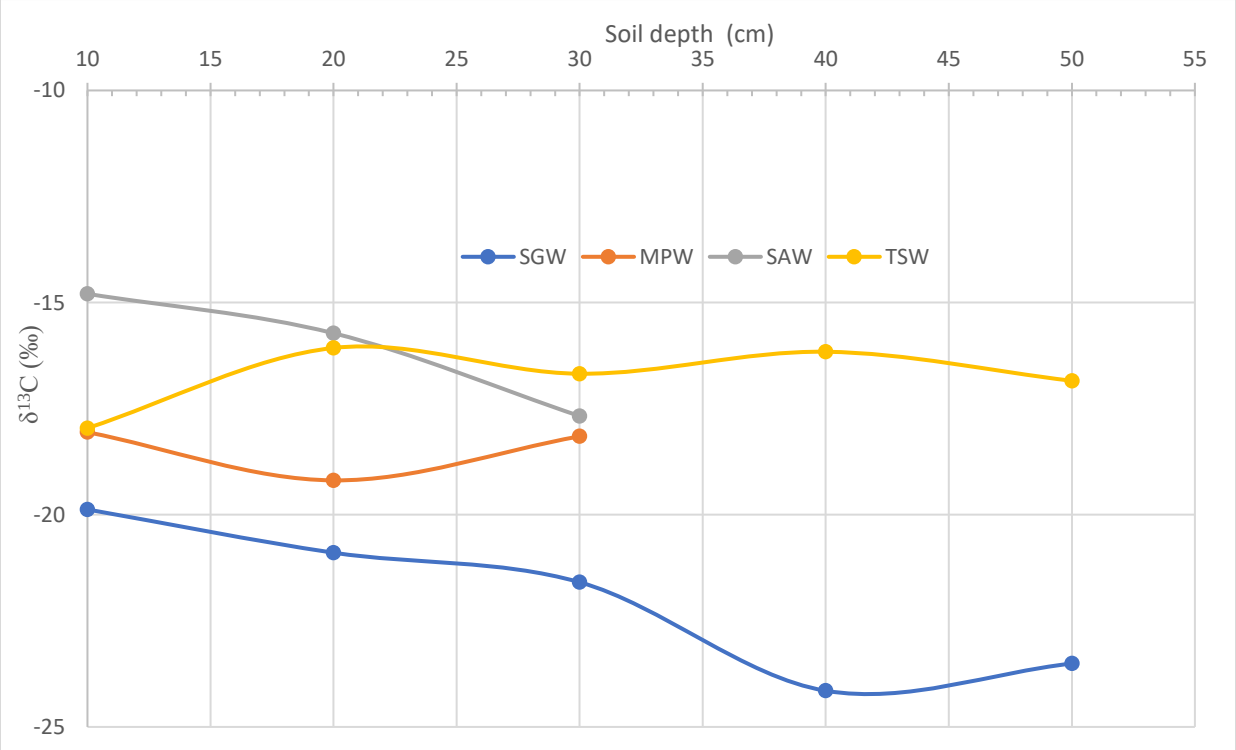

Figure 6.5: Plot of the soil depth against $\delta^{13}C$ at Siloam, Sagole, Tshipise and Mphephu in winter.

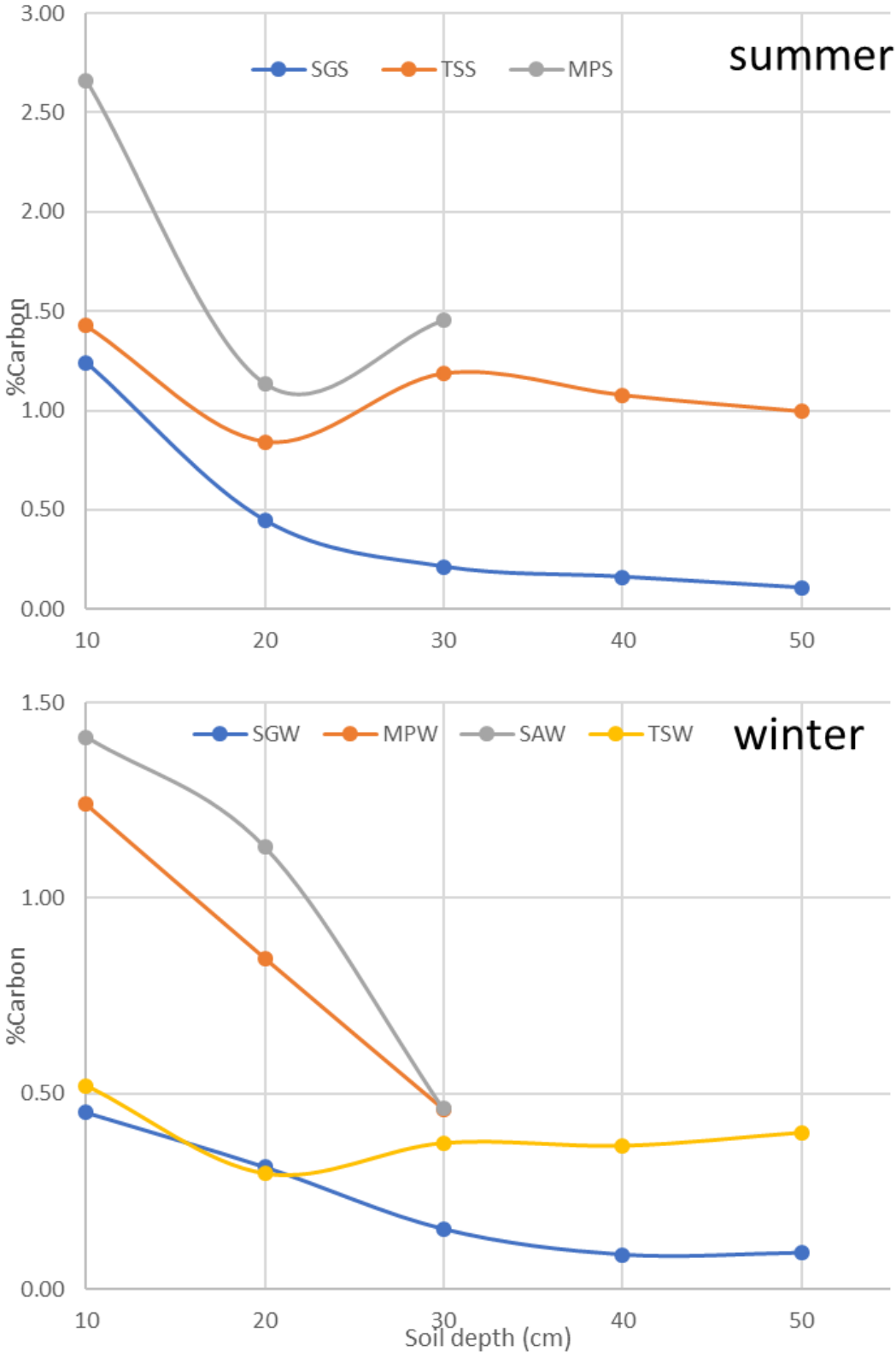

Figure 6.6: Plot of soil depth against % carbon Siloam, Sagole, Tshipise and Mphephu for both seasons.

A one-way analysis of variance (ANOVA) shows there is a significant difference between $\delta^{13}C$ values of soil at different depths in winter and summer (P = 0.04, Table 6.3). This indicates that the $\delta^{13}C$ approach is sensitive enough to differentiate the sources of organic matter in the catchments. This implies that the $\delta^{13}C$ values at depth reflect the respiration, whereas values near the surface are more affected by the atmosphere (Schmidt and Gleixner, 2005).

Table 6.3: ANOVA for $\delta^{13}C$ values within Soutpansberg region in both seasons

Source of Variation	SS	df	MS	F	P-value	F critical
Between Groups	32.6477	1	32.6477	4.599152	0.041145	4.210008
Within Groups	191.6631	27	7.098635			
Total	224.3108	28				

Generally, the soils at all the four sites show a similar trend of δD and $\delta^{13}C$ with respect to soil depth except for few a exceptions. The soil types differ, ranging from sandy, sand loamy and clay loamy for Sagole, Tshipise and Mphephu and Siloam soils, respectively, which play a vital role in isotopic fractionantion. All the soil types covered in studied areas were typically the major type classifications.

It can be deduced that δD is directly proportional to the depth and $\delta^{13}C$ is inversely proportional to the depth. The relationship between δD and $\delta^{13}C$ varies with season (Figures 6.7 and 6.8). Hence, equations connecting δD and $\delta^{13}C$ deduced from Figures 6.7 and 6.8 are:

For winter (Positive correlation);

$$\delta^{13}C = 0.0812\delta D - 10.657 \quad \text{.....6.1}$$

And for summer (Negative correlation);

$$\delta^{13}C = -0.0278\delta D - 21.945 \quad \text{.....6.2}$$

The differences in equations could be attributed to the enrichment from rainwater during summer leading to less depletion of δD and vice versa. The equations could be used to determine $\delta^{13}C$ if δD is known and vice versa.

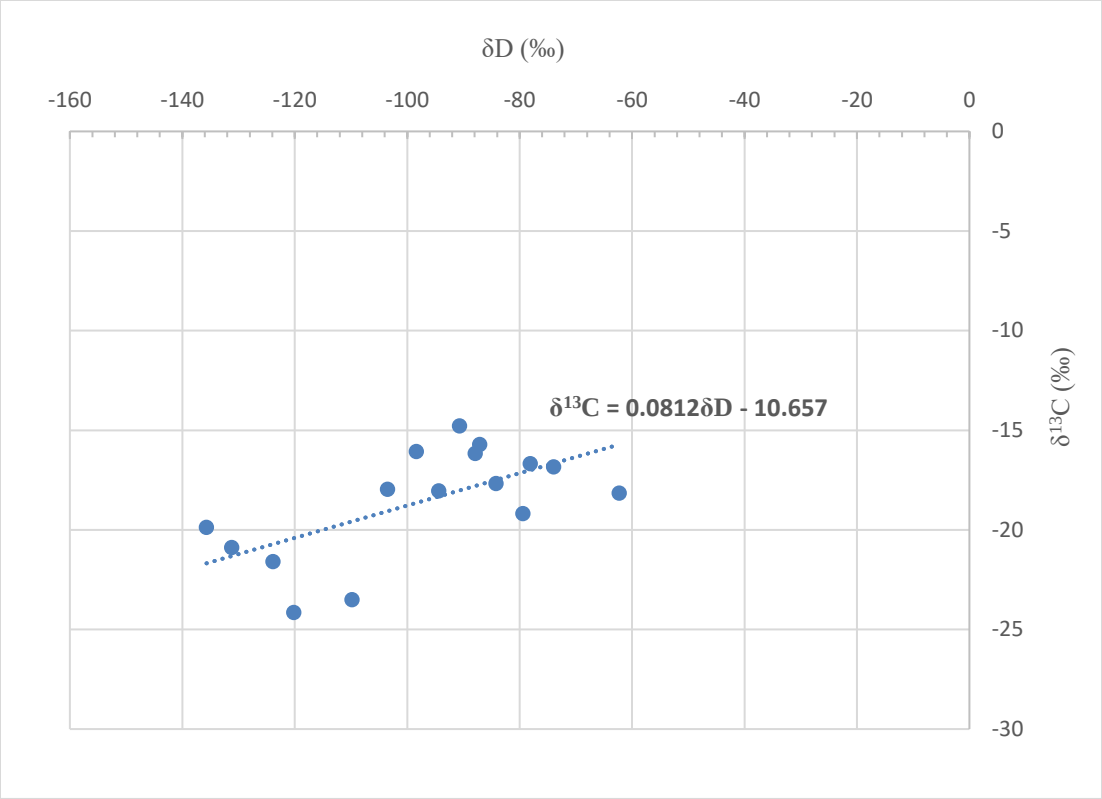

Figure 6.7: Relationship between $\delta^{13}C$ and δD for winter in Soutpansberg region.

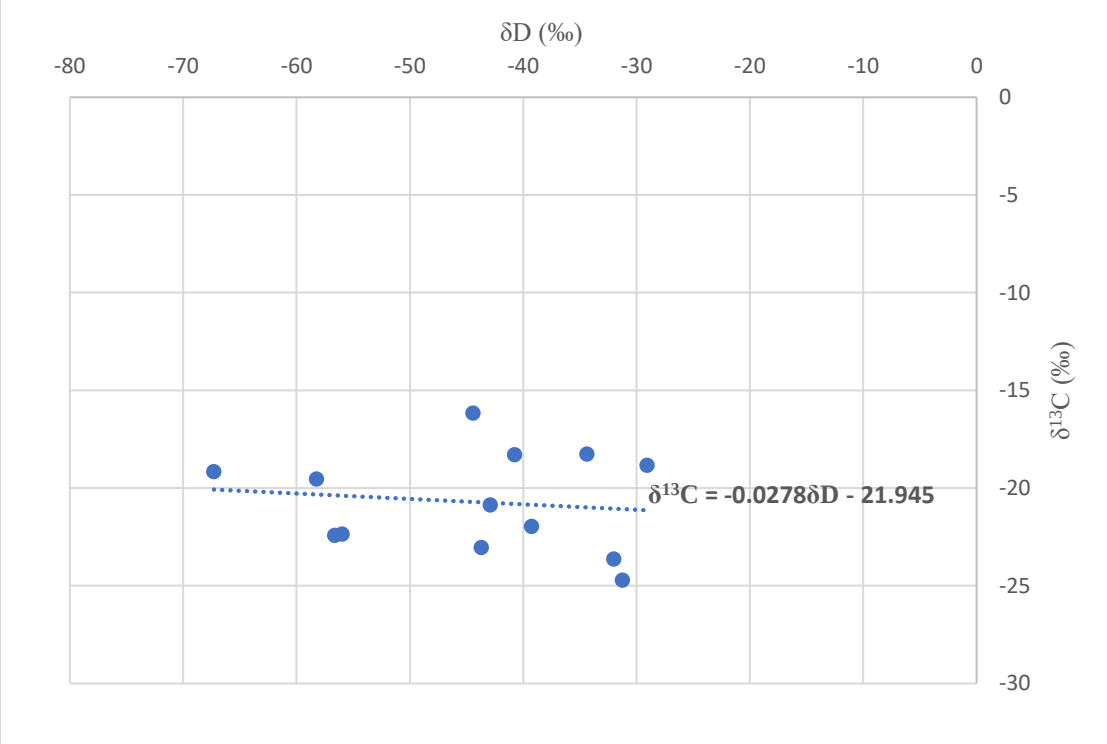

Figure 6.8: Relationship between $\delta^{13}C$ and δD for summer in Soutpansberg region.

6.3 Stable isotopic compositions (Hydrogen and Carbon) in vegetation

The stable isotopic compositions (δD and $\delta^{13}C$) vary with different indigenous trees present at each site (Table 6.4). Also, different parts of vegetation (core, leaf and bark) showed different variations in their compositions.

Table 6.4: Mean isotopic composition (Hydrogen and Carbon) in vegetation

		δD (‰)			$\delta^{13}C$ (‰)			%C		
Sites	Plant species	Core	Leaf	Bark	Core	Leaf	Bark	Core	Leaf	Bark
	Amarula tree	-55.54	-78.50	-94.10	-29.30	-34.50	-30.17	13.40	14.03	13.75
	Lowveld	-61.60	-71.80	-77.10	-26.50	-28.60	-29.30	15.21	11.35	13.18
Sagole	Leadwood	-56.13	-70.70	-110.60	-23.70	-25.60	-14.20	12.26	13.37	11.25
	Acacia tree	-53.49	-82.30	-66.30	-17.87	-17.46	-18.85	14.73	16.21	15.89
	Fig tree	-48.21	-71.60	-60.70	-14.63	-24.81	-18.19	16.31	16.21	16.26
Mphephu	Amarula tree	-44.57	-93.00	-78.60	-25.49	-28.17	-29.84	11.69	14.79	16.21
	Sausage tree	-48.10	-42.70	-72.50	-13.71	-19.26	-17.64	13.03	9.32	10.52
	Amarula tree	-55.50	-82.30	-66.70	-26.86	-30.17	-28.69	11.59	10.52	-
Tshipise	Acacia tree	-73.50	-72.50	-49.50	-15.72	-17.95	-16.30	13.62	11.06	11.31
	Amarula tree	-53.60	-79.80	-88.30	-21.82	-23.47	-22.46	14.11	15.23	15.06
	Guava tree	-38.90	-47.40	-40.20	-17.94	-18.38	-16.43	12.97	15.63	16.87
Siloam	Mango tree	-62.60	-86.70	-78.90	-18.81	-24.92	-20.08	13.95	15.32	15.89

The δD values in vegetation were heavier than the mean δD value in soil (summer and winter). This implies that the plant has access to more evaporation-influence and

isotopically heavier surface water/groundwater and tree roots sourcing deeper, isotopically lighter soil water (Krull *et al.,* 2006). As highlighted earlier in soil-water, there is also a link with the atmospheric δD from the rainwater since it's value ranges from -110.60‰ to -38.90‰. Although, the relationship of δD differs among various parts of the vegetation: with the core part having heavier δD (less negative value) than other parts in all the sites, except for the Acacia tree at Tshipise (Figure 6.9). This could be as a result of evaporative enrichment of the leaf water transmitting to another part, hence making δD in leaves lighter (more negative value) (Krull *et al.,* 2006; Seki *et al.,* 2010). The core of Sausage tree at Tshipise is also lighter in δD than the leaf part. Hence, there is no uniform trend of distribution for δD in different parts of the vegetations, but generally, the core part has heavier δD than other parts (Figures 6.9 and 6.10). Variations of δD among the core, leaves and barks show no significant difference between the different parts of the plant at all sites ($P > 0.05$) except for Siloam (Table 6.5). This implies that there is variation of δD among the different parts of each plant, but the variation is not statistically significant. At Siloam, there is a significant difference in the variation of δD in core, leaves and barks of Amarula, Guava and Mango trees (Table 6.5). Interestingly, δD composition with Amarula tree differs at the four sites and this could be attributed to the different soil types in different sites.

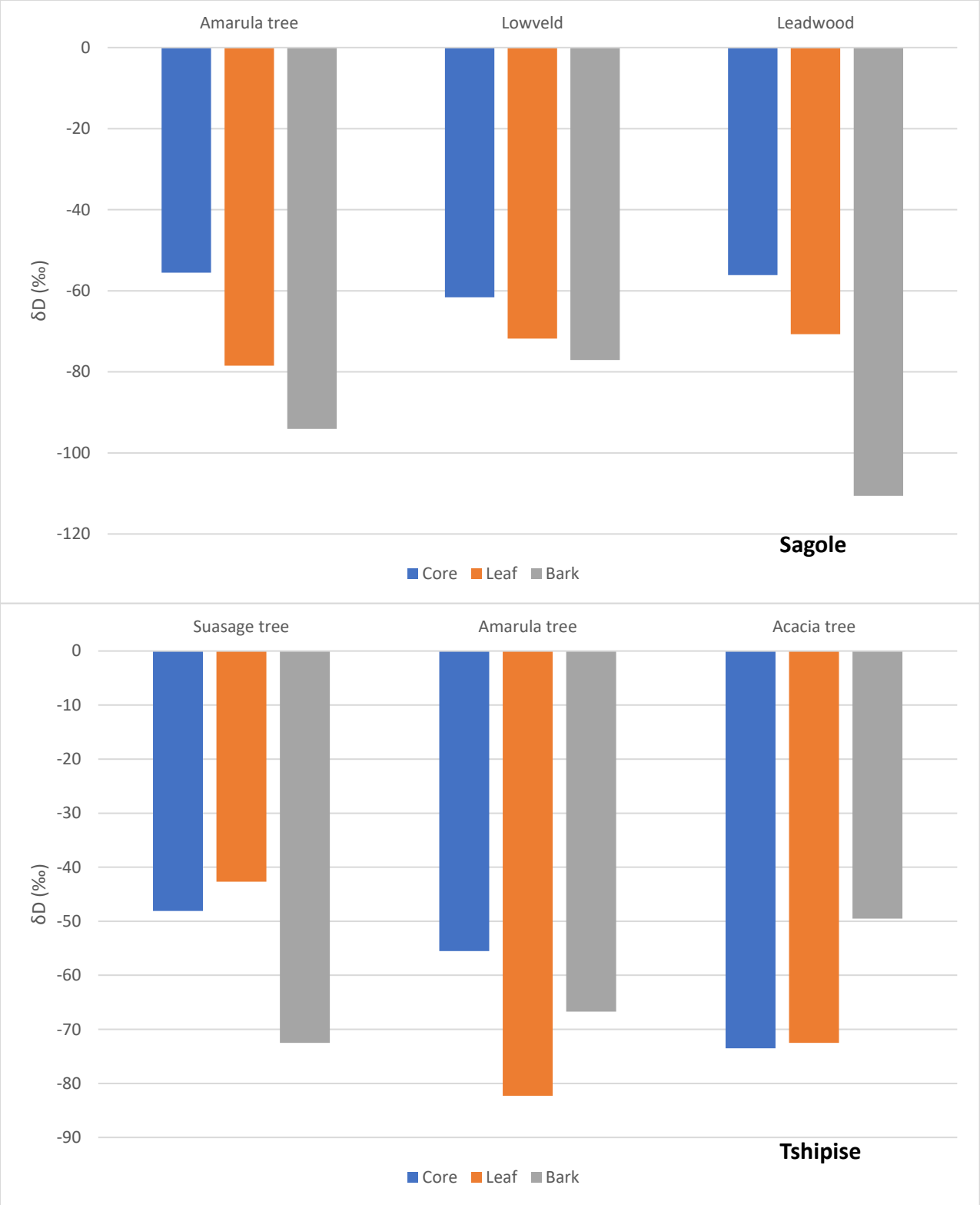

Figure 6.9: Variations of δD among different parts of various vegetation at Sagole Tshipise

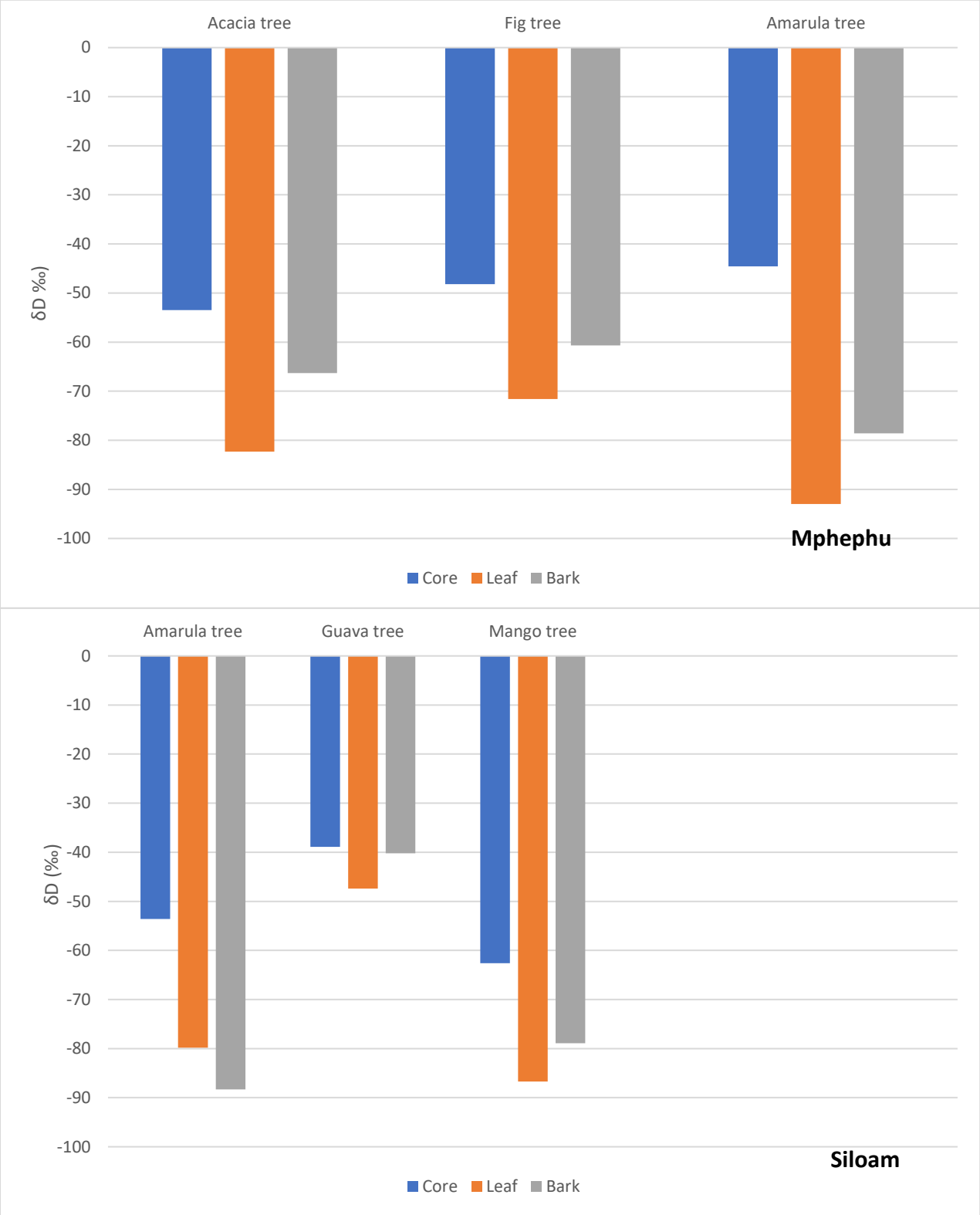

Figure 6.10: Variations of δD among different parts of various vegetation at Mphephu and Siloam.

Table 6.5: ANOVA for δD variations in different parts of the vegetation at Soutpansberg region

Source of Variation	SS	df	MS	F	P-value	F critical
Sagole						
Between Groups	124.73	2	62.37	0.152	0.862	5.143
Within Groups	2467.01	6	411.17			
Total	2591.74	8				
Mphephu						
Between Groups	215.09	2	107.54	0.335	0.728	5.143
Within Groups	1927.77	6	321.30			
Total	2142.86	8				
Tshipise						
Between Groups	312.81	2	156.40	0.760	0.508	5.143
Within Groups	1235.20	6	205.87			
Total	1548.01	8				
Siloam						
Between Groups	2160.91	2	1080.45	6.492	0.032	5.143
Within Groups	998.63	6	166.44			
Total	3159.54	8				

The $\delta^{13}C$ composition in plant-water varies from one vegetation to another and from one part to another in the different sites (Table 6.4). Like δD in plant water, the $\delta^{13}C$ value in core part was higher than in leaves and barks (Figure 6.11). The composition of $\delta^{13}C$ in plant water ranges wide from -34.50 to -13.71‰ (Table 6.4), which indicate the presence of C3, CAM and C4 plants. Different fractionation in $\delta^{13}C$ in the plant were used to determine the biosynthetic pathway of the plant and classify the plant type. Generally, the C3 plants include Amarula, Lowveld and Leadwood trees; C4 plants include Acacia and Sausage plants; and CAM plants include Fig, Guava and Mango trees (Table 6.6). But from the soil-water, the $\delta^{13}C$ obtained showed that the carbon soil is induced by Crassulacean Acid Metabolism (CAM), resulting in CAM soils. Studies have shown that there is the possibility of having a CAM soil with either C3 or C4 or CAM plants, which

this study has also supported (Ehleringer *et al.,* 1993; Lajtha and Michener, 1994; Krull *et al.,* 2005; Seki *et al.,* 2010).

Table 6.6: Plant type classification based on $\delta^{13}C$ values within the Soutpansberg region

Sites	Vegetation analysed	Plant type
Sagole	Amarula tree	C3
	Lowveld	C3
	Leadwood	C3
Mphephu	Acacia tree	C4
	Fig tree	CAM
	Amarula tree	C3
Tshipise	Sausage tree	C4
	Amarula tree	C3
	Acacia tree	C4
Siloam	Amarula tree	C3
	Guava tree	CAM
	Mango tree	CAM

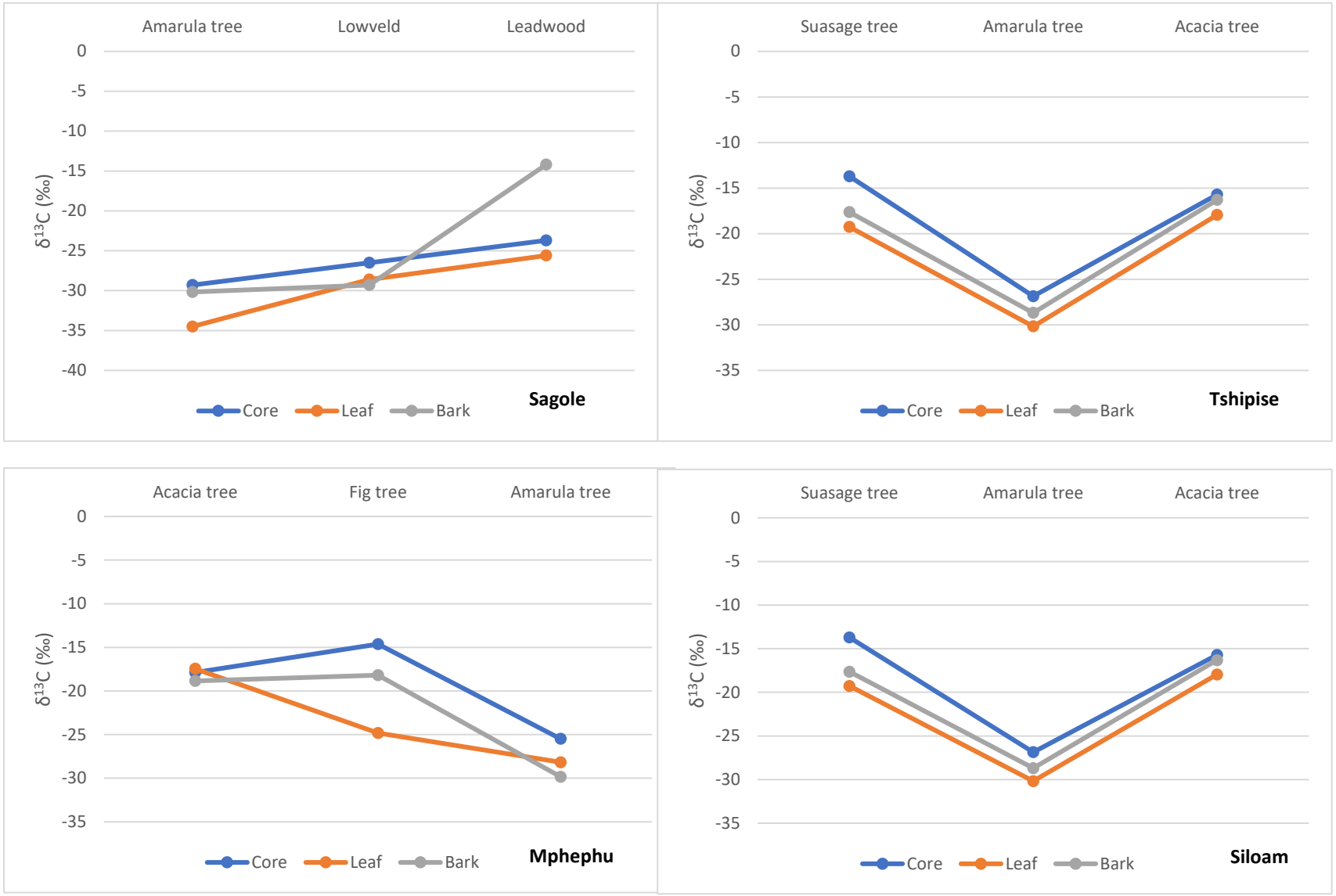

Figure 6.11: Variations of $\delta^{13}C$ among different parts of various vegetation at Sagole, Tshipise, Mphephu and Siloam.

Also, this study has shown that different plant types could be on the same soil type. For instance, Siloam with CAM soil having an Amarula tree (C3), and Guava and Mango trees (CAM). Amarula tree was classified as C3 plant at all the sites, which supports reports from Ruwimbo (2017).

Statistically, there are significant differences in the $\delta^{13}C$ in plant water at different parts of the indigenous trees (Table 6.7). This implies that the difference in $\delta^{13}C$ values among the core, leaves and barks of each tree at each site were not by chance but real. Hence, this accounts for the reliability of the results obtained in this study because previous studies only examined the leaf part of the selected tree in an area. The $\delta^{13}C$ in the core were higher than in the leaves and bark because the soil water is transported via core to leaves and bark before respiration takes place.

Table 6.7: ANOVA for $\delta^{13}C$ variations in different parts of the vegetation within Soutpansberg region

Source of Variation	SS	df	MS	F	P-value	F critical
Sagole						
Between Groups	161.868	2	80.934	5.146	0.049	5.143
Within Groups	94.369	6	15.728			
Total	256.237	8				
Mphephu						
Between Groups	171.202	2	85.601	8.022	0.020	5.143
Within Groups	64.028	6	10.671			
Total	235.231	8				
Tshipise						
Between Groups	279.020	2	139.510	34.213	0.001	5.143
Within Groups	24.466	6	4.078			
Total	303.487	8				
Siloam						
Between Groups	40.316	2	20.158	4.984	0.053	5.143
Within Groups	24.266	6	4.044			
Total	64.583	8				

6.4 Interconnectivity of δD and $\delta^{13}C$ within the environmental media

Water source used by indigenous plants should be used to understand the function of these plants and the feedback mechanisms involved in soil-vegetation systems in semi-arid zones. Rainwater is the main water source for revegetated ecosystems, and its isotopic composition varies significantly with the seasons. A conceptual model that shows the interconnectivity of the stable isotopes of δD and $\delta^{13}C$ in water, soil and vegetation is presented in Figure 6.12. Earlier in chapter 4, it was mentioned that the rainwater is a fundamental component of the geothermal springs/boreholes. That is groundwater is recharged by infiltration of rainwater. Hence, the geothermal spring/borehole water reflects the isotopic signatures (δD and $\delta^{13}C$) of rainwater and are trapped in the soils. The root of the plant absorbs the soil-water and its signature is then transported via the core part to other parts such as leaves and barks. Then, δD and $\delta^{18}O$ in plant water in the leaves and barks are then evaporated to form evaporated water which via evapotranspiration process forms evapotranspired water. This evapotranspired water in turn rains when it becomes saturated in the atmosphere.

Soil-water comes in contact with carbonic compound in which the soil microbes break down by respiration leading to generation of respired CO_2. Also, the plant water $\delta^{13}C$ from the soil water is transmitted via core to the leaves and barks when respiration takes place. Some of the respired CO_2 travels back to the atmosphere (CO_2 in the air) and to the photosynthate (product of photosynthesis). Hence, this process is a cycle and is summarised in Figures 6.9.

Statistically, there were strong positive and negative correlations in the variation of δD and $\delta^{13}C$ isotopes in water to soil; soil to plant and water to plant. The positive correlation coefficient ranges from 0.771 to 1, whereas the negative correlation coefficient ranges from 0.086 to 1 (Table 6.8). The weak negative correlation was observed in soil $\delta^{13}C$ vs plant $\delta^{13}C$ at Tshipise and Mphephu. Generally, the relationship of δD and $\delta^{13}C$ in water and soil; water and plant were very strong with significant differences at all sites except for Siloam ($P > 0.05$). There is also a relationship of δD and $\delta^{13}C$ in soil and plant in all the sites, but significant difference (Table 6.8). Therefore, it can be concluded that δD and $\delta^{13}C$ isotope in water, soil and plant are correlated to one another to form a cycle

(that is water to soil to plant) (Table 6.7; Figure 6.13). Although, this relationship does not support conceptual model 100%.

Table 6.8: Spearman correlation analyses of the δD and $\delta^{13}C$ isotopes in water (W), soil (S) and vegetation (P) within Soutpansberg region

	Tshipise	**Mphephu**	**Sagole**	**Siloam**
Variables	Correlation Coefficient (P-value)	Correlation Coefficient (P-value)	Correlation Coefficient (P-value)	Correlation Coefficient (P-value)
W-$\delta^{13}C$ vs S-$\delta^{13}C$	-1.000 (0.000)	-1.000 (0.000)	1.000 (0.000)	-
W-δD vs S-δD	1.000 (0.000)	-1.000 (0.000)	1.000 (0.000)	-0.866 (0.333)
S-$\delta^{13}C$ vs P-$\delta^{13}C$	-0.086 (0.877)	-0.400 (0.600)	0.771 (0.072)	-0.500 (0.667)
S- δD vs P-δD	-0.429 (0.397)	-1.000 (0.000)	-0.714 (0.111)	-0.500 (0.667)
W- $\delta^{13}C$ vs P- $\delta^{13}C$	1.000 (0.000)	-1.000 (0.000)	-1.000 (0.000)	-
W- δD vs P- δD	-1.000 (0.000)	1.000 (0.000)	1.000 (0.000)	-0.866 (0.333)

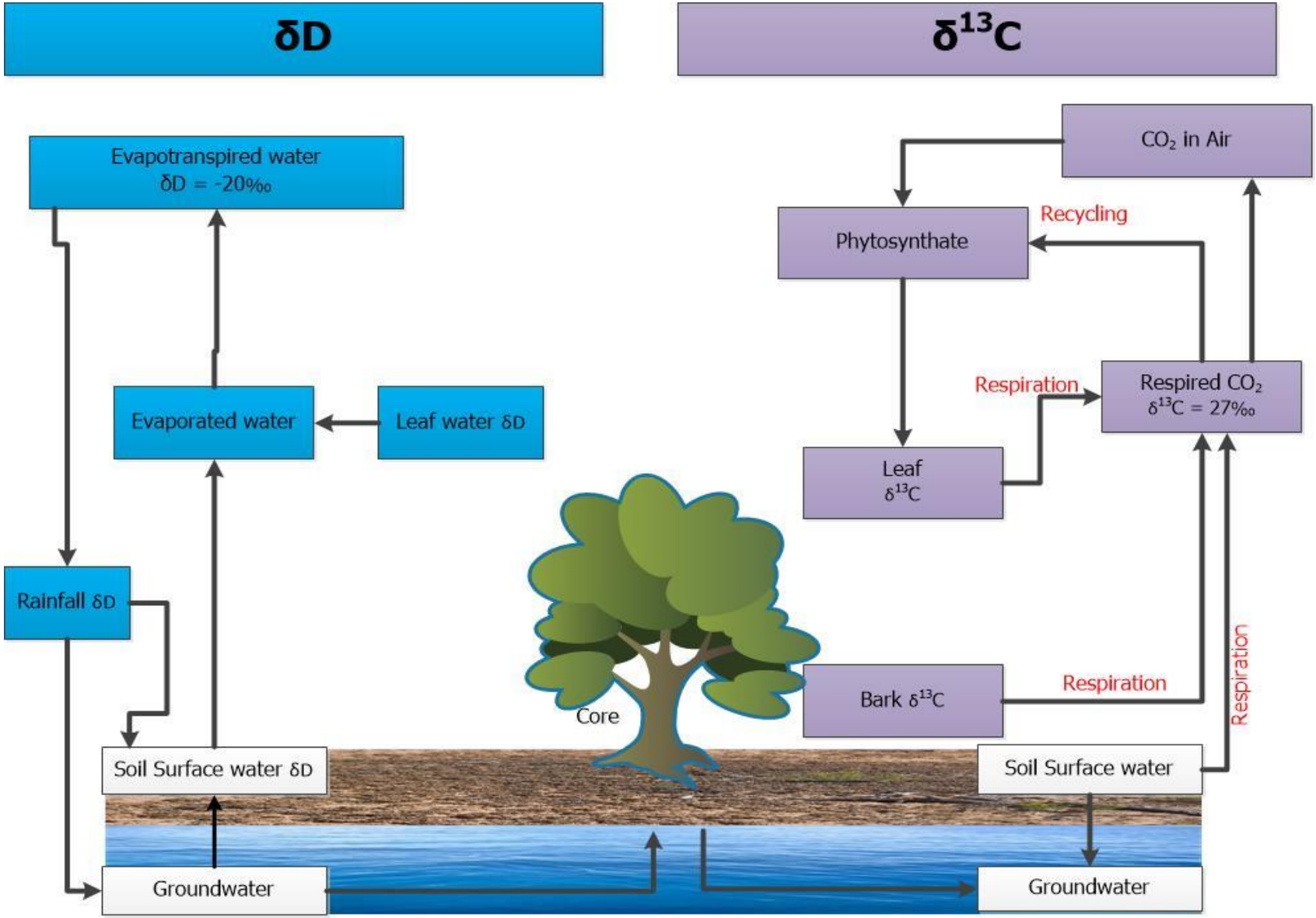

Figure 6.12: Conceptual model summarising the interconnectivity of δD and $\delta^{13}C$ isotopes within the environmental media.

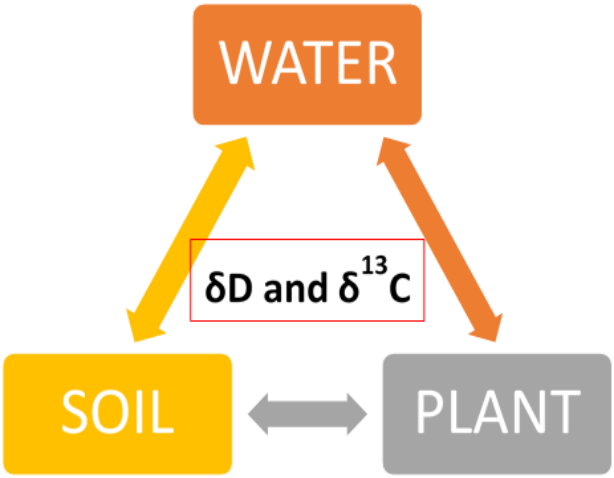

Figure 6.13: Interconnectivity of δD and $\delta^{13}C$ isotopes in water, soil and plant.

6.5 Synopsis

The objective of this chapter was to determine the stable isotopes compositions (hydrogen, carbon) in the surrounding soils and vegetation; and their interconnectivity within the study areas (Specific Objective 3). The following results were obtained:

- δD values of soil water increase with depth at all sites such that the top soil has the least concentrations but the composition of $\delta^{13}C$ in soil water decreases with depth. Hence, it can be deduced that δD is directly proportional to the depth and $\delta^{13}C$ is inversely proportional to the depth of the soil. Two equations connecting δD and $\delta^{13}C$ in soil-water were deduced per season for soil-water (Equations 6.1 and 6.2)
- The composition of $\delta^{13}C$ in soil water ranges from -24.15 to -14.79‰, which is an indication of Crassulacean Acid Metabolism (CAM) (mixture of C3 and C4 photosynthetic cycles) with a stronger C4 trend. This result corroborates with the $\delta^{13}C$ of the geothermal springs, which suggested that the carbon in the soil is induced by Crassulacean Acid Metabolism (CAM).
- The composition of $\delta^{13}C$ in plant water ranges wide from -34.50 to -13.71‰, which indicates the presence of C3 plants, CAM Plants and C4 plants. The C3 plants include Amarula, Lowveld and Leadwood trees; C4 plants include Acacia and

Sausage trees; and CAM plants include Fig, Guava and Mango trees. Hence, this study shows that with CAM soils, there is a possibility of having either C3, C4 or CAM vegetation on it. From literature, only Amarula and Acacia trees have been documented for isotopic compositions, which this study has given additional information on other indigenous plants such as Lowveld, Leadwood, Sausage, Fig, Guava and Mango trees.

- This study has shown that the δD and $\delta^{13}C$ isotopes in water, soil and vegetation are interconnected (conceptual model). Statistically, there is a strong correlation among the environmental media with respect to δD and $\delta^{13}C$ isotopic compositions. Therefore, surrounding soils and vegetation of geothermal springs have similar stable isotopic compositions and are interconnected.

CHAPTER SEVEN

ASSESSSMENT OF TRACE METALS CONCENTRATIONS AND ASSOCIATED HUMAN HEALTH RISK WITHIN THE NEIGBOURHOOD OF THE GEOTHERMAL SPRINGS

7.1 Preamble

The chapter presents results and discussion on the trace metals concentrations and evaluate possible human health risks associated with the trace metals from geothermal springs and the surrounding soils. In addition, it explores the phytoremediative ability of the surrounding vegetation (Specific objective 4). This chapter elucidates on the possible sources of these trace metals using principal component analysis (PCA), factor analysis (FA) and correlation; and their potential health risk (cancer and non-cancer) using the USEPA health risk model. Hence, the findings will be communicated via the appropriate channel to the community members and various stakeholders. The chapter is based on Hypothesis 4, which states that "the studied geothermal spring water and surrounding soils have potential health risk on the inhabitants".

7.2 Trace metals concentrations from the geothermal springs and boreholes

Table 7.1 shows the mean values for trace metals concentrations in the geothermal springs, hot boreholes and tepid boreholes. Results show that geothermal springs are highly mineralised owing to their geological formations as supported by Todd (1980). More mineralisation of the geothermal springs was aided by the thermal gradient (temperature) leading to more mineral dissolution in water (Odiyo and Makungo, 2012). The obtained values were compared with the standard guidelines for drinking water by SANS (2015) and WHO (2004). Generally, the trace metals concentrations of the geothermal spring and boreholes within the Soutpansberg were within the drinking water permissible guidelines by the SABS and WHO, except for Mercury (Hg) which is high in summer (>1 µg/L). This high mercury concentration could be associated with igneous activity and circulating geothermal fluids that precipitate around mineral springs, geysers and fumaroles, particularly during summer, when there is high rainfall (Barringer *et al*., 2013). Though trace metals concentrations were within the drinking water guidelines, the

accumulation in the human body could result in adverse effect considering that some of these metals are carcinogenic in nature.

Generally, the mean trace metals concentrations were higher in summer compared to winter except for some trace metals such as Be, Ni, Cu, Zn, Se, Ba at different sites with anomalous concentrations. This could be attributed to the temperature differences and more rainfall leading to more dissolution of the host rock (minerals) in summer (Figures 7.1 and 7.2). Figures 7.1 and 7.2 show clearly the variations in the trace metal concentrations in the geothermal spring and boreholes (hot and tepid).

The mean trace metals concentrations within the study areas were in relatively good agreement during summer for geothermal springs (Table 7.1). As stated earlier, more rainfall in summer (wet) enhances more rock-water interaction at the deep aquifer of the geothermal spring and more trace metals were released into the water body at the surface. Therefore, there are more trace metals in the geothermal spring water during summer (wet) than in the winter (dry). At Siloam, anomalous trend was found among the geothermal spring, hot borehole and tepid boreholes, where the boreholes were in some cases more enriched with trace metals than the geothermal spring. This could possibly be linked to the geology of the area, although, the geology of an area is complex and differs from one point to another (Olivier *et al*., 2008; 2011). For instance, two houses where the borehole water was sampled are next to one another and their water characteristics are different (one is hot and the other is cold). Hence, there is possibility of common host rock and minor faults connecting the aquifer of geothermal spring and boreholes.

Table 7.1: Mean trace metal concentrations of the geothermal springs and boreholes within Soutpansberg region

	SABS; WHO	TSS	TSW	SGS	SGW	MPS	MPW	SAW	SH1	SH2	BH1	BH2	SCC	TTP
Temp(°C)		55.4.	54.60	44.80	42.40	42.70	41.30	67.70	45.20	48.40	22.40	21.40	20.10	22.50
pH	6-9	8.47	8.46	7.98	8.82	8.15	8.05	9.39	8.86	9.19	8.17	8.1	7.17	8.17
EC	<750	745.00	746.67	347.33	330.00	365.00	335.00	340.00	630.00	330.00	690.00	730.00	90.00	290.00
Alkalinity		10.75	11.12	6.5	10.50	6.00	12.5	107.52	10.00	12.00	25.50	17.50	2.00	11.50
Be (µg/l)		1.83	5.84	1.34	0.01	2.60	5.13	0.05	3.21	3.53	4.37	6.76	5.06	0.01
V (µg/l)		18.36	16.74	13.51	14.59	16.28	13.96	3.21	13.54	17.63	5.12	12.46	17.83	4.62
Cr (µg/l)	50; 100	12.46	8.64	10.48	6.64	10.57	8.40	0.09	10.40	11.08	6.99	6.48	12.14	9.03
Mn (µg/l)	500; 1000	2.67	2.22	10.30	25.55	36.60	1.06	0.24	1.25	1.95	107.50	1.66	1.52	14.69
Co (µg/l)		0.21	0.28	0.43	0.36	0.29	0.36	0.04	0.19	0.26	3.42	0.51	0.24	0.17
Ni (µg/l)	20; 150	2.25	2.64	0.99	1.11	2.14	0.84	0.71	0.82	1.48	12.52	0.55	1.88	1.57
Cu (µg/l)	2000; 1000	11.97	18.75	30.58	0.06	1.28	0.01	0.35	0.01	1.84	31.39	0.34	2.15	4.82
Zn (µg/l)	3000; 5000	312.90	464.85	294.38	194.59	49.35	21.00	0.95	0.01	0.01	350.90	0.01	0.01	44.86
As (µg/l)	10; 10	2.04	2.01	1.35	1.97	2.72	2.10	1.01	1.03	3.04	1.92	1.29	3.05	1.30
Se (µg/l)		5.83	6.18	3.86	5.74	10.02	6.42	0.68	5.07	10.95	5.85	3.62	10.94	3.25
Cd (µg/l)		0.06	0.02	0.01	0.05	0.01	0.14	0.02	0.01	0.01	0.73	0.01	0.01	0.05
Sb (µg/l)	5; 5	0.05	0.02	0.03	0.06	0.04	0.17	0.03	0.01	0.02	0.12	0.08	0.01	0.10
Ba (µg/l)		1.54	26.39	0.78	42.39	8.79	29.00	10.42	0.38	7.20	67.32	71.98	6.84	0.01
Hg (µg/l)	1; 1	**6.11**	0.62	**3.26**	0.40	**1.82**	0.43	0.35	0.66	0.80	0.15	**1.60**	0.46	0.72
Pb (µg/l)	10; 20	0.28	0.33	0.49	0.01	0.01	0.01	0.09	0.17	0.01	0.01	0.01	0.01	0.06

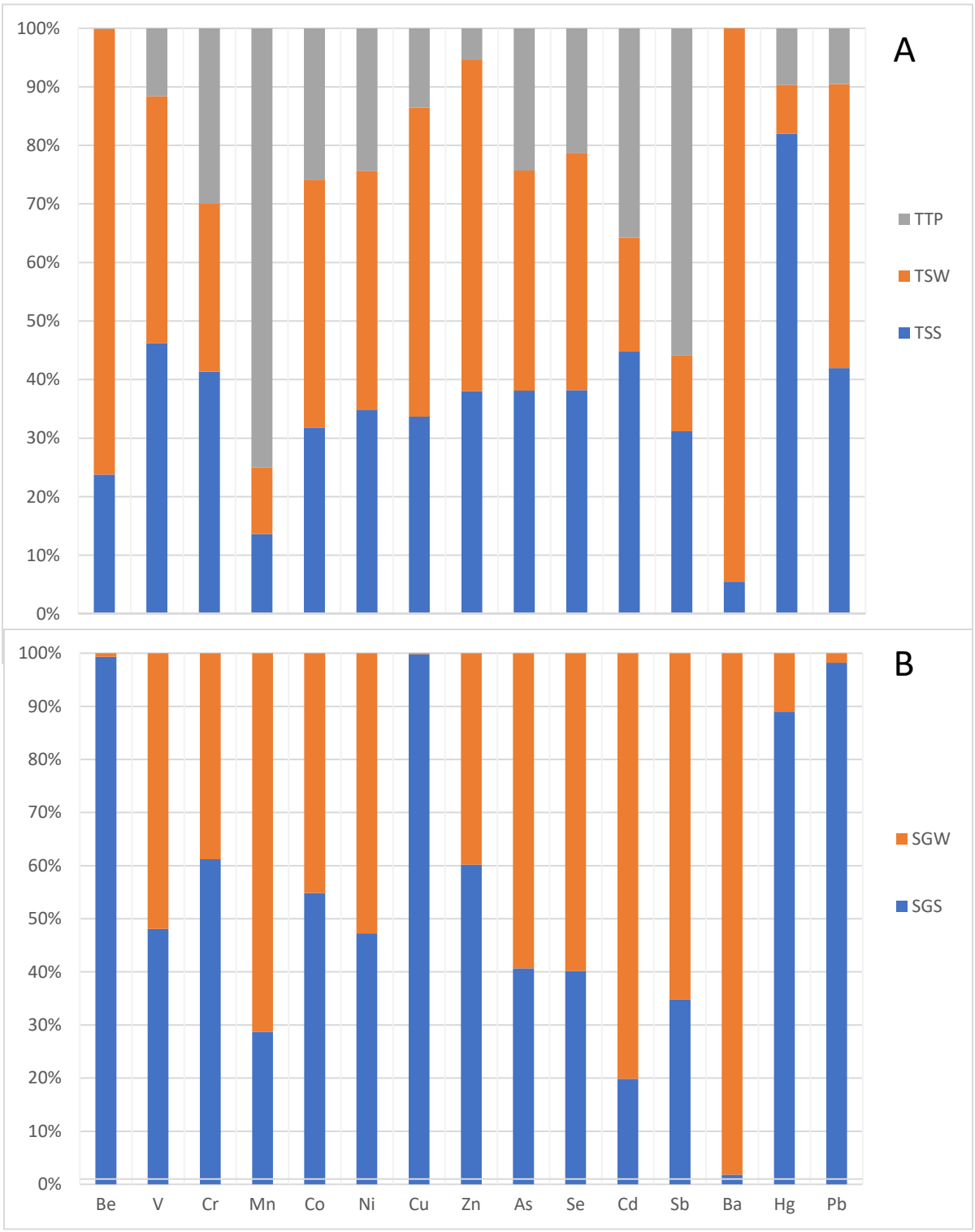

Figure 7.1: Variations of trace metals concentrations in (A) Tshipise geothermal spring and tepid borehole (B) Sagole geothermal spring.

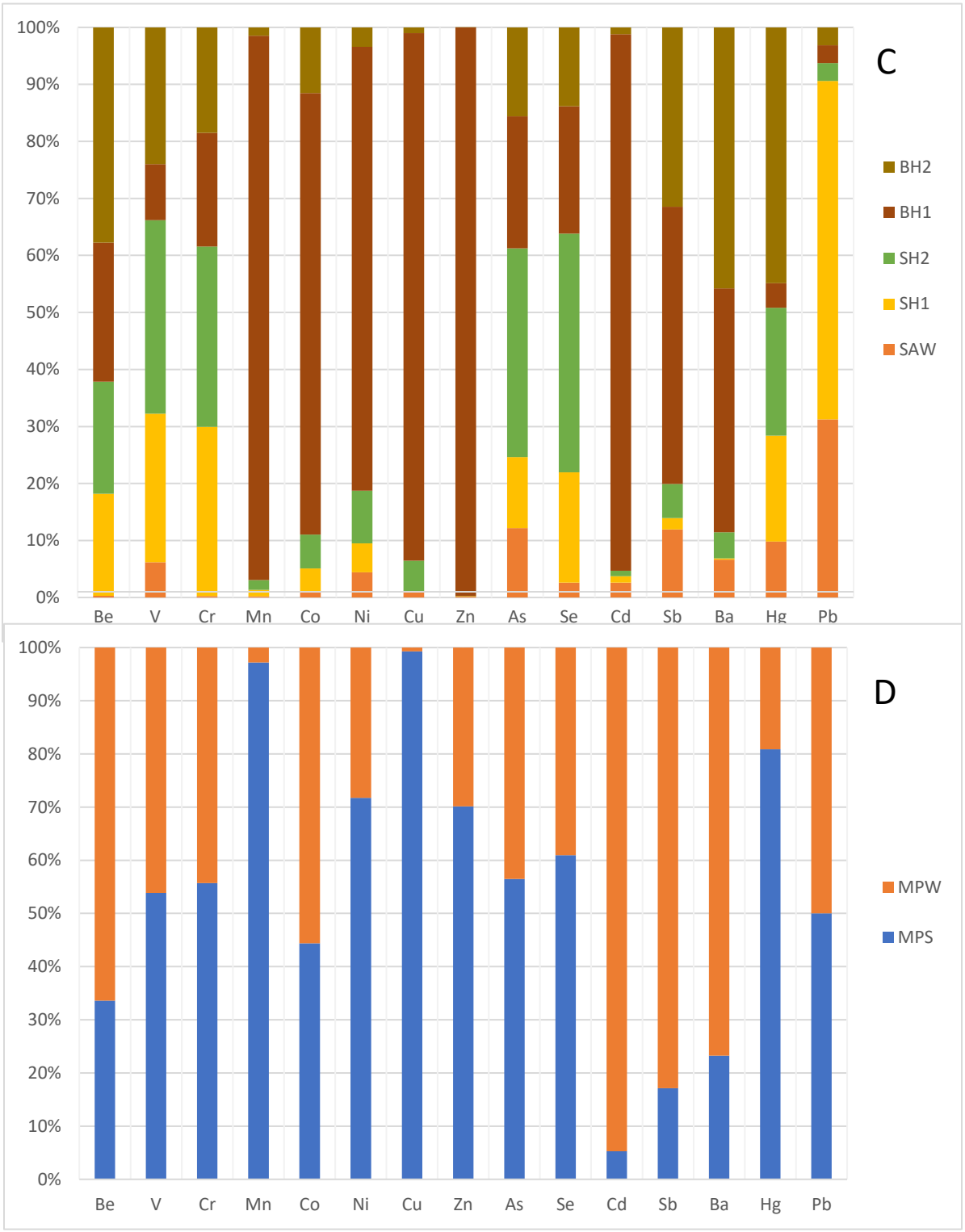

Figure 7.2: Variations of trace metals concentrations in (C) Siloam geothermal spring, hot and tepid boreholes (D) Mphephu geothermal spring.

Relationships of trace metals in water with some physicochemical parameters were evaluated using the Pearson's test (Table 7.2). There is a direct relationship between temperature and alkalinity, pH, EC, V, Zn, Hg and Pb. This means that an increase in water temperature results to increase in EC, pH (leading to high alkalinity) and trace metals such as V, Zn, Hg, Pb. This is an indication of dissolution of minerals (rock-water interaction) under high temperature. Also, there was a negative correlation between temperature and other trace metals (Be, Cr, Mn, Co, Ni, Cu, As, Se, Cd, Sb, Ba). This means that these trace metals are in good agreement with one another or perhaps have some common minerals in their compositions. This study revealed that pH has a negative correlation with all the trace metals (Be, Cr, Mn, Co, Ni, Cu, As, Se, Cd, Sb, Ba, V, Zn, Hg) except Pb. This means that increase in pH (basic) results to decrease in trace metals concentrations in the geothermal springs/boreholes; which shows that there is less indication of trace metals pollution (insoluble) (USEPA, 1992b). This is in support of a previous study that stated that most metals seem to be more toxic in acidic state (Witeska and Jezierska, 2003). The conductivity values had a significant positive relationship with all trace metals such as Be, V, Mn, Co, Ni, Cu, Zn, Cd, Sb, Ba, Hg, Pb except alkalinity, Cr, As and Se. It could be inferred that the changes of physicochemical parameters depend on how seasons affect the levels of some metals (Radulescu *et al*., 2014).

The relationships among the trace metals were further determined by hierarchical cluster analysis (HCA) using XLSTAT statistical software (Shan *et al*., 2012). They were grouped into clusters based on the similarities and dissimilarities between different metals (Figure 7.3). Dendrogram analysis produced 6 clusters for the spatial distribution of trace metals of the samples; clusters 2 and 5 include pH and all the trace metals except Cu. These metals are likely present in the geothermal springs/boreholes due to agricultural run-off or atmospheric deposition in the study areas (Iqbal and Shah, 2013). This corroborated by the findings from the Pearson correlation matrix; trace metals are insoluble at higher pH (basic medium), hence the negative correlation. Clusters 1, 3, 4, and 6 are temperature, conductivity, alkalinity and Cu, respectively, occurred independently. The results of cluster analysis supported the correlation results, which suggested that the selected metals are from anthropogenic and natural sources.

Table 7.2: Pearson correlation matrix showing the relationships between trace metals and physicochemical parameters in geothermal springs and boreholes water

Variables	Temp	pH	EC	Alk	Be	V	Cr	Mn	Co	Ni	Cu	Zn	As	Se	Cd	Sb	Ba	Hg	Pb
Temp	**1.00**																		
pH	**0.71**	**1.00**																	
EC	0.13	0.21	**1.00**																
Alkalinity	0.48	**0.55**	-0.04	**1.00**															
Be	-0.36	-0.42	0.37	-0.33	**1.00**														
V	0.13	-0.22	0.02	**-0.65**	0.37	**1.00**													
Cr	-0.25	-0.48	-0.04	**-0.86**	0.22	**0.72**	**1.00**												
Mn	-0.38	-0.13	0.20	-0.03	0.00	-0.40	-0.12	**1.00**											
Co	-0.42	-0.17	0.34	0.00	0.23	-0.39	-0.13	**0.93**	**1.00**										
Ni	-0.34	-0.16	0.34	0.00	0.19	-0.34	-0.05	**0.92**	**0.96**	**1.00**									
Cu	-0.06	-0.23	0.35	-0.12	0.05	-0.15	0.12	0.54	**0.63**	**0.64**	**1.00**								
Zn	0.18	-0.06	0.53	-0.18	0.03	0.10	0.11	0.38	0.41	0.49	**0.81**	**1.00**							
As	-0.14	-0.30	-0.35	-0.44	0.30	**0.64**	0.54	0.08	0.02	0.12	-0.11	-0.03	**1.00**						
Se	-0.21	-0.32	-0.29	**-0.58**	0.37	**0.70**	**0.68**	0.06	0.00	0.09	-0.15	-0.11	**0.95**	**1.00**					
Cd	-0.35	-0.12	0.30	0.06	0.17	-0.44	-0.17	**0.90**	**0.98**	**0.96**	**0.58**	0.39	0.00	-0.04	**1.00**				
Sb	-0.36	-0.24	0.09	-0.04	0.15	-0.37	-0.21	0.37	0.44	0.34	0.09	0.03	-0.13	-0.22	0.54	**1.00**			
Ba	-0.42	-0.10	0.43	0.03	0.48	-0.22	-0.41	0.51	**0.62**	0.48	0.16	0.19	-0.09	-0.15	**0.57**	0.51	**1.00**		
Hg	0.26	-0.09	0.33	-0.21	-0.18	0.38	0.44	-0.19	-0.20	-0.15	0.26	0.33	-0.02	-0.05	-0.21	-0.13	-0.30	**1.00**	
Pb	0.43	0.00	0.30	-0.10	-0.15	0.19	0.23	-0.26	-0.19	-0.15	**0.60**	**0.61**	-0.34	-0.31	-0.22	-0.34	-0.39	**0.56**	**1.00**

Values in bold are different from 0 with a significance level alpha=0.05, Alk - Alkalinity

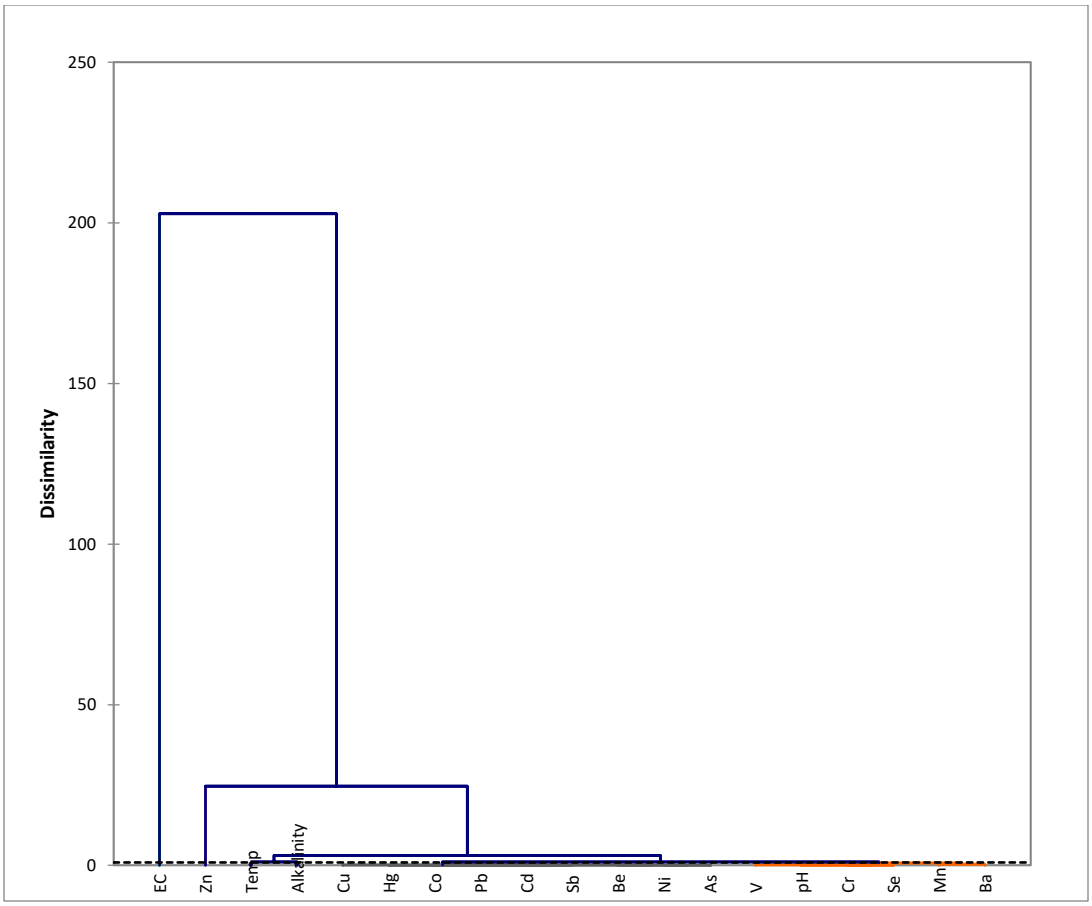

Figure 7.3: Dendrogram showing the spatial clustering of trace metals in geothermal spring/borehole water samples based on the hierarchical cluster analysis using Ward's method.

The PCA/FA loading factors for the trace metals in the geothermal springs/borehole samples taken within Soutpansberg are shown in Table 7.3. For both seasons (winter and summer), five important principal components (PCs) were significant with eigenvalues > 1, explaining higher total variance of 30.27, 53.20, 70.59, 79.00 and 86.61% respectively (Table 7.3 and Figure 7.4). The factor loadings show that F1 (30.27%) has high loadings of Mn, Co, Ni, Cu, Cd, Sb, Ba; F2 (22.93%) with high loadings of V, Cr, As, Se; F3 (17.39%) with high loading of EC, Cu, Zn, Hg, Pb; F4 (8.42%) with the highest loading of Be; F5 (7.60%) with high loadings of pH. Multivariate analysis using PCA/FA is very useful as a monitoring tool to identify the multiple sources of contaminants and relationships with trace metals in the groundwater (Figure 7.4). The five factors are interrelated and are indicative of rock-water interaction, such as thermal gradient, mineral dissolution and ion exchange as the major geochemical processes governing the

groundwater chemistry. This supports the previous findings in water types and confirms that the rock-water interaction is one of the major processes controlling the chemistry of the geothermal spring/boreholes.

Table 7.3: Factor loadings of the trace metals concentrations and some physicochemical parameters

	F1	F2	F3	F4	F5
Temperature	-0.4432	-0.4625	0.4421	-0.2965	0.4432
pH	-0.1900	-0.6551	0.0840	-0.2828	**0.5248**
EC	0.3886	-0.0839	**0.5363**	0.4553	0.4652
Alkalinity	0.0419	-0.8558	-0.1334	-0.1990	0.1804
Be	0.2417	**0.5150**	-0.1384	**0.5436**	0.4214
V	-0.4874	**0.7351**	0.2189	0.0749	0.3380
Cr	-0.2476	**0.8574**	0.2698	-0.0474	-0.1765
Mn	**0.8936**	0.0911	-0.0276	-0.3416	-0.0365
Co	**0.9687**	0.0988	0.0185	-0.1507	0.0416
Ni	**0.9219**	0.1502	0.0891	-0.2885	0.0746
Cu	**0.6030**	0.1119	**0.6812**	-0.1419	-0.1886
Zn	0.4386	0.1176	**0.7799**	-0.0682	0.1081
As	-0.1061	0.7733	-0.2425	-0.4112	0.2689
Se	-0.1487	**0.8540**	-0.2373	-0.3470	0.2594
Cd	0.9591	0.0341	-0.0101	-0.1859	0.0197
Sb	**0.5607**	-0.0521	-0.2696	0.3223	-0.2290
Ba	**0.7120**	-0.0234	-0.2423	0.4370	0.3215
Hg	-0.2335	0.1716	**0.6983**	0.0980	-0.1280
Pb	-0.1928	-0.0659	**0.9167**	0.0710	-0.1803
Eigenvalue	5.7517	4.3560	3.3038	1.5992	1.4443
Variability (%)	30.2721	22.9262	17.3885	8.4166	7.6015
Cumulative (%)	**30.2721**	**53.1983**	**70.5868**	**79.0034**	**86.6050**

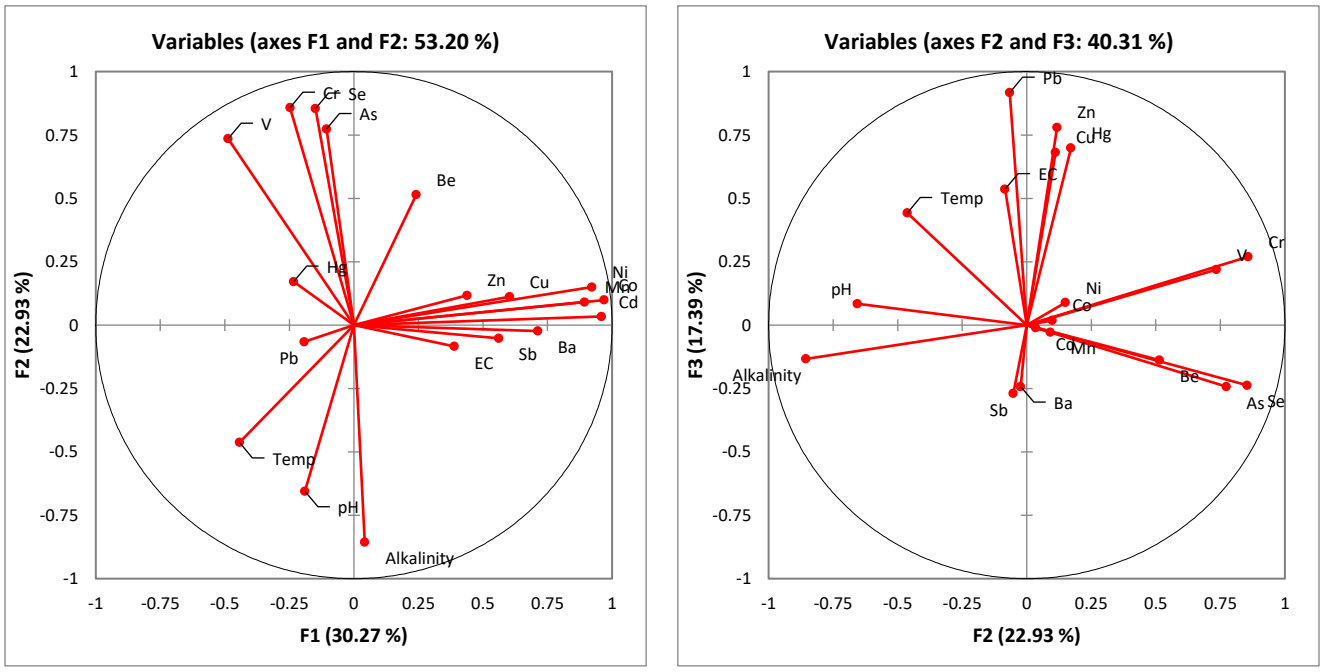

Figure 7.4: The principal component analysis (PCA) biplots showing the relationships between trace metals in the geothermal spring/borehole samples.

7.3 Evaluation of human health risk associated with trace metals in geothermal springs and boreholes

The level of exposure through ingestion and dermal contact were estimated since these are the major exposure pathways of geothermal springs and boreholes in the communities. Possible health risk associated with the exposure through ingestion depends on the weight, age and volume of groundwater consumed by an individual (children and adults) as presented in Table 7.4. In most of the study areas, the children's chronic daily intake was higher than the adults, indicating that children are more susceptible to potential health risk associated with the consumption of trace metals. When hazard quotient (HQ) and hazard index (HI) are less than one, there is no obvious risk to the population, but if these values exceed one, there may be concern for potential non-carcinogenic effects (Naveedullah *et al*., 2014; Asare-Donkor *et al*., 2016). The calculated cumulative hazard quotients (HI) for all the trace metals served as a conservative assessment tool to estimate high-end risk rather than low end-risk in order to protect the public. Calculated HI served as a screen value to determine whether there is a major significant health risk that exposure of trace metals in the groundwater may pose on the

communiinity and if there is any difference in total health risk during the study period. For the adult population, the calculated values for HQ were less than one in dermal intakes (Appendix 7.1). Although, calculated HI (summation of the HIs) for all the exposure pathways was 1.23, a value greater than one is due to the ingestion pathways. Trace metals such as Be, Cr, Hg and As are the main drivers (HI values ranges from 0.1 – 0.5), hence, the adult population was at risk of non-carcinogenic diseases.

For children, calculated HI (summation of the HIs) was 54.7 with Be, Se, As, Mn, Cr, Hg and V (Appendix 7.1) being the major drivers (HI values ranges from 1.04 – 9.94), through ingestion pathway. This high value indicated trace metal pollution that may pose a very high non-cancer health risk to children living in those communities. In general, health risk assessment index using the overall non-carcinogenic risk assessment (HI), CDI and HQ via ingestion and dermal adsorption routes were greater than one. This is an indication that groundwater poses more significant health threats to both adults and children via the pathways (Asare-Donkor *et al*., 2016; Naveedullah *et al*., 2014), however measures should be made to avoid accumulation of heavy metals that pose adverse health problems especially in children.

The carcinogenic risk of only Cr, Cd, As and Pb were calculated for both adults and children because the values of carcinogenic slope factors for the other trace metals could not be found in literature. According to regulatory bodies, the acceptable carcinogenic risk values ranges between 10^{-6} and 10^{-4} for an individual (children and adults) (USEPA, 2004; Government of South Africa, 2006). In this study, Cr, Cd and As were found to be the highest contributors to the cancer risk in adults and children, respectively (Table 7.5). Pb poses carcinogenic risk to children in all the sites in both seasons and this is of great concern and requires attention. Whereas Cd also poses cancer risk in children at all sites but fall within the acceptable limit for adult population except for MPW and BH1. Hence, Cd poses cancer risk in adult at MPW and BH1. SAW (Siloam) having 4.04E-05 in Cr, it does not pose cancer risk to its population unlike other sites. Therefore, proper monitoring and control measures (civic education, routine sampling, remediation among others) to protect human health within the study areas should be implemented for safety by relevant stakeholders.

Table 7.4: Average chronic daily intake (CDI) values in mg/kg/day of geothermal water/boreholes for adults and children within Soutpansberg

		TSS	TSW	SGS	SGW	MPS	MPW	SAW	SH1	SH2	BH1	BH2	SCC	TTP
Be	Children	2.19E-01	7.01E-01	1.61E-01	1.08E-03	3.12E-01	6.16E-01	6.00E-03	3.85E-01	4.23E-01	5.24E-01	8.11E-01	6.07E-01	1.08E-03
	Adult	5.74E-02	1.83E-01	4.21E-02	2.83E-04	8.16E-02	1.61E-01	1.57E-03	1.01E-01	1.11E-01	1.37E-01	2.13E-01	1.59E-01	2.83E-04
V	Children	2.20E+00	2.01E+00	1.62E+00	1.75E+00	1.95E+00	1.68E+00	3.85E-01	1.62E+00	2.12E+00	6.14E-01	1.50E+00	2.14E+00	5.54E-01
	Adult	5.77E-01	5.26E-01	4.25E-01	4.59E-01	5.12E-01	4.39E-01	1.01E-01	4.26E-01	5.54E-01	1.61E-01	3.92E-01	5.60E-01	1.45E-01
Cr	Children	1.50E+00	1.04E+00	1.26E+00	7.97E-01	1.27E+00	1.01E+00	1.08E-02	1.25E+00	1.33E+00	8.39E-01	7.78E-01	1.46E+00	1.08E+00
	Adult	3.92E-01	2.71E-01	3.29E-01	2.09E-01	3.32E-01	2.64E-01	2.83E-03	3.27E-01	3.48E-01	2.20E-01	2.04E-01	3.82E-01	2.84E-01
Mn	Children	3.20E-01	2.67E-01	1.24E+00	3.07E+00	4.39E+00	1.28E-01	2.88E-02	1.50E-01	2.34E-01	1.29E+01	1.99E-01	1.83E-01	1.76E+00
	Adult	8.38E-02	6.99E-02	3.24E-01	8.03E-01	1.15E+00	3.35E-02	7.54E-03	3.94E-02	6.12E-02	3.38E+00	5.20E-02	4.79E-02	4.62E-01
Co	Children	2.51E-02	3.34E-02	5.18E-02	4.27E-02	3.49E-02	4.37E-02	4.80E-03	2.23E-02	3.13E-02	4.11E-01	6.10E-02	2.86E-02	2.04E-02
	Adult	6.58E-03	8.75E-03	1.36E-02	1.12E-02	9.15E-03	1.15E-02	1.26E-03	5.85E-03	8.20E-03	1.08E-01	1.60E-02	7.48E-03	5.34E-03
Ni	Children	2.69E-01	3.16E-01	1.19E-01	1.33E-01	2.56E-01	1.01E-01	8.52E-02	9.80E-02	1.78E-01	1.50E+00	6.54E-02	2.26E-01	1.89E-01
	Adult	7.06E-02	8.28E-02	3.12E-02	3.47E-02	6.72E-02	2.65E-02	2.23E-02	2.57E-02	4.66E-02	3.93E-01	1.71E-02	5.92E-02	4.94E-02
Cu	Children	1.44E+00	2.25E+00	3.67E+00	7.70E-03	1.54E-01	1.08E-03	4.20E-02	1.08E-03	2.21E-01	3.77E+00	4.13E-02	2.58E-01	5.78E-01
	Adult	3.76E-01	5.89E-01	9.61E-01	2.02E-03	4.02E-02	2.83E-04	1.10E-02	2.83E-04	5.78E-02	9.87E-01	1.08E-02	6.76E-02	1.51E-01
Zn	Children	3.75E+01	5.58E+01	3.53E+01	2.34E+01	5.92E+00	2.52E+00	1.14E-01	1.08E-03	1.08E-03	4.21E+01	1.08E-03	1.08E-03	5.38E+00
	Adult	9.83E+00	1.46E+01	9.25E+00	6.12E+00	1.55E+00	6.60E-01	2.99E-02	2.83E-04	2.83E-04	1.10E+01	2.83E-04	2.83E-04	1.41E+00
As	Children	2.45E-01	2.42E-01	1.62E-01	2.37E-01	3.27E-01	2.52E-01	1.21E-01	1.24E-01	3.65E-01	2.30E-01	1.55E-01	3.66E-01	1.56E-01
	Adult	6.42E-02	6.33E-02	4.25E-02	6.20E-02	8.55E-02	6.59E-02	3.17E-02	3.24E-02	9.56E-02	6.03E-02	4.07E-02	9.59E-02	4.09E-02
Se	Children	6.99E-01	7.42E-01	4.63E-01	6.89E-01	1.20E+00	7.70E-01	8.16E-02	6.08E-01	1.31E+00	7.02E-01	4.34E-01	1.31E+00	3.90E-01
	Adult	1.83E-01	1.94E-01	1.21E-01	1.80E-01	3.15E-01	2.02E-01	2.14E-02	1.59E-01	3.44E-01	1.84E-01	1.14E-01	3.44E-01	1.02E-01
Cd	Children	6.76E-03	2.94E-03	1.60E-03	6.46E-03	9.20E-04	1.65E-02	2.40E-03	1.08E-03	8.40E-04	8.71E-02	1.08E-03	8.40E-04	5.40E-03
	Adult	1.77E-03	7.70E-04	4.19E-04	1.69E-03	2.41E-04	4.32E-03	6.29E-04	2.83E-04	2.20E-04	2.28E-02	2.83E-04	2.20E-04	1.41E-03
Sb	Children	6.36E-03	2.64E-03	3.76E-03	7.06E-03	4.28E-03	2.07E-02	3.60E-03	6.00E-04	1.80E-03	1.46E-02	9.48E-03	1.08E-03	1.14E-02
	Adult	1.67E-03	6.91E-04	9.85E-04	1.85E-03	1.12E-03	5.42E-03	9.43E-04	1.57E-04	4.71E-04	3.83E-03	2.48E-03	2.83E-04	2.99E-03
Ba	Children	1.84E-01	3.17E+00	9.36E-02	5.09E+00	1.06E+00	3.48E+00	1.25E+00	4.55E-02	8.64E-01	8.08E+00	8.64E+00	8.21E-01	1.08E-03
	Adult	4.83E-02	8.29E-01	2.45E-02	1.33E+00	2.76E-01	9.11E-01	3.27E-01	1.19E-02	2.26E-01	2.12E+00	2.26E+00	2.15E-01	2.83E-04
Hg	Children	7.33E-01	7.45E-02	3.91E-01	4.83E-02	2.18E-01	5.17E-02	4.20E-02	7.94E-02	9.58E-02	1.84E-02	1.92E-01	5.52E-02	8.64E-02
	Adult	1.92E-01	1.95E-02	1.02E-01	1.27E-02	5.71E-02	1.35E-02	1.10E-02	2.08E-02	2.51E-02	4.81E-03	5.03E-02	1.45E-02	2.26E-02
Pb	Children	3.38E-02	3.91E-02	5.87E-02	1.08E-03	1.08E-03	1.08E-03	1.08E-02	2.05E-02	1.08E-03	1.08E-03	1.08E-03	1.08E-03	7.68E-03
	Adult	8.86E-03	1.02E-02	1.54E-02	2.83E-04	2.83E-04	2.83E-04	2.83E-03	5.37E-03	2.83E-04	2.83E-04	2.83E-04	2.83E-04	2.01E-03

Table 7.5: Carcinogenic risk assessment of Cr, Cd, As and Pb from geothermal springs and boreholes within Soutpansberg through ingestion pathway for adults and children

	Cr		Cd		As		Pb	
Code	Children	Adults	Children	Adults	Children	Adults	Children	Adults
TSS	2.49E-01	5.59E-03	4.26E-02	9.56E-04	1.22E+00	2.71E-02	8.22E-05	5.84E-08
TSW	1.73E-01	3.88E-03	1.85E-02	4.16E-04	1.21E+00	1.82E-02	9.50E-05	6.75E-08
SGS	2.10E-01	4.70E-03	1.01E-02	2.26E-04	8.12E-01	2.66E-02	1.43E-04	1.01E-07
SGW	1.33E-01	2.98E-03	4.07E-02	9.13E-04	1.18E+00	3.67E-02	2.62E-06	1.86E-09
MPS	2.11E-01	4.75E-03	5.80E-03	1.30E-04	1.63E+00	2.82E-02	2.62E-06	1.86E-09
MPW	1.68E-01	3.77E-03	1.04E-01	2.33E-03	1.26E+00	1.36E-02	2.62E-06	1.86E-09
SAW	1.80E-03	4.04E-05	1.51E-02	3.39E-04	6.06E-01	1.39E-02	2.62E-05	1.86E-08
SH1	2.08E-01	4.67E-03	6.80E-03	1.53E-04	6.19E-01	4.10E-02	4.98E-05	3.54E-08
SH2	2.22E-01	4.97E-03	5.29E-03	1.19E-04	1.83E+00	2.59E-02	2.62E-06	1.86E-09
BH1	1.40E-01	3.14E-03	5.49E-01	1.23E-02	1.15E+00	1.74E-02	2.62E-06	1.86E-09
BH2	1.30E-01	2.91E-03	6.80E-03	1.53E-04	7.76E-01	4.11E-02	2.62E-06	1.86E-09
SCC	2.43E-01	5.45E-03	5.29E-03	1.19E-04	1.83E+00	1.75E-02	2.62E-06	1.86E-09
TTP	1.81E-01	4.05E-03	3.40E-02	7.64E-04	7.80E-01	3.35E-01	1.87E-05	1.32E-08

7.4 Trace metals concentrations from surrounding soils

The surrounding soils were sampled vertically from a depth of 10 cm, 30 cm and 50 cm and mean values of trace metals concentrations are presented in Table 7.6 and descriptive statistics are included in Appendix 7.2 for both seasons. Although, depths of 10 cm and 30 cm were used for sampling soil at Mphephu and Siloam owing to the nature of their soils (rocky soil), the concentrations of the trace metals varied from different sampling points at different site. At Sagole, the coefficient of variation of some trace metals such as As, Sb, Ba and Hg were 151.66, 141.51, 159.91 and 139.94 for summer, respectively, and 161.66 of Hg in winter (Appendix 7.2). These high coefficients of variations suggest anthropogenic inputs as their main source. Most of the trace metals were within acceptable limits (Department of Environmental Affairs, 2010) except for Cu at Siloam and Mphephu soils, and at sampling depth W50 in Tshipise; Cr at all the sites except for Sagole (S30, S50 and W50); As at Sagole (S50) and Pb in Siloam (S10 and S30) (Table 7.6). Hence, the soils in the sites where the trace metals concentrations

exceed the standards are contaminated. Generally, the pH ranges from acidic to alkaline and this account for the solubility of the trace metals in soil. The pH varied from 7.5 to 8.55, 3.1 to 9.9, 6.62 to 6.97 for summer at Tshipise, Sagole and Mphephu, respectively. Whereas pH varied from 8.01 to 8.05, 9.31 to 9.72, 7.47 to 7.76 for winter at Tshipise, Sagole and Mphephu, respectively. Siloam sampling points have pH, which ranges from 6.67 to 7.15. The slightly acidic and slightly alkaline nature of the soil in the study sites, for example at Mphephu and Siloam enhances the solubility of trace metals (Witeska and Jezierska, 2003).

Generally, trace metals concentrations are comparable in both seasons (Figures 7.5 – 7.8), though in some cases the concentrations at given depths in each of the sites are higher either in summer or winter. Though one would have expected the deeper depths of the soil to be more enriched with trace metals than the top surface of the soil due to leaching from the top soil to the bottom soil, the complexity of the soil environment and the source or location of the trace metal and their solubility makes this convoluted. The soil at Siloam was the most enriching in trace metals and to some extent Mphephu soils and this was due to the clayey nature of the soil. Though, the soil was loosely packed with rocky materials, its clayey texture (implying high retention capacity) accounts for higher trace metal concentrations than others. The soil types are sandy, sand loamy and clay loamy for Sagole, Tshipise and Mphephu soils, respectively (Olivier *et al*., 2008; Durowoju, 2015). Therefore, based on the retention capacity of the soil (soil type), the average magnitude of the absorbed trace metals was in this order of sequence; Siloam > Mphephu > Tshipise > Sagole.

Table 7.6: Mean concentrations of the trace metals from the surrounding soil of the geothermal springs

		Tshipise (mg/Kg)						Sagole (mg/Kg)						Siloam (mg/Kg)		Mphephu (mg/Kg)			
	DEA, 2010	S10	S30	S50	W10	W30	W50	S10	S30	S50	W10	W30	W50	S10	S30	S10	S30	W10	W30
pH		7.5	8.55	8.32	8.05	8.05	8.01	9.9	9.14	3.1	9.72	9.33	9.31	7.15	6.67	6.62	6.97	7.76	7.47
EC		154.2	89.4	253.9	95.8	90.1	130.2	1441	124.1	973	376	253.7	195.8	90.6	116.9	217.5	111.2	27.4	40.8
TDS		98.7	57.2	162	613	57.6	83.3	922	79.4	623	241	162	125	58	74.8	139	71.1	17.5	26.1
Be	-	0.188	0.138	0.212	0.226	0.214	0.299	0.11	0.05	0.754	0.093	0.058	0.04	0.588	0.643	0.626	0.337	0.198	0.312
V	150	17.13	12.24	16.39	18.27	16.82	25.23	6.864	4.152	7.016	6.534	5.381	4.134	165.1	172.4	68.17	58.5	49.02	48.14
Cr	6.5	**46.23**	**37.93**	**42.85**	**37.5**	**36.93**	**44.9**	**9.977**	3.765	4.493	**7.81**	**7.267**	4.707	**90.54**	**96.35**	**36.1**	**35.32**	**27.92**	**38.38**
Mn	740	113.2	99.98	144	130.3	120.3	157.1	68.76	18.07	33.11	53.96	30.15	24.59	118.3	119	35.41	47.22	46.96	71.84
Co	300	5.084	3.623	5.284	4.96	4.61	7.781	2.293	0.888	2.124	1.518	1.117	0.999	28.66	28.67	14.66	13.8	19.12	21.52
Ni	91	34.44	24.46	31.59	26.1	26.84	37.03	11.27	2.414	4.311	6.13	4.439	3.405	51.65	57.39	21.1	15.72	11.6	21.45
Cu	16	12.7	8.519	12.16	13.73	15.05	**19.13**	8.687	8.108	9.229	7.141	5.796	5.628	**97.07**	**103.6**	**33.45**	**25.09**	**19.3**	**25.39**
Zn	240	15.24	14.16	15.75	16.15	15.49	21.25	17.17	10.64	2.512	4.93	3.827	6.104	48.62	48.94	37.74	15.52	8.082	19.77
As	5.8	0.382	0.222	0.309	0.369	0.673	0.925	0.333	0.337	**7.41**	0.587	0.263	0.326	0.787	0.794	1.098	0.435	0.103	0.668
Se	-	0.27	0.092	0.091	0.177	0.182	0.18	0.07	0.14	0.093	0.098	0.083	0.001	0.264	0.252	1.534	0.36	0.114	0.332
Cd	7.5	0.034	0.043	0.024	0.024	0.028	0.035	0.022	0.01	0.012	0.01	0.006	0.017	0.257	0.357	0.094	0.04	0.018	0.037
Sb	-	0.014	0.017	0.013	0.021	0.037	0.033	0.019	0.022	0.295	0.02	0.012	0.012	0.029	0.022	0.037	0.017	0.01	0.013
Ba	-	12.29	11.09	13.88	14.51	16.23	20.81	10.54	3.169	253.2	19.87	5.69	3.437	48.4	51.48	45.36	23.8	18.03	41.58
Hg	0.93	0.229	0.15	0.105	0.066	0.291	0.025	0.118	0.001	0.017	0.001	0.043	0.001	0.001	0.001	0.005	0.001	0.001	0.001
Pb	20	2.358	1.996	2.417	2.959	3.89	5.742	6.084	1.74	1.425	1.486	1.148	1.153	**85.02**	**30.6**	9.453	4.078	2.963	3.51

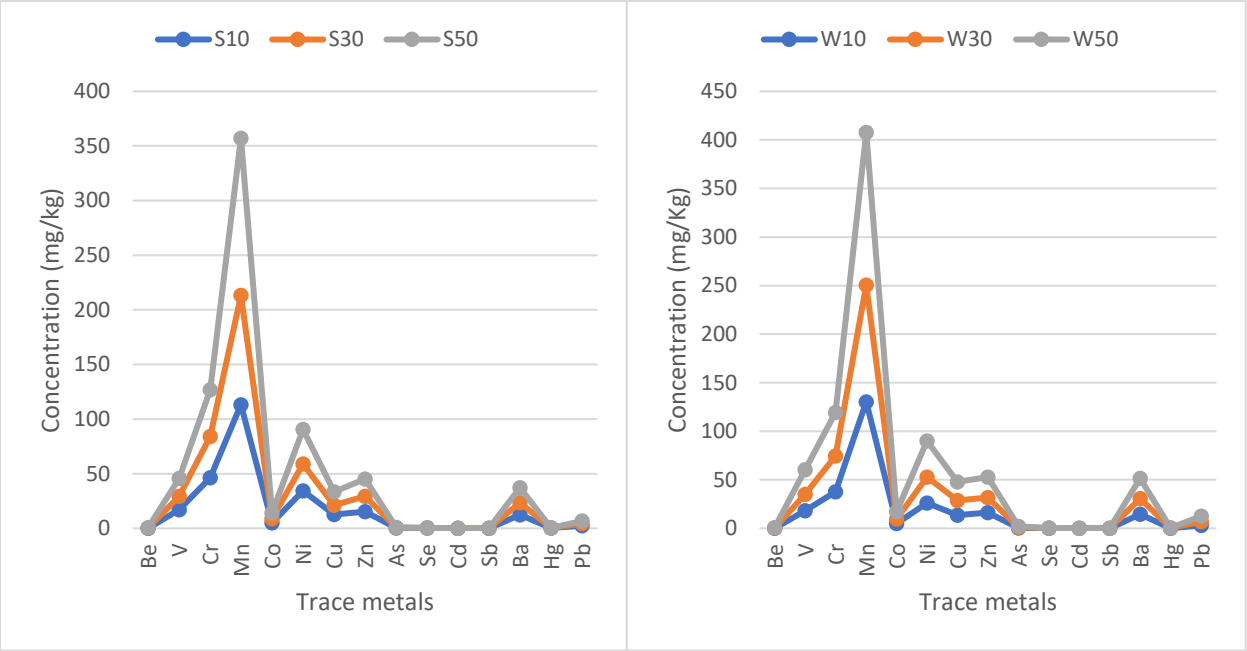

Figure 7.5: Trace metals concentrations and physicochemical parameters of soils at different depth at Tshipise.

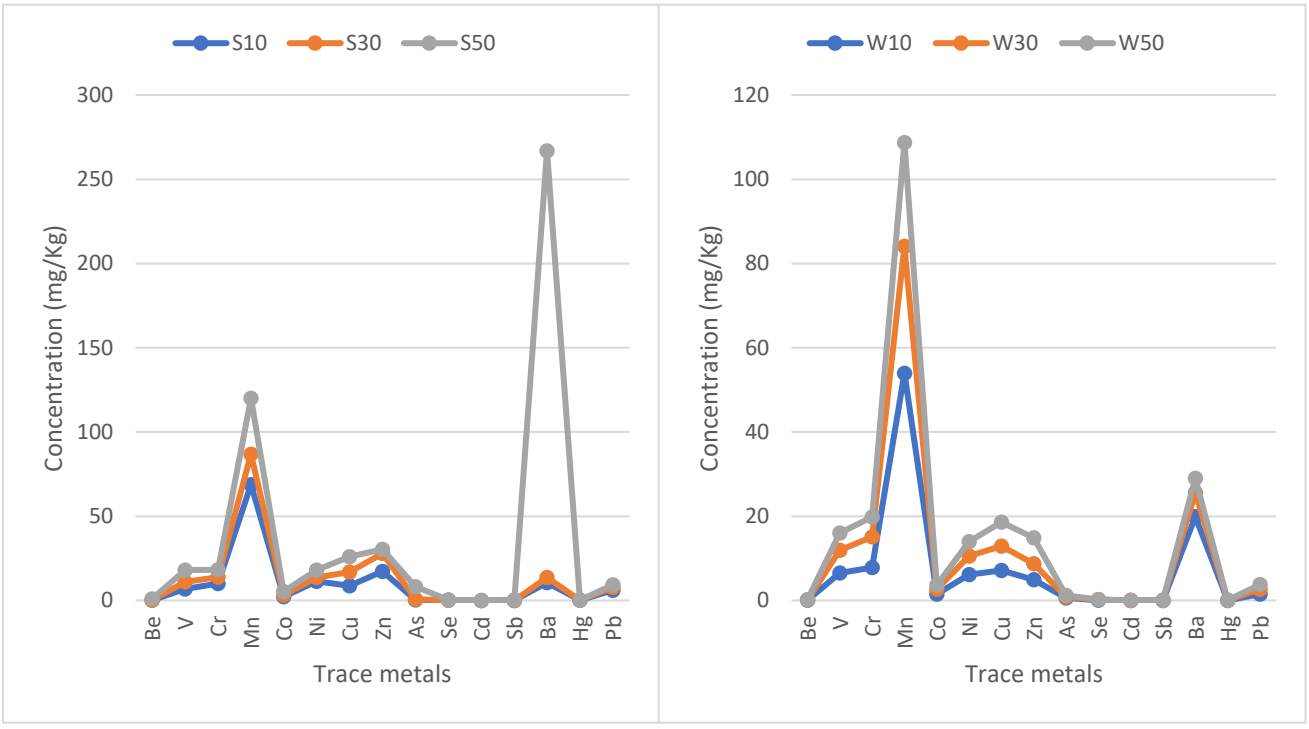

Figure 7.6: Trace metals concentrations and physicochemical parameters of soils at different depth at Sagole.

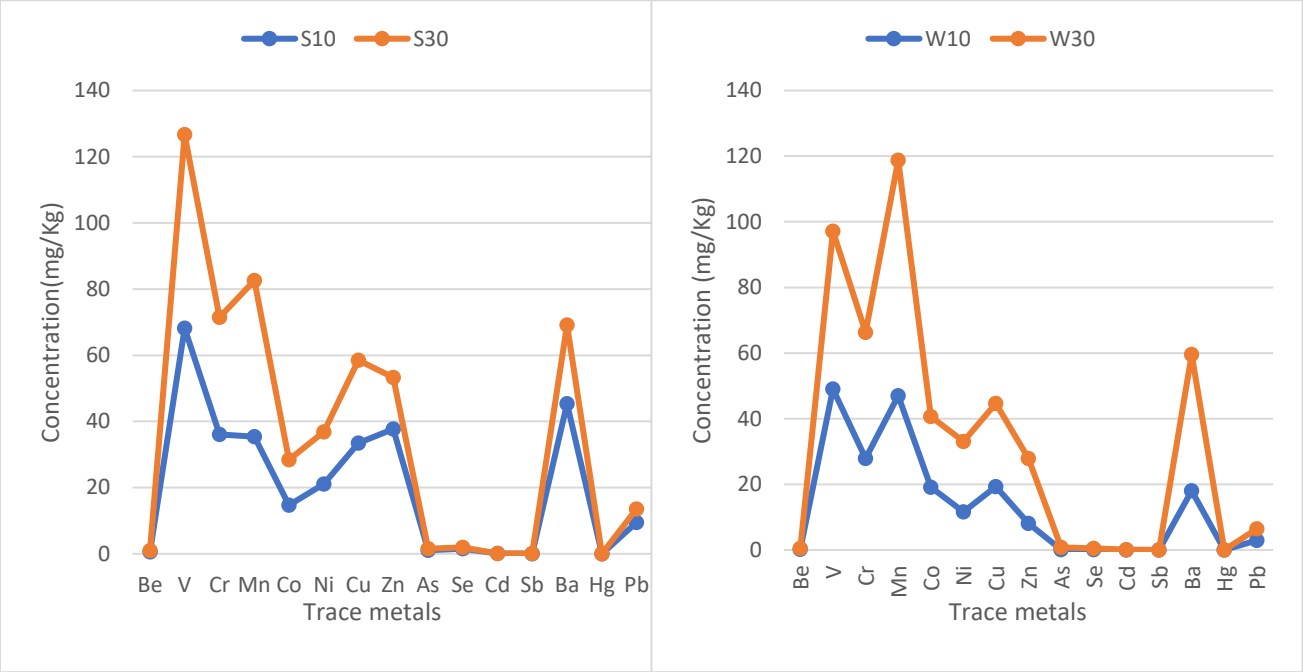

Figure 7.7: Trace metals concentrations and physicochemical parameters of soils at different depth at Mphephu.

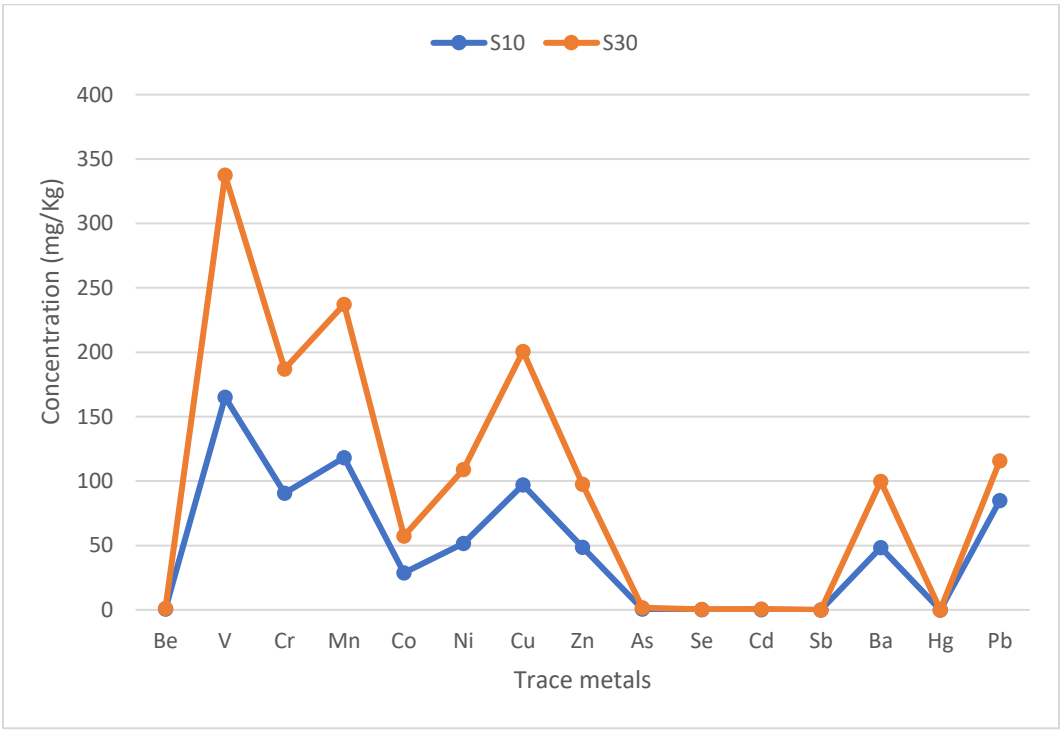

Figure 7.8: Trace metals concentrations and physicochemical parameters of soils at different depth at Siloam.

Pearson correlation shows the relationship between trace metals concentrations and physicochemical parameters (Table 7.7). The pH values showed a negative correlation with all the trace metals except for Hg and Mn (very weak positive correlation). This means that the higher the pH of the soil, the lesser the trace metals concentrations in soil and vice versa. Invariably, this relationship justifies the fact that trace metals are more soluble in acidic soils and tend to be insoluble in alkaline soil. Very strong negative correlation was observed between the pH and trace metals Be, As, Sb and Ba. EC and TDS showed a positive correlation with Be, As, Sb, Ba and Hg. This is an indication of similar source. Generally, most of the trace metals had positive correlations with each other.

The relationships among the trace metals were further determined using a dendrogram (HCA) (Figure 7.9). Dendrogram analysis produced 5 clusters for the spatial distribution of trace metals of the soil samples; Cluster 1 has pH, Be, As, Se, Cd, Se and Hg; Cluster 4 has V, Cr, Co, Ni, Cu, Ba and Pb; and EC, TDS and Mn are independent clusters 2, 3 and 5, respectively. The dendrogram further strengthens the relationship observed by Pearson's correlation by revealing the major clusters (1 and 4).

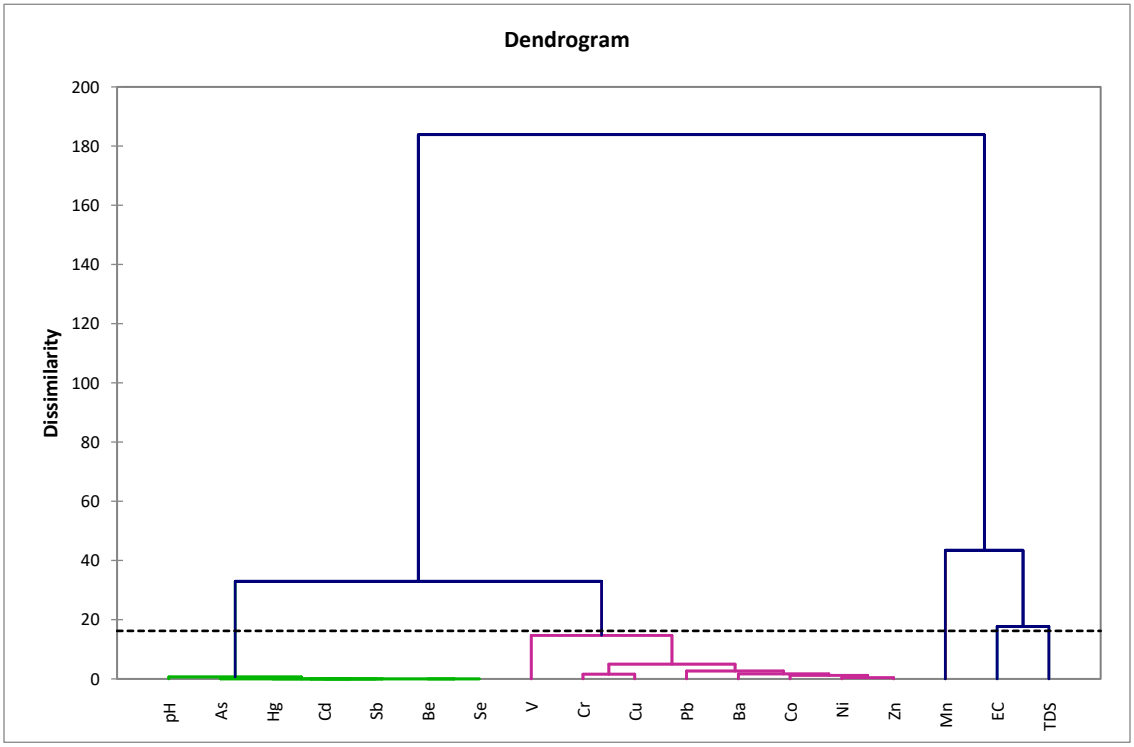

Figure 7.9: Dendrogram showing the spatial clustering of trace metals in surrounding soil samples based on the hierarchical cluster analysis using Ward's method.

Table 7.7: Pearson correlation matrix showing the relationship between the physicochemical parameters and trace metals in surrounding soils of geothermal springs

Variables	pH	EC	TDS	Be	V	Cr	Mn	Co	Ni	Cu	Zn	As	Se	Cd	Sb	Ba	Hg	Pb
pH	**1.00**																	
EC	-0.07	**1.00**																
TDS	-0.05	**0.86**	**1.00**															
Be	**-0.87**	0.07	0.03	**1.00**														
V	-0.34	-0.29	-0.32	**0.66**	**1.00**													
Cr	-0.27	-0.42	-0.37	**0.53**	**0.87**	**1.00**												
Mn	0.00	-0.23	-0.07	0.12	0.26	**0.67**	**1.00**											
Co	-0.35	-0.37	-0.40	**0.60**	**0.92**	**0.80**	0.23	**1.00**										
Ni	-0.22	-0.35	-0.29	**0.47**	**0.75**	**0.97**	**0.81**	**0.66**	**1.00**									
Cu	-0.32	-0.24	-0.27	**0.65**	**0.99**	**0.88**	0.32	**0.87**	**0.78**	**1.00**								
Zn	-0.23	-0.22	-0.22	**0.62**	**0.90**	**0.87**	0.42	**0.79**	**0.83**	**0.90**	**1.00**							
As	**-0.81**	0.46	0.38	**0.62**	-0.07	-0.19	-0.21	-0.11	-0.18	-0.04	-0.16	**1.00**						
Se	-0.29	-0.15	-0.16	**0.48**	0.29	0.20	-0.15	0.32	0.14	0.22	**0.49**	0.00	**1.00**					
Cd	-0.28	-0.20	-0.23	**0.62**	**0.95**	**0.86**	0.32	**0.79**	**0.78**	**0.98**	**0.89**	-0.04	0.20	**1.00**				
Sb	**-0.78**	**0.48**	0.41	**0.58**	-0.12	-0.23	-0.21	-0.17	-0.22	-0.09	-0.21	**1.00**	-0.04	-0.09	**1.00**			
Ba	**-0.87**	0.42	0.34	**0.72**	0.08	-0.07	-0.19	0.06	-0.09	0.10	-0.04	**0.98**	0.04	0.09	**0.97**	**1.00**		
Hg	0.15	0.06	0.06	-0.28	-0.33	0.04	0.45	-0.36	0.17	-0.28	-0.14	-0.15	-0.15	-0.22	-0.10	-0.21	**1.00**	
Pb	-0.18	-0.13	-0.16	**0.50**	**0.82**	**0.72**	0.29	**0.69**	**0.64**	**0.85**	**0.77**	-0.03	0.10	**0.78**	-0.06	0.08	-0.21	**1.00**

Values in bold are different from 0 with a significance level alpha=0.05

The PCA/FA loadings for the trace metals in the surrounding soil samples taken within study sites are shown in Table 7.8. Three principal components (PCs) were significant with eigenvalues > 1, explaining higher total cumulative variance of 80.78% (Table 7.8 and Figure 7.10). The factor loadings show that F1 (44.24%) has high loadings of V, Cr, Co, Cu, Zn, Be, Cd, Pb and Ni; F2 (26.16%) with the high loadings of EC, As, Sb and Ba: F3 (10.37%) with the high loadings of Mn, As and Hg. F1 could be attributed to soil pedogenesis. Soil contains trace quantities of these elements based on its parent material and soil forming factors (soil pedogenesis) (Siegel, 2002). F2 could be attributed to groundwater-surface soil interaction in which the soil absorbs trace elements resulting in their accumulation (Lakshmanan *et al*., 2003). Geothermal water and groundwater are used for irrigation purposes at all the sites and there is a high tendency of the trace elements mobility to the soil surface. The EC and TDS in the F2 are useful indicators which show the solubility of the trace metals from the groundwater into the surrounding soil, which, bioaccumulate with time (Durowoju *et al*., 2016b). F3 suggests anthropogenic source such as wastewater discharges and sewage sludge around the study sites. The pH has direct relationship with trace metals from the varimax (Figure 7.10) and is also indicative of anthropogenic activities leading to the release of Hg to the soil.

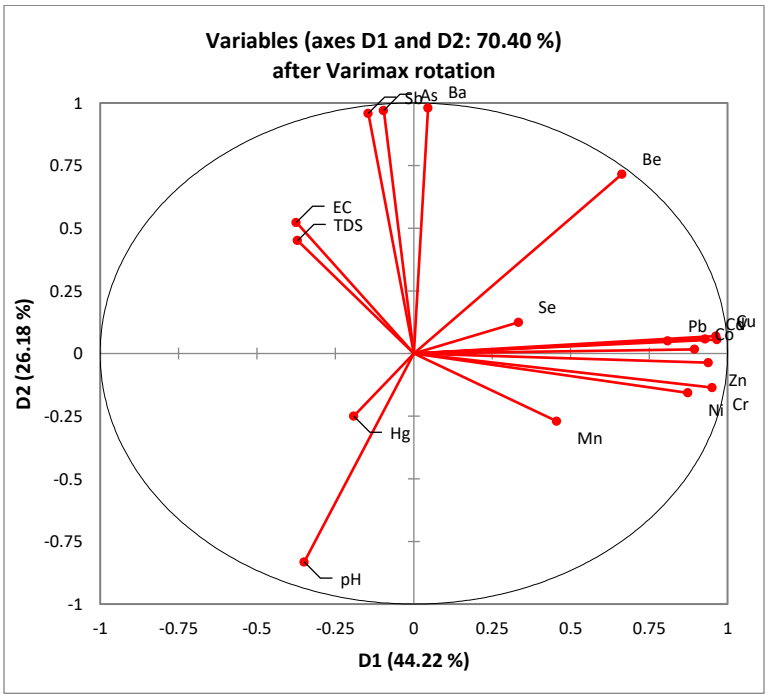

Figure 7.10: The principal component analysis (PCA) biplots showing the relationships between trace metals in the surrounding soils within the Soutpansberg region.

Table 7.8: Factor loadings of the trace metals concentrations and some physicochemical parameters of surrounding soils

	F1	F2	F3
pH	-0.377	-0.819	0.006
EC	-0.357	0.536	0.310
TDS	-0.355	0.463	0.404
Be	0.687	0.693	-0.046
V	0.968	0.023	-0.137
Cr	0.946	-0.168	0.237
Mn	0.447	-0.286	0.746
Co	0.895	-0.014	-0.240
Ni	0.868	-0.187	0.419
Cu	0.966	0.037	-0.043
Zn	0.937	-0.068	0.021
As	-0.063	0.973	0.086
Se	0.338	0.113	-0.423
Cd	0.930	0.027	0.013
Sb	-0.113	0.963	0.119
Ba	0.078	0.978	0.045
Hg	-0.200	-0.243	0.731
Pb	0.811	0.023	0.034
Eigenvalue	7.963	4.709	1.867
Variability (%)	44.241	26.162	10.372
Cumulative %	44.241	70.403	80.776

7.5 Evaluation of human health risk due to trace metals from the surrounding soils

Trace metals concentrations in the topmost soil (0 - 10 cm) were considered in the risk assessment for both children and adults because of its closeness to the human activities such as agriculture and exposure to dust compared to deeper soils. The trace metals concentrations were used to estimate intake from different pathways (ingestion, inhalation

and dermal) using standard USEPA's exposure equations highlighted above. Appendix 7.3 shows that the ingestion pathway is the major exposure to the surrounding soil at all sites followed by dermal and inhalation pathways. Hence, soil ingestion was the most significant contributor to the total health risk, except for a few trace metals that do not have RFD value for dermal exposure. Findings from this study also support the general observation that children are more susceptible/vulnerable to potential health risk associated with these trace metals in the environment (Figure 7.11) (USEPA, 1989; Sundararajan *et al*., 2016; Hu *et al*., 2018). The results from the ingestion, inhalation and dermal pathways for non-carcinogenic risks were presented in terms of HQs in Table 7.9.

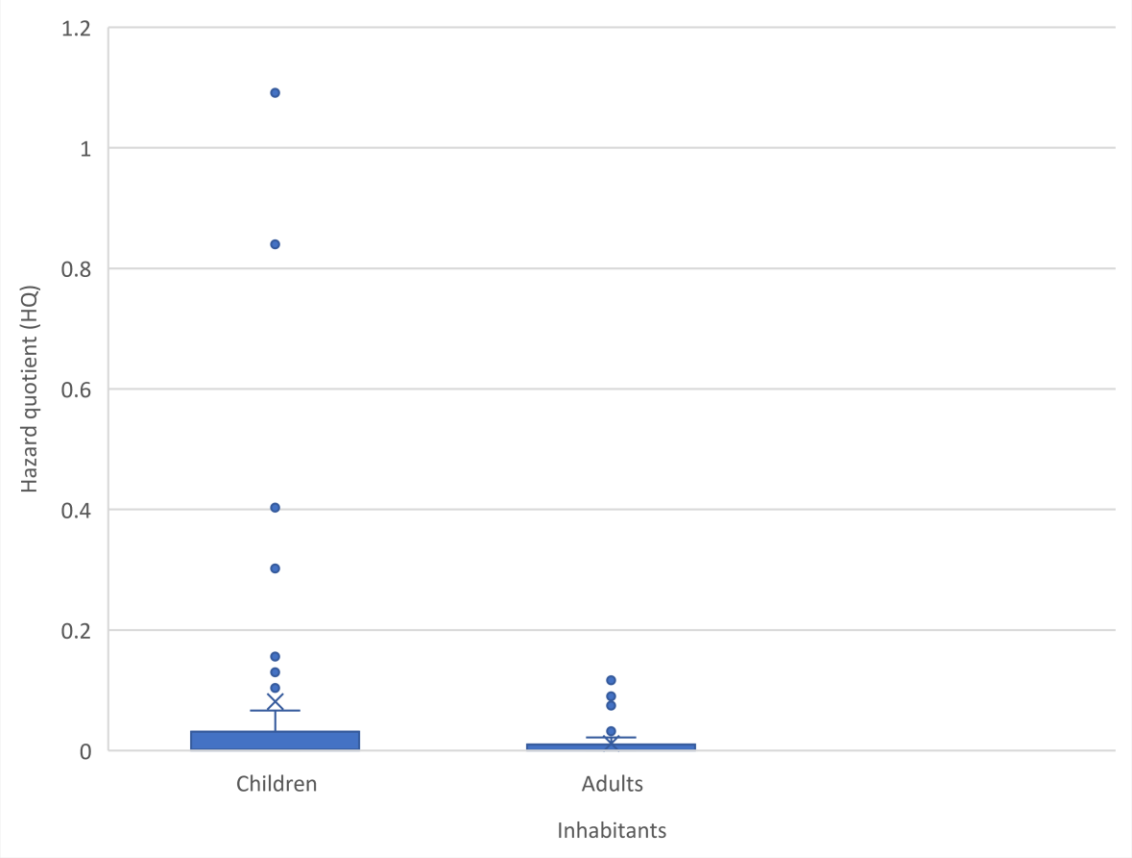

Figure 7.11: Biplot variant of the hazard quotient risk among children and adults Within Soutpansberg region.

Table 7:9: Average daily intake (ADI) values in mg/kg/day for adults and children in surrounding soils from the geothermal springs for non-carcinogenic risk calculations within Soutpansberg region

	Be						V						Cr					
	Ingestion		inhalation		dermal		Ingestion		inhalation		dermal		Ingestion		inhalation		dermal	
	Children	Adults	Children	Adults	Children	Adults	Children	Adults	Children	Adults	Children	Adults	Children	Adults	Children	Adults	Children	Adults
TSS	2.40E-06	2.58E-07	6.60E-11	2.83E-11	5.05E-09	1.05E-08	2.19E-04	2.35E-05	6.02E-09	2.58E-09	4.60E-07	9.53E-07	5.91E-04	6.33E-05	1.62E-08	6.96E-09	1.24E-06	2.57E-06
TSW	2.89E-06	3.10E-07	7.94E-11	3.40E-11	6.07E-09	1.26E-08	2.34E-04	2.50E-05	6.42E-09	2.75E-09	4.91E-07	1.02E-06	4.79E-04	5.14E-05	1.32E-08	5.65E-09	1.01E-06	2.09E-06
SGS	1.41E-06	1.51E-07	3.86E-11	1.66E-11	2.95E-09	6.12E-09	8.78E-05	9.40E-06	2.41E-09	1.03E-09	1.84E-07	3.82E-07	1.28E-04	1.37E-05	3.50E-09	1.50E-09	2.68E-07	5.55E-07
SGW	1.19E-06	1.27E-07	3.27E-11	1.40E-11	2.50E-09	5.17E-09	8.35E-05	8.95E-06	2.30E-09	9.84E-10	1.75E-07	3.63E-07	9.99E-05	1.07E-05	2.74E-09	1.18E-09	2.10E-07	4.34E-07
SAW	7.52E-06	8.05E-07	2.07E-10	8.85E-11	1.58E-08	3.27E-08	2.11E-03	2.26E-04	5.80E-08	2.49E-08	4.43E-06	9.18E-06	1.16E-03	1.24E-04	3.18E-08	1.36E-08	2.43E-06	5.04E-06
MPS	8.00E-06	8.58E-07	2.20E-10	9.42E-11	1.68E-08	3.48E-08	8.72E-04	9.34E-05	2.39E-08	1.03E-08	1.83E-06	3.79E-06	4.62E-04	4.95E-05	1.27E-08	5.43E-09	9.69E-07	2.01E-06
MPW	2.53E-06	2.71E-07	6.95E-11	2.98E-11	5.32E-09	1.10E-08	6.27E-04	6.72E-05	1.72E-08	7.38E-09	1.32E-06	2.73E-06	3.57E-04	3.82E-05	9.81E-09	4.20E-09	7.50E-07	1.55E-06
	Mn						Co						Ni					
TSS	1.45E-03	1.55E-04	3.98E-08	1.70E-08	3.04E-06	6.30E-06	6.50E-05	6.96E-06	1.79E-09	7.65E-10	1.37E-07	2.83E-07	4.40E-04	4.72E-05	1.21E-08	5.18E-09	9.25E-07	1.92E-06
TSW	1.67E-03	1.78E-04	4.58E-08	1.96E-08	3.50E-06	7.25E-06	6.34E-05	6.79E-06	1.74E-09	7.47E-10	1.33E-07	2.76E-07	3.34E-04	3.58E-05	9.17E-09	3.93E-09	7.01E-07	1.45E-06
SGS	8.79E-04	9.42E-05	2.42E-08	1.04E-08	1.85E-06	3.82E-06	2.93E-05	3.14E-06	8.05E-10	3.45E-10	6.16E-08	1.28E-07	1.44E-04	1.54E-05	3.96E-09	1.70E-09	3.03E-07	6.27E-07
SGW	6.90E-04	7.39E-05	1.90E-08	8.12E-09	1.45E-06	3.00E-06	1.94E-05	2.08E-06	5.33E-10	2.29E-10	4.08E-08	8.44E-08	7.84E-05	8.40E-06	2.15E-09	9.23E-10	1.65E-07	3.41E-07
SAW	1.51E-03	1.62E-04	4.16E-08	1.78E-08	3.18E-06	6.58E-06	3.66E-04	3.93E-05	1.01E-08	4.31E-09	7.70E-07	1.59E-06	6.60E-04	7.08E-05	1.81E-08	7.78E-09	1.39E-06	2.87E-06
MPS	4.53E-04	4.85E-05	1.24E-08	5.33E-09	9.51E-07	1.97E-06	1.87E-04	2.01E-05	5.15E-09	2.21E-09	3.94E-07	8.15E-07	2.70E-04	2.89E-05	7.41E-09	3.18E-09	5.67E-07	1.17E-06
MPW	6.00E-04	6.43E-05	1.65E-08	7.07E-09	1.26E-06	2.61E-06	2.44E-04	2.62E-05	6.72E-09	2.88E-09	5.13E-07	1.06E-06	1.48E-04	1.59E-05	4.07E-09	1.75E-09	3.11E-07	6.45E-07
	Cu						Zn						As					
TSS	1.62E-04	1.74E-05	4.46E-09	1.91E-09	3.41E-07	7.06E-07	1.95E-04	2.09E-05	5.35E-09	2.29E-09	4.09E-07	8.48E-07	4.88E-06	5.23E-07	1.34E-10	5.75E-11	1.03E-08	2.12E-08
TSW	1.76E-04	1.88E-05	4.82E-09	2.07E-09	3.69E-07	7.64E-07	2.06E-04	2.21E-05	5.67E-09	2.43E-09	4.34E-07	8.98E-07	4.72E-06	5.05E-07	1.30E-10	5.55E-11	9.91E-09	2.05E-08
SGS	1.11E-04	1.19E-05	3.05E-09	1.31E-09	2.33E-07	4.83E-07	2.20E-04	2.35E-05	6.03E-09	2.58E-09	4.61E-07	9.55E-07	4.26E-06	4.56E-07	1.17E-10	5.01E-11	8.94E-09	1.85E-08
SGW	9.13E-05	9.78E-06	2.51E-09	1.07E-09	1.92E-07	3.97E-07	6.30E-05	6.75E-06	1.73E-09	7.42E-10	1.32E-07	2.74E-07	7.51E-06	8.04E-07	2.06E-10	8.84E-11	1.58E-08	3.26E-08
SAW	1.24E-03	1.33E-04	3.41E-08	1.46E-08	2.61E-06	5.40E-06	6.22E-04	6.66E-05	1.71E-08	7.32E-09	1.31E-06	2.70E-06	1.01E-05	1.08E-06	2.76E-10	1.18E-10	2.11E-08	4.38E-08
MPS	4.28E-04	4.58E-05	1.17E-08	5.04E-09	8.98E-07	1.86E-06	4.83E-04	5.17E-05	1.33E-08	5.68E-09	1.01E-06	2.10E-06	1.40E-05	1.50E-06	3.86E-10	1.65E-10	2.95E-08	6.11E-08
MPW	2.47E-04	2.64E-05	6.78E-09	2.91E-09	5.18E-07	1.07E-06	1.03E-04	1.11E-05	2.84E-09	1.22E-09	2.17E-07	4.49E-07	1.32E-06	1.41E-07	3.62E-11	1.55E-11	2.77E-09	5.73E-09

	Se						Cd						Sb					
	Ingestion		inhalation		dermal		Ingestion		inhalation		dermal		Ingestion		inhalation		dermal	
	Children	Adults	Children	Adults	Children	Adults	Children	Adults	Children	Adults	Children	Adults	Children	Adults	Children	Adults	Children	Adults
TSS	3.45E-06	3.70E-07	9.48E-11	4.06E-11	7.25E-09	1.50E-08	4.35E-07	4.66E-08	1.19E-11	5.12E-12	9.13E-10	1.89E-09	1.79E-07	1.92E-08	4.92E-12	2.11E-12	3.76E-10	7.79E-10
TSW	2.26E-06	2.42E-07	6.22E-11	2.66E-11	4.75E-09	9.84E-09	3.07E-07	3.29E-08	8.43E-12	3.61E-12	6.44E-10	1.33E-09	2.68E-07	2.88E-08	7.38E-12	3.16E-12	5.64E-10	1.17E-09
SGS	8.95E-07	9.59E-08	2.46E-11	1.05E-11	1.88E-09	3.89E-09	2.81E-07	3.01E-08	7.73E-12	3.31E-12	5.91E-10	1.22E-09	2.43E-07	2.60E-08	6.67E-12	2.86E-12	5.10E-10	1.06E-09
SGW	1.25E-06	1.34E-07	3.44E-11	1.48E-11	2.63E-09	5.45E-09	1.28E-07	1.37E-08	3.51E-12	1.51E-12	2.68E-10	5.56E-10	2.56E-07	2.74E-08	7.02E-12	3.01E-12	5.37E-10	1.11E-09
SAW	3.38E-06	3.62E-07	9.27E-11	3.97E-11	7.09E-09	1.47E-08	3.29E-06	3.52E-07	9.03E-11	3.87E-11	6.90E-09	1.43E-08	3.71E-07	3.97E-08	1.02E-11	4.37E-12	7.79E-10	1.61E-09
MPS	1.96E-05	2.10E-06	5.39E-10	2.31E-10	4.12E-08	8.53E-08	1.20E-06	1.29E-07	3.30E-11	1.42E-11	2.52E-09	5.23E-09	4.73E-07	5.07E-08	1.30E-11	5.57E-12	9.93E-10	2.06E-09
MPW	1.46E-06	1.56E-07	4.00E-11	1.72E-11	3.06E-09	6.34E-09	2.30E-07	2.47E-08	6.32E-12	2.71E-12	4.83E-10	1.00E-09	1.28E-07	1.37E-08	3.51E-12	1.51E-12	2.68E-10	5.56E-10
	Ba						Hg						Pb					
TSS	1.57E-04	1.68E-05	4.32E-09	1.85E-09	3.30E-07	6.84E-07	2.93E-06	3.14E-07	8.04E-11	3.45E-11	6.15E-09	1.27E-08	3.01E-05	3.23E-06	8.28E-10	3.55E-10	6.33E-08	1.31E-07
TSW	1.86E-04	1.99E-05	5.10E-09	2.18E-09	3.90E-07	8.07E-07	8.44E-07	9.04E-08	2.32E-11	9.94E-12	1.77E-09	3.67E-09	3.78E-05	4.05E-06	1.04E-09	4.45E-10	7.94E-08	1.65E-07
SGS	1.35E-04	1.44E-05	3.70E-09	1.59E-09	2.83E-07	5.86E-07	1.51E-06	1.62E-07	4.14E-11	1.78E-11	3.17E-09	6.56E-09	7.78E-05	8.33E-06	2.14E-09	9.16E-10	1.63E-07	3.38E-07
SGW	2.54E-04	2.72E-05	6.98E-09	2.99E-09	5.33E-07	1.11E-06	1.28E-08	1.37E-09	3.51E-13	1.51E-13	2.68E-11	5.56E-11	1.90E-05	2.04E-06	5.22E-10	2.24E-10	3.99E-08	8.26E-08
SAW	6.19E-04	6.63E-05	1.70E-08	7.29E-09	1.30E-06	2.69E-06	1.28E-08	1.37E-09	3.51E-13	1.51E-13	2.68E-11	5.56E-11	1.09E-03	1.16E-04	2.99E-08	1.28E-08	2.28E-06	4.73E-06
MPS	5.80E-04	6.21E-05	1.59E-08	6.83E-09	1.22E-06	2.52E-06	6.39E-08	6.85E-09	1.76E-12	7.53E-13	1.34E-10	2.78E-10	1.21E-04	1.29E-05	3.32E-09	1.42E-09	2.54E-07	5.26E-07
MPW	2.31E-04	2.47E-05	6.33E-09	2.71E-09	4.84E-07	1.00E-06	1.28E-08	1.37E-09	3.51E-13	1.51E-13	2.68E-11	5.56E-11	3.79E-05	4.06E-06	1.04E-09	4.46E-10	7.96E-08	1.65E-07

When HQ and HI values are less than a unit, there is no obvious risk to the population, but if these values exceed one, there may be concern for potential non-carcinogenic effects (USEPA, 2004) as explained earlier. Most of these metals are associated with negative neurological impacts on humans (e.g., mental retardation and developmental delay) (Jacob *et al*., 2002; Madl *et al*., 2007; Bouchard *et al*., 2008). For both children and adults, the calculated HQ was less than one for the three pathways within Soutpansberg. This implies that there is no significant non-carcinogenic risk in their population. The total HQ for Cr in child population was, however, greater than one and therefore implies that there is a possible non-carcinogenic risk to their population. Hence, there is a need for necessary mitigation strategies (such as civic education, routine sampling) to reduce concentrations and limit human exposure in the selected communities. In addition, the HI values were less than one in both populations at all sites implying that there is no significant non-carcinogenic risk to their population, but the relatively high value of Cr is of great concern as explained (Table 7.10).

The excess lifetime cancer risks for adults and children are calculated separately from the average concentrations of individual metals in soil for all the exposure pathways using equations (3.9 – 3.13). Based on the carcinogenic risk values of the calculated ADI and HQ values presented in Tables 7.11 and 7.12, respectively, the results of the excess lifetime cancer risk are presented in Table 7.13. The HQ values for the three exposure pathways were presented in Appendix 7.4.

Table 7.10: Hazard index (HI) for non-carcinogenic risk from the surrounding soils within Soutpansberg region.

		TSS	TSW	SGS	SGW	SAW	MPS	MPW
Be	Children	1.20E-02	1.44E-02	7.03E-03	5.95E-03	3.76E-02	4.00E-02	1.27E-02
	Adults	1.29E-03	1.55E-03	7.54E-04	6.37E-04	4.03E-03	4.29E-03	1.36E-03
V	Children	4.35E-02	4.63E-02	1.74E-02	1.66E-02	4.19E-01	1.73E-01	1.24E-01
	Adults	4.66E-03	4.97E-03	1.87E-03	1.78E-03	4.49E-02	1.85E-02	1.33E-02
Cr	Children	1.98E-01	1.61E-01	4.27E-02	3.34E-02	3.88E-01	1.55E-01	1.20E-01
	Adults	2.22E-02	1.80E-02	4.79E-03	3.75E-03	4.35E-02	1.73E-02	1.34E-02
Mn	Children	6.24E-02	7.19E-02	3.79E-02	2.98E-02	6.52E-02	1.95E-02	2.59E-02
	Adults	1.09E-02	1.25E-02	6.60E-03	5.18E-03	1.14E-02	3.40E-03	4.51E-03
Co	Children	5.68E-03	5.54E-03	2.56E-03	1.69E-03	3.20E-02	1.64E-02	2.13E-02
	Adults	5.32E-03	5.19E-03	2.40E-03	1.59E-03	3.00E-02	1.53E-02	2.00E-02
Ni	Children	2.22E-02	1.68E-02	7.26E-03	3.95E-03	3.33E-02	1.36E-02	7.47E-03
	Adults	2.70E-03	2.05E-03	8.84E-04	4.81E-04	4.05E-03	1.65E-03	9.10E-04
Cu	Children	4.40E-03	4.76E-03	3.01E-03	2.48E-03	3.37E-02	1.16E-02	6.69E-03
	Adults	5.00E-04	5.40E-04	3.42E-04	2.81E-04	3.82E-03	1.32E-03	7.59E-04
Zn	Children	6.55E-04	6.94E-04	7.38E-04	2.12E-04	2.09E-03	1.62E-03	3.47E-04
	Adults	8.09E-05	8.57E-05	9.11E-05	2.62E-05	2.58E-04	2.00E-04	4.29E-05
As	Children	1.63E-02	1.58E-02	1.42E-02	2.51E-02	3.36E-02	4.69E-02	4.40E-03
	Adults	1.82E-03	1.75E-03	1.58E-03	2.79E-03	3.74E-03	5.22E-03	4.89E-04
Se	Children	6.90E-04	4.53E-04	1.79E-04	2.51E-04	6.75E-04	3.92E-03	2.92E-04
	Adults	7.40E-05	4.85E-05	1.92E-05	2.69E-05	7.23E-05	4.20E-04	3.12E-05
Cd	Children	4.36E-04	3.08E-04	2.82E-04	1.28E-04	3.29E-03	1.20E-03	2.31E-04
	Adults	4.86E-05	3.43E-05	3.14E-05	1.43E-05	3.67E-04	1.34E-04	2.57E-05
Sb	Children	4.48E-04	6.71E-04	6.07E-04	6.39E-04	9.27E-04	1.18E-03	3.20E-04
	Adults	4.80E-05	7.19E-05	6.51E-05	6.85E-05	9.93E-05	1.27E-04	3.43E-05
Ba	Children	7.86E-04	9.28E-04	6.74E-04	1.27E-03	3.09E-03	2.90E-03	1.15E-03
	Adults	8.42E-05	9.94E-05	7.22E-05	1.36E-04	3.32E-04	3.11E-04	1.24E-04
Hg	Children	9.78E-03	2.82E-03	5.04E-03	4.27E-05	4.27E-05	2.14E-04	4.27E-05
	Adults	1.09E-03	3.14E-04	5.61E-04	4.75E-06	4.75E-06	2.38E-05	4.75E-06
Pb	Children	8.73E-03	1.10E-02	2.25E-02	5.50E-03	3.15E-01	3.50E-02	1.10E-02
	Adults	1.17E-03	1.47E-03	3.03E-03	7.39E-04	4.23E-02	4.70E-03	1.47E-03

Table 7.11: Average daily intake (ADI) values in mg/kg/day for adults and children in surrounding soils from the geothermal springs for carcinogenic risk calculations within Soutpansberg region.

	Be						V						Cr					
	Ingestion		inhalation		dermal		Ingestion		inhalation		dermal		Ingestion		inhalation		dermal	
	Children	Adults	Children	Adults	Children	Adults	Children	Adults	Children	Adults	Children	Adults	Children	Adults	Children	Adults	Children	Adults
TSS	2.06E-07	1.10E-07	5.66E-12	1.21E-11	4.33E-10	4.48E-09	1.88E-05	1.01E-06	5.16E-10	1.11E-10	3.94E-08	4.08E-07	5.07E-05	2.71E-05	1.39E-09	2.98E-10	1.06E-07	1.10E-06
TSW	2.48E-07	1.33E-07	6.80E-12	1.46E-11	6.07E-09	5.39E-09	2.00E-05	1.07E-06	5.50E-10	1.18E-10	4.20E-08	4.35E-07	4.11E-05	2.20E-05	1.13E-09	2.42E-10	8.63E-08	8.94E-07
SGS	1.21E-07	6.46E-08	3.31E-12	7.10E-12	2.95E-09	2.62E-09	7.52E-06	4.03E-07	2.07E-10	4.43E-11	1.58E-08	1.64E-07	1.09E-05	5.86E-06	3.00E-10	6.44E-11	2.30E-08	2.38E-07
SGW	1.02E-07	5.46E-08	2.80E-12	6.00E-12	2.50E-09	2.22E-09	7.16E-06	3.84E-07	1.97E-10	4.22E-11	1.50E-08	1.56E-07	8.56E-06	4.59E-06	2.35E-10	5.04E-11	1.80E-08	1.86E-07
SAW	6.44E-07	3.45E-07	1.77E-11	3.79E-11	1.58E-08	1.40E-08	1.81E-04	9.69E-06	4.97E-09	1.07E-09	3.80E-07	3.94E-06	9.92E-05	5.32E-05	2.73E-09	5.84E-10	2.08E-07	2.16E-06
MPS	6.86E-07	3.68E-07	1.88E-11	4.04E-11	1.68E-08	1.49E-08	7.47E-05	4.00E-06	2.05E-09	4.40E-10	1.57E-07	1.62E-06	3.96E-05	2.12E-05	1.09E-09	2.33E-10	8.31E-08	8.60E-07
MPW	2.17E-07	1.16E-07	5.96E-12	1.28E-11	5.32E-09	4.72E-09	5.37E-05	2.88E-06	1.48E-09	3.16E-10	1.13E-07	1.17E-06	3.06E-05	1.64E-05	8.41E-10	1.80E-10	6.43E-08	6.65E-07
	Mn						Co						Ni					
TSS	1.24E-04	6.65E-05	3.41E-09	7.30E-09	2.61E-07	2.70E-06	5.57E-06	2.98E-06	1.53E-10	3.28E-10	1.17E-08	1.21E-07	3.77E-05	2.02E-05	1.04E-09	2.22E-09	7.93E-08	8.21E-07
TSW	1.43E-04	7.65E-05	3.92E-09	8.41E-09	3.00E-07	3.11E-06	5.44E-06	2.91E-06	1.49E-10	3.20E-10	1.14E-08	1.18E-07	2.86E-05	1.53E-05	7.86E-10	1.68E-09	6.01E-08	6.22E-07
SGS	7.54E-05	4.04E-05	2.07E-09	4.44E-09	1.58E-07	1.64E-06	2.51E-06	1.35E-06	6.90E-11	1.48E-10	5.28E-09	5.47E-08	1.24E-05	6.62E-06	3.39E-10	7.27E-10	2.59E-08	2.69E-07
SGW	5.91E-05	3.17E-05	1.62E-09	3.48E-09	1.24E-07	1.29E-06	1.66E-06	8.91E-07	4.57E-11	9.79E-11	3.49E-09	3.62E-08	6.72E-06	3.60E-06	1.85E-10	3.95E-10	1.41E-08	1.46E-07
SAW	1.30E-04	6.95E-05	3.56E-09	7.63E-09	2.72E-07	2.82E-06	3.14E-05	1.68E-05	8.63E-10	1.85E-09	6.60E-08	6.83E-07	5.66E-05	3.03E-05	1.56E-09	3.33E-09	1.19E-07	1.23E-06
MPS	3.88E-05	2.08E-05	1.07E-09	2.28E-09	8.15E-08	8.44E-07	1.61E-05	8.61E-06	4.41E-10	9.46E-10	3.37E-08	3.49E-07	2.31E-05	1.24E-05	6.35E-10	1.36E-09	4.86E-08	5.03E-07
MPW	5.15E-05	2.76E-05	1.41E-09	3.03E-09	1.08E-07	1.12E-06	2.10E-05	1.12E-05	5.76E-10	1.23E-09	4.40E-08	4.56E-07	1.27E-05	6.81E-06	3.49E-10	7.48E-10	2.67E-08	2.76E-07
	Cu						Zn						As					
TSS	1.39E-05	7.46E-06	3.82E-10	8.19E-10	2.92E-08	3.03E-07	1.67E-05	8.95E-06	4.59E-10	9.83E-10	3.51E-08	3.63E-07	4.19E-07	2.24E-07	1.15E-11	2.46E-11	8.79E-10	9.11E-09
TSW	1.50E-05	8.06E-06	4.13E-10	8.86E-10	3.16E-08	3.27E-07	1.77E-05	9.48E-06	4.86E-10	1.04E-09	3.72E-08	3.85E-07	4.04E-07	2.17E-07	1.11E-11	2.38E-11	8.49E-10	8.80E-09
SGS	9.52E-06	5.10E-06	2.62E-10	5.60E-10	2.00E-08	2.07E-07	1.88E-05	1.01E-05	5.17E-10	1.11E-09	3.95E-08	4.09E-07	3.65E-07	1.95E-07	1.00E-11	2.15E-11	7.66E-10	7.94E-09
SGW	7.83E-06	4.19E-06	2.15E-10	4.61E-10	1.64E-08	1.70E-07	5.40E-06	2.89E-06	1.48E-10	3.18E-10	1.13E-08	1.18E-07	6.43E-07	3.45E-07	1.77E-11	3.79E-11	1.35E-09	1.40E-08
SAW	1.06E-04	5.70E-05	2.92E-09	6.26E-09	2.23E-07	2.31E-06	5.33E-05	2.85E-05	1.46E-09	3.14E-09	1.12E-07	1.16E-06	8.62E-07	4.62E-07	2.37E-11	5.08E-11	1.81E-09	1.88E-08
MPS	3.67E-05	1.96E-05	1.01E-09	2.16E-09	7.70E-08	7.97E-07	4.14E-05	2.22E-05	1.14E-09	2.43E-09	8.69E-08	9.00E-07	1.20E-06	6.45E-07	3.31E-11	7.08E-11	2.53E-09	2.62E-08
MPW	2.12E-05	1.13E-05	5.81E-10	1.25E-09	4.44E-08	4.60E-07	8.86E-06	4.74E-06	2.43E-10	5.21E-10	1.86E-08	1.93E-07	1.13E-07	6.05E-08	3.10E-12	6.65E-12	2.37E-10	2.46E-09

	Se						Cd						Sb					
	Ingestion		inhalation		dermal		Ingestion		inhalation		dermal		Ingestion		inhalation		dermal	
	Children	Adults	Children	Adults	Children	Adults	Children	Adults	Children	Adults	Children	Adults	Children	Adults	Children	Adults	Children	Adults
TSS	2.96E-07	1.59E-07	8.13E-12	1.74E-11	6.21E-10	6.44E-09	3.73E-08	2.00E-08	1.02E-12	2.19E-12	7.82E-11	8.10E-10	1.53E-08	8.22E-09	4.21E-13	9.03E-13	3.22E-11	3.34E-10
TSW	1.94E-07	1.04E-07	5.33E-12	1.14E-11	4.07E-10	4.22E-09	2.63E-08	1.41E-08	7.23E-13	1.55E-12	5.52E-11	5.72E-10	2.30E-08	1.23E-08	6.32E-13	1.35E-12	4.83E-11	5.01E-10
SGS	7.67E-08	4.11E-08	2.11E-12	4.52E-12	1.61E-10	1.67E-09	2.41E-08	1.29E-08	6.62E-13	1.42E-12	5.06E-11	5.24E-10	2.08E-08	1.12E-08	5.72E-13	1.23E-12	4.37E-11	4.53E-10
SGW	1.07E-07	5.75E-08	2.95E-12	6.32E-12	2.26E-10	2.34E-09	1.10E-08	5.87E-09	3.01E-13	6.45E-13	2.30E-11	2.38E-10	2.19E-08	1.17E-08	6.02E-13	1.29E-12	4.60E-11	4.77E-10
SAW	2.89E-07	1.55E-07	7.95E-12	1.70E-11	6.08E-10	6.29E-09	2.82E-07	1.51E-07	7.74E-12	1.66E-11	5.91E-10	6.13E-09	3.18E-08	1.70E-08	8.73E-13	1.87E-12	6.67E-11	6.91E-10
MPS	1.68E-06	9.01E-07	4.62E-11	9.90E-11	3.53E-09	3.66E-08	1.03E-07	5.52E-08	2.83E-12	6.06E-12	2.16E-10	2.24E-09	4.05E-08	2.17E-08	1.11E-12	2.39E-12	8.52E-11	8.82E-10
MPW	1.25E-07	6.69E-08	3.43E-12	7.35E-12	2.62E-10	2.72E-09	1.97E-08	1.06E-08	5.42E-13	1.16E-12	4.14E-11	4.29E-10	1.10E-08	5.87E-09	3.01E-13	6.45E-13	2.30E-11	2.38E-10
	Ba						Hg						Pb					
TSS	1.35E-05	7.22E-06	3.70E-10	7.93E-10	2.83E-08	2.93E-07	2.51E-07	1.34E-07	6.89E-12	1.48E-11	5.27E-10	5.46E-09	2.58E-06	1.38E-07	7.10E-11	1.52E-10	5.43E-09	5.62E-08
TSW	1.59E-05	8.52E-06	4.37E-10	9.36E-10	3.34E-08	3.46E-07	7.23E-08	3.87E-08	1.99E-12	4.26E-12	1.52E-10	1.57E-09	3.24E-06	1.74E-07	8.91E-11	1.91E-10	6.81E-09	7.05E-08
SGS	1.16E-05	6.19E-06	3.17E-10	6.80E-10	2.43E-08	2.51E-07	1.29E-07	6.93E-08	3.55E-12	7.61E-12	2.72E-10	2.81E-09	6.67E-06	3.57E-07	1.83E-10	3.93E-10	1.40E-08	1.45E-07
SGW	2.18E-05	1.17E-05	5.98E-10	1.28E-09	4.57E-08	4.74E-07	1.10E-09	5.87E-10	3.01E-14	6.45E-14	2.30E-12	2.38E-11	1.63E-06	8.72E-08	4.47E-11	9.59E-11	3.42E-09	3.54E-08
SAW	5.30E-05	2.84E-05	1.46E-09	3.12E-09	1.11E-07	1.15E-06	1.10E-09	5.87E-10	3.01E-14	6.45E-14	2.30E-12	2.38E-11	9.32E-05	4.99E-06	2.56E-09	5.49E-09	1.96E-07	2.03E-06
MPS	4.97E-05	2.66E-05	1.37E-09	2.93E-09	1.04E-07	1.08E-06	5.48E-09	2.94E-09	1.51E-13	3.23E-13	1.15E-11	1.19E-10	1.04E-05	5.55E-07	2.85E-10	6.10E-10	2.18E-08	2.25E-07
MPW	1.98E-05	1.06E-05	5.43E-10	1.16E-09	4.15E-08	4.30E-07	1.10E-09	5.87E-10	3.01E-14	6.45E-14	2.30E-12	2.38E-11	3.25E-06	1.74E-07	8.92E-11	1.91E-10	6.82E-09	7.06E-08

Table 7.12: Hazard index for carcinogenic risk for from the surrounding soils within Soutpansberg region

		TSS	TSW	SGS	SGW	SAW	MPS	MPW
Be	Children	1.03E-03	1.24E-03	6.03E-04	5.10E-04	3.22E-03	3.43E-03	1.08E-03
	Adults	5.52E-04	6.63E-04	3.23E-04	2.73E-04	1.73E-03	1.84E-03	5.81E-04
V	Children	3.72E-03	3.97E-03	1.49E-03	1.42E-03	3.59E-02	1.48E-02	1.07E-02
	Adults	2.00E-04	2.13E-04	8.00E-05	7.61E-05	1.92E-03	7.94E-04	5.71E-04
Cr	Children	1.70E-02	1.38E-02	3.66E-03	2.87E-03	3.32E-02	1.33E-02	1.02E-02
	Adults	9.42E-03	7.64E-03	2.03E-03	1.59E-03	1.85E-02	7.36E-03	5.69E-03
Mn	Children	5.35E-03	6.16E-03	3.25E-03	2.55E-03	5.59E-03	1.67E-03	2.22E-03
	Adults	4.66E-03	5.36E-03	2.83E-03	2.22E-03	4.87E-03	1.46E-03	1.93E-03
Co	Children	4.87E-04	4.75E-04	2.19E-04	1.45E-04	2.74E-03	1.40E-03	1.83E-03
	Adults	2.28E-03	2.23E-03	1.03E-03	6.81E-04	1.29E-02	6.58E-03	8.58E-03
Ni	Children	1.90E-03	1.44E-03	6.22E-04	3.38E-04	2.85E-03	1.16E-03	6.40E-04
	Adults	1.16E-03	8.77E-04	3.79E-04	2.06E-04	1.74E-03	7.09E-04	3.90E-04
Cu	Children	3.77E-04	4.08E-04	2.58E-04	2.12E-04	2.88E-03	9.94E-04	5.74E-04
	Adults	2.14E-04	2.32E-04	1.46E-04	1.20E-04	1.64E-03	5.64E-04	3.25E-04
Zn	Children	5.61E-05	5.95E-05	6.33E-05	1.82E-05	1.79E-04	1.39E-04	2.98E-05
	Adults	3.47E-05	3.67E-05	3.91E-05	1.12E-05	1.11E-04	8.59E-05	1.84E-05
As	Children	1.40E-03	1.35E-03	1.22E-03	2.15E-03	2.88E-03	4.02E-03	3.77E-04
	Adults	7.78E-04	7.52E-04	6.78E-04	1.20E-03	1.60E-03	2.24E-03	2.10E-04
Se	Children	5.92E-05	3.88E-05	1.53E-05	2.15E-05	5.79E-05	3.36E-04	2.50E-05
	Adults	3.17E-05	2.08E-05	8.22E-06	1.15E-05	3.10E-05	1.80E-04	1.34E-05
Cd	Children	3.74E-05	2.64E-05	2.42E-05	1.10E-05	2.82E-04	1.03E-04	1.98E-05
	Adults	2.08E-05	1.47E-05	1.35E-05	6.12E-06	1.57E-04	5.75E-05	1.10E-05
Sb	Children	3.84E-05	5.75E-05	5.21E-05	5.48E-05	7.95E-05	1.01E-04	2.74E-05
	Adults	2.06E-05	3.08E-05	2.79E-05	2.94E-05	4.26E-05	5.43E-05	1.47E-05
Ba	Children	6.73E-05	7.95E-05	5.78E-05	1.09E-04	2.65E-04	2.49E-04	9.88E-05
	Adults	3.61E-05	4.26E-05	3.09E-05	5.83E-05	1.42E-04	1.33E-04	5.29E-05
Hg	Children	8.38E-04	2.42E-04	4.32E-04	3.66E-06	3.66E-06	1.83E-05	3.66E-06
	Adults	4.67E-04	1.34E-04	2.40E-04	2.04E-06	2.04E-06	1.02E-05	2.04E-06
Pb	Children	7.49E-04	9.39E-04	1.93E-03	4.72E-04	2.70E-02	3.00E-03	9.41E-04
	Adults	1.47E-04	1.84E-04	3.78E-04	9.24E-05	5.29E-03	5.88E-04	1.84E-04

The carcinogenic risk was calculated for trace metals (As, Cd, Cr, Co and Pb) with an available carcinogenic slope factor from literature (Table 3.5). Cr, As and Co were found to be the highest contributors (value greater than recommended standard from 10^{-4} to 10^{-6}) to cancer risk in the selected communities. Cd does not pose cancer risk to children at all the sites except for Siloam (SAW). The cancer risk from winter to summer ranges from 1.56E-02 to 1.37E-02; 2.84E-02 to 2.69E-02; 5.98E-03 to 6.15E-02; 1.22E-02 to 9.30E-03; 2.71E-02 to 2.38E-02; 7.19E-02 to 8.73E-02 for children and adults, respectively (Table 7.13 and Figure 7.12). There is high possibility of cancer risk at the study areas and there is need for intervention. Therefore, the cancer risk is high in the general population, that is 1 in 72-162 individuals in children's population and 1 in 7-107 individuals for adult population. The ingestion route seems to be the major contributor to excess lifetime cancer risk followed by the dermal pathway. This quantitative evidence demonstrates the critical need for mitigation strategies to protect the residents especially the children.

Table 7.13: Carcinogenic risk assessment of Cr, Cd, As, Co and Pb from surrounding soils within Soutpansberg region

	Cr		Cd		As		Pb		Co	
	Children	Adults	Children	Adults	Children	Adults	Children	Adults	Children	Adults
TSS	8.48E-03	4.71E-03	2.35E-04	1.31E-04	2.10E-03	1.17E-03	6.36E-06	1.25E-06	4.77E-03	2.24E-02
TSW	6.88E-03	3.82E-03	1.66E-04	9.25E-05	2.03E-03	1.13E-03	7.99E-06	1.56E-06	4.65E-03	2.18E-02
SGS	1.83E-03	1.02E-03	1.52E-04	8.48E-05	1.83E-03	1.02E-03	1.64E-05	3.22E-06	2.15E-03	1.01E-02
SGW	1.43E-03	7.96E-04	6.92E-05	3.86E-05	3.22E-03	1.79E-03	4.01E-06	7.86E-07	1.42E-03	6.67E-03
SAW	1.66E-02	9.23E-03	1.78E-03	9.91E-04	4.32E-03	2.40E-03	2.29E-04	4.49E-05	2.69E-02	1.26E-01
MPS	6.63E-03	3.68E-03	6.51E-04	3.62E-04	6.03E-03	3.35E-03	2.55E-05	5.00E-06	1.37E-02	6.45E-02
MPW	5.12E-03	2.85E-03	1.25E-04	6.94E-05	5.66E-04	3.15E-04	8.00E-06	1.57E-06	1.79E-02	8.41E-02

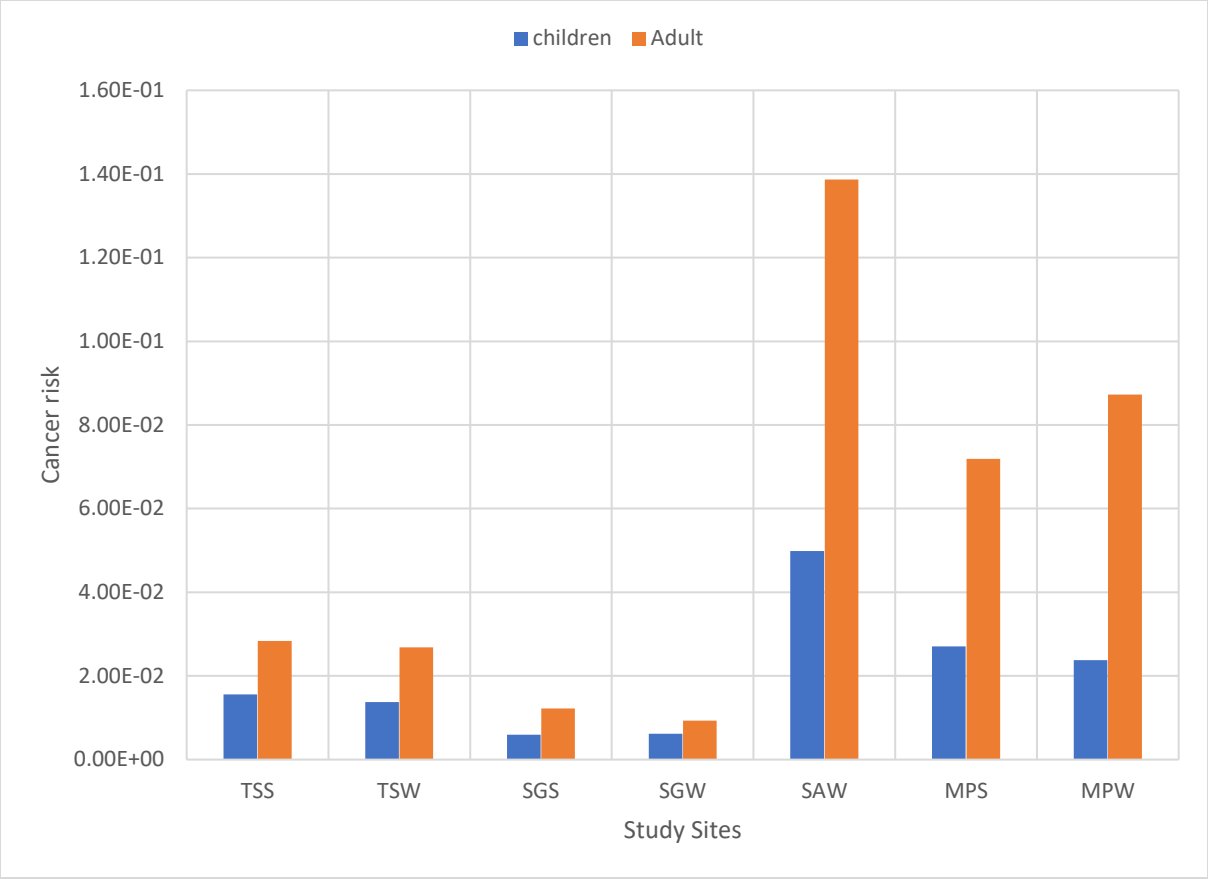

Figure 7.12: Cancer risk values of trace metals for adults and children in surrounding soil within Soutpansberg region.

7.6 Trace metals concentrations from surrounding vegetation

The trace metals from geothermal springs and their surrounding soils were also measured in the vegetation except for Be, As and Se because they are below the detection limit (BDL) of the instrument. Table 7.14 summarises the mean trace metals concentrations in various parts of different vegetation at specific sites. Generally, vegetation growing on soil has a tendency of absorbing trace metals through its root system and transporting them to other parts of the plant (Otieno *et al*., 2005; Ojekunle *et al*., 2014). In addition to the study by Durowoju (2015), this study has shown that geothermal spring water contaminates the surrounding surface soil with trace metals. Since plants depend on soil for their nutrients, there is a high possibility of them absorbing and transmitting these trace metals via their various parts. Also, vegetation has the potential capacity to reduce the concentrations of absorbed trace metals to a harmless state (Phyto-remediation).

Table 7.14: Mean trace metals concentrations (mg/kg) in the surrounding vegetation within Soutpansberg

			V	Cr	Mn	Co	Ni	Cu	Zn	Cd	Sb	Ba	Hg	Pb
Sagole	Amarula	Core	0.489	1.220	12.060	0.372	4.373	2.380	8.297	0.098	0.019	31.300	0.090	0.990
		Leaf	1.034	16.970	50.500	0.462	19.210	21.178	22.090	0.000	0.016	32.380	1.019	0.000
		Bark	1.958	2.901	29.910	0.864	10.605	5.089	10.805	0.052	0.018	39.765	0.115	0.562
	Lowveld mangosteen	Core	0.000	0.477	0.554	0.000	2.406	2.266	11.385	0.000	0.000	2.367	0.000	0.000
		Leaf	0.621	7.842	40.915	0.323	7.506	3.940	43.890	0.000	0.018	6.430	0.319	1.295
		Bark	3.499	6.485	54.860	2.005	14.680	26.390	35.080	0.055	0.024	16.940	0.090	1.597
	leadwood tree	Core	0.488	1.145	15.035	0.475	8.498	3.002	10.031	0.000	0.013	59.305	0.058	0.000
		Leaf	0.412	3.254	66.885	2.313	5.332	6.578	29.650	0.000	0.026	19.915	0.367	0.000
		Bark	1.999	3.653	47.370	1.100	15.315	6.061	12.505	0.000	0.013	96.810	0.089	0.636
Mphephu	Acacia tree	Core	0.266	0.558	9.020	0.137	1.472	1.773	8.509	0.090	0.019	21.510	0.080	0.980
		Leaf	0.515	1.167	81.305	0.238	2.003	8.246	40.935	0.143	0.026	45.290	0.498	0.000
		Bark	0.759	2.672	24.200	0.605	10.308	8.067	27.500	0.117	0.011	54.150	0.075	0.000
	Fig tree	Core	2.128	1.339	3.921	0.057	6.425	2.721	26.160	0.000	0.022	14.755	0.354	0.000
		Leaf	0.644	1.113	29.175	0.228	7.259	6.758	10.892	0.000	0.017	43.130	0.456	0.000
		Bark	1.622	4.396	17.800	0.585	12.755	3.719	13.235	0.000	0.015	68.585	0.000	0.000
	Amarula	Core	0.000	0.340	4.430	0.087	3.453	1.781	8.877	0.000	0.000	38.985	0.000	0.000
		Leaf	23.200	16.565	163.900	5.264	11.820	13.560	31.005	0.000	0.011	82.155	0.195	1.924
		Bark	0.567	1.832	14.880	0.278	3.661	3.048	8.574	0.000	0.011	58.550	0.000	0.000
Tshipise	Suage tree	Core	0.000	0.872	7.919	0.068	2.777	4.760	26.640	0.070	0.012	12.425	0.072	0.727
		Leaf	0.000	0.730	8.828	0.075	5.104	5.486	19.210	0.187	0.011	11.085	0.189	0.000
		Bark	2.711	6.594	29.310	0.514	6.054	10.158	15.010	0.000	0.015	23.875	0.000	0.710
	Amarula	Core	0.000	0.487	6.617	0.128	6.763	3.244	10.760	0.000	0.000	20.760	0.058	0.000
		Leaf	0.323	1.281	22.130	0.290	2.892	2.814	13.300	0.000	0.000	24.885	0.308	0.000
		Bark	0.359	2.054	10.414	0.248	6.055	4.024	10.475	0.000	0.015	20.375	0.000	0.000
	Acacia tree	Core	0.000	0.518	5.376	0.251	5.656	3.273	7.548	0.259	0.017	35.215	0.000	0.000
		Leaf	0.190	1.043	27.520	5.179	4.036	7.294	38.360	0.000	0.012	19.995	0.237	0.000
		Bark	0.326	0.806	5.797	0.428	4.625	3.104	11.375	0.000	0.000	68.775	0.000	0.000
Siloam	Amarula	Core	0.000	0.547	1.112	0.063	4.975	2.105	8.948	0.000	0.000	21.940	0.000	0.000
		Leaf	8.330	4.629	37.200	1.399	4.564	7.857	11.899	0.000	0.016	22.525	0.125	0.000
		Bark	1.056	9.158	29.435	0.371	12.420	9.292	19.125	0.000	0.015	45.350	0.142	0.000
	Guava	Core	0.000	0.477	0.554	0.000	2.406	2.266	11.385	0.000	0.000	2.367	0.000	0.000
		Leaf	0.208	0.605	8.669	0.159	5.683	4.913	17.815	0.462	0.014	26.915	0.000	1.960
		Bark	0.992	1.931	57.075	0.394	12.335	13.855	12.315	0.000	0.016	28.240	0.118	0.000
	Mango	Core	0.000	0.430	2.857	0.023	2.755	1.180	9.545	0.000	0.000	2.653	0.000	0.000
		Leaf	4.480	2.659	40.950	0.989	4.730	5.364	11.190	0.000	0.012	38.030	0.066	0.756
		Bark	0.719	8.332	124.850	0.250	8.743	4.583	13.620	0.061	0.016	39.115	0.111	0.000

Phytoremediation pathway involves phytoextraction, phytodegradation, phytovolatilation, phytostabilisation and phytostimulation of the absorbed trace metals from the soil. Hence, either of the phytoremediation pathways take place in the plant metabolism. The total concentrations of the trace metals in the different parts of vegetation at all the sites showed a similar decreasing trend from the root to the core (that is root – leaf – core). This seems to be the general trend for all plants in the process of their metabolism. This shows that the root system absorbs trace metals from the surrounding soil before transmitting via core to the leaves. The inner core has the lowest concentrations of trace metals because it serves as channel for transpiration compared to bark and leaves that could store before metabolism; except for the Amarula tree at all the sites which shows a contrary trend from the others, with the trend being from leaf to the core (that is a leaf – bark – core). Amarula tree has the largest leaves, and therefore contained more trace elements than its roots.

Statistically, there are significant differences in variances of trace metals concentrations from different parts (core, leaves and barks) in Amarula, Lowveld and Leadwood at Sagole ($P < 0.05$). This means that the variations of trace metals concentrations in core, leaves and barks of the plants were significant and not random. Significant variations of trace metals concentrations were observed in two different types of vegetation at Mphephu (Acacia and Fig trees), Tshipise (Sausage tree and Amarula tree) and Siloam (Amarula tree and Mango tree) ($P < 0.05$). However, no significant differences were observed in Amarula, Acacia and Guava trees in Mphephu, Tshipise and Siloam, respectively (Table 7.15).

Figures 7.13 – 7.16 show clearly that the various plant parts (core, leaves and barks) absorb trace metals concentrations differently from different sites. From this study, it can be inferred that the leaf part of the Amarula tree absorbs more trace metals than other plants' leaves. However, the barks of mango and Leadwood trees also absorb more trace metals than barks of other vegetation. This further confirms the significant variations of the trace metals concentrations among the various parts of the vegetation at different sites.

Table 7.15: ANOVA for variations of the different parts of vegetation

	Source of Variation	SS	df	MS	F	P-value	F critical
SAGOLE	**Amarula**						
	Between Groups	4387.88	11	398.90	8.407	4.56E-04	2.717
	Within Groups	569.41	12	47.45			
	Lowveld						
	Between Groups	5655.27	11	514.12	12.973	5.05E-05	2.717
	Within Groups	475.57	12	39.63			
	Leadwood						
	Between Groups	10279.73	11	934.52	3.351	2.42E-02	2.717
	Within Groups	3346.10	12	278.84			
MPHEPHU	**Acacia tree**						
	Between Groups	8922.34	11	811.12	4.968	6.58E-03	2.818
	Within Groups	1795.81	11	163.26			
	Fig tree						
	Between Groups	5847.26	11	531.57	15.291	2.12E-05	2.717
	Within Groups	417.17	12	34.76			
	Amarula						
	Between Groups	19286.61	11	1753.33	1.739	1.78E-01	2.717
	Within Groups	12101.15	12	1008.43			
TSHIPISE	**Sausage tree**						
	Between Groups	1253.00	11	113.91	4.105	1.12E-02	2.717
	Within Groups	332.99	12	27.75			
	Amarula						
	Between Groups	1283.16	11	116.65	15.749	1.81E-05	2.717
	Within Groups	88.88	12	7.41			
	Acacia tree						
	Between Groups	4189.27	11	380.84	2.525	6.33E-02	2.717
	Within Groups	1810.09	12	150.84			
SILOAM	**Amarula**						
	Between Groups	3329.18	11	302.65	9.412	2.61E-04	2.717
	Within Groups	385.87	12	32.16			
	Guava						
	Between Groups	2901.61	11	263.78	2.526	6.31E-02	2.717
	Within Groups	1252.93	12	104.41			
	Mango						
	Between Groups	13249.04	11	1204.46	4.065	1.16E-02	2.717
	Within Groups	3555.22	12	296.27			

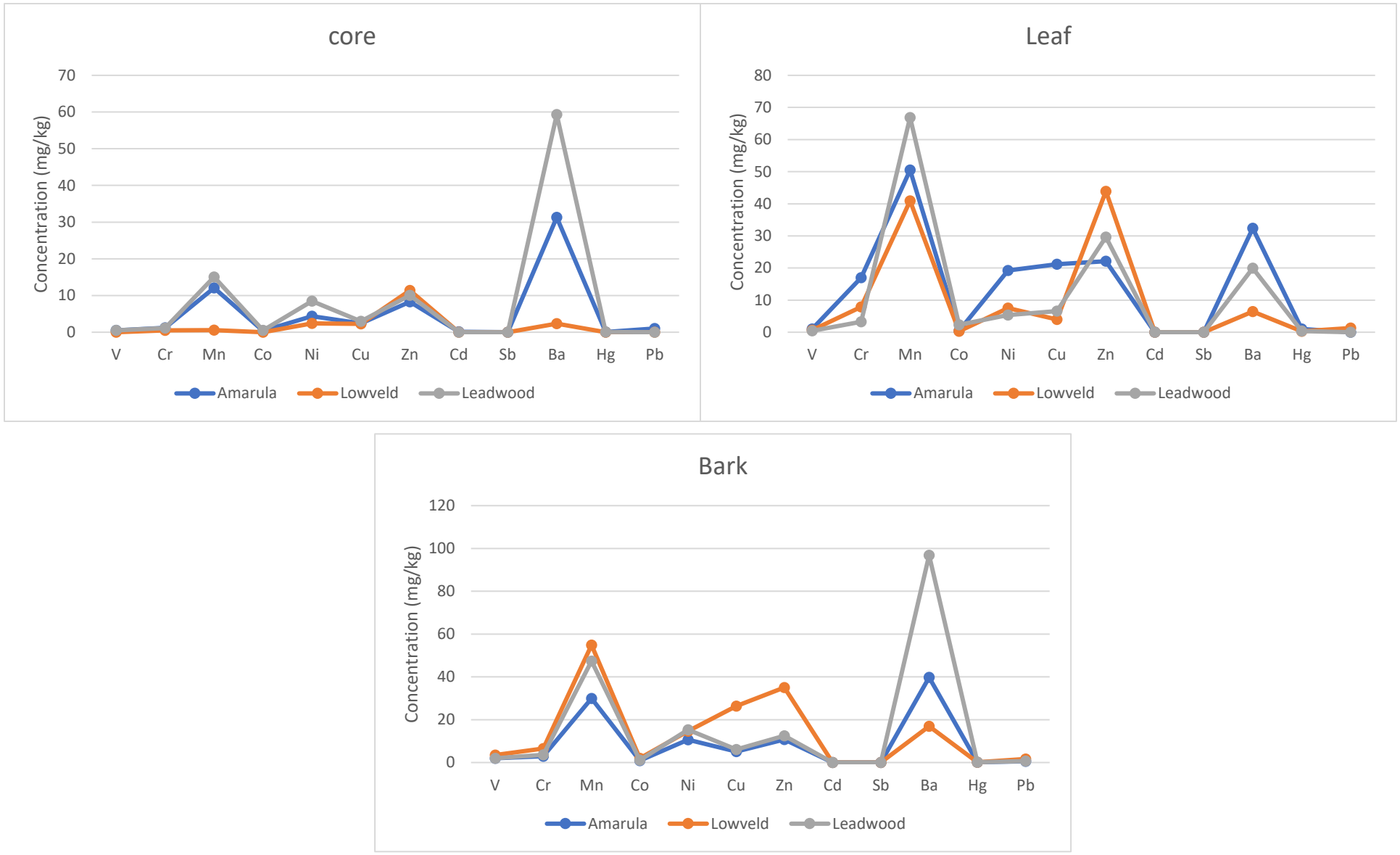

Figure 7.13: Variations of trace metals concentrations in the different parts of the vegetation at Sagole.

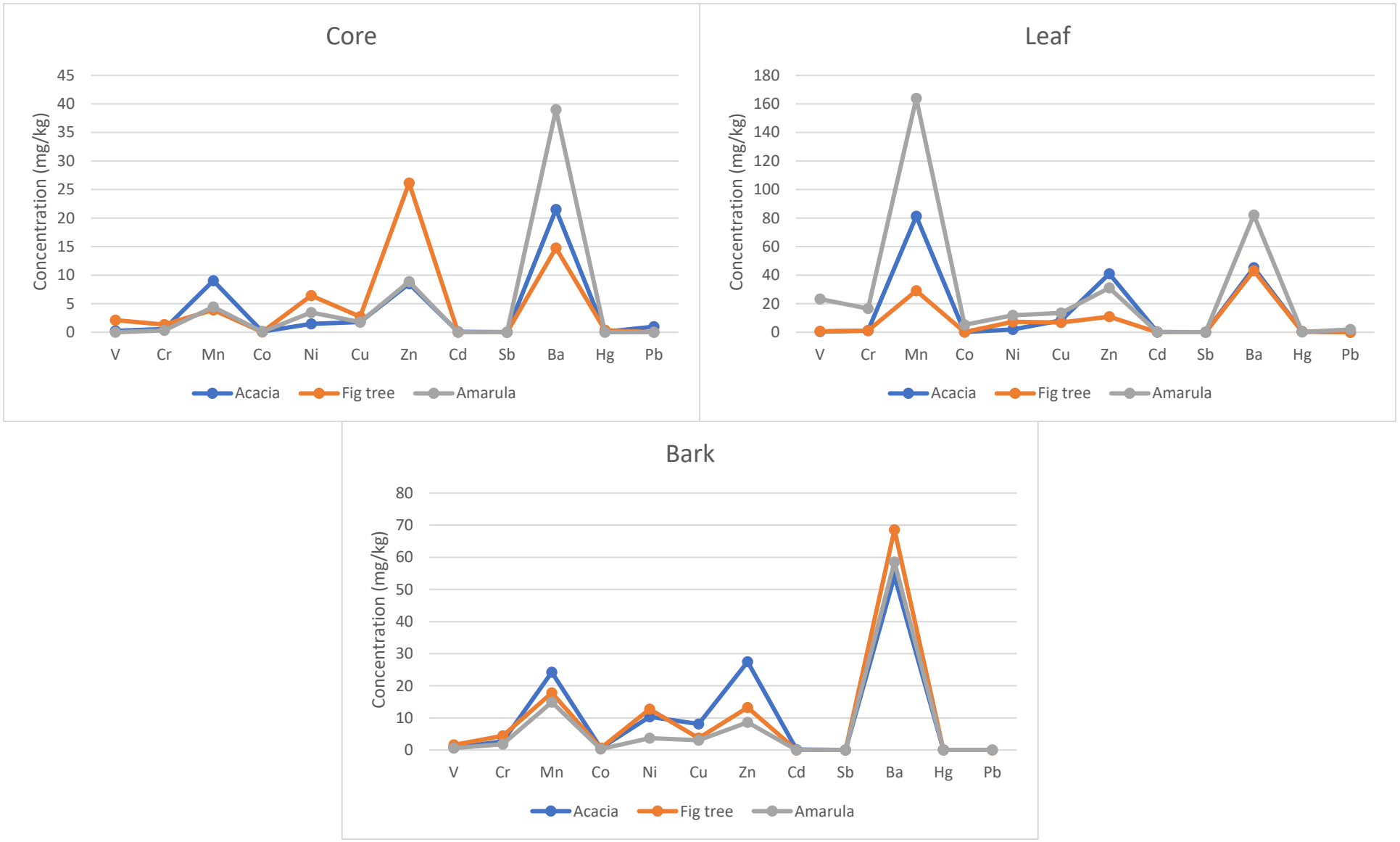

Figure 7.14: Variations of trace metals concentrations in the different parts of the vegetation at Mphephu.

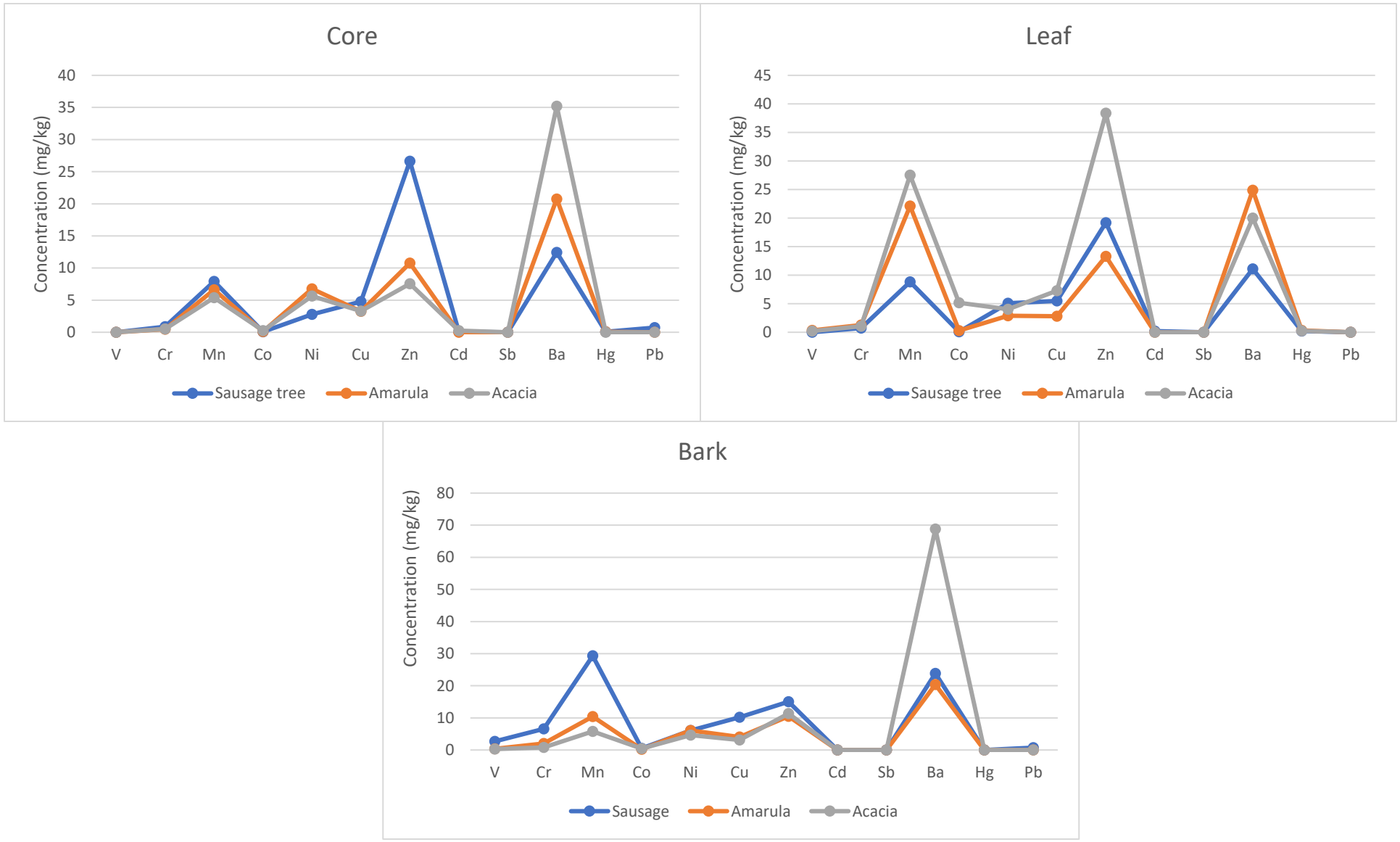

Figure 7.15: Variations of trace metals concentrations in the different parts of the vegetation at Tshipise.

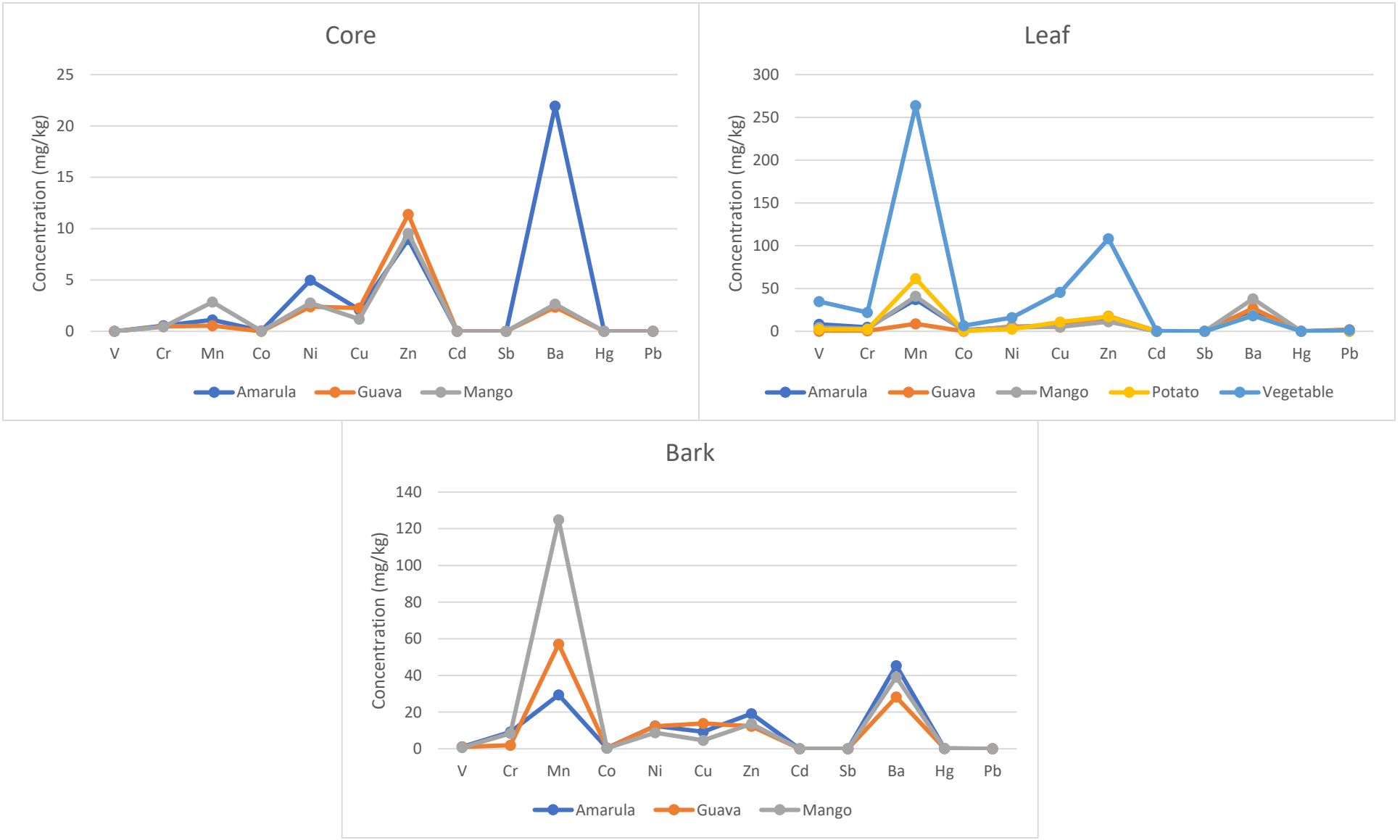

Figure 7.16: Variations of trace metals concentrations in the different parts of the vegetation at Siloam.

7.7 Uptake efficiency of the trace metals in parts of the vegetation

This study adopts the passive monitoring/observation of analysing trace metals in selected indigenous plants to explore their bioaccumulative/phytoremediative capacity (Ceburnis and Valiulis, 1999). Various plants have been used as bio-indicators to assess the impact of pollution sources in their vicinity due to high metal accumulation in plants (Onder and Dursun, 2006). The percentage uptake of the trace elements core, barks and leaves of the plant were calculated using the formula by Lawal *et al*. (2011):

% Conc. of uptake = Conc. of plant's part ÷ (Conc. of plant's part + Conc. of soil) × 100

The total trace metals concentrations for soil used for the uptake efficiency are 125.30 mg/kg, 260.36 mg/kg, 270.49 mg/kg and 722.89 mg/kg (Table 7.6) for Sagole, Mphephu, Tshipise and Siloam, respectively. These values were obtained from the average, summation of trace metals analysed in both seasons. The percentage uptake results indicate that different tree species have different uptake capacities with respect to different parts of the tree. The percentage mean trace element uptake by Amarula tree, Lowveld mangosteen and Leadwood trees were 32.99%, 56.82%, 45.03%; 13.44%, 47.44%, 56.34%; 43.90%, 51.81%, 59.69% for inner core, leaves and barks, respectively at Sagole (Figure 7.17). These species of trees have shown high uptake capacity in this magnitude: Leadwood tree > Amarula tree > Lowveld mangosteen with the leaf and bark as the most absorptive parts. At Mphephu, % uptake by Acacia tree, Fig tree and Amarula tree were 14.57%, 40.92%, 33.04%; 18.19%, 27.68%, 32.03%; 18.21%, 57.31%, 25.98% for inner core, leaves and barks, respectively (Figure 7.17). The uptake capacity decreases in this magnitude; Amarula tree, Acacia tree and Fig tree. Similarly, the leaves and barks of these species of tree are more absorptive. At Tshipise, % uptake by Sausage tree, Amarula tree, Acacia tree was 17.24%, 15.84%, 25.98%; 15.29%, 20.14%, 16.65%; 17.68%, 27.75%, 26.04% for inner core, leaves and barks, respectively (Figure 7.17). The uptake capacity decreases in this magnitude; Acacia tree, Sausage tree and Amarula trees, respectively. Although, the leaf and bark parts of these species of tree are the most absorptive parts as observed at Sagole and Mphephu but % uptake rate is lower compared to other sites.

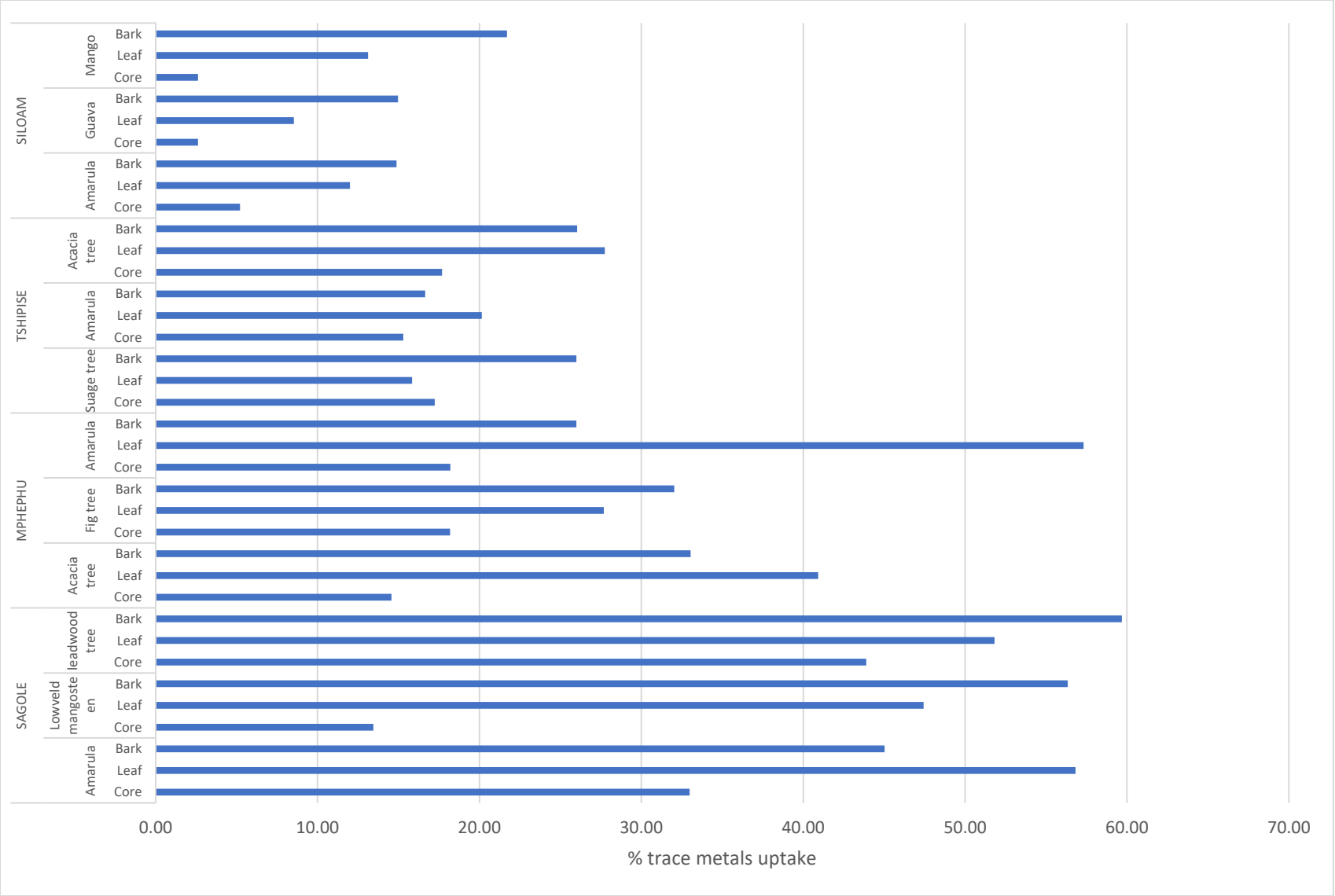

Figure 7.17: Percentage uptake concentrations of the mean trace metal in the vegetation within the Soutpansberg region.

The percentage uptake by Amarula tree, Guava tree and Mango tree were 5.20%, 12.00%, 14.88%; 2.62%, 8.53%, 14.97%; 2.62%, 13.13%, 21.70% for inner core, leaves and barks, respectively at Siloam (Figure 7.17). The uptake capacity decreases in this magnitude; Mango tree, Amarula tree and Guava tree. Similarly, the leaves and barks of these species of trees are more absorptive. The determination of the percentage uptake ensured the level of bioaccumulation of these trace elements by each tree. All the indigenous trees could be used as bio-indicators to access the level of contamination of trace elements in the soil since their uptake capacity is high. However, the study by Ojekunle *et al*. (2014) showed that mango tree and guava have high uptake capability for some selected heavy metals, which the present study cannot justify. This could be as a result of the broader scope of this study considering about 12 trace metals collectively at four different sites rather than selecting a few elements to evaluate their % uptake individually. This study recommends the use of indigenous trees such as Amarula tree, Acacia tree, Fig tree, mango tree, guava tree, Lowveld mangosteen, Leadwood and Sausage tree for remediation of trace metals contaminated soil. Hence, Amarula tree is selected as the best among others based on its uptake consistency at different sites.

7.8 Synopsis

The study aimed to assess trace metals concentrations and evaluate the potential health risk of inhabitants (adult and children) from the geothermal spring water and surrounding soils (Specific Objective 4). The following results were obtained:

- Trace metals concentrations of the geothermal springs and boreholes were within drinking permissible guidelines by SABS and WHO, with the exception of Mercury (Hg) which is high in summer. Presence of Hg could be associated with igneous activity and circulating geothermal fluids that precipitate around geothermal springs, geysers and fumaroles, especially during summer when there is high rainfall. Mean trace metals concentrations were higher in summer compared to winter except for a few anomalious concentrations in some metals. This could be attributed to the temperature differences (approximately 1°C) and more rainfall leading to more dissolution of the host rock (minerals) in summer. Pearson's correlation revealed that there is a strong relationship between the temperature

and pH; and inversely correlated to most of the trace metals. This is an indication of dissolution of minerals (rock-water interaction) under high temperature. HCA and PCA/FA further elucidated the relationship and possible sources of the trace metals. It can be inferred that the rock-water interaction is the main geochemical process governing the formation of trace metals in groundwater.

- Even though trace metals concentrations were within the drinking guideline, the accumulations in the human body could result in adverse effect considering that some of these metals are carcinogenic in nature. HI values for both children and adults were higher than one and this implies that the communities have a high risk of non-cancer health conditions. The ingestion pathway is the major pathway with trace metals such as As, Be, Se, Cr, Co, Mn, Hg, V and Zn as the main drivers. As, Cr and Cd were found to be the highest contributors to the cancer risk in study areas with children having a higher risk than adults. Therefore, proper monitoring and control measures to protect human health, particularly in children, within the study areas should be implemented for safety.
- The concentrations of the trace metals at different depths of the surrounding soil were found within the acceptable limits of the Department of Environmental Affairs (DEA) except for Cu, Cr, As and Pb at Siloam and Mphephu; Siloam, Tshipise and Mphephu; Sagole; and Siloam, respectively. The trace metals concentrations were higher at deeper depths at all sites (leaching effects). The soil type plays a vital role in the trace metals retention capacity in the soil, making Siloam, the most enriched soil among others. The relationship of the trace metals and physicochemical parameters was assessed using Pearson's correlation matrix, HCA and PCA/FA. This study showed that trace metals are more soluble in acidic soil and tends to be insoluble in alkaline soil. The sources of trace metals are soil pedogenesis (geogenic), groundwater-surface soil interaction and anthropogenic sources.
- From the risk assessment of trace metals in soil, it was confirmed that ingestion pathway is the major exposure to the surrounding soil at all sites followed by dermal and inhalation pathways. Hence, soil ingestion was the most significant contributor to the total health risk. The findings from this study also support the

general observations that children are more susceptible/vulnerable to potential health risk associated with these trace metals in the environment. For both children and adult population, the calculated HQ was less than one for the three pathways; this means that there is no significant non-carcinogenic risk in their population. Cr, As and Co were found to be the highest contributors to the cancer risk in the selected communities. Therefore, the cancer risk is high in the general population; that is 1 in 72-162 individuals in child population and 1 in 7-107 individuals for adult populations. The ingestion route seems to be the major contributor to excess lifetime cancer risk followed by the dermal pathway.

- The trace metals in the surrounding trees within the geothermal springs were determined to assess the phytoremediative capacity of the plants. The total concentrations of the trace metals in the different parts of vegetation at all the sites showed a similar decreasing trend from the root to the core (that is root – leaf – core). Statistically, there is a significant difference in variance of trace metals concentrations from different parts for every surrounding plant analysed at different sites. The determination of the percentage uptake ensured the level of bioaccumulation of these trace metals by each tree. All the surrounding trees could be used as bio-indicators to access the level of contamination of trace metals in the soil since their uptake capacity is high. Although, all the surrounding trees are good for remediations of contaminated soils, this study recommends Amarula tree based on its high uptake consistency at different sites.

CHAPTER EIGHT

CONCLUSIONS AND RECOMMENDATIONS

8.1 Overview of the study

Geothermal springs within Soutpansberg (Siloam, Mphephu, Sagole and Tshipise) were studied comprehensively to elucidate on isotopic and trace metals compositions in relation to their surrounding soils and vegetation. This is an eco-hydrological study that shows the interconnectivity of isotopic signatures among water (rainwater, geothermal springs and boreholes), soils and vegetation. It has been shown that rainwater is one of the major components of recharge of geothermal spring, which is isotopically depleted as it infiltrates through the soil. The signatures from soil-water is absorbed by the plant (plant water) and which is evapotranspired via the leaves and barks to the atmosphere. This study has provided better comprehensive understanding of the geochemical processes, sources, reservoir temperatures and suitability of these geothermal springs. Also, the local meteoric water line was generated, which will be useful for future isotopic research within the locality. Assessment of trace metals concentrations of geothermal springs, surrounding soils and vegetation was carried out; possible health risk associated with these trace metals concentrations in geothermal springs and surrounding soils were assessed in adults and children.

8.2 Conclusions

Conclusions drawn from this research are as follows:

1) The physicochemical, geochemical and isotopic compositions of rainwater, geothermal springs and boreholes led to the following conclusions:

- Temperature plays a vital and significant role in the geochemical processes of groundwater. Na-Cl and Na-HCO_3 are water types, which are typical of marine and deep/deeper groundwaters which are influenced by the ion - exchange processes. Gibb's plot indicates that rock-water interaction process leads to chemical weathering of the rock-forming minerals. The reservoir temperature of all the geothermal springs within Soutpansberg concentrated in range between 95°C to 185°C. Most of geothermal springs and borehole sources were characterised with

high chlorine from the Na-Cl water type, they are affected by geothermal water mixed with salt water, which is not native water. Whereas, Na-HCO_3-Cl water indicating water rising from periphery of hot granitic source (Siloam).

- The geothermal springs and boreholes water are not fit for drinking due to high fluoride content, except for the treated water such as water from SCC and TTP. According to Wilcox (US salinity) diagram, all geothermal and boreholes water samples were suitable for irrigation purposes. Other indices such as SAR, RSC, PI, and EC showed similar results except for KR and SP, implying that the geothermal springs /boreholes water fall under excellent to good category in both seasons with respect to these parameters. Although, geothermal springs/boreholes water are not fit for drinking due to high fluoride content but could be used for the following; domestic uses due to its softness, direct heating in refrigeration, green-housing, spa, therapeutic uses, aquaculture, sericulture, concrete curing and coal washing.

- The δD values of the rainwater varied from -76.3 ‰ to +22.7 ‰ (SMOW) with a weighted mean of – 9.8 ‰ and $\delta^{18}O$ values ranged from -10.78 ‰ to +3.07 ‰ (SMOW) with a weighted mean of -2.7 ‰ (n=12). Rain formation processes at Thohoyandou occurred under isotopic equilibrium conditions with minor evaporation effect during the precipitation, as reflected by the slope of the local meteoric water line of $\delta D = 7.56\delta^{18}O + 10.64$. The slightly high d-excess value is an indication that the rainwater is formed from water vapour near the land surface that is, either by re-condensation of the evaporated rainfall or evaporation of surface waters.

- The δD and $\delta^{18}O$ values of the geothermal springs/boreholes water confirm that the waters are of meteoric origin, which implies that rainfall is the fundamental component of these groundwaters. That is, the groundwater was derived from the infiltration of local precipitation, with significant contribution of another type of water in the deeper part of the aquifer. Stable isotopic composition of the geothermal

spring and boreholes water further confirms the significant role of evaporation on the groundwater chemistry of the studied areas with rock-water interaction being the main process. The isotopic signatures further confirm that there is an interconnectivity between the hot boreholes and geothermal spring at Siloam. Hence, this could be attributed to the minor faults connecting the shallow aquifer of hot boreholes to the deep aquifer of the geothermal spring.

2) The geothermal springs have higher tritium values in summer compared to winter. This implies that the geothermal springs were recharged before 1952 (submodern) for winter and recharged before and after 1952 (Mixture of modern and submodern) for the summer season. Radiocarbon values of the geothermal spring range from 2700 BP to 7350 BP (where the BP- Before Present, which is 1950) without correction. The radiocarbon further the longer residence time in the aquifer in winter compared to summer, where there is a mixture of modern and submodern water for recharge. From several carbon-14 correction models employed in this study, Vogel model which is an empirical model showed a good result with respect to the uncorrected radiocarbon age (apparent age). Incorporating the tritium age, Ingerson and Pearson, Eichinger and Fontes and Garnier correction models results proved to be the most appropriate models for radiocarbon correction of groundwater, particularly in semi-arid region.

3) The composition of $\delta^{13}C$ in soil water ranges from -24.15 to -14.79‰, which is an indication of Crassulacean Acid Metabolism (CAM) (mix of C3 and C4 photosynthetic cycles) with a stronger C4 trend. It can be deduced that δD is directly proportional to the depth and $\delta^{13}C$ is inversely proportional to the depth of the soil. Therefore, δD of the soil is inversely proportional to the $\delta^{13}C$ of the soil, where the depth of the soil is constant. The composition of $\delta^{13}C$ in plant water ranges wide from -35.50 to -10.42‰, which indicates the presence of C3 plants, CAM plants and C4 plants. The C3 plants include Amarula tree, Lowveld tree and Leadwood tree; C4 plants include Acacia tree and Sausage tree; and CAM plants include Fig tree, Guava tree and Mango tree. Hence, this study shows that with

CAM soils, there is a possibility of having either C3, C4 or CAM vegetation on it. This study has shown that the δD and $\delta^{13}C$ isotopes in water, soil and vegetation are interconnected. The study statistically justified that there is a strong correlation among the environmental media with respect to δD and $\delta^{13}C$ isotopes.

4) Assessment of trace metals concentrations and their associated health risk in adults and children from geothermal spring water and surrounding soils led to the following conclusions:

- Trace metals concentrations of the geothermal springs/boreholes were within permissible drinking guidelines by the SABS and WHO, with exception of Mercury (Hg) which is high in summer season. Pearson's correlation reveals that there is a strong relationship between the temperature and pH; and inversely correlated to most of the trace metals. This is an indication of dissolution of minerals (rock-water interaction) under high temperature. HCA and PCA/FA further elucidate the relationship and possible sources of the trace metals. It can be inferred that the rock-water interaction is the main geochemical process governing the formation of trace metals in groundwater.

- HI values for both children and adults were higher than one and this implies that the communities are at high risk of non-cancer health effects. The ingestion pathway is the major pathway with trace metals such as As, Be, Se, Cr, Co, Mn, Hg, V and Zn as the main drivers. As, Cr and Cd were found to be the highest contributors to the cancer risk in study areas with children having a higher risk than adults. Therefore, proper monitoring and control measures to protect human health, particularly the children, within the study areas should be implemented for safety.

- The concentrations of the trace metals at different depths of the surrounding soil were found within acceptable limit set by the Department of Environmental Affairs (DEA) except for Cu, Cr, As and Pb at Siloam and Mphephu; Siloam, Tshipise and Mphephu; Sagole; and Siloam, respectively. The relationship of

the trace metals and physicochemical parameters was assessed using Pearson's correlation matrix, HCA and PCA/FA. This study shows that trace metals are more soluble in acidic soil and tends to be insoluble in alkaline soil. The sources of trace metals are soil pedogenesis (geogenic), groundwater-surface soil interaction and anthropogenic sources.

- It was confirmed that ingestion pathway is the major exposure to the surrounding soil at all sites followed by dermal and inhalation pathways. For both children and adult population, the calculated HQ was less than one of the three pathways, which means that there was no significant non-carcinogenic risk in their population. Cr, As and Co were found to be the highest contributors to the cancer risk in the selected communities. Therefore, the cancer risk is high in the general population, that is (1 in 72-162 individuals in child population and 1 in 7-107 individuals for adult population). The ingestion route seems to be the major contributor to excess lifetime cancer risk followed by the dermal pathway.

- The determination of the percentage uptake ensured the level of bioaccumulation of these trace metals by each surrounding tree. All the surrounding trees could be used as bioindicators to access the level of contamination of trace elements in the soil since their uptake capacity is high. Although, all the surrounding trees are good for remediation of contaminated soils, but this study recommended Amarula tree based on its uptake consistency at different sites.

8.3 Recommendations

Though this research on isotopic signatures and trace metals in geothermal springs and their environmental media within Soutpansberg in Limpopo Province, South Africa contributed to the body of knowledge of geothermal springs in South Africa, it also gave room for future research. The following are recommendations for future research:

- Long term monitoring of the isotopic composition of rainwater across the province to generate a regional, meteoric water line which will help in proper water management across the province.
- Isotopic characterisation of surface water and groundwater within the Soutpansberg. This will provide detailed information on surface and groundwater interactions.
- Compound specific δD and $\delta^{13}C$ analyses of n-alkane should be carried out to differentiate the water sources of different vegetation types.
- Extensive mineralogical study to ascertain the deductions from this present study on trace metals concentrations.

REFERENCES

Aastri, J.C. (1994). Groundwater chemical quality in river basins, hydrogeochemical facies and hydrogeochemical modelling. PhD thesis Bharathidasan University, Tiruchirapalli, Tamil Nadu, India.

Abiye, T.A. (2011). Provenance of groundwater in the crystalline aquifer of Johannesburg area, South Africa. *Int. J. Physical Science*, 6(1), 98-111.

Abiye, T.A. (2013). The use of isotope hydrology to characterize and assess water resources in South (ern) Africa, WRC Project No. K5/1907.

Abiye, T.A., Mengistu, H. and Demlie, M.B. (2011). Groundwater resource in the crystalline rocks of the Johannesburg area, South Africa. *J. Water Resources and Protection,* 3(4), 199-212.

Adomako, D., Gibrilla, A., Maloszewski, P., Ganyaglo, S.Y. and Rai, S.P. (2015). Tracing stable isotopes ($\delta^{2}H$ and $\delta^{18}O$) from meteoric water to groundwater in the Densu River basin of Ghana. *Environ Monit Assess*, 187:264–278.

Agarwal, K., Sharma, A. and Talukder, G. (1990). Clastogenic effects of copper sulphate on the bone marrow chromosomes of mice in vivo. Mutation Research, vol. 243, pp. 1–6.

Aghazadeh, N., Mogaddam, A.A. (2010). Assessment of groundwater quality and its suitability for drinking and agricultural uses in the Oshnavieh area, Northwest of Iran, *Jour. of Environ. Protect*, 1:30-40.

Alloway, B.J. and Ayres, D.C. (1997). Chemical Principles of Environmental Pollution. Second Edition, Chapman and Hall, London, pp.140-167.

Al-Saudi, A. and Yaseen, I.A.B. (2017). Geochemical and Geo-thermometers Characteristics of Thermal Groundwater at Khan Ezabeeb Area, in Central Jordan, *Journal of Natural Sciences Research,* 7, 4.

Ako, A.A. (2011). Hydrological study on groundwater in the Banana Plain and Mount Cameroon area-Cameroon Volcanic line (CVL). Unpublished PhD thesis from Kumamoto University, Japan.

Ako, A.A., Shimada, J., Ichiyanagi, K., Koike, K., Hosono, T., Eyong, G.E.T. and Iskandar, I. (2010). Isotope hydrology and hydrochemistry of water resources in the banana plain (mungo-division) of the Cameroon Volcanic line, *Journal of Env. Hydrology*, 18(4), 1-20.

APEC (2010). Drinking water contaminants: Mercury. Free Drinking Water (http://www.freedrinkingwater.com) accessed November 12, 2016.

Arnorsson, S., Gunnlaugsson, E. and Svavarsson, H. (1983). The chemistry of geothermal waters in Iceland III. Chemical geothermometry in geothermal investigations. *Geochim. Cosmochim. Acta*, 47, 567-577

Asare-Donkor, N.K., Boadu, T.A. and Adimado, A.A. (2016). Evaluation of groundwater and surface water quality and human risk assessment for trace metals in human settlements around the Bosomtwe Crater Lake in Ghana. *SpringerPlus*, 5(1):1812

Baradacs, E., Hunyadi, I., Dezso, Z., Csige, I. and Szerbin, P. (2001). ^{226}Ra in geothermal and bottled mineral waters of Hungary. Radiation Measurement, 34: 385-390.

Barker, O.B. (1979). A contribution to the geology of the Soutpansberg group, Waterberg supergroup, northern Transvaal. Unpublished Master's thesis, University of Witwatersrand, Johannesburg, 116.

Barker, O.B., Brandl, G., Callagham, C.C., Eriksson, P.G. and Van der Neut, M. (2006). The Soutpansberg and Waterberg Groups and the Blouberg Formation. In: M.R. Johnson, C.R. Anhaeusser & R. J. Thomas, Eds. The Geology of South Africa, Pretoria: Geological Society of South Africa & Council for Geoscience, 301-318.

Barringer, J.L., Szabo, Z. and Reilly, P.A. (2013). Occurrence and Mobility of Mercury in Groundwater, Current Perspectives in Contaminant Hydrology and Water Resources Sustainability, Paul M. Bradley, IntechOpen, DOI: 10.5772/55487.

Barton, J.M. (1979). The chemical compositions, Rb-Sr isotopic systematics and tectonic setting of certain post-kinematic mafic igneous rocks, Limpopo Mobile Belt, Southern Africa, *Precambrian Res*., 9, 57 – 80.

Bjornsson, O. (2000). Therapeutic bathing, medical science and culture, (in Icelandic). Orkustofnun, Reykjavik, Report OS-2000/027, 104 p.

Blasch, K.W. and Bryson, J.R. (2007). Distinguishing sources of groundwater recharge by using delta H-2 and delta O-18, *Groundwater*, 45, 294 – 308.

Boekstein, M. (1998). Hot spring holidays: Visitor's guide to hot springs and mineral spa resorts in southern Africa, Cape Town: Mark Boekstein.

Bond, G.W. (1946). A geochemical survey of the underground water supplies of the Union of South Africa. *Memoirs Geol. Surv. S. Afr*., 41, 208.

Booyens, B. (1981). Bronwaters van genesing - Die tradisionele waterkuur in ons volksgeneeskunde. Kaapstad: Tafelberg.

Bouchard, M., Mergler, D., Baldwin, M.E. and Panisset, M. (2008). Manganese cumulative exposure and symptoms: a follow-up study of alloy workers. *Neurotoxicology*, 29:577–583.

Brandl, G. (1986). The geology of the Pietersburg area. Explanation sheet, geological survey of South Africa. vol. 2328 (Pietersburg), pp. 43

Brandl, G. (1999). Soutpansberg Group. Catalogue of South Africa Lithostratigraphic Units. SA Committee for Stratigraphy, Council for Geoscience, pp. 6-41.

Brandl, G. (2002). The geology of the Alldays area. Explanation sheet geological Survey South Africa. 2228 (Alldays), pp. 71.

Brubaker, K.L., Entekhabi, D. and Eagleson, P.S. (1993). Estimation of continental precipitation recycling. *J. Climate*, 6, 1077–1089.

Bruvold, W.H. and Ongerth, H.J. (1969). Taste Quality of Mineralized Water. Journal of the American Water works Association, vol. 61, pp. 170.

Buckau, G., Artinger, R., Geyer, S., Wolf, M., Fritz, P. and Kim, J.I. (2000). ^{14}C dating of Gorleben groundwater. *Applied Geochemistry,* 15, 583–597.

Cassidy, D.P., Werkema, D.D., Atekwana, E.A., Sauck, W.A., Rossbach, S. and Duris, J. (2001). The effects of LNAPL biodegradation products on electrical conductivity measurements. Journ. Enviro Eng Geo, vol. 6 (1), pp. 47-52.

Ceburnis, D. and Valiulis, D. (1999). Investigation of absolute metal uptake efficiency from precipitation in moss. *The Science of the Total Environment,* 226, 247- 253

Chandrasekharam, D. and Bundschuh, J. (2008). Low-Enthalpy Geothermal Resources for Power Generation. Taylor & Francis Group, London, UK, 172pp.

Cheney, E.S., Barton, J.M. and Brandl, G. (1990). Extent and age of the Soutpansberg sequences of Southern Africa. *S. Afri. J. Geo.* 93, 644-675.

Chrostowski, P.C. (1994). Exposure assessment principles. In: Patrick, D.R. (Ed.), Toxic Air Pollution Handbook. Van Nostrand Reinhold, New York, 133–163.

Chrotowski, P., Durda, J.L. and Edelman, K.G. (1991). The uses of natural processes for the control of chromium migration. Remediation, pp. 341-351.

Churchill, R.K. and Clinkenbeard, J.P. (2005). Perspectives on mercury contributions to watersheds from historic mercury mines and non-mine mercury sources: examples from the sulphur creek mining district. Cordilleran Section – 101st Annual Meeting. Piedmont, Italy, 29 April – 1 May 2005.

Clark, I. and Fritz, P (1997) Environmental Isotopes in Hydrology. Lewis, Boca Raton, Fl.

Cohen, A.S., Talbot, M.R.S., Awramik, M.D., Dettman, l. and Abell, P.I. (1997). Lake level and paleoenvironmental history of Lake Tanganyika, Africa, as inferred from Late Holocene and modern stromatolites, *Geol. Soc. Am. Bull*., 109(4), 444 – 460, doi:10.1130/0016-7606(1997) 109<0444:LLAPHO>2.3.CO;2.

Coplen, T.B., Herczeg, A.L. and Barnes, C. (2000). Isotope engineering-using stable isotopes of water molecule to solve practical problems. In: Cook, P., Herczeg, A.L

(eds) Environmental tracers in catchment hydrology. Kluwer Academic Publishers, Norwell, 79–110

Craig, H. (1961). Standards for reporting concentrations of deuterium and oxygen 18 in natural waters. Science 133, 1833–1834.

Craig, H., 1963: The isotopic geochemistry of water and carbon in geothermal areas. In: Tongiorgi, E. (ed.), Nuclear geology on geothermal areas. Consiglio Nazionale delle Ricerche, Laboratorio di Geologia Nucleare, Pisa, 17-53.

Cox, S.E (2003). Estimates of Residence Time and Related Variations in Quality of Ground Water Beneath Submarine Base Bangor and Vicinity, Kitsap County, Washington, U.S. Geological Survey, Water-Resources Investigations Report 03-4058, Tacoma, Washington 2003.

Dansgaard W. (1964). Stable isotopes in precipitation. *Tellus* 16: 436–468. DOI:10.1111/j.2153-3490. 1964.tb00181.x

Datta, P. S., and Tyagi, S. K. (1996). Major ion chemistry of groundwater in Delhi area: Chemical weathering processes and groundwater flow regime. *Journal of Geological Society of India*, 47, 179–188.

Deines, P. (1970). The carbon and oxygen isotopic composition of carbonates from the Oka carbonatite complex, Quebec, Canada, *Geochim Cosmochim Acta*, 34, 1199.

Deines, P. (1980). The isotopic composition of reduced organic carbon. In: Fritz, P. and Fontes, J.C. (eds), Handbook of Environmental Isotope Geochemistry. The Terrestrial Environmental, Elsevier, Amsterdam, pp. 329-409.

Department of Environmental Affairs (DEA) (2010). The Framework for the Management of Contaminated Land, South Africa. Available online: http://sawic.environment.gov.za/documents/562.pdf (accessed on 5/11/2017).

Department of Water Affairs and Forestry (DWAF) (1996). South African Water Quality Guidelines, Vol. 1: Domestic Water Use (2nd edn.). Department of Water Affairs and Forestry, Pretoria.

Department of Water Affairs and Forestry (DWAF) (2001). Luvuvhu/Letaba Water Management Area: Water resource situation assessment report NO P0200/00/030/. WSM (pty) Ltd.

Dhansay, T., Musekiwa, C., Ntholi, T., Chevallier, L., Cole, D. and De Wit, M.J. (2017). South Africa's geothermal energy hotspots inferred from subsurface temperature and geology. *S Afr J Sci*., 113(11/12), doi.org/10.17159/ sajs.2017/20170092.

Diamond, R. (1997). Stable isotopes of thermal springs of the Cape Fold Belt. University of Cape Town, Department of geological sciences, published Master dissertation, South Africa, 1997.

Dissanayake, C.B., Senaratne, A. and Weerassoriya, V.R. (1992). Geochemistry of well water and cardiovascular diseases in Siri Lanka. *International Journal of Environmental Studies*, 19, 195–203.

Doan, V., Tran Anh, V. and Nguyen, T.T. (2014). Geochemical Characteristics of Geothermal Hot Water Sources on the Territory of Vietnam, Proceedings, Thirty-Eighth Workshop on Geothermal Reservoir Engineering Stanford University, Stanford, California, February 24-26, SGP-TR-202

Dolnikowski GG. (1995). A New Sample Preparation Method for Isotope Ratio Mass Spectrometry of 2H-Enriched Samples Generated by the Doubly Labeled Water Method. *Obesity*, DOI: 10.1002/j.1550-8528.1995.tb00010.x

Doneen, L.D. (1964). Notes on Water Quality in Agriculture. 1st Edn., Department of Water Science and Engineering, University of California, Davis. pp: 96.

Drever, J.I. (1997). Weathering processes. In: Saether, O.M. and Caritat, P (ed): Geochemical Processes, weathering and groundwater recharge in catchments. pp 3-19.

Du, T., Kang, S., Zhang, J., Li, F. and Yan, B. (2008). Water use efficiency and fruit quality of table grape under alternate partial root-zone drip irrigation. *Agric Water Manag*., 95: 659-668

Dubbert, M., Cuntz, M., Piayda, A., Maguas, C. and Werner, C. (2013). Partitioning evapotranspiration- testing the Craig and Gordon model with field measurement of oxygen isotope ratios if evaporative fluxes, *J. Hydrol*., 496, 142-153.

Durov, S.A. (1948). Classification of natural waters and graphical representation of their composition. Dokl. Akad. Nauk. USSR. 59(1):87-90.

Durowoju, O.S. (2015). Trace element concentrations in geothermal springs and their impact on soil and vegetation in Siloam and Tshipise, Unpublished Master's dissertation, University of Venda, South Africa.

Durowoju, O.S., Odiyo, J.O. and Ekosse, G.E. (2015). Hydrogeochemical setting of geothermal springs in Limpopo Province, South Africa - A Review. *Res. J. Chem. Environ*., 19, 77–88.

Durowoju, O.S, Odiyo, J.O., and Ekosse, G.E. (2016a). Variations of heavy metals from geothermal spring to surrounding soil and *Mangifera indica*-Siloam Village, Limpopo Province, *Sustainability*, 8, 60; doi:10.3390/su8010060

Durowoju, O.S, Odiyo, J.O., and Ekosse, G.E. (2016b). Horizontal variation in trace elements and soil characteristics at Siloam and Tshipise geothermal springs, Limpopo Province, South Africa, *Water SA*, 42(4), 694-702.

Durowoju, O.S, Odiyo, J.O. and Ekosse, G.E. (2018). Geochemistry of Siloam and Tshipise Geothermal Springs, Limpopo Province, South Africa, *American J. of Environmental Sciences*, DOI: 10.3844/ajessp.2018.

Durvey, V.S., Shama, L.L., Saini, V.P and Sharma, B.K. (1991). Handbook on the methodology of water quality assessment. India: Rajasthan Agriculture University

Duvert, C., Stewart, M. K., Cendón, D. I. and Raiber, M. (2016). Time series of tritium, stable isotopes and chloride reveal short-term variations in groundwater contribution to a stream, *Hydrol. Earth Syst. Sci*., 20, 257–277.

Eaton, E.M. (1950). Significance in carbonate in irrigation water*. Soil Science*, 69, 123–133.

Eglinton, T.I. and Eglinton, G. (2008). Molecular proxies for paleoclimatology. *Earth and Planetary Science Letters,* 275, 1-16.

Ehleringer, J.R., Hall, A.E. and Farquhar, G.D. (1993). Stable isotopes and plant carbon-water relations, Academic Press, San Diego.

Ehleringer, J.R., Cerling T.E and Dearing, M.D. (2005). A History of Atmospheric CO_2 and its Effects on Plants, Animals and Ecosystems. Springer.

Eichinger L. (1983). A contribution to the interpretation of ^{14}C groundwater ages considering the example of a partially confined sandstone aquifer. Radiocarbon, 5(2):347–356.

Elliot, T., Andrews, J.N. and Edmunds, W.M. (1999). Hydrochemical trends, palaeorecharge and groundwater ages in the fissured chalk aquifer of the London and Berkshire Basins, UK. *Appl. Geoch*. 14, 333-363

El-Kadi, A.I., Plummer, L.N and Aggarwal, P. (2010). NETPATH-WIN: An Interactive User Version of the Mass-Balance Model, NETPATH,*GROUND WATER*, 49(4), 593–599.

Enzenberger, F. (2015). ^{14}C - Dating - Method for radiochemical age determination, September 2015, http: // www.c14 method.de.v

Estep, M.F and Dabrowski H. (1980). Tracing food webs with stable hydrogen isotopes. *Science*, 209, 1537-1538.

Estep, M.F and Hoering T.C. (1980). Biogeochemistry of the stable hydrogen isotopes. *Geochimicaet Cosmochimica Acta,* 44, 1197-1206.

European Commission (EC), (1999). Blue Book on Geothermal Resources: A Strategic Plan for the Development of European Geothermal Sector, Alterner: Luxembourg.

European Union (EU), (1998). Council Directive 98/83/EEC of 3 November 1998 on the quality intended for human consumption, Official journal of the European Communities, L330 (5.12.98), pp. 32-53.

Fawzia, M.A and Mohamed, S. (2004). Hydrochemical Processes and Environmental Isotopic Study of Groundwater in Kuwait, *Water International*, 29:2, 158-166, DOI: 10.1080/02508060408691765

Flanagan, L.B., Ehleringer, J.R. and Pataki, D.E. (Eds.) (2005). Stable isotopes and biosphere-atmosphere interactions, Elsevier Academic Press, San Diego, US, 318.

Fontes, J.ch. and Garnier, J.M. (1979). Determination of the initial ^{14}C activity of the total dissolved carbon: a review of the existing models and new approach. *Water Resources Research,* 15, 399-413

Fontes, J.C. (1980). Environmental isotopes in groundwater hydrology. In: P.Fritz and J.C Fontes (Eds.) Handbook of environmental isotope geochemistry, 1. The terrestrial environment (pp. 75-134). Amsterdam; Elsevier

Fontes, J.C. (1992). Chemical and isotopic constraints on ^{14}C dating of groundwater. In: Taylor RE, Long A, Kra RS, editors. Radiocarbon dating after four decades: an interdisciplinary perspective. New York: SpringerVerlag. p 242–261.

Fournier, R.O. (1979): A revised equation for the Na/K geothermometer. Geothermal Resources Council Transactions. Volume 3, 221-224.

Fritz, P. and Mozeto, A.A. (1981). Considerations on radiocarbon dating of groundwater. In; Interamerican Symposium on isotope Hydrology, Bogota. IAEA, Vienna, pp.221-224

Fry, B. (2006). Stable isotope ecology, Springer, New York, USA, 308

Gallagher, D., McGee, E.J., Kalin, R.M and Mitchell, P.I. (2000). Performance of models for radiocarbon dating of groundwater: An appraisal using selected irish aquifers, *Radiocarbon*, 42(2), 235-248, DOI10.2458/azu_js_rc.42.3841

Garg, V.K., Suthar, S., Sheoran, A., Garima, M and Jain, S. (2009). Drinking water quality of southwestern Haryana India: Assessing human health risks associated with hydrochemistry. *Environmental Geology*. Doi:10.1007/s00254-008-1636-y

Gartley, K. (2011). Recommended Soluble Salts Test., In the North Coordinating Committee for Soil Testing, Recommended Soil Testing Procedures for the Northeastern United States. Northeastern Regional Publication, 493, 3rd (edn).

Gat, J.R. and Gonfiantini, R. (1981). Stable isotope hydrology: Deuterium and Oxygen-18 in water cycle. International Atomic Energy Agency, Vienna, Austria

Gat, J.R. (1996). Oxygen and hydrogen isotopes in the hydrologic cycle. *Annu Rev Earth Planet Sci,* 24:225–262

Gat, J.R. (2010). Isotope hydrology: a study of the water cycle. Series on environmental science and management, Imperial College Press, London, 6.

Gemici, U., Tarcan, G., Mumtaz, C. and Helvaci, C. (2004). Hydrogeochemical and hydrogeolocial investigations of thermal waters in the Emet area (Kutahya, Turkey). *Applied Geochemistry*, 19: 105-117.

Geo-Heat Center (2005). What is Geothermal? Oregon Institute of Technology, Klamath Falls, (http://geoheat.oit.edu/whatgeo.htm) accessed November 10, 2014.

George, M. (2003). Selenium and Tellurium. Minerals yearbook, Bureau of Mines, U.S., U.S Government printing office, Washington D.C.

Gibbs, R.J. (1970). Mechanisms controlling world water chemistry. *Science*, 170:1088-1090

Giggenbach, W.F. (1988). Geothermal solute equilibria. *Geochimica. Cosmochim. Acta,* 52, 2749 - 2765.

Giggenbach, W.F. (1991). Chemical techniques in geothermal exploration; Application of Geochemistry in Geothermal Reservoir Development (D'Amore F., Ed.), UNITAR/UNDP Center on Small Energy Resources, Rome, 119-144.

Giggenbach, W.F. (1992). Isotopic shifts in waters from geothermal and volcanic systems along convergent plate boundaries and their origin. *Earth Planet. Sci. Lett*. 113, 495–510.

Glover, E.T., Akiti, T.T. and Osae, S. (2012). Major ion chemistry and identification of hydrogeochemical processes of groundwater in Accra Plains, *Elixir Geoscience*, 50:10279-10288

Godwin, H. (1962). Half-life of radiocarbon, *Nature,* 195, 984.

Goldsmith, G.R., Munoz-Villers, L.E., Holwerda, F., McDonnell J.J., Asbjornsen, H. and Dawson T.E. (2011). Stable isotopes reveal linkages among ecohydrological processes in a seasonally dry topical montane cloud forewst. *Ecohydrology, DOI: 10.1002/eco.268*

Gonfiantini, R. (1988). Carbon isorope exchange in Karst groundwater. In: 21st Congress on Karst Hydrology and karst Environment Protecction, Vol. XXI. Part 2, pp.832-837.

Gonfiantini, R. (1998). On the Isotopic Composition of Precipitation. Hydrologie et Geochimie Isotopique In: Causse, C., Gasse, F. (Eds) 1998. Proc. Int. Symposium in memory of J.-Ch.Fontes, Paris, June 1995,ORSTOM, Paris.pp.3-22

Gonfiantini, R., Frohlich, K., Araguás-Araguás, L. and Rozanski, K. (1998). Isotopes in groundwater hydrology. In: Kendal, C and McDonnell, J. (eds), Isotope Tracers in Catchments Hydrology. Elsevier, Amsterdam. 203-246.

Gonfiantini, R., Roche, M.A., Olivry, J.C., Fontes, J.Ch., Zuppi, G.M. (2001). The altitude effect on the isotopic composition of tropical rains. *Chem Geol*, 181:147–167

Government of South Africa. Regulation Gazette: No. 8454, Vol 490, No. 28755; Government of South Africa: Pretoria, South Africa, 2006.

Gray, N.F. (2008). Drinking water quality (2nd edn). Cambridge University press, New York, pp. 191-200, ISBN- 978-0-521-87825-8.

Griffiths, H. (Ed.) (1998). Stable Isotopes – integration of biochemical, ecological and geochemical processes, BIOS Scientific Publishers Ltd, Oxford.

Grossman, E.L., Coffman, B.K., Fritz, J.S. and Wada, H. (1989). Bacterial production of methane and its influence on groundwater chemistry – east central Texas aquifers. *Geology,* 17, 495-499.

Gupta, S.K and Deshpande, R.D. (2003). Synoptic hydrology of India from the data of isotopes in precipitation. *Curr Sci*., 85:1591–1595.

Gurdak, J.J., Hanson, R.T., McMahon, P.B., Bruce, B.W., McCray, J.E., Thyne, G.D. and Reedy, R.C. (2007). Climate variability controls on unsaturated water and chemical movement, High Plans Aquifer, USA. Vadose Zone J 6:533–547

Gustafson, L., Showers, W. and Kwak, T., Levine, J. and Stoskopf, M. (2007). Temporal and spatial variability in stable isotope compositions of freshwater mussel: Implications for biomonitoring and ecological studies, *Oecologia*, 152, 140-150

Harris, C., Oom, B.M., Diamond, R.E. (1999). Preliminary investigation of the urban isotope hydrology of the Cape Town area: *Water SA*, 25, 15-24.

Hartnady, C.J.H. and Jones, M.Q.W (2007). Geothermal Studies of the Table Mountain Group Aquifer Systems, Water Research Commission, Report No. 1403/1/07.

Harvey, D. (2000). Modern analytical chemistry. International edition. Mc Graw-Hill company. ISBN: 0-07-116953-9

Hayashi, H. (2008). The scientific benefits of drinking alkaline ionised water, Alkaline Water Health, (http://www.AlkalineWaterHeath.com) accessed February 18, 2014.

Hobson, K.A. (1999). Tracing origins and migration of wildlife using stable isotopes- A review, *Oecologia*, 120, 314-326

Hodder, A.P.W. (2005). Geothermal waters: a source of energy and metals, Department of Earth Sciences, University of Waikato) XIII-Water-AGeothermal-10, (http://nzic.org.nz/ChemProcesses/water/13A.pdf) accessed in 12/12/2014.

Hoole, R.J. (2001). The Development of Lilani Hot Springs: An Analysis of socio-economic and environmental impacts, Dissertation submitted in fulfilment of the

degree of Master of Science in the Department of Geography, University of Natal: Pietermaritzburg.

Hu, Z.M., Wen, X.F., Sun, X.M., Li, L.H., Yu, G.R., Lee, X.H. and Li, S.G. (2014). Partitioning of evapotranspiration through oxygen isopotic measurement of water pools and fluxes in temperate grassland, *J. Geophys. Res. Biogeo*., 119, 358-371.

Hu, B., Zhao, R., Chen, S., Zhou, Y., Jin, B., Li, Y. and Shi, Z. (2018). Heavy metal pollution delineation based on uncertainty in a coastal industrial city in the Yangtze River Delta, China. *Int. J. Environ. Res. Public Health*, 15, 710

Huang, L and Zhang, Z. (2015). Stable Isotopic Analysis on Water Utilization of Two Xerophytic Shrubs in a Revegetated Desert Area: Tengger Desert, China, *Water*, 7, 1030-1045; doi:10.3390/w7031030

Ingerson, E. and Pearson, F.J. (1964). Estimation of age and rate of motion of groundwater by the 14C-method, in Recent Researches in the Fields of Atmosphere, Hydrosphere, and Nuclear Geochemistry, Sugawara Festival Volume: Maruzen Co. Tokyo, p 263-283.

Ingraham, N.L. (1998). Isotopic variations in precipitation. In: Kendall C., McDonell J.J (eds). Isotope tracers in catchment hydrology. Elsevier, Amsterdam, 87–118.

International Atomic Energy Agency (IAEA) (1976). Procedure and Technique Critique for Tritium Enrichment by Electrolysis at the IAEA Laboratory Isotope Hydrology Laboratory, Technical Procedure Note No. 19

International Atomic Energy Agency (IAEA) (1977). Consultants' meeting on stable isotope standards and intercalibration in Hydrology and in Geochemistry, Internal report. IAEA, Vienna, 35

International Atomic Energy Agency (IAEA) (2001). Environmental Isotopes in the hydrological cycle. Principles and applications IHP-V Technical Documents in Hydrology, Nº 39. UNESCO

International Atomic Energy Agency (IAEA) (2011). Dating old groundwater: a guidebook. IAEA, Vienna.

International Atomic Energy Agency/ World Meteorological Organization (IAEA/WMO) (2015). Global network of isotopes in precipitation. The GNIP database Accessible at http://www.iaea.org/water

International Organization for Standardization (ISO) (1986). Water quality—determination of cobalt, nickel, copper, zinc, cadmium and lead—flame atomic absorption spectrometric methods. Geneva, 1986 (ISO 8288:1986).

Ishaku, J.M., Ahmed, A.S. and Abubakar, M.A. (2011). Assessment of groundwater quality using chemical indices and GIS mapping in Jada area, Northeastern Nigeria, *Journal of Earth Sciences and Geotechnical Engineering*, 1(1), 35-60.

Iqbal. J. and Shah, M.H. (2013). Health risk assessment of metals in surface water from freshwater source lakes Pakistan. *Hum Ecol Risk Assess Inter J*., 19(6):1530–1543.

Jacobs, I.A., Taddeo, J., Kelly, K. and Valenziano, C. (2002). Poisoning as a result of barium styphnate explosion. *American Journal of Industrial Medicine*, 41:285–288.

Jansen, H. (1975). The Soutpansberg trough (northern Transvaal) — an aulacogen. *Transactions of the Geological Society of South Africa*, 78, 129–36.

Jarup, L., Berglund, M., Elinder, C.G., Nordberg, G and Vahter, M. (1998). Health Effects of Cadmium Exposure--a Review of the Literature and a Risk Estimate. Scandinavian Journal of Work, Environment & Health, vol. 24(1), pp. 1-51.

Jashechko, S., Sharp, Z.D., Gibson, J.J., Birks, S.J., Yi, Y. and Fawcett, P.J. (2013). Terrestrial fluxes dominated by transpiration, *Nature*, 494, 347-350

Johnson, M.R., Anhaeusser, C.R. and Thomas, R.J. (2006). The geology of South Africa. Published jointly by the geological society of South Africa, Johannesburg and the council for geosciences, Pretoria, pp. 301 – 318.

Johnson, R. and Scherer, T. (2009). Drinking water quality: Testing and interpreting your results, North Dakota State University (NDSU), (http://www.ag.ndsu.edu) accessed November 10, 2014.

Joseph, A., Frangi, J.P. and Aranyossy, J.F. (1992). Isotope characteristics of meteoric water and groundwater in the Sahelo-Sudanese zone. *J Geophys Res*, 97, 7543–7551.

Kamtchueng, B.T., Fantong, W.Y., Wirmvem, M.J., Tiodjio, R.E., Takounjou, A.F., Asai, K. and Bopda Djomou, S.L. (2015). A multi-tracer approach for assessing the origin, apparent age and recharge mechanism of shallow groundwater in the Lake Nyos catchment, Northwest, Cameroon, *Journal of Hydrology*, 523, 790-803.

Karingithi, C.W and Wambugu, J. (2009). Geochemical survey case study of Arus and Bogoria geothermal prospects, presented at Short Course IV on Exploration for Geothermal Resources, organised by UNU-GTP, KenGen and GDC, at Lake Naivasha, Kenya, November 1-22, 2009.

Karingithi, C.W. (2014). Chemical geothermometers for geothermal exploration, Presented at Short Course IX on Exploration for Geothermal Resources, organized by UNU-GTP, GDC and KenGen, at Lake Bogoria and Lake Naivasha, Kenya, Nov. 2-23, 2014.

Kebede, S. (2013). Groundwater in Ethiopia, Springer Hydrogeology, DOI:10.1007/978-3-642-30391-3_5, Berlin Heidelberg, 187-203

Kebede, S. and Travi, Y. (2012). Origin of the $\delta^{18}O$ and $\delta^{2}H$ composition of meteoric waters in Ethiopia. *Quart Int*, 257:4–12

Kelly, W.P. (1946). Permissible composition and concentration of irrigation waters. Proc. ASC

Kempster, P.L., van Vliet, H.R. and Kuhn, A. (1997). The need for guidelines to bridge the gap between ideal drinking water quality and that quality which is practically achievable and acceptable, *Water SA*, 23(2); 163-167

Kendall, C. and McDonnell, J.J (Eds) (1998). Isotope Tracers in Catchment Hydrology in Fundamentals of Isotope geochemistry by Kendall, C. and Caldwell, E.A., Elsevier Science B.V., Amsterdam. pp. 51-86.

Kent, L. E. (1942). The Letaba hot spring. *The Transaction of the Royal Society of South Africa*, 29 (2), 35-47

Kent, L.E. (1948). The warm springs of Loubad, near Nylstroom, Transvaal. Trans. *Royal Soc. South Afr.* 31:151-168

Kent, L.E. (1949). Thermal waters of the Union of South Africa and South West Africa. *Trans. Geol. Soc. WS. Afr.*, 52, 231–264.

Kent, L.E. (1969). The Thermal Waters in the Republic of South Africa, International Geological Congress, Report of the Twenty-Third session, Czechoslovakia, Proceedings of Symposium II, Mineral and Thermal Waters of the world-Overseas countries, 19, 143-164.

Kortelainen, N. (2009). Isotopic composition of atmospheric precipitation and shallow groundwater in Olkiluoto: ^{18}O, ^{2}H and ^{3}H. Working report 2009-06, Posiva.

Kottek, M., Grieser, J., Beck, C., Rudolf, B. and Rubel, F. (2006). World Map of the Köppen-Geiger climate classification updated, *Meteorologische Zeitschrift*, 15(3), 259-263

Koziet J. (1997) Isotope ratio mass spectrometric method for the on-line determinartion of oxygen-18 inorganic matter. *J. Mass Spectrom*., 32: 103-108.

KrishnaKumar, S., Bharani, R., Magesh, N.S., Godson, P.S. and Chandrasekar, N. (2014). Hydrogeochemistry and groundwater quality appraisal of partof south Chennai coastal aquifers, Tamil Nadu, India using WQIand fuzzy logic method, *Appl Water Sci*., DOI 10.1007/s13201-013-0148-4.

Krull, E., Sachse, D., Mugler, I., Thiele, A and Gleixner, G. (2006). Compound-specific $\delta^{13}C$ and $\delta^{2}H$ analyses of plant and soil organic matter: A preliminary assessment of the effects of vegetation change on ecosystem hydrology. *Soil Biology & Biochemistry,* 38, 3211–3221

Kuitcha, D., Takounjou, A.L.F., Ndjama, J., Eneke, G.T., Awah, M.T., Beyala, K.K. and Ekodeck, G.E. (2012). Chemical and isotopic signal of precipitation in Yaounde-Cameroon. *Arch Appl Sci Res*, 4:2591–2597

Kyser, K.T. (1986). Stable isotope variations in the mantle, in Stable Isotopes in High Temperature Geologic Processes, edited by J. W. Valley, B. E. Taylor and J. R. O'Neil, p. 141-164, Mineral. Soc. Am., Washington.

Labasque, T., Aquilina, L., Vergnaud, V., Hochreutener, R., Barbecot, F. and Casile, G. (2014). Intercomparison exercises on dissolved gases for groundwater dating - (1) Goals of the exercise and site choice, validation of the sampling strategy. *Appl. Geochemistry*, 40, 119-125

La Moreaux, P.E and Tanner, J.T. (2001). Springs and Bottled Waters of the World, Ancient History, Source, Occurrence, Quality and Use, Springer: Berlin.

Lajtha, K. and Michener, R.H. (1994). Stable Isotopes in Ecology and Environmental Science. Blackwell Scientific Publications, Oxford.

Lakshmanan, E., Kannan, R. and Senthil Kumar, M. (2003). Major ion chemistry and identification of hydrogeochemical processes of ground water in a part of Kancheepuram district, Tamil Nadu, India. *Journal of Environmental Geosciences*, v. 10: no. 4, p. 157-166.

Lawal, A.O., Batagarawa, S.M., Oyeyinka, O.D. and Lawal, M.O (2011). Estimation of Heavy Metals in Neem Tree Leaves along Katsina – Dutsinma – Funtua, Highway in Katsina State of Nigeria, *J. Appl. Sci. Environmental Management*.,15 (2), 327 – 330.

Lenntech (1998-2009). Selenium (Se) chemical properties, health and environmental effects, (http://www.lenntech.com/periodic/elements/se.htm) accessed May 25, 2014.

Lemay, G.T. (2002). Carbon-14 Dating of Groundwater from Selected Wells in Quaternary and Quaternary–Tertiary Sediments, Athabasca Oil Sands (In Situ) Area, Alberta, Alberta Geological Survey, EUB /AGS Geo-Note 2002-03 (December 2002).

Li, J.Z., Wang, G.A. and Liu, X.Z. (2009). Variations in carbon isotope ratios of C3 plants and distribution of C4 plants along an altitudinal transect on the eastern slope of Mount Gongga. *Sci China Ser D,* 52: 1714–1723.

Li, S.Y. and Zhang, Q.F. (2010) Spatial characterization of dissolved trace elements and heavy metals in the upper Han River (China) using multivariate statistical techniques. *J Hazard Mater*, 176(1–3):579

Lipfert, G., Reeve, A.S. Sidle, W. and Marvinney, R. (2004). Geochemical patterns in an arsenic – tainted, fracture – bedrock groundwater system in Northport, Maine USA, *Applied Geochemistry* (In review).

Liu, W., Liu, W., Li, P., Duan, W. and Li, H. (2010). Dry season water uptake by two dominant canopy tree species in a tropical seasonal rainforest of Xishuangbanna, SW China. *Agricultural and Forest Meteorology*, 150: 380–388.

Liu, X., Song, X., Zhang, Y., Xia, J., Zhang, X., Yu, J., Long, D., Li, F. and Zhang, B. (2010). Spatio-temporal variations of d2H and d18O in precipitation and shallow groundwater in the Hilly Loess Region of the Loess Plateau, China, *Environ Earth Sci*, DOI 10.1007/s12665-010-0785-y

Liu, J., Xiao, C., Ding, M. and Ren, J. (2014). Variations in stable hydrogen and oxygen isotopes in atmospheric water vapor in the marine boundary layer across a wide latitude range. *J Environ Sci*, 26:2266–2276

Liu, F., Song, X., Yang, L., Zhang, Y., Han, D., Ma, Y. and Bu, H. (2015). Identifying the origin and geochemical evolution of groundwater using hydrochemistry and stable isotopes in the Subei Lake basin, Ordos energy base, Northwestern China, *Hydrol. Earth Syst. Sci*., 19, 551–565, doi:10.5194/hess-19-551-2015

Locsey, K.L. and Cox, M.E. (2003). Statistical and hydrochemical methods to compare basalt and basement rockhosted ground waters: Atherton Tablelands, northeastern Australia. *Environ. Geol*., 43, 698-713.

Low, A.B. and Rebelo, A.G. (eds) (1996). Vegetation of South Africa, Lesotho and Swaziland. Department of Environmental Affairs and Tourism, Pretoria, South Africa

Lund, J.W. (2000). Balneological use of thermal water in the USA, GHC Bulletin, September, pp. 31-34.

Lund, J.W. and Freeston, D.H. (2001). World-wide direct uses of geothermal energy 2000. *Geothermics*, 30, 29-68.

Macko, S.A. and Ostrom, N.E. (1994). Pollution studies using stable isotopes. In: Lajtha K, Michener RH (eds) Stable isotopes in ecology and environmental science. Blackwell, Oxford, 45-62

Madl, A.K., Brown, J.L., Kolanz, M.E. and Kent, M.S. (2007). Exposure-response analysis for beryllium sensitization and chronic beryllium disease among workers in a beryllium metal machining plant. *Journal of Occupational and Environmental Hygiene*, 4:448–466

Makungo, T.E. (2008). The adequacy of water supply to meet the demand in Siloam Village of Limpopo Province of South Africa, Honours dissertation, Department of Hydrology Water Resources, University of Venda, South Africa. pp 92.

Makungo, R., Odiyo, J.O., Ndiritu, J.G. and Mwaka, B. (2010). Rainfall–runoff modelling approach for ungauged catchments: A case study of Nzhelele River sub-quaternary catchment.

Mamba, B.B., Rietveld, I.C. and Verbeck J.I.Q.C. (2008). SA drinking water standards under the microscope. *The Water Wheel,* 7 (1), 24-27.

Manda, L. and Suzuki, K.T. (2002). Arsenic round the world: a review. *Talanta*, vol. 58 (1); 201-235.

Martin-Gomez, P., Barbeta, A., Voltas, J., Penuelas, J., Dennis, K., Palacio, S., Dawson, T.E. and Ferrio, J.P. (2015). Isotope-ratio infrared spectroscopy: a reliable tool for the investigation of plant-water source? *New phytologist*, doi.10.1111/nph.13376

Mazor, E. and Verhagen, B.Th. (1983). Dissolved ions, stable and radioactive isotopes and noble gases in thermal waters of South Africa. *J. of Hydrol.* 63, 315-329

Mbonu, M.and Travi, Y. (1994). Labelling of precipitation by stable isotopes (^{18}O, ^{2}H) over the Jos Plateau and the surrounding plains (north-central Nigeria). *J Afr Earth Sci*, 19:91–98.

Mekiso, F.M. (2011). Hydrological Processes, Chemical Variability, and Multiple Isotopes tracing of Water Flow Paths in the Kudumela Wetland-Limpopo Province, South Africa. Rhodes University, Grahamstown.

Mekiso, F.A., Snyman, J. and Ochieng, G.M. (2015). Recent findings in Tritium Isotopes in Small Catchment: A Case of the Middle Mohlapitsi Wetland, South Africa, *Int'l Journal of Control Theory and Applications*, 8(4), 1621-1630.

Merwe van der, N.J. and Medina, E. (1989). Photosynthesis and $^{13}C/^{12}C$ ratios in Amazonian rain forests. *Geochim Cosmochim Acta*, 53, 1091-1094

Merwe van der, N.J., Lee-Thorp, J.A., Thackeray, J.F., Hall-Martin, A., Kruger, F.J., Coetzees, H., Bell, R.H.V. and Lindeque, M. (1990). Source-area determination of elephant ivory by isotopic analysis. *Nature,* 346, 744-746.

Mook, W.G. (1980). Carbon-14 in Hydrogeological studies. In: Fritz, P. & Fontes, J. Ch. (eds), Handbook of Environmental Isotope Geochemistry, Vol. 1, The Terrestrial Environmental. pp 49-74. Elsevier, Amsterdam

Mook, W.G. (2006). Introduction to Isotope Hydrology: Stable and Radioactive isotopes of Hydrogen, Oxygen and Carbon: Taylor & Francis Group, London, Great Britain, 226 p.

Mook, W.G. and de Vries, J.J. (2001). Environmental Isotopes in the Hydrological cycle: Principles and Application, volume I: Introduction, Theory, Methods, Review (W.G. Mook, editor), UNESCO/IAEA, Vienna, Austria and Paris France, 280

Moore, R., Clark, W.D. and Vodopich, D.S. (2003). Botany. 2nd ed. Boston, Massachusetts: McGraw-Hill. p. 130-162.

Moran, J.E. (2007). Introduction to Groundwater Age Dating, in C. Kendall and J.E. Moran, Isotope Methods of Groundwater Investigation Course: Groundwater Resources Association of California, March 28, 2007, Hilton Hotel, Concord, CA.

Mucina, L. and Rutherford, M.C. (eds.) 2006. The Vegetation of South Africa, Lesotho and Swaziland. Strelitizia 19. South African National Biodiversity Institute, Pretoria, South Africa. (808 pp with CD GIS-database)

Muhammad, S.B. and Sadiq, U. (2014). Analysis of stable isotopic composition of precipitation in Katsina state in Nigeria as an indication of water cycle. *Advances in physics theories and applications*, 33, 28-34

Mundalamo H.R. (2003). Investigation of water quality in Nzhelele valley, Limpopo province, South Africa, honours mini-dissertation (Unpublished), University of Venda, Thohoyandou.

Nadeem A.B. and Jeelani, Gh. (2016). Quantification of Groundwater - Surface Water Interactions using Environmental Isotopes; A Case Study of Bringi Watershed, Kashmir Himalayas, India, *Journal of Earth System Science*, https://www.ias.ac.in/public/Volumes/jess/forthcoming/JESS-D-16-00594.pdf

Nagaraju, A., Sunil Kumar, K. and Thejaswi, A. (2014). Assessment of groundwater quality for irrigation: a case study from Bandalamottu lead mining area, Guntur District, Andhra Pradesh, South India, *Appl Water Sci*, 4: 385. https://doi.org/10.1007/s13201-014-0154-1

National Health and Medical Research Council (NHMRC) (2004). Australian Drinking Water Guidelines, (http://www.nhmrc.gov.au/publications/synopses/eh19sun.htm) accessed March 30, 2014.

Naveedullah, M.Z.H., Yu, C., Shen, H., Duan, D., Shen, C., Lou, L. and Chen, Y. (2014). Concentration and human health risk assessment of selected heavy metals in surface water of the siling reservoir watershed in Zhejiang Province, China. *Pol J Environ Stud*, 23(3):801–811.

New Hampshire Department of Environmental Services (2007). Beryllium in drinking water, Environmental Fact Sheet, New Hampshire, (www.des.nh.gov) accessed January 21, 2014.

New Mexico Environment Department, (2002). Use Attainability of Sulphur Creek Sandoval County, New Mexico. Surface Water Quality Bureau, 15 April 2002.

Nguyen, K. (2007). Answers to a nation's prayers. City Press. Accessed 7 October 2017.

NIOSH (2003). Method 7303: Elements by ICP (Hot Block/HCl/HNO3 Ashing), NIOSH Manual of Analytical Methods, Fourth Edition, Issue 1, March 15, 2003, pp. 1-6.

Njitchoua, R., Sigha-Nkamdjou, L., Dever, L. (1999). Variations of the stable isotopic compositions of rainfall events from the Cameroon rain forest, Central Africa. *J Hydrol*, 223:17–26.

Nordberg, G.F., Goyer, R.A. and Clarkson, T.W. (1985). Impact of effects of acid precipitation on toxicity of metals. Environmental Health Perspectives, vol. 68, pp. 169–180.

Ntsoane, O. (2001). A typology of indigenous cultural heritage sites as educational material. A paper presented to the South African Heritage Resource agency and Local Government seminar held in Grahamstown, 15 February 2002.

O'Leary, M.H. (1993). Biochemical basis of carbon isotope fractionation. In: Ehleringer, J.R., Hall, A.E., Farquhar, G.D. (Eds.), Stable Isotopes and Plant Carbon –Water Relations. Academic Press, pp. 19 – 28

Ochieng, E.Z., Lalah, J.O. and Wandiga, S.O. (2007). Analysis of heavy metals in water and surface sediment in five Rift Valley Lakes in Kenya for assessment of recent increase in anthropogenic activities, *Bull Environ Contam Toxicol*., 79,570-576

Odiyo, J.O. and Makungo, R. (2012). Fluoride concentrations in groundwater and impact on human health in Siolam Village, Limpopo Province, South Africa. *Water SA*, 38, 731–736.

Odiyo, J.O. and Makungo, R. (2018). Chemical and Microbial Quality of Groundwater in Siloam Village, Implications to Human Health and Sources of Contamination. *Int J Environ Res Public Health,* 15(2): 317, doi:10.3390/ijerph15020317

Ohmoto, H. and Rye, R.O. (1979). Isotopes of Sulfur and Carbon, in Geochemistry of Hydrothermal Ore Deposits, edited by H. Barnes, pp., John Wiley and Sons, New York.

Ojekunle, Z.O., Ubani, D.R and Sangowusi, R.O. (2014). Effectiveness of Neem, Cashew and Mango trees in uptake of heavy metals in mechanic village, *Merits Res. Journ. Envin. Sci. and Tox*., 2(8), 185 – 190.

Olivier, J., Van Niekerk, H.J. and Van Der Walt, I.J. (2008). Physical and chemical characteristics of thermal springs in the Waterberg area of Limpopo Province, South Africa. *Water SA,* 34 (2), 163-174.

Olivier, J., Venter, J.S. and Jonker, C.Z. (2011). Thermal and Chemical Characteristics of Thermal Springs in the Northern Part of the Limpopo Province, South Africa. *Water SA*, 34, 163–174.

Olivier, J., Venter, J.S. and Van Niekerk., H.J. (2010). Physical and Chemical Characteristics of Thermal Springs in Limpopo Province, South Africa, proceedings of World Geothermal Congress 2010, Bali, Indonesia, pp. 13.

Onder, S. and Dursun, S. (2006). Air borne heavy metal pollution of Cedrus libani (A. Rich.) in city center of Konya (Turkey). *Atmospher. Environ*., 40 (6), 1122- 1133.

Otieno, D., Schmidt, M.U.I., Adiku, S.T.K. and Tenhunen, J.D. (2005). Physiological and morphological responses to water stress in two acacia species from contrasting habitats, *Tree Physiology*, 25, 361-371.

Pair, C.H. (1983). Irrigation. The Irrigation Assoc., Arlington, VA. 680pp

Pais, I. and Jones, J.B. (1997). The handbook of trace elements. St. Lucie Press, Boca Raton, FL.

Pang, Z., Shivanna, K., Abidin, Z., Tafif, A., Young, K.G., Koh, Y., Suratman, S., Javino, F., Hussin, U.D., Choudhry, M.A., Hafeez, M.A., Ogena, M., Salonga, N.D., A snachinda, P. and Praserdvigai, S. (2006). Isotope composition of geothermal waters in East Asia and the Pacific Region: hydrological and geothermal energy implications, Proceedings of the 7th Asian Geothermal Symposium, July 25-26.

Pankurst, R. (1990). The use of thermal baths in treatment of skin diseases in old time Ethiopia. *International Journal of Dermatology*, 29(6), 451-456.

Pearson, F.J. and white, D.E. (1967). ^{14}C ages and flow rates of water in Carrizo Sand, Atascosa Country, TX, *Water Resources Research*, 3, 251-261

Pearson, Jr. and Hanshaw, F.J., (1970). Sources of dissolved carbonate species in groundwater and their effect on C-14 dating. In: Isotope Hydrology 1970, Proc. Symp. IAEA, Vienna, pp 271-286.

Pearson, F.J.Jr. and Rightmire, C.T. (1980). Sulphur and oxygen isotopes in aqueous sulphur compounds, In: Fritz, P. and Fontes, LL-Ch., Handbook of Environmental Isotope Geochemistry, Vol.1. Elsevier Scientific Publishing Company, Amsterdam-Oxford-New

Perkin M.R., Craven, J., Logan, K., Strachan, D., Marrs, T., Radulovic, S., Campbell, L.E., MacCallum, S.F., McLean, W.H.I., Lack, G., Flohr, C. (2016). The association between Domestic Water Hardness, Chlorine and Atopic Dermatitis Risk in Early Life: A Population-Based Cross-Sectional Study. *Journal of Allergy and Clinical Immunology*, DOI: 10.1016/j.jaci.2016.03.031

Piper, A.M. (1944). A graphic procedure in geochemical interpretation of water analyses. *Trans Am Geophys Union*, 25, 914–923.

Pleysier, L.J. (1995). Soil sampling and sample preparation. IITA Research Guide

Plummer, L.N., Prestemon, E.C. and Parkhurst, D.L. (1994) An interactive code (NETPATH) for modelling NET Geochemical reactions along a flow Path Version 2.0 U.S. Geological Survey Water-Resources Investigations Report 94-4169, 132

Plummer, L.N. and Sprinkle, C.L. (2001). Radiocarbon dating of dissolved inorganic carbon in groundwater from confined parts of the Upper Floridan aquifer, Florida, USA. *Hydrogeology Journal*, 9(2):127–50.

Plummer, L.N., L.M. Bexfield, S.K. Anderholm, W.E. Sanford, and E. Busenberg. (2004). Geochemical characterisation of ground-water flow in the Santa Fe Group aquifer system, Middle Rio Grande Basin, New Mexico. Water-Resources Investigations Report 03-4131. Reston, Virginia: U.S. Geological Survey, 395. http://pubs.usgs.gov/wri/wri034131/.

Popovski, K and Vasilevska, S.P. (2003). What about further development of geothermal energy use in agriculture? Problems and possibilities, European Geothermal Conference 2003, Session: Agricultural direct use,

Press, F. and Siever, R. (1986). Earth, 4th ed., W.H. Freeman and Company: New York.

Pyle, S.M., Nocerino, J.M., Deming, S.N., Palasota, J.A., Palasota, J.M., Miller, E.L., Hillman, D. C., Kuharic, C.A., Cole, W.H., Fitzpatrick, P.M., Watson, M.A. and Nichols, K.D. (1996). Comparison of AAS, ICP-AES, PSA, and XRF in determining Lead and Cadmium in Soil. *Environmental Science and Technology*, 30, 204-213

Qin, D., Turner, J.V. and Pang, Z. (2005). Hydrogeochemistry and groundwater circulation in the Xi'an geothermal field, China, *Geothermics*, 34, 471–494.

Radulescu, C., Dulama, I.D., Stihi, C., Ionita, I., Chilian, A., Necula, C. and Chelarescu, E.D. (2014). Determination of heavy metal levels in water and Therapeutic mud by Atomic Absorption Spectrometry, *Rom. Journ. Phys*., 59 (9–10), 1057–1066.

Rai, S.P., Purushothaman, P., Kumar, B., Jacob, N. and Rawat, Y.S. (2013). Stable isotopic composition of precipitation in the River Bhagirathi Basin and identification of source vapour. *Environ Earth Sci*, 71:4835–4847

Ranjit, M. (1994). Geochemical studies of some thermal springs in Nepal, geothermal training programme, Orkustofnun, Grensasvegur, 9, 15-108, Report 11, Reykjavik, Iceland.

Raven, P.H., Evert, R.F and Curtis, H. (1981). Biology of Plants. Worth Publishers, New York, pp. 106 – 112

Ravikumar, P. and Somashekar, R.K. (2011). Environmental Tritium (^{3}H) and hydrochemical investigations to evaluate groundwater in Varahi and Markandeya river basins, Karnataka, India, Journal of Environmental Radioactivity, 102, 153-162, doi:10.1016/j.jenvrad.2010.11.006

Ravikumar, P., Mohammad, A.M and Somashekar, R.K. (2015). Interpretation of Groundwater Quality and Radon Estimation in the Selected Region of Bangalore North Taluk, Karnataka, India, Research & Reviews: *Journal of Ecology and Environmental Sciences*, 3:2, 73-81

Richards, L.A. (1954). Diagnosis and improvement of saline and alkali soils. Washington: US Department of Agriculture

Rindl, M. (1936). The Medicinal Springs of South Africa, South African Railways and Harbours: Pretoria.

Risi, C., Bony, S., Vimeux, F., Descroix, L., Ibrahim, B., Lebreton, E., Mamadou, I. and Sultan, B. (2008). What controls the isotopic composition of the African monsoon precipitation? Insights from event-based precipitation collected during the 2006 AMMA field campaign. *Geophys Res Lett*, 35: L24808

Robinson, M.S., Anthony, T.R., Littau, S.R., Herckes, P., Nelson, X., Poplin, G.S. and Burgess, J.L. (2008). Occupational PAH exposures during prescribed pile burns. *Ann. Occ. Hyg*., 52(6), 497–50.

Romero, L., Alomso, H., Campano, P., Fanfani, L., Cidu, R., Dadea, C., Keegan, T., Thornton, I. and Farago, M. (2003). Arsenic enrichment in waters and sediments of the Rio Loa (Second Region, Chile). *Appl. Geochem*., 18 (9):1399-1416.

Rothfuss, Y., Biron, P., Braud, I., Canale, L., Durand, J.L., Gaudet, J.P., Richard, P., Vauclin, M., and Bariac, T. (2010). Partitioning evapotranspiration fluxes into soil evaporation and plant transpiration using water stable isotopes under controlled conditions, *Hydrol. Process*., 24, 3177–3194.

Rozanski, K., Ara Aragua´s-Aragua´s, L. and Gonfiantini, R. (1993). Isotope patterns in modern global precipitation. In: Swart PK, Lohmann.

Russell, J. M., and T. C. Johnson (2006), The water balance and stable isotope hydrology of Lake Edward, Uganda-Congo, *J. Great Lakes Res*., 32, 77– 90,

Ruwimbo, M. (2017). The development and use of stable isotope analysis of felids' whiskers as a tool to study their feeding ecology. Masters dissertation, Cape Peninsula University of Technology, South Africa.

Sachse D., Billault I., Bowen G.J., Chikaraishi Y., Dawson T.E., Feakins S.J., Freeman K.H., Magill C.R., McInerney F.A., van der Meer B.T.J., Polissar P., Robins R.J., Sachs J.P., Schmidt H.L., Sessions A.L., White J.W.C., West J.B. and Kahmen A. (2012). Molecular paleohydrology: interpreting the hydrogen-isotopic composition of lipid, biomarkers from photosynthesizing organisms. *Annual Review of Earth and Planetary Sciences,* 40, 221-249.

Saeze, H. and Rikhotso, C. (2013). Hydrogeochemistry of thermal spring of Limpopo Province assessed by water chemistry and environmental isotopes in hydrology. Unpublished.

Salati, E., Dallolio, A., Matsui, E. and Gat, J.R. (1979). Recycling of water in the Amazon Basin: an isotopic study. *Water Resour Res*, 15:1250–1258

Sanchez-Murillo, R., Esquivel-Hernandez, G. and Welsh, K. (2013). Spatial and temporal variation of stable isotopes in precipitation across Costa Rica: an analysis of historic GNIP records. *Open J Mod Hydrol*, 3:226–240.

Sarolkar, P.B. (2005). Geochemical Characters of Hot Springs of West Coast, Maharashtra State, India, Proceedings World Geothermal Congress 2005, Antalya, Turkey, 24-29 April 2005.

Saunders, M, Lewis, P. and Thornhill, A. (2012). Research methods for business students. Sixth edition. Pearson Education Limited, England. ISBN: 978-0-273-75075-8

Schaffner, F.C. and Swart, P.K. (1991). Influence of diet and environmental water on the carbon and oxygen isotopic signatures of seabird eggshell carbonate. *Bull Mar Sci* 48, 23-38

Schmidt, M.W and Gleixner G. (2005). Carbon and nitrogen isotope composition of bulk soils, particle-size fractions and organic material after treatment with hydrofluoric acid, *European Journal of Soil Science*, 56, 407–416

Schoeller, H. (1977). Geochemistry of groundwater, In: Groundwater Studies – An international Guide for Research and Practice, UNESCO, Paris, 1-18.

Scholl, M.A., Gingerich, S.B. and Tribble, G.W. (2002). The influence of microclimate and fog on stable isotope signature used in interpretation of regional hydrology, East Maui, *Hawaii journal of hydrology*, 264, 170-184.

Scholl, M., Eugster, W. and Burkard, R. (2011). Understanding the role of fog in forest hydrology: stable isotopes as tool for determining input and partitioning of cloud water in montane forests. *Hydrol. Process*., 25, 353-366.

Scott, L. and Vogel, J.C., (2000). Evidence for environmental conditions during the last 20,000 years in southern Africa from ^{13}C in fossil hyrax dung. *Global and Planetary Change* 26, 207–215.

Scott-Samuel A. (1998). Health impact assessment — theory into practice. *J Epidemiol Community Health*, 52:704–5.

Scott-Samuel A. (2005). Health impact assessment: an international perspective. N S W *Public Health Bull*, 16:110–3.

Seki, O., Nakatsuka, T., Shibata, H. and Kawamura, K. (2010). A compound-specific n-alkane $\delta^{13}C$ and $\delta^{2}H$ approach for assessing source and delivery processes of terrestrial organic matter within a forested watershed in northern Japan. *Geochimica et Cosmochimica Acta,* 74, 599–613

Shan, M.H., Iqbal, J., Shaheen, N., Khan, N., Choudhary, M.A. and Akhter, G. (2012) Assessment of background levels of trace metals in water and soil from a remote region of Himalaya. *Environ Monit Assess*, 184(3):1243–1252

Sheppard, S.M.F. (1986) Characterization and isotopic variations in natural waters. Pp. 165-183 in: Stable Isotopes in High Temperature Geological Processes (J.W. Valley, H.P. Taylor Jr. and J.R. O'Neil, editors). Reviews in Mineralogy Vol. 16, Mineralogical Society of America, Washington, D.C.

Siegel, F.R. (2002). Environmental Geochemistry of Potentially Toxic Metals, Springer-Verlag, Berlin, 218.

Skapare, I. (2001). Commercially profitable utilisation of geothermal water in the Riga/Jurmala region of Latvia for recreation and health. Pre-Feasibility study for an outdoor thermal swimming pool. Geothermal training programme, UNU, Reykjavik, 32 p.

Skapare, I., Kreslins, A. and Gjunsburgs, B. (2003). Balneological properties of the geothermal water in Latvia, Proceedings of the European Geothermal Conference, Hungary,(http://www.geothermie.de/egec-geothernet/proceedings/szeged/o-6-03) accessed May 7, 2014.

Skapare, I., Kreslins, A. and Gjunsburgs, B. (2005). Balneological properties of the geothermal water in Latvia, Institute of Heat, Gas and Water Technology. Riga Technical University

Smith, G.T., Goldman, M.S., Greenbaum, P.E. and Christiansen, B.A. (1995). Expectancy for social facilitation for drinking: the divergent paths of high expectancy and low expectancy adolescents. J. Abnorm. Psycho., vol. 104 (1), pp. 32-42.

Spalding, R.F. and Exner, M. E. (1993) Occurrence of nitrate in groundwater—a review: Journal of Environmental Quality, v. 22, p. 392–402.

South African Bureau of Standards (SABS) (1999). Class 1 Potable Water Standards. SABS 241:1999. South African Bureau of Standards Pretoria, South Africa.

South African National Standards (SANS) (2015). Drinking water, Part 2: Application of SANS 241-1, published by South African Bureau of Standards Pretoria, South Africa.

Spicer, S. and Nepgen, J. (2005). Holistic holidays in South Africa-health spas, hot springs, magical places and sacred spaces. Cape Town, Human & Rousseau.

SR ISO 11466 – (1999). Soil quality - Extraction of trace elements soluble in aqua regia. International Organization for Standardization, Geneva, Switzerland.

Staddon, P.L. (2004). Carbon isotopes in functional soil ecology- A review, *TRENDS in Ecology and Evolution*, 19, 3

Sternberg, L.S.L. (1989). Oxygen and hydrogen isotope ratios in plant cellulose: mechanisms and applications. In Stable Isotopes in Ecological Research. (eds. P. W. Rundel, J. R. Ehleringer and K. A. Nagy), Springer, New York, pp. 124–141.

Subtavewung, P., Raksaskulwong, M. and Tulyatid, J. (2005). The Characteristic and Classification of Hot Springs in Thailand. Proceedings World Geothermal Congress 2005, Antalya, Turkey, 24-29 April 2005

Sundararajan, S., Khadanga, M.K., Kumar, P.J., Raghumaran, S., Vijaya, R. and Jena, B.K. (2016). Ecological risk assessment of trace metal accumulation in sediments of Veraval Harbor, Gujarat, Arabian Sea, *Marine pollution bulletin*, 114(1), 592-601.

Talma, A.S., Vogel, J.C. and Stiller, M. (1997). The radiocarbon content of the Dead Sea. In TM. Niemi, Z. Ben-Avraham & J.R Gat (eds), The Dead Sea: the lake and its settings. Oxford: Oxford University Press.

Tamers, M.A. (1967). Surface-water infiltration and groundwater movement in arid zones of Venezuela. Isotopes in hydrology. Vienna: IAEA. p 339–51.

Tamers, M.A. (1975). Validity of radiocarbon dates on groundwater: *Geophysical surveys*, 2, 217-239

Tao, S. (1995). The formation of geothermal water near Xi'an. *Hydrogeol. Eng. Geol*. 5, 6–11.

Tarcan, G. and Gemici, Ü. (2003). Water geochemistry of the Seferihisar geothermal area, Izmir, Turkey. *Journal of Volcanology and Geothermal Research*. 126, 225-242.

Taupin, J.D., Coudrain-Ribstein, A., Gallaire, R., Zuppi, G.M., Filly, A. (2000). Rainfall characteristics (d18O, d2H, DT and DHr) in western Africa: regional scale and influence of irrigated areas. *J Geophys Res*, 105:11911–11924

Tekere, M., Adele, L., Olivier, J., Jonker, N., and Venter, F. (2012). Metagenomic analysis of bacterial diversity of Siloam hot water spring, Limpopo, South Africa. *Afri. J. Biotechnol*., 10, 18005-18012.

Tieszen, L.L and Archer, S. (1990). Isotopic assessment of vegetation changes in grassland and woodland systems. In: Osmond, C.B., Pitelka, L.F., Hidy, G.M. (Eds.), Plant Biology of the Basin and Range. Springer-Verlag, New York, pp. 293 – 321.

Todd, D.K. (1980). Groundwater Hydrology, 2nd edition. xiii + 535 pp., numerous figs and tables. New York, Chichester, Brisbane, Toronto: John Wiley. ISBN 0 471 87616X

Truesdell, A.H. and Hulston, J.R. (1980). Isotopic evidence of environments of geothermal systems, In: Fritz, P and Fontes, J.Ch (eds), Handbook of Environmental Isotope Geochemistry, Vol. 1, The Terrestrial Environment., A. Elsevier, Amsterdam, The Netherlands: 179-226

Tshibalo, A.E. (2011). Strategy for the sustainable development of thermal springs: A case study for Sagole in Limpopo province. Unpublished PhD. Thesis, University of South Africa.

U.S. Environmental Protection Agency (1989). Risk Assessment Guidance for Superfund Volume 1: Human Health Evaluation Manual (Part A); Office of Emergency and Remedial Response: Washington, DC, USA.

U.S. Environmental Protection Agency (1991). Human Health Evaluation Manual, Supplemental Guidance: Standard Default Exposure Factors; USEPA: Washington, DC, USA.

U.S. Environmental Protection Agency (1992a). Guidelines for Exposure Assessment, EPA/600/Z-92/001, Risk Assessment Forum, Washington, DC

U.S. Environmental Protection Agency (1992b). Ground water issue: behavior of metals in soils. Office of Solid Waste and Emergency Response, Washington, DC; EPA 540-S-92-018.

U.S. Environmental Protection Agency, (1993). Clean Water Act. Standards for the use and disposal of sewage sludge. Code of Federal Regulations (CFR) Part 503, vol. 58, No. 32. U.S. Environmental Protection Agency, Washington, DC

U.S. Environmental Protection Agency (2001). Risk assessment guidance for superfund: Volume III – Part A, Process for conducting probabilistic risk assessment. Washington, DC.: US Environmental Protection Agency, Report EPA 540-R-02-002.

U.S. Environmental Protection Agency (2002). Child-specific exposure factors handbook. Washington, DC.: US Environmental Protection Agency, Report EPA-600-P-00-002B.

U.S. Environmental Protection Agency (2004a). Risk assessment guidance for superfund, Volume I: Human health evaluation manual (Part E, Supplemental guidance for dermal risk assessment). Washington, DC.: Office of Superfund Remediation and Technology Innovation, US Environmental Protection Agency, Report EPA/540/R/99/005.

U.S. Environmental Protection Agency (EPA) (2004b). Guideline for Water Reuse. EPA, Washington DC, EPA/625/R-04/108.

U.S. Environmental Protection Agency (2008). Child-specific exposure factors handbook. Washington, DC.: USA

U.S. Environmental Protection Agency (2009) Drinking water standards and health advisories, EPA 822-R-09–011. Office of water, Washington, DC, USA

Van Eeden, O.R., Visser, H.N., Van Zyl, J.S., Coertze, F.J. and Wessel, J.T. (1955). The geology of the eastern Soutpansberg and the Lowveld to the north. Explanation Sheet 42 (Soutpansberg), geological Survey of South Africa, 117.

Van Vuuren, K. (1990). Die Warmwaterbronne van Suidwes-Kaapland: HulleVerbreiding, Eienskappe en Benutting. B.A. Honours dissertation, University of Stellenbosch.

Virk, H.S., Sharma, A.K and Kurma, N. (1998). Radon/Helium survey of thermal springs of Parbati, Beas, Sutlej Valleys in Himachal. Journal of the Geological Society of India, vol. 52(5), pp. 523-528.

Visser, A., Fourre, E., Barbecot, F., Aquilina, L., Labasque, T., Vergnaud, V. and Esser, B.K. (2014). Intercomparison of tritium and noble gases analyses, apparent $^{3}H/^{3}He$ ages and other derived Parameters. *Appl. Geochem*., 50, 130-141.

Visser, A., Moran, J.E., Hillegonds, D., Singleton, M.J., Kulongoski, J.T. and Belitz, K. (2016). Geostatistical analysis of tritium, groundwater age and other noble gas derived parameters in California, *Water research*, 91, 314-330.

Vogel JC and Ehhalt D. (1963). The use of carbon isotopes in groundwater studies. Radioisotopes in hydrology. Vienna: IAEA. p 383–95.

Vogel, J.C. (1970). Carbon 14 dating of groundwater. In: *Isotope Hydrology*.p. 225-239.

Vogel, J.C. (1978). Isotopic assessment of the dietary habits of ungulates. *S. Afr. J. Sci.* 74:298-301.

Vogel, J.C. (1993). Variability of carbon isotopes fractionation during photosynthesis. In stable isotopes and Plant carbon: Water Relations (eds J.R. Ehleringer, A.E Hall, and G.D Farquhari). Academic Press, pp. 29-46.

Vogel, J.C., Eglington, B. and Auret, J.M. (1990). Isotope fingerprints in elephant bone and ivory. *Nature* 346, 747-749

Voss, M., Larsen, B., Leivuori, M. and Vallius, H. (2000). Stable isotope signals of eutrophication in Baltic sea sediments, *Journal of Marine system*, 25, 287-298.

Wang, S. and Xie, G. (2003). Geothermal water for multiple purposes in Beijing, Beijing Institute of Geological Engineering and Exploration, China.

Water UK (2001). Cadmium briefing paper, Water UK: London.

Werner, R. A., Buchmann, N., Siegwolf, R. T. W., Kornexl, B. E. and Gessler, A. (2011). Metabolic fluxes, carbon isotope fractionation and respiration – lessons to be learned from plant biochemistry, *New Phytol*., 191, 10–15.

White W.M. (2015). Isotope geochemistry, Wiley-Blackwell, 361-420, ISBN; 978-0-470-65670-9

Wilcox, L. V. (1958). The quality of water for irrigation. US Department of Agriculture

Wirmvem, M.J., Ohba, T., Fantong, W.Y., Ayonghe, S.N., Suila, J.Y., Asaah, A.N.E., Asai, K., Tanyileke, G., Hell, J.V. (2014). Monthly d18O, dD and Cl- characteristics of precipitation in the Ndop plain, Northwest Cameroon: baseline data. *Quat Int*, 338:35–41

Wirmvem, M.J., Ohba, T., Kamtchueng, B.T., Taylor, E.T., Fantong, W.Y. and Ako, A.K. (2016). Variation in stable isotope ratios of monthly rainfall in the Douala and Yaounde cities, Cameroon: local meteoric lines and relationship to regional precipitation cycle. *Appl Water Sci*, DOI 10.1007/s13201-016-0413-4

Witcher, J.C. (2002). Masson Radium Springs Farm. Southwest Technology Institute, New Mexico State University.

Witeska, M. and Jezierska, B. (2003). The effects of environmental factors on metal toxicity to fish. *Fresenius Environmental Bulletin*, 12(8), 824-829.

World Health Organization (WHO), (1989). Health guidelines for use of wastewater in agriculture and aquaculture. WHO Geneva.

World Health Organisation (WHO), (2000). Bottled drinking water, Geneva: World Health Organization (http://www.who.int/mediacentre/factsheets/fs256/en/print.html).

World Health Organisation (WHO) (2003). Selenium in drinking water, Background document for development of WHO Guidelines for Drinking-water Quality, WHO: Geneva.

World Health Organization (WHO), (2004). Guidelines for drinking water quality. Geneva: World Health Organization

World Health Organization (eds) (WHO), (2006a), Cobalt and inorganic cobalt compounds. Concise International Chemical Assessment Document 69, WHO: Geneva.

World Health Organization (eds) (WHO), (2006b) Guidelines for drinking water quality, vol 1. Recommendations, Geneva, p 595

World Health Organisation (WHO) (2008). Guideline for Drinking-water Quality, 3rd ed., Incorporating the First and Second Addenda, Volume 1, Recommendations, WHO: Geneva.

World Health Organisation (WHO) (2009). Beryllium in Drinking-water, Background document for development of WHO Guidelines for Drinking-water Quality, WHO/HSE/WSH/09.01/5, WHO: Geneva

World Health Organization (WHO) (2011), Guidelines for drinking-water quality, Fourth edition, Volume 1, 2011, WHO: Geneva

Wu, H., Chen, J., Qian, H. and Zhang, X. (2015). Chemical Characteristics and Quality Assessment of Groundwater of Exploited Aquifers in Beijiao Water Source of Yinchuan, China: A Case Study for Drinking, Irrigation, and Industrial Purposes, *Journal of Chemistry*, http://dx.doi.org/10.1155/2015/726340

Yahaya, M.I., Mohammad, S. and Abdullahi, B.K. (2009). Seasonal variations of heavy metal concentration in Abattoir dumping site soil in Nigeria. *J. Appl. Sci. Environ. Manage*., 13(4), 9-13.

Yakir, D. and Sternberg, L. (2000). The use of stable isotopes to study ecosystem gas exchange, *Oecologia*, 123, 297–311.

Yeh, H-F. and Lee, J-W. (2018). Stable hydrogen and oxygen isotopes for groundwater sources of Penghu Islands, Taiwan, *Geosciences*, 8, 84; doi:10.3390/geosciences8030084

Yepez, E.A., Huxman, T.E., Ignace, D.D., English, N.B., Weltzin, J.F., Castellanos, A.E. and Williams, D.G. (2005). Dynamics of transpiration and evaporation following a moisture pulse in semiarid grassland: A chamber-based isotope method for partitioning flux components, *Agr. Forest Meteorol*., 132, 359–376.

Zhou, X., Li, R., Zhang, H. and Zhang, L. (2006). Characteristics of natural low pH groundwater in the coastal aquifers near Beihai, China. Chinese J. Geochemistry, vol. 25 (1), pp. 228.

Zimmerman, U., Ehhalt, D., and Munnich, K.O. (1967). Soil-water movement and evapotranspiration: changes in the isotopic composition of the water. Proc. IAEA Symp. Isot. Hydrol., IAEA Vienna, pp. 567-584

Zongyu, C., Jixiang, Q., Jianming, X., Jiaming, X., Hao, Y. and Yunju, N. (2003). Paleoclimatic interpretation of the past 30 ka from isotopic studies of the deep confined aquifer of the North China plain. *Applied Geochemistry,* 18, 1009.

Zouari, K., Hkir, N. and Ouda, B. (2003). Palaeoclimatic Variation in Maknassi Basin (Central Tunisia) during Holocene Period Using Pluridisplinary Approaches. Technical document. IAEA, Vienna. 2:80e88.

APPENDICES

Appendix 5.1: Images of outcome obtained from NETPATH software for ^{14}C correction

Initial Carbon-14, A0, (percent modern) for Total Dissolved Carbon — TSS

	Model	Initial well	Age
1	Original Data	45.20	0.00
2	Mass Balance	409.95	18227.38
3	Vogel	85.00	5220.83
4	Tamers	50.30	884.32
5	Ingerson and Pearson	64.92	2993.01
6	Mook	73.66	4036.61
7	Fontes and Garnier	68.73	3464.60
8	Eichinger	65.11	3017.64
9	User-defined	100.00	6564.32
10	Revised F&G gas ex	74.58	4139.42
11	Revised F&G solid ex	65.42	3056.77

Initial Carbon-14, A0, (percent modern) for Total Dissolved Carbon — TSW

	Model	Initial well	Age
1	Original Data	41.20	0.00
2	Mass Balance	358.55	17885.85
3	Vogel	85.00	5986.81
4	Tamers	50.31	1652.04
5	Ingerson and Pearson	36.28	-1051.28
6	Mook	22.39	-5041.73
7	Fontes and Garnier	34.87	-1378.92
8	Eichinger	31.80	-2141.24
9	User-defined	100.00	7330.30
10	Revised F&G gas ex	22.36	-5051.64
11	Revised F&G solid ex	31.93	-2107.76

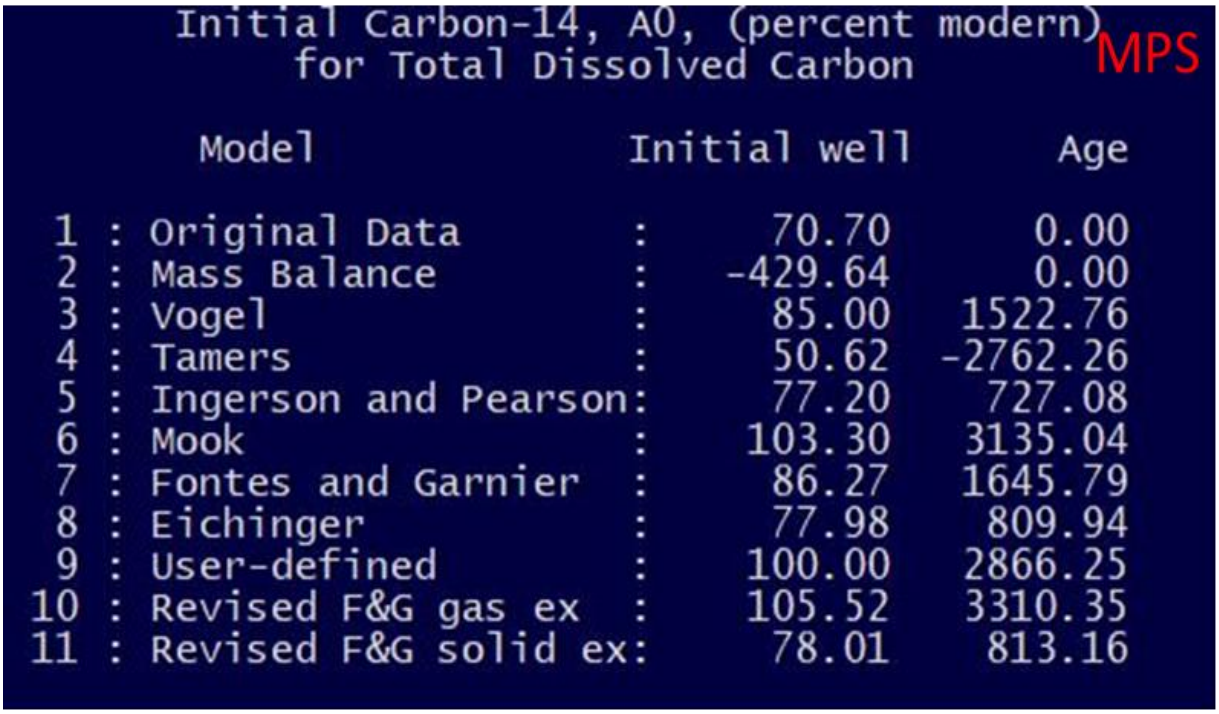

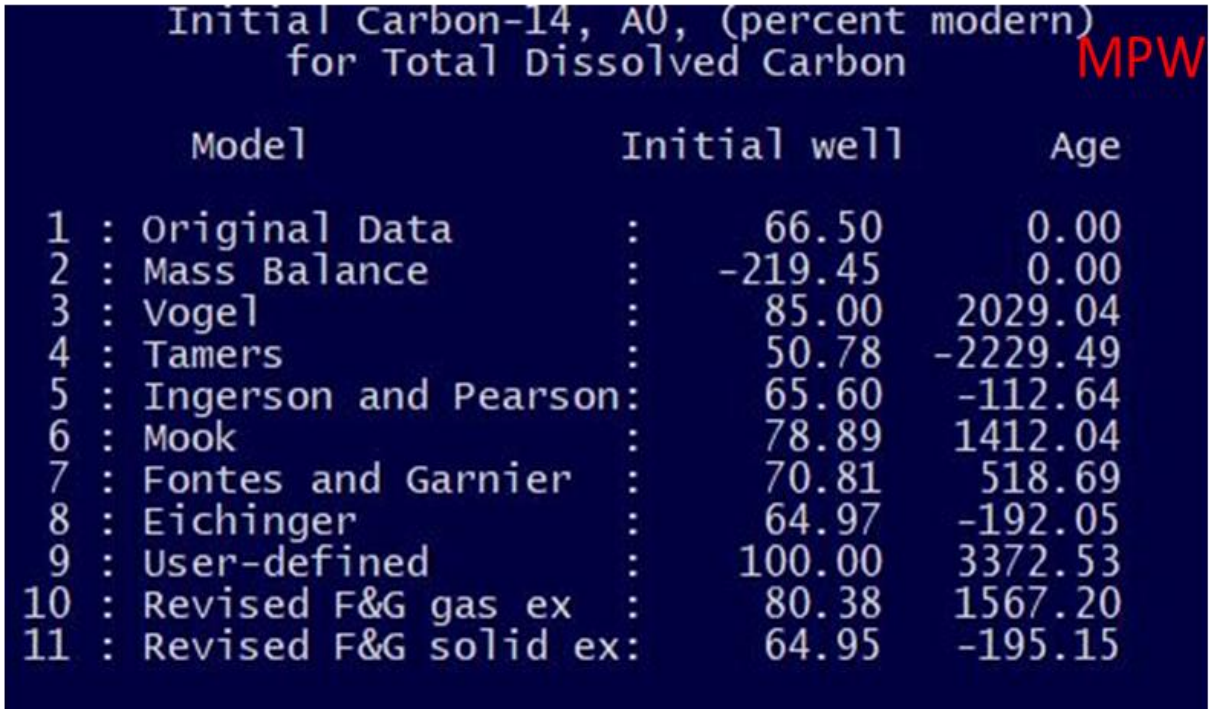

Initial Carbon-14, A0, (percent modern) for Total Dissolved Carbon — SGS

	Model	Initial well	Age
1	Original Data	49.80	0.00
2	Mass Balance	133.58	8156.69
3	Vogel	85.00	4419.65
4	Tamers	50.93	186.05
5	Ingerson and Pearson	63.04	1948.90
6	Mook	71.92	3038.39
7	Fontes and Garnier	67.00	2452.23
8	Eichinger	62.30	1851.72
9	User-defined	100.00	5763.13
10	Revised F&G gas ex	72.76	3134.26
11	Revised F&G solid ex	62.25	1844.62

Initial Carbon-14, A0, (percent modern) for Total Dissolved Carbon — SGW

	Model	Initial well	Age
1	Original Data	44.40	0.00
2	Mass Balance	212.26	12933.71
3	Vogel	85.00	5368.46
4	Tamers	50.14	1005.22
5	Ingerson and Pearson	52.96	1457.39
6	Mook	54.18	1645.61
7	Fontes and Garnier	53.93	1607.16
8	Eichinger	51.06	1155.20
9	User-defined	100.00	6711.94
10	Revised F&G gas ex	55.12	1787.91
11	Revised F&G solid ex	51.36	1203.75

Appendix 5.2: Plots of outcome obtained from NETPATH software for ^{14}C correction

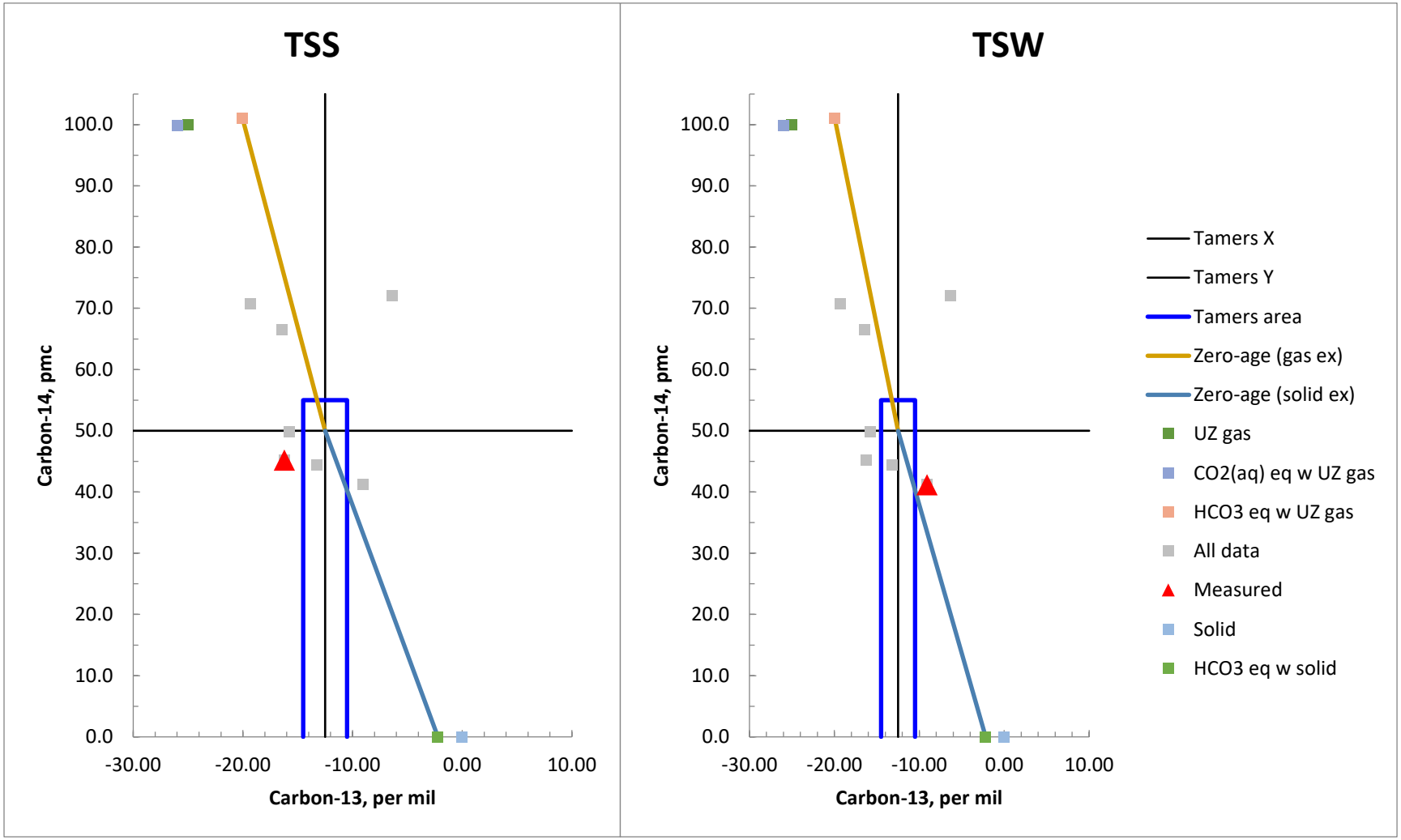

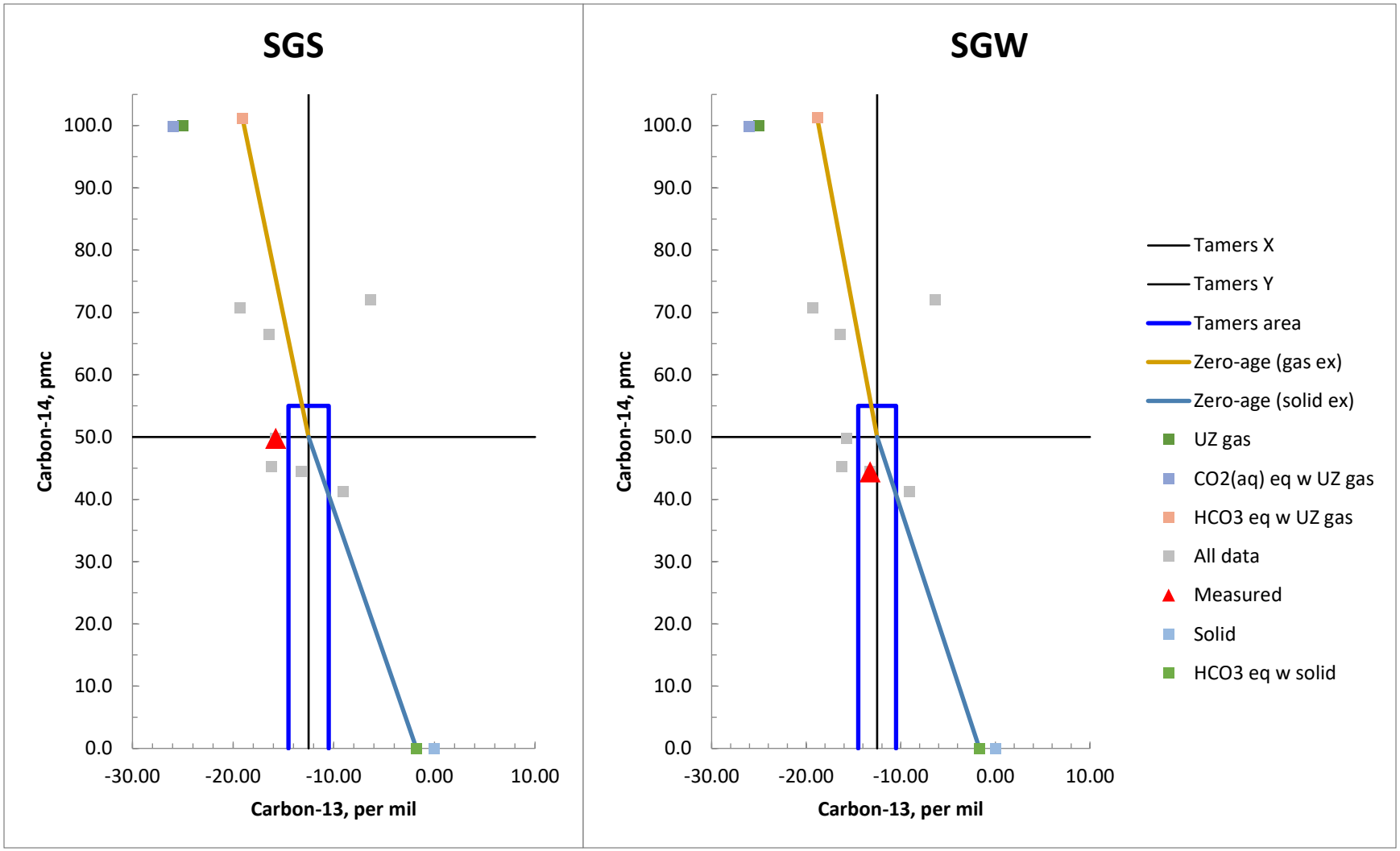

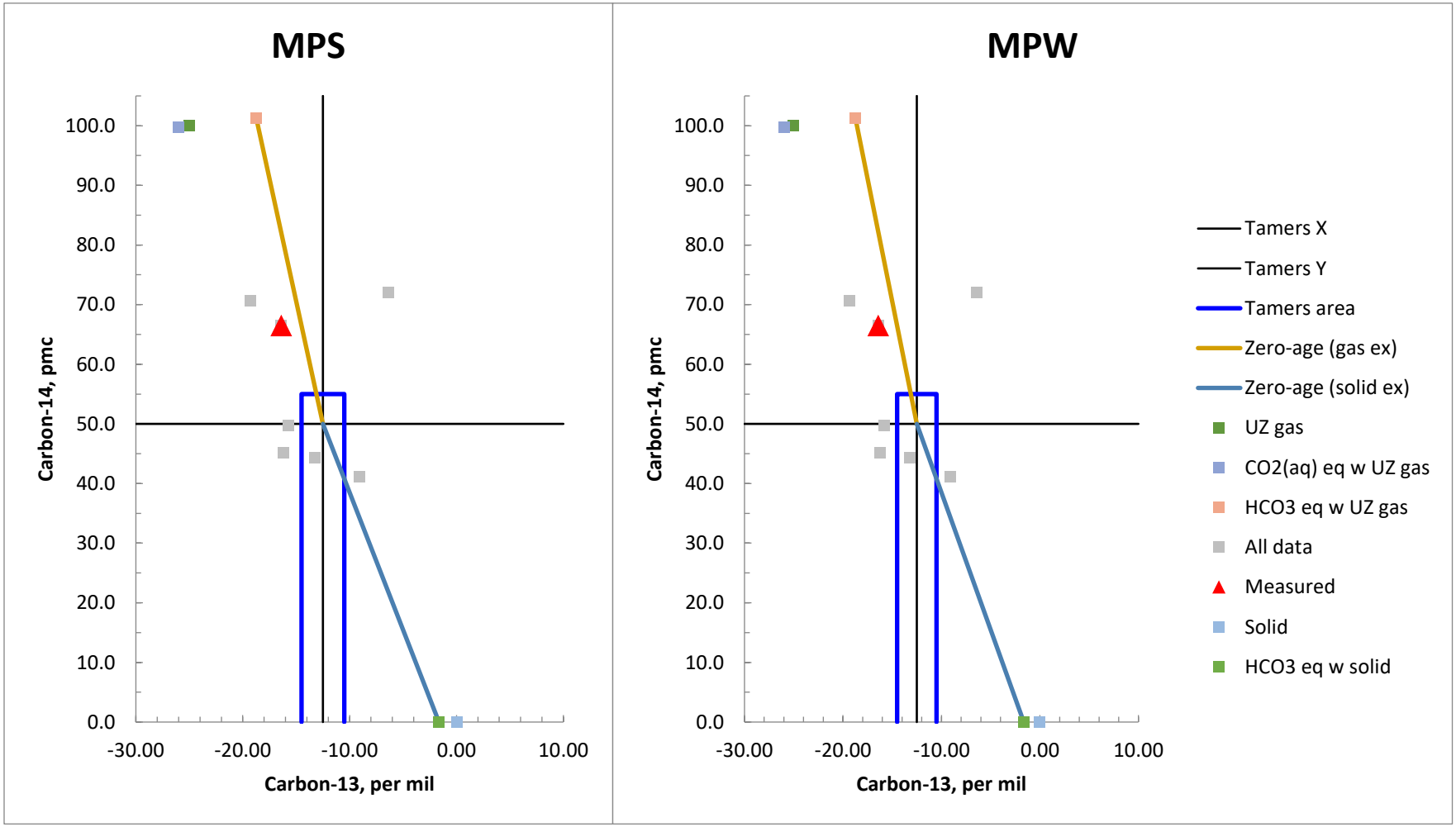

Appendix 7.1: Hazard quotient for geothermal springs and boreholes within Soutpansberg

Hazard Quotient															
		TSS	**TSW**	**SGS**	**SGW**	**MPS**	**MPW**	**SAW**	**SH1**	**SH2**	**BH1**	**BH2**	**SCC**	**TTP**	**HI-total**
							Be								
	Ingestion	1.10E+00	3.50E+00	8.03E-01	5.40E-03	1.56E+00	3.08E+00	3.00E-02	1.92E+00	2.12E+00	2.62E+00	4.06E+00	3.04E+00	5.40E-03	**2.38E+01**
Children	Dermal	-	-	-	-	-	-	-	-	-	-	-	-	-	**-**
	Ingestion	2.46E-02	7.86E-02	1.80E-02	1.21E-04	3.50E-02	6.91E-02	6.73E-04	4.32E-02	4.75E-02	5.88E-02	9.11E-02	6.82E-02	1.21E-04	**5.35E-01**
Adult	Dermal	-	-	-	-	-	-	-	-	-	-	-	-	-	**-**
							V								
	Ingestion	4.37E-01	3.98E-01	3.22E-01	3.47E-01	3.88E-01	3.32E-01	7.64E-02	3.22E-01	4.20E-01	1.22E-01	2.97E-01	4.25E-01	1.10E-01	**4.00E+00**
Children	Dermal	-	-	-	-	-	-	-	-	-	-	-	-	-	**-**
	Ingestion	9.81E-03	8.94E-03	7.22E-03	7.80E-03	8.70E-03	7.46E-03	1.72E-03	7.24E-03	9.42E-03	2.74E-03	6.66E-03	9.53E-03	2.47E-03	**8.97E-02**
Adult	Dermal	-	-	-	-	-	-	-	-	-	-	-	-	-	**-**
							Cr								
	Ingestion	4.98E-01	3.46E-01	4.19E-01	2.66E-01	4.23E-01	3.36E-01	3.60E-03	4.16E-01	4.43E-01	2.80E-01	2.59E-01	4.86E-01	3.61E-01	**4.54E+00**
Children	Dermal	1.83E-03	1.27E-03	1.54E-03	9.74E-04	1.55E-03	1.23E-03	1.32E-05	1.53E-03	1.63E-03	1.03E-03	9.51E-04	1.78E-03	1.32E-03	**1.66E-02**
	Ingestion	1.12E-02	7.76E-03	9.41E-03	5.97E-03	9.49E-03	7.55E-03	8.08E-05	9.34E-03	9.95E-03	6.28E-03	5.82E-03	1.09E-02	8.10E-03	**1.02E-01**
Adult	Dermal	5.31E-05	3.68E-05	4.47E-05	2.83E-05	4.50E-05	3.58E-05	3.84E-07	4.43E-05	4.72E-05	2.98E-05	2.76E-05	5.17E-05	3.85E-05	**4.83E-04**
							Mn								
	Ingestion	1.33E-02	1.11E-02	5.15E-02	1.28E-01	1.83E-01	5.32E-03	1.20E-03	6.27E-03	9.73E-03	5.38E-01	8.28E-03	7.62E-03	7.35E-02	**1.04E+00**
Children	Dermal	8.21E-04	6.84E-04	3.17E-03	7.86E-03	1.13E-02	3.28E-04	7.38E-05	3.86E-04	5.99E-04	3.31E-02	5.09E-04	4.69E-04	4.52E-03	**6.38E-02**
	Ingestion	2.99E-04	2.50E-04	1.16E-03	2.87E-03	4.11E-03	1.19E-04	2.69E-05	1.41E-04	2.18E-04	1.21E-02	1.86E-04	1.71E-04	1.65E-03	**2.33E-02**
Adult	Dermal	2.38E-05	1.99E-05	9.21E-05	2.28E-04	3.27E-04	9.52E-06	2.15E-06	1.12E-05	1.74E-05	9.61E-04	1.48E-05	1.36E-05	1.31E-04	**1.85E-03**
							Co								
	Ingestion	1.26E-03	1.67E-03	2.59E-03	2.13E-03	1.75E-03	2.19E-03	2.40E-04	1.12E-03	1.57E-03	2.05E-02	3.05E-03	1.43E-03	1.02E-03	**4.05E-02**
Children	Dermal	1.62E-02	2.15E-02	3.33E-02	2.75E-02	2.25E-02	2.81E-02	3.09E-03	1.44E-02	2.01E-02	2.64E-01	3.92E-02	1.84E-02	1.31E-02	**5.21E-01**
	Ingestion	2.82E-05	3.75E-05	5.82E-05	4.79E-05	3.92E-05	4.91E-05	5.39E-06	2.51E-05	3.52E-05	4.61E-04	6.84E-05	3.21E-05	2.29E-05	**9.10E-04**
Adult	Dermal	4.69E-04	6.25E-04	9.69E-04	7.98E-04	6.53E-04	8.17E-04	8.97E-05	4.17E-04	5.85E-04	7.67E-03	1.14E-03	5.34E-04	3.81E-04	**1.52E-02**

							Ni								
	Ingestion	1.35E-02	1.58E-02	5.95E-03	6.63E-03	1.28E-02	5.06E-03	4.26E-03	4.90E-03	8.89E-03	7.51E-02	3.27E-03	1.13E-02	9.43E-03	**1.77E-01**
Children	Dermal	1.08E-08	1.26E-08	4.75E-09	5.30E-09	1.02E-08	4.04E-09	3.40E-09	3.92E-09	7.11E-09	6.00E-08	2.61E-09	9.03E-09	7.53E-09	**1.41E-07**
	Ingestion	3.02E-04	3.55E-04	1.34E-04	1.49E-04	2.88E-04	1.13E-04	9.56E-05	1.10E-04	2.00E-04	1.69E-03	7.34E-05	2.54E-04	2.12E-04	**3.97E-03**
Adult	Dermal	5.13E-06	6.02E-06	2.26E-06	2.52E-06	4.88E-06	1.92E-06	1.62E-06	1.87E-06	3.38E-06	2.86E-05	1.24E-06	4.30E-06	3.59E-06	**6.73E-05**
							Cu								
	Ingestion	3.88E-02	6.08E-02	9.92E-02	2.08E-04	4.15E-03	2.92E-05	1.14E-03	2.92E-05	5.96E-03	1.02E-01	1.12E-03	6.98E-03	1.56E-02	**3.36E-01**
Children	Dermal	2.19E-04	3.44E-04	5.61E-04	1.18E-06	2.35E-05	1.65E-07	6.42E-06	1.65E-07	3.37E-05	5.75E-04	6.31E-06	3.94E-05	8.83E-05	**1.90E-03**
	Ingestion	8.71E-04	1.37E-03	2.23E-03	4.67E-06	9.32E-05	6.55E-07	2.55E-05	6.55E-07	1.34E-04	2.29E-03	2.50E-05	1.57E-04	3.51E-04	**7.54E-03**
Adult	Dermal	6.37E-06	9.99E-06	1.63E-05	3.42E-08	6.82E-07	4.79E-09	1.86E-07	4.79E-09	9.80E-07	1.67E-05	1.83E-07	1.15E-06	2.57E-06	**5.52E-05**
							Zn								
	Ingestion	1.25E-01	1.86E-01	1.18E-01	7.78E-02	1.97E-02	8.40E-03	3.80E-04	3.60E-06	3.60E-06	1.40E-01	3.60E-06	3.60E-06	1.79E-02	**6.94E-01**
Children	Dermal	1.84E-03	2.73E-03	1.73E-03	1.14E-03	2.90E-04	1.23E-04	5.57E-06	5.28E-08	5.28E-08	2.06E-03	5.28E-08	5.28E-08	2.63E-04	**1.02E-02**
	Ingestion	7.30E-04	2.34E-03	5.35E-04	3.60E-06	1.04E-03	2.05E-03	2.00E-05	1.28E-03	1.41E-03	1.75E-03	2.70E-03	2.02E-03	3.60E-06	**1.59E-02**
Adult	Dermal	5.33E-05	7.92E-05	5.02E-05	3.32E-05	8.41E-06	3.58E-06	1.62E-07	1.53E-09	1.53E-09	5.98E-05	1.53E-09	1.53E-09	7.65E-06	**2.96E-04**
							As								
	Ingestion	8.17E-01	8.05E-01	5.41E-01	7.89E-01	1.09E+00	8.39E-01	4.04E-01	4.13E-01	1.22E+00	7.68E-01	5.18E-01	1.22E+00	5.20E-01	**9.94E+00**
Children	Dermal	2.99E-03	2.95E-03	1.98E-03	2.89E-03	3.99E-03	3.07E-03	1.48E-03	1.51E-03	4.46E-03	2.82E-03	1.90E-03	4.47E-03	1.91E-03	**3.64E-02**
	Ingestion	1.83E-02	1.81E-02	1.21E-02	1.77E-02	2.44E-02	1.88E-02	9.07E-03	9.27E-03	2.73E-02	1.72E-02	1.16E-02	2.74E-02	1.17E-02	**2.23E-01**
Adult	Dermal	8.70E-05	8.58E-05	5.77E-05	8.41E-05	1.16E-04	8.93E-05	4.30E-05	4.40E-05	1.30E-04	8.18E-05	5.51E-05	1.30E-04	5.54E-05	**1.06E-03**
							Se								
	Ingestion	1.40E-01	1.48E-01	9.25E-02	1.38E-01	2.41E-01	1.54E-01	1.63E-02	1.22E-01	2.63E-01	1.40E-01	8.68E-02	2.63E-01	7.79E-02	**1.88E+00**
Children	Dermal	-	-	-	-	-	-	-	-	-	-	-	-	-	**-**
	Ingestion	3.14E-03	3.33E-03	2.08E-03	3.09E-03	5.40E-03	3.46E-03	3.66E-04	2.73E-03	5.90E-03	3.15E-03	1.95E-03	5.89E-03	1.75E-03	**4.22E-02**
-	Dermal	-	-	-	-	-	-	-	-	-	-	-	-	-	**-**
							Cd								
	Ingestion	6.76E-03	2.94E-03	1.60E-03	6.46E-03	9.20E-04	1.65E-02	2.40E-03	1.08E-03	8.40E-04	8.71E-02	1.08E-03	8.40E-04	5.40E-03	**1.34E-01**
Children	Dermal	2.48E-05	1.08E-05	5.87E-06	2.37E-05	3.37E-06	6.05E-05	8.80E-06	3.96E-06	3.08E-06	3.19E-04	3.96E-06	3.08E-06	1.98E-05	**4.91E-04**
Adult	Ingestion	1.52E-04	6.60E-05	3.59E-05	1.45E-04	2.07E-05	3.70E-04	5.39E-05	2.42E-05	1.89E-05	1.96E-03	2.42E-05	1.89E-05	1.21E-04	**3.01E-03**

	Dermal	7.20E-07	3.13E-07	1.70E-07	6.88E-07	9.80E-08	1.76E-06	2.56E-07	1.15E-07	8.95E-08	9.28E-06	1.15E-07	8.95E-08	5.75E-07	**1.43E-05**
							Sb								
	Ingestion	1.59E-02	6.60E-03	9.40E-03	1.76E-02	1.07E-02	5.18E-02	9.00E-03	1.50E-03	4.50E-03	3.66E-02	2.37E-02	2.70E-03	2.85E-02	**2.18E-01**
Children	Dermal	-	-	-	-	-	-	-	-	-	-	-	-	-	**-**
	Ingestion	3.57E-04	1.48E-04	2.11E-04	3.96E-04	2.40E-04	1.16E-03	2.02E-04	3.37E-05	1.01E-04	8.22E-04	5.32E-04	6.06E-05	6.40E-04	**4.90E-03**
Adult	Dermal	-	-	-	-	-	-	-	-	-	-	-	-	-	**-**
							Ba								
	Ingestion	9.22E-04	1.58E-02	4.68E-04	2.54E-02	5.28E-03	1.74E-02	6.25E-03	2.27E-04	4.32E-03	4.04E-02	4.32E-02	4.10E-03	5.40E-06	**1.64E-01**
Children	Dermal	-	-	-	-	-	-	-	-	-	-	-	-	-	**-**
	Ingestion	2.07E-05	3.55E-04	1.05E-05	5.71E-04	1.18E-04	3.91E-04	1.40E-04	5.10E-06	9.70E-05	9.07E-04	9.70E-04	9.21E-05	1.21E-07	**3.68E-03**
Adult	Dermal	-	-	-	-	-	-	-	-	-	-	-	-	-	**-**
							Hg								
	Ingestion	2.44E+00	2.48E-01	1.30E+00	1.61E-01	7.27E-01	1.72E-01	1.40E-01	2.65E-01	3.19E-01	6.12E-02	6.40E-01	1.84E-01	2.88E-01	**6.95E+00**
Children	Dermal	8.96E-03	9.11E-04	4.78E-03	5.90E-04	2.67E-03	6.31E-04	5.13E-04	9.71E-04	1.17E-03	2.24E-04	2.35E-03	6.75E-04	1.06E-03	**2.55E-02**
	Ingestion	5.49E-02	5.58E-03	2.93E-02	3.62E-03	1.63E-02	3.87E-03	3.14E-03	5.94E-03	7.17E-03	1.37E-03	1.44E-02	4.13E-03	6.47E-03	**1.56E-01**
Adult	Dermal	2.60E-04	2.65E-05	1.39E-04	1.72E-05	7.74E-05	1.83E-05	1.49E-05	2.82E-05	3.40E-05	6.52E-06	6.81E-05	1.96E-05	3.07E-05	**7.41E-04**
							Pb								
	Ingestion	9.67E-03	1.12E-02	1.68E-02	3.09E-04	3.09E-04	3.09E-04	3.09E-03	5.86E-03	3.09E-04	3.09E-04	3.09E-04	3.09E-04	2.19E-03	**5.09E-02**
Children	Dermal	2.36E-04	2.73E-04	4.10E-04	7.54E-06	7.54E-06	7.54E-06	7.54E-05	1.43E-04	7.54E-06	7.54E-06	7.54E-06	7.54E-06	5.36E-05	**1.24E-03**
	Ingestion	2.17E-04	2.51E-04	3.77E-04	6.93E-06	6.93E-06	6.93E-06	6.93E-05	1.32E-04	6.93E-06	6.93E-06	6.93E-06	6.93E-06	4.93E-05	**1.14E-03**
Adult	Dermal	6.87E-06	7.94E-06	1.19E-05	2.19E-07	2.19E-07	2.19E-07	2.19E-06	4.16E-06	2.19E-07	2.19E-07	2.19E-07	2.19E-07	1.56E-06	**3.62E-05**

Appendix 7.2: Statistical summary of the trace metals concentrations from the surrounding soil of the geothermal springs

		Tshipise S	Tshipise W	Mphephu S	Mphephu W	Sagole S	Sagole W	Siloam
pH	Min	7.50	8.01	6.62	7.47	3.10	9.31	6.67
	Max	8.55	8.05	6.97	7.76	9.90	9.72	7.15
	Mean	8.12	8.04	6.80	7.62	7.38	9.45	6.91
	SD	0.55	0.02	0.25	0.21	3.73	.23	0.34
	CV	6.79	0.29	3.64	2.69	50.49	2.45	4.91
EC	Min	89.40	90.10	111.20	27.40	124.10	165.80	90.60
	Max	253.90	130.20	217.50	40.80	1441.00	376.00	116.90
	Mean	165.83	105.37	164.35	34.10	846.03	275.17	103.75
	SD	82.86	21.69	75.17	9.48	667.57	92.00	18.60
	CV	49.97	20.59	45.73	27.79	78.91	33.43	17.92
TDS	Min	57.20	57.60	71.10	17.50	79.40	125.00	58.00
	Max	162.00	613.00	139.00	26.10	922.00	241.00	74.80
	Mean	105.97	251.30	105.05	21.80	541.47	176.00	66.40
	SD	52.78	313.50	48.01	6.08	427.18	59.25	11.88
	CV	49.80	124.75	45.70	27.90	78.89	33.67	17.89
Be	Min	0.14	0.21	0.34	0.20	0.05	0.04	0.59
	Max	0.21	0.30	0.63	0.31	0.75	0.09	0.64
	Mean	0.18	0.25	0.48	0.26	0.30	0.06	0.62
	SD	0.04	0.05	0.20	0.08	0.39	0.03	0.04
	CV	21.05	18.68	42.44	31.61	128.10	42.33	6.32
V	Min	12.24	16.82	58.50	48.14	4.15	4.13	165.10
	Max	17.13	25.23	68.17	49.02	7.02	6.53	172.40
	Mean	15.25	20.11	63.34	48.58	6.01	5.35	168.75
	SD	2.64	4.50	6.84	0.62	1.61	1.20	5.16
	CV	17.28	22.36	10.80	1.28	26.81	22.44	3.06
Cr	Min	37.93	36.93	35.32	27.92	3.77	4.71	90.54
	Max	46.23	44.90	36.10	38.38	9.98	7.81	96.35
	Mean	42.34	39.78	35.71	33.15	6.08	6.59	93.45
	SD	4.17	4.45	0.55	7.40	3.40	1.66	4.11
	CV	9.86	11.18	1.54	22.31	55.87	25.13	4.40
Mn	Min	99.98	120.30	35.41	46.96	18.07	24.59	118.30
	Max	144.00	157.10	47.22	71.84	68.76	53.96	119.00
	Mean	119.06	135.90	41.32	59.40	39.98	36.23	118.65
	SD	22.59	19.03	8.35	17.59	26.03	15.60	0.49
	CV	18.97	14.00	21.21	29.62	65.12	43.06	0.42
Co	Min	3.62	4.61	13.80	19.12	0.89	1.00	28.66
	Max	5.28	7.78	14.66	21.52	2.29	1.52	28.67
	Mean	4.66	5.78	14.23	20.32	1.77	1.21	28.67
	SD	0.91	1.74	0.61	1.70	0.77	0.27	0.01
	CV	19.44	30.06	4.27	8.35	43.38	22.46	0.02
Ni	Min	24.46	26.10	15.72	11.60	2.41	3.41	51.65
	Max	34.44	37.03	21.10	21.45	11.27	6.13	57.39
	Mean	5.14	29.99	18.41	.16.53	6.00	4.66	54.52
	SD	30.16	6.11	3.80	6.97	4.66	1.3	4.06
	CV	17.04	20.37	20.66	42.15	77.74	29.53	7.44

Cu	Min	8.52	13.73	25.09	19.30	8.11	5.63	97.07
	Max	12.70	19.13	33.45	25.39	9.23	7.14	103.60
	Mean	11.13	15.97	29.27	22.35	8.67	6.19	100.34
	SD	2.27	2.82	5.91	4.31	0.56	0.83	4.62
	CV	20.44	17.63	20.20	19.27	6.46	13.40	4.60
Zn	Min	14.16	1549	15.52	8.08	2.51	3.83	48.62
	Max	15.75	21.25	37.74	19.77	17.17	6.10	48.94
	Mean	15.05	17.63	26.63	13.93	10.11	4.95	48.78
	SD	0.81	3.15	15.71	8.26	7.34	1.14	0.23
	CV	5.39	17.88	59.00	59.35	72.66	22.99	0.46
As	Min	0.22	0.37	0.44	0.10	0.33	0.26	0.79
	Max	0.38	0.93	1.10	0.67	7.41	0.59	0.79
	Mean	0.30	0.66	0.77	0.39	2.69	0.39	0.79
	SD	0.08	0.28	0.47	0.40	4.08	0.17	0.00
	CV	26.32	42.46	61.16	103.64	151.66	43.82	0.63
Se	Min	0.09	0.18	0.36	0.11	0.07	0.00	0.25
	Max	0.27	0.18	1.53	0.33	0.14	0.10	0.26
	Mean	0.15	0.18	0.95	0.22	0.10	0.06	0.26
	SD	0.10	0.00	0.83	0.15	0.04	0.05	0.01
	CV	68.25	1.40	87.66	69.13	35.33	86..07	3.29
Cd	Min	0.02	0.02	0.04	0.02	0.01	0.01	0.26
	Max	0.04	0.04	0.09	0.04	0.02	0.02	0.36
	Mean	0.03	0.03	0.07	0.03	0.01	0.01	0.31
	SD	0.01	0.01	0.04	0.01	0.01	0.01	0.07
	CV	28.23	19.20	56.99	48.85	43.83	50.62	23.03
Sb	Min	0.01	0.02	0.02	0.01	0.02	0.01	0.02
	Max	0.02	0.04	0.04	0.01	0.30	0.02	0.03
	Mean	0.01	0.03	0.03	0.01	0.11	0.01	0.03
	SD	0.00	0.01	0.01	0.00	0.16	0.00	0.00
	CV	14.19	27.45	52.38	18.45	141.51	31.49	19.41
Ba	Min	11.09	14.51	23.80	18.03	3.17	3.44	48.40
	Max	13.88	20.81	45.36	41.58	253.20	19.87	51.48
	Mean	12.42	17.18	34.58	29.81	88.97	9.67	49.94
	SD	1.40	3.26	15.25	16.65	142.28	8.91	2.18
	CV	11.27	18.95	44.09	55.87	159.91	92.17	4.36
Hg	Min	0.11	0.03	0.00	0.00	0.00	0.00	0.00
	Max	0.23	0.29	0.01	0.00	0.12	0.04	0.00
	Mean	0.16	013	0.00	0.00	0.05	0.02	0.00
	SD	0.06	0.14	0.00	0.00	0.06	0.02	0.00
	CV	38.91	112.47	94.28	0.00	139.94	161.66	0.00
Pb	Min	2.00	2.96	4.08	2.96	1.43	1.15	30.60
	Max	2.42	5.74	9.45	3.51	6.08	1.49	85.02
	Mean	2.26	4.20	6.77	3.24	3.08	1.26	57.81
	SD	0.23	1.42	3.80	0.39	2.60	0.19	38.48
	CV	10.10	33.75	56.18	11.95	84.45	15.35	66.56

Appendix 7.3: Hazard quotient (Non-cancer) for surrounding soils of the geothermal springs within Soutpansberg

	Be						V						Cr					
	Ingestion		Inhalation		Dermal		Ingestion		Inhalation		Dermal		Ingestion		Inhalation		Dermal	
	Children	Adults	Children	Adults	Children	Adults	Children	Adults	Children	Adults	Children	Adults	Children	Adults	Children	Adults	Children	Adults
TSS	1.20E-02	1.29E-03	3.30E-07	1.42E-07	-	-	4.35E-02	4.66E-03	1.19E-06	5.12E-07	-	-	1.97E-01	2.11E-02	5.41E-04	2.32E-04	4.14E-04	8.57E-04
TSW	1.44E-02	1.55E-03	3.97E-07	1.70E-07	-	-	4.63E-02	4.97E-03	1.27E-06	5.46E-07	-	-	1.60E-01	1.71E-02	4.39E-04	1.88E-04	3.36E-04	6.95E-04
SGS	7.03E-03	7.53E-04	1.93E-07	8.28E-08	-	-	1.74E-02	1.87E-03	4.78E-07	2.05E-07	-	-	4.25E-02	4.56E-03	1.17E-04	5.01E-05	8.93E-05	1.85E-04
SGW	5.95E-03	6.37E-04	1.63E-07	7.00E-08	-	-	1.66E-02	1.78E-03	4.55E-07	1.95E-07	-	-	3.33E-02	3.57E-03	9.14E-05	3.92E-05	6.99E-05	1.45E-04
SAW	3.76E-02	4.03E-03	1.03E-06	4.43E-07	-	-	4.19E-01	4.49E-02	1.15E-05	4.93E-06	-	-	3.86E-01	4.13E-02	1.06E-03	4.54E-04	8.10E-04	1.68E-03
MPS	4.00E-02	4.29E-03	1.10E-06	4.71E-07	-	-	1.73E-01	1.85E-02	4.75E-06	2.04E-06	-	-	1.54E-01	1.65E-02	4.23E-04	1.81E-04	3.23E-04	6.69E-04
MPW	1.27E-02	1.36E-03	3.48E-07	1.49E-07	-	-	1.24E-01	1.33E-02	3.42E-06	1.46E-06	-	-	1.19E-01	1.27E-02	3.27E-04	1.40E-04	2.50E-04	5.18E-04
	Mn						**Co**						**Ni**					
	Ingestion		Inhalation		Dermal		Ingestion		Inhalation		Dermal		Ingestion		Inhalation		Dermal	
	Children	Adults	Children	Adults	Children	Adults	Children	Adults	Children	Adults	Children	Adults	Children	Adults	Children	Adults	Children	Adults
TSS	6.03E-02	6.46E-03	1.66E-06	7.10E-07	2.13E-03	4.40E-03	3.25E-03	3.48E-04	3.13E-05	1.34E-05	2.39E-03	4.96E-03	2.20E-02	2.36E-03	6.05E-07	2.59E-07	1.65E-04	3.42E-04
TSW	6.94E-02	7.44E-03	1.91E-06	8.17E-07	2.45E-03	5.07E-03	3.17E-03	3.40E-04	3.06E-05	1.31E-05	2.34E-03	4.84E-03	1.67E-02	1.79E-03	4.58E-07	1.96E-07	1.25E-04	2.59E-04
SGS	3.66E-02	3.92E-03	1.01E-06	4.31E-07	1.29E-03	2.67E-03	1.47E-03	1.57E-04	1.41E-05	6.06E-06	1.08E-03	2.24E-03	7.20E-03	7.72E-04	1.98E-07	8.48E-08	5.40E-05	1.12E-04
SGW	2.87E-02	3.08E-03	7.90E-07	3.38E-07	1.01E-03	2.10E-03	9.70E-04	1.04E-04	9.35E-06	4.01E-06	7.15E-04	1.48E-03	3.92E-03	4.20E-04	1.08E-07	4.61E-08	2.94E-05	6.09E-05
SAW	6.30E-02	6.75E-03	1.73E-06	7.42E-07	2.22E-03	4.60E-03	1.83E-02	1.96E-03	1.77E-04	7.57E-05	1.35E-02	2.80E-02	3.30E-02	3.54E-03	9.07E-07	3.89E-07	2.48E-04	5.13E-04
MPS	1.89E-02	2.02E-03	5.18E-07	2.22E-07	6.65E-04	1.38E-03	9.37E-03	1.00E-03	9.03E-05	3.87E-05	6.91E-03	1.43E-02	1.35E-02	1.45E-03	3.71E-07	1.59E-07	1.01E-04	2.10E-04
MPW	2.50E-02	2.68E-03	6.87E-07	2.95E-07	8.82E-04	1.83E-03	1.22E-02	1.31E-03	1.18E-04	5.05E-05	9.01E-03	1.87E-02	7.42E-03	7.95E-04	2.04E-07	8.73E-08	5.56E-05	1.15E-04
	Cu						**Zn**						**As**					
	Ingestion		Inhalation		Dermal		Ingestion		Inhalation		Dermal		Ingestion		Inhalation		Dermal	
	Children	Adults	Children	Adults	Children	Adults	Children	Adults	Children	Adults	Children	Adults	Children	Adults	Children	Adults	Children	Adults
TSS	4.39E-03	4.70E-04	1.21E-07	5.17E-08	1.42E-05	2.94E-05	6.49E-04	6.96E-05	1.78E-08	7.65E-09	5.46E-06	1.13E-05	1.63E-02	1.74E-03	4.47E-07	1.92E-07	3.42E-05	7.08E-05
TSW	4.74E-03	5.08E-04	1.30E-07	5.59E-08	1.54E-05	3.18E-05	6.88E-04	7.37E-05	1.89E-08	8.10E-09	5.78E-06	1.20E-05	1.57E-02	1.68E-03	4.32E-07	1.85E-07	3.30E-05	6.84E-05
SGS	3.00E-03	3.22E-04	8.25E-08	3.53E-08	9.72E-06	2.01E-05	7.32E-04	7.84E-05	2.01E-08	8.62E-09	6.15E-06	1.27E-05	1.42E-02	1.52E-03	3.90E-07	1.67E-07	2.98E-05	6.17E-05
SGW	2.47E-03	2.64E-04	6.78E-08	2.91E-08	7.99E-06	1.65E-05	2.10E-04	2.25E-05	5.77E-09	2.47E-09	1.76E-06	3.66E-06	2.50E-02	2.68E-03	6.87E-07	2.95E-07	5.25E-05	1.09E-04
SAW	3.35E-02	3.59E-03	9.22E-07	3.95E-07	1.09E-04	2.25E-04	2.07E-03	2.22E-04	5.69E-08	2.44E-08	1.74E-05	3.61E-05	3.35E-02	3.59E-03	9.21E-07	3.95E-07	7.04E-05	1.46E-04
MPS	1.16E-02	1.24E-03	3.18E-07	1.36E-07	3.74E-05	7.75E-05	1.61E-03	1.72E-04	4.42E-08	1.89E-08	1.35E-05	2.80E-05	4.68E-02	5.01E-03	1.29E-06	5.51E-07	9.83E-05	2.04E-04
MPW	6.67E-03	7.15E-04	1.83E-07	7.85E-08	2.16E-05	4.47E-05	3.44E-04	3.69E-05	9.46E-09	4.06E-09	2.89E-06	5.99E-06	4.39E-03	4.70E-04	1.21E-07	5.17E-08	9.22E-06	1.91E-05

	Se						Cd						Sb					
	Ingestion		Inhalation		Dermal		Ingestion		Inhalation		Dermal		Ingestion		Inhalation		Dermal	
	Children	Adults	Children	Adults	Children	Adults	Children	Adults	Children	Adults	Children	Adults	Children	Adults	Children	Adults	Children	Adults
TSS	6.90E-04	7.40E-05	1.90E-08	8.13E-09	-	-	4.35E-04	4.66E-05	2.10E-07	8.98E-08	9.13E-07	1.89E-06	4.47E-04	4.79E-05	1.23E-08	5.27E-09	-	-
TSW	4.53E-04	4.85E-05	1.24E-08	5.33E-09	-	-	3.07E-04	3.29E-05	1.48E-07	6.34E-08	6.44E-07	1.33E-06	6.71E-04	7.19E-05	1.84E-08	7.90E-09	-	-
SGS	1.79E-04	1.92E-05	4.92E-09	2.11E-09	-	-	2.81E-04	3.01E-05	1.36E-07	5.81E-08	5.91E-07	1.22E-06	6.07E-04	6.51E-05	1.67E-08	7.15E-09	-	-
SGW	2.51E-04	2.68E-05	6.88E-09	2.95E-09	-	-	1.28E-04	1.37E-05	6.16E-08	2.64E-08	2.68E-07	5.56E-07	6.39E-04	6.85E-05	1.76E-08	7.53E-09	-	-
SAW	6.75E-04	7.23E-05	1.85E-08	7.95E-09	-	-	3.29E-03	3.52E-04	1.58E-06	6.79E-07	6.90E-06	1.43E-05	9.27E-04	9.93E-05	2.55E-08	1.09E-08	-	-
MPS	3.92E-03	4.20E-04	1.08E-07	4.62E-08	-	-	1.20E-03	1.29E-04	5.79E-07	2.48E-07	2.52E-06	5.23E-06	1.18E-03	1.27E-04	3.25E-08	1.39E-08	-	-
MPW	2.92E-04	3.12E-05	8.01E-09	3.43E-09	-	-	2.30E-04	2.47E-05	1.11E-07	4.75E-08	4.83E-07	1.00E-06	3.20E-04	3.42E-05	8.78E-09	3.76E-09	-	-

	Ba						Hg						Pb					
	Ingestion		Inhalation		Dermal		Ingestion		Inhalation		Dermal		Ingestion		Inhalation		Dermal	
	Children	Adults	Children	Adults	Children	Adults	Children	Adults	Children	Adults	Children	Adults	Children	Adults	Children	Adults	Children	Adults
TSS	7.86E-04	8.42E-05	2.16E-08	9.25E-09	-	-	9.76E-03	1.05E-03	9.35E-07	4.01E-07	2.05E-05	4.25E-05	8.61E-03	9.23E-04	2.37E-07	1.01E-07	1.21E-04	2.50E-04
TSW	9.28E-04	9.94E-05	2.55E-08	1.09E-08	-	-	2.81E-03	3.01E-04	2.70E-07	1.16E-07	5.91E-06	1.22E-05	1.08E-02	1.16E-03	2.97E-07	1.27E-07	1.51E-04	3.13E-04
SGS	6.74E-04	7.22E-05	1.85E-08	7.93E-09	-	-	5.03E-03	5.39E-04	4.82E-07	2.07E-07	1.06E-05	2.19E-05	2.22E-02	2.38E-03	6.11E-07	2.62E-07	3.11E-04	6.45E-04
SGW	1.27E-03	1.36E-04	3.49E-08	1.50E-08	-	-	4.26E-05	4.57E-06	4.08E-09	1.75E-09	8.95E-08	1.85E-07	5.43E-03	5.82E-04	1.49E-07	6.39E-08	7.60E-05	1.57E-04
SAW	3.09E-03	3.32E-04	8.50E-08	3.64E-08	-	-	4.26E-05	4.57E-06	4.08E-09	1.75E-09	8.95E-08	1.85E-07	3.11E-01	3.33E-02	8.53E-06	3.66E-06	4.35E-03	9.01E-03
MPS	2.90E-03	3.11E-04	7.97E-08	3.41E-08	-	-	2.13E-04	2.28E-05	2.04E-08	8.75E-09	4.47E-07	9.27E-07	3.45E-02	3.70E-03	9.49E-07	4.07E-07	4.83E-04	1.00E-03
MPW	1.15E-03	1.23E-04	3.17E-08	1.36E-08	-	-	4.26E-05	4.57E-06	4.08E-09	1.75E-09	8.95E-08	1.85E-07	1.08E-02	1.16E-03	2.97E-07	1.27E-07	1.52E-04	3.14E-04

Appendix 7.4: Hazard quotient (Cancer) for surrounding soils of the geothermal springs within Soutpansberg

	Be						V						Cr					
	Ingestion		inhalation		dermal		Ingestion		inhalation		dermal		Ingestion		inhalation		dermal	
	Children	Adults	Children	Adults	Children	Adults	Children	Adults	Children	Adults	Children	Adults	Children	Adults	Children	Adults	Children	Adults
TSS	1.03E-03	5.52E-04	2.83E-08	6.06E-08	-	-	3.72E-03	2.00E-04	1.02E-07	2.19E-08	-	-	1.69E-02	9.05E-03	4.64E-05	9.94E-06	3.55E-05	3.67E-04
TSW	1.24E-03	6.63E-04	3.40E-08	7.29E-08	-	-	3.97E-03	2.13E-04	1.09E-07	2.34E-08	-	-	1.37E-02	7.34E-03	3.76E-05	8.06E-06	2.88E-05	2.98E-04
SGS	6.03E-04	3.23E-04	1.66E-08	3.55E-08	-	-	1.49E-03	8.00E-05	4.10E-08	8.79E-09	-	-	3.64E-03	1.95E-03	1.00E-05	2.15E-06	7.65E-06	7.93E-05
SGW	5.10E-04	2.73E-04	1.40E-08	3.00E-08	-	-	1.42E-03	7.61E-05	3.90E-08	8.36E-09	-	-	2.85E-03	1.53E-03	7.84E-06	1.68E-06	5.99E-06	6.21E-05
SAW	3.22E-03	1.73E-03	8.85E-08	1.90E-07	-	-	3.59E-02	1.92E-03	9.86E-07	2.11E-07	-	-	3.31E-02	1.77E-02	9.09E-05	1.95E-05	6.95E-05	7.19E-04
MPS	3.43E-03	1.84E-03	9.42E-08	2.02E-07	-	-	1.48E-02	7.94E-04	4.07E-07	8.73E-08	-	-	1.32E-02	7.06E-03	3.62E-05	7.76E-06	2.77E-05	2.87E-04
MPW	1.08E-03	5.81E-04	2.98E-08	6.39E-08	-	-	1.07E-02	5.71E-04	2.93E-07	6.27E-08	-	-	1.02E-02	5.46E-03	2.80E-05	6.00E-06	2.14E-05	2.22E-04
	Mn						Co						Ni					
TSS	5.17E-03	2.77E-03	1.42E-07	3.04E-07	1.82E-04	1.89E-03	2.79E-04	1.49E-04	2.69E-06	5.75E-06	2.05E-04	2.13E-03	1.89E-03	1.01E-03	5.18E-08	1.11E-07	1.42E-05	1.47E-04
TSW	5.95E-03	3.19E-03	1.63E-07	3.50E-07	2.10E-04	2.17E-03	2.72E-04	1.46E-04	2.62E-06	5.61E-06	2.00E-04	2.07E-03	1.43E-03	7.66E-04	3.93E-08	8.42E-08	1.07E-05	1.11E-04
SGS	3.14E-03	1.68E-03	8.63E-08	1.85E-07	1.11E-04	1.15E-03	1.26E-04	6.73E-05	1.21E-06	2.60E-06	9.26E-05	9.59E-04	6.18E-04	3.31E-04	1.70E-08	3.64E-08	4.63E-06	4.80E-05
SGW	2.46E-03	1.32E-03	6.77E-08	1.45E-07	8.68E-05	8.99E-04	8.32E-05	4.46E-05	8.02E-07	1.72E-06	6.13E-05	6.35E-04	3.36E-04	1.80E-04	9.23E-09	1.98E-08	2.52E-06	2.61E-05
SAW	5.40E-03	2.89E-03	1.48E-07	3.18E-07	1.90E-04	1.97E-03	1.57E-03	8.41E-04	1.51E-05	3.24E-05	1.16E-03	1.20E-02	2.83E-03	1.52E-03	7.78E-08	1.67E-07	2.12E-05	2.20E-04
MPS	1.62E-03	8.66E-04	4.44E-08	9.52E-08	5.70E-05	5.90E-04	8.03E-04	4.30E-04	7.74E-06	1.66E-05	5.92E-04	6.13E-03	1.16E-03	6.19E-04	3.18E-08	6.81E-08	8.67E-06	8.98E-05
MPW	2.14E-03	1.15E-03	5.89E-08	1.26E-07	7.56E-05	7.83E-04	1.05E-03	5.61E-04	1.01E-05	2.16E-05	7.72E-04	8.00E-03	6.36E-04	3.41E-04	1.75E-08	3.74E-08	4.77E-06	4.94E-05
	Cu						Zn						As					
TSS	3.76E-04	2.02E-04	1.03E-08	2.21E-08	1.22E-06	1.26E-05	5.57E-05	2.98E-05	1.53E-09	3.28E-09	4.68E-07	4.84E-06	1.40E-03	7.48E-04	3.83E-08	8.21E-08	2.93E-06	3.04E-05
TSW	4.07E-04	2.18E-04	1.12E-08	2.39E-08	1.32E-06	1.36E-05	5.90E-05	3.16E-05	1.62E-09	3.47E-09	4.96E-07	5.13E-06	1.35E-03	7.22E-04	3.70E-08	7.94E-08	2.83E-06	2.93E-05
SGS	2.57E-04	1.38E-04	7.07E-09	1.51E-08	8.33E-07	8.63E-06	6.27E-05	3.36E-05	1.72E-09	3.69E-09	5.27E-07	5.46E-06	1.22E-03	6.52E-04	3.34E-08	7.16E-08	2.55E-06	2.65E-05
SGW	2.12E-04	1.13E-04	5.81E-09	1.25E-08	6.85E-07	7.09E-06	1.80E-05	9.65E-06	4.95E-10	1.06E-09	1.51E-07	1.57E-06	2.14E-03	1.15E-03	5.89E-08	1.26E-07	4.50E-06	4.66E-05
SAW	2.88E-03	1.54E-03	7.90E-08	1.69E-07	9.31E-06	9.64E-05	1.78E-04	9.51E-05	4.88E-09	1.05E-08	1.49E-06	1.55E-05	2.87E-03	1.54E-03	7.90E-08	1.69E-07	6.04E-06	6.25E-05
MPS	9.91E-04	5.31E-04	2.72E-08	5.83E-08	3.21E-06	3.32E-05	1.38E-04	7.39E-05	3.79E-09	8.12E-09	1.16E-06	1.20E-05	4.01E-03	2.15E-03	1.10E-07	2.36E-07	8.42E-06	8.72E-05
MPW	5.72E-04	3.06E-04	1.57E-08	3.37E-08	1.85E-06	1.92E-05	2.95E-05	1.58E-05	8.11E-10	1.74E-09	2.48E-07	2.57E-06	3.76E-04	2.02E-04	1.03E-08	2.22E-08	7.90E-07	8.18E-06

	Se						Cd						Sb					
	Ingestion		inhalation		dermal		Ingestion		inhalation		dermal		Ingestion		inhalation		dermal	
	Children	Adults	Children	Adults	Children	Adults	Children	Adults	Children	Adults	Children	Adults	Children	Adults	Children	Adults	Children	Adults
TSS	5.92E-05	3.17E-05	1.63E-09	3.48E-09	-	-	3.73E-05	2.00E-05	1.80E-08	3.85E-08	7.82E-08	8.10E-07	3.84E-05	2.05E-05	1.05E-09	2.26E-09	-	-
TSW	3.88E-05	2.08E-05	1.07E-09	2.28E-09	-	-	2.63E-05	1.41E-05	1.27E-08	2.72E-08	5.52E-08	5.72E-07	5.75E-05	3.08E-05	1.58E-09	3.39E-09	-	-
SGS	1.53E-05	8.22E-06	4.21E-10	9.03E-10	-	-	2.41E-05	1.29E-05	1.16E-08	2.49E-08	5.06E-08	5.24E-07	5.21E-05	2.79E-05	1.43E-09	3.06E-09	-	-
SGW	2.15E-05	1.15E-05	5.90E-10	1.26E-09	-	-	1.10E-05	5.87E-06	5.28E-09	1.13E-08	2.30E-08	2.38E-07	5.48E-05	2.94E-05	1.51E-09	3.23E-09	-	-
SAW	5.79E-05	3.10E-05	1.59E-09	3.41E-09	-	-	2.82E-04	1.51E-04	1.36E-07	2.91E-07	5.91E-07	6.13E-06	7.95E-05	4.26E-05	2.18E-09	4.68E-09	-	-
MPS	3.36E-04	1.80E-04	9.24E-09	1.98E-08	-	-	1.03E-04	5.52E-05	4.96E-08	1.06E-07	2.16E-07	2.24E-06	1.01E-04	5.43E-05	2.78E-09	5.97E-09	-	-
MPW	2.50E-05	1.34E-05	6.86E-10	1.47E-09	-	-	1.97E-05	1.06E-05	9.51E-09	2.04E-08	4.14E-08	4.29E-07	2.74E-05	1.47E-05	7.53E-10	1.61E-09	-	-
	Ba						Hg						Pb					
TSS	6.73E-05	3.61E-05	1.85E-09	3.96E-09	-	-	8.37E-04	4.48E-04	8.02E-08	1.72E-07	1.76E-06	1.82E-05	7.38E-04	3.96E-05	2.03E-08	4.35E-08	1.03E-05	1.07E-04
TSW	7.95E-05	4.26E-05	2.18E-09	4.68E-09	-	-	2.41E-04	1.29E-04	2.31E-08	4.95E-08	5.06E-07	5.24E-06	9.26E-04	4.96E-05	2.55E-08	5.45E-08	1.30E-05	1.34E-04
SGS	5.78E-05	3.09E-05	1.59E-09	3.40E-09	-	-	4.31E-04	2.31E-04	4.13E-08	8.85E-08	9.05E-07	9.38E-06	1.90E-03	1.02E-04	5.23E-08	1.12E-07	2.67E-05	2.76E-04
SGW	1.09E-04	5.83E-05	2.99E-09	6.41E-09	-	-	3.65E-06	1.96E-06	3.50E-10	7.50E-10	7.67E-09	7.95E-08	4.65E-04	2.49E-05	1.28E-08	2.74E-08	6.51E-06	6.75E-05
SAW	2.65E-04	1.42E-04	7.29E-09	1.56E-08	-	-	3.65E-06	1.96E-06	3.50E-10	7.50E-10	7.67E-09	7.95E-08	2.66E-02	1.43E-03	7.31E-07	1.57E-06	3.73E-04	3.86E-03
MPS	2.49E-04	1.33E-04	6.83E-09	1.46E-08	-	-	1.83E-05	9.78E-06	1.75E-09	3.75E-09	3.84E-08	3.97E-07	2.96E-03	1.59E-04	8.13E-08	1.74E-07	4.14E-05	4.29E-04
MPW	9.88E-05	5.29E-05	2.71E-09	5.82E-09	-	-	3.65E-06	1.96E-06	3.50E-10	7.50E-10	7.67E-09	7.95E-08	9.28E-04	4.97E-05	2.55E-08	5.46E-08	1.30E-05	1.35E-04

Appendix 8: Spectrogram from IRMS

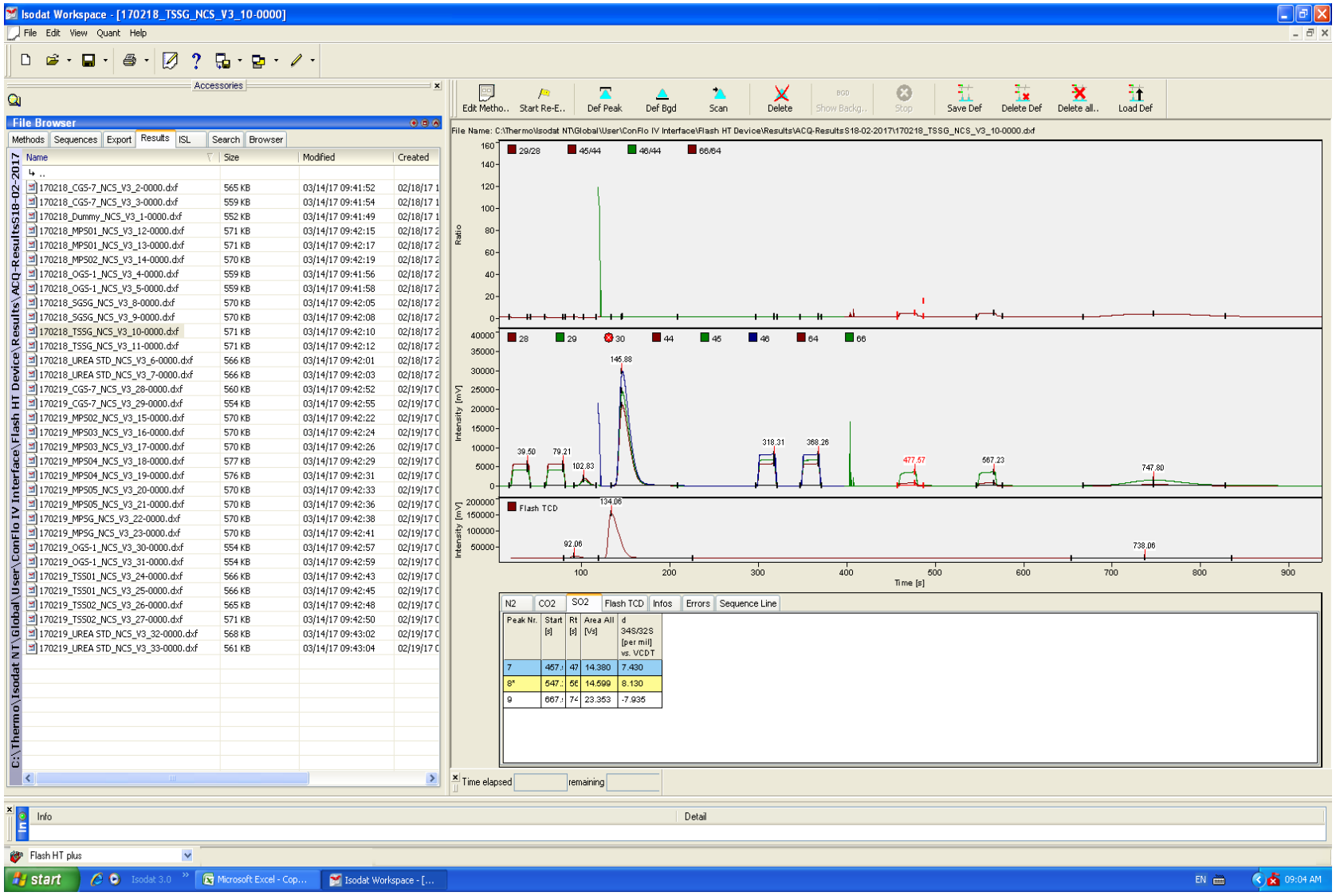

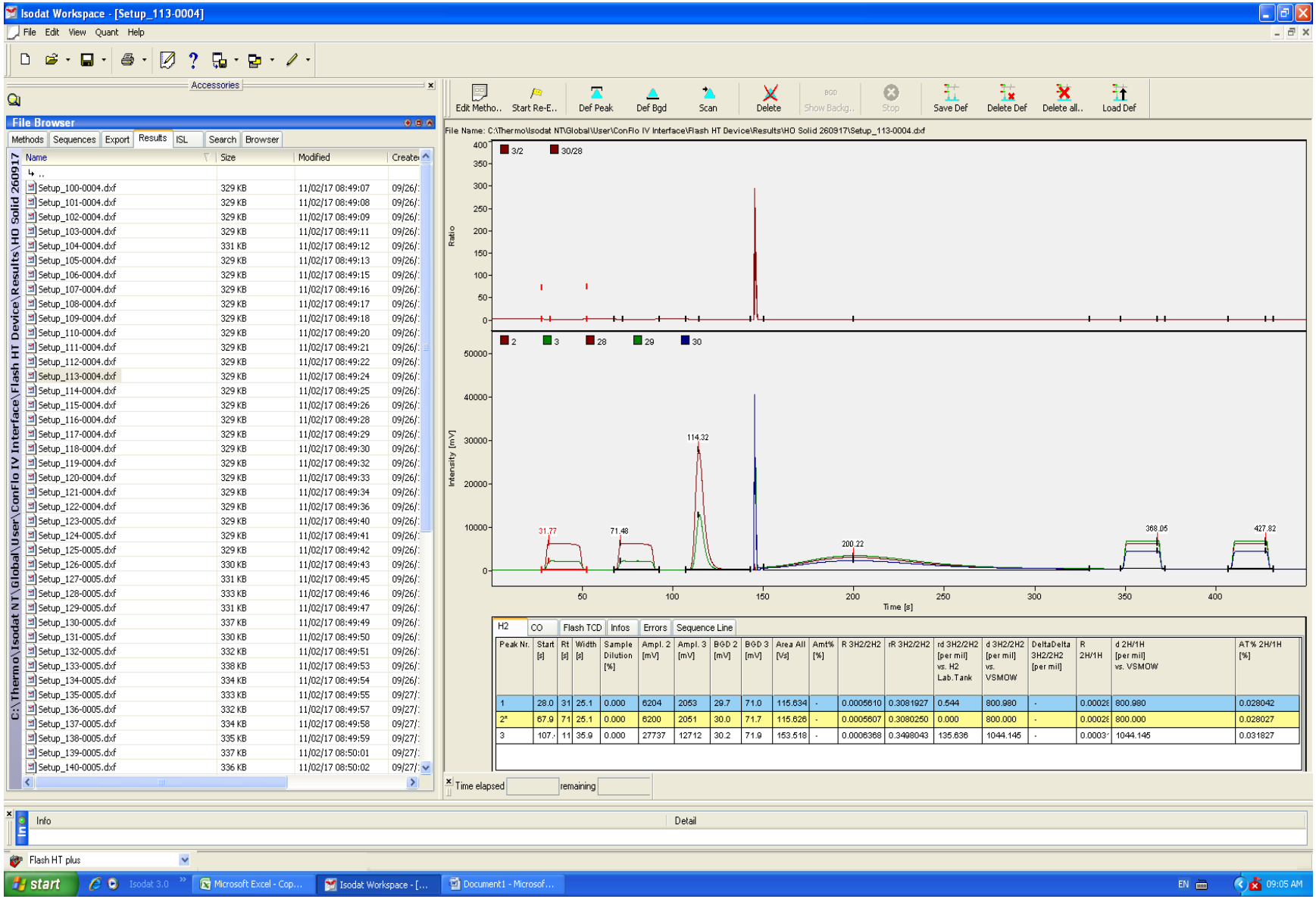

Appendix 9: Request and Permission letters obtained for/during the study

SCHOOL OF ENVIRONMENTAL SCIENCES
OFFICE OF THE DEAN

TO: THE MANAGER, FOREVER RESORTS TSHIPISE

FROM: DEAN, SCHOOL OF ENVIRONMENTAL SCIENCES

SUBJECT: REQUEST FOR PERMISSION TO CONDUCT RESEARCH

DATE: 11 APRIL 2017

Mr. Durowoju Olatunde (student number 11634830) is a PhD student in the School of Environmental Sciences at the University of Venda. He is researching on "Isotopic signatures from thermal springs and environmental media within Soutpansberg". Kindly allow him to collect water samples from the springs. The data collected will solely be used for research purposes.

Thanks for your consideration.

SCHOOL OF ENVIRONMENTAL SCIENCES
FOR YOUR INFORMATION
2017 -04- 11
OFFICE OF THE DEAN
UNIVERSITY OF VENDA

Yours faithfully,

Prof J.O. Odiyo
Head, Department of Hydrology and Water Resources

University of Venda

PRIVATE BAG X5050 THOHOYANDOU 0950 SOUTH AFRICA
TEL: +27 15 962 8511; E-mail: john.odiyo@univen.ac.za
"A quality driven, financially sustainable, rural-based comprehensive university"

Gmail OLATUNDE DUROWOJU <durotunde@gmail.com>

Permission to conduct Research

Pieter Erasmus <pieter@foreversa.co.za> 13 April 2017 at 07:46
To: durotunde@gmail.com
Cc: Beauty Maseka <info@foreversa.co.za>

Dear Durowoju,

I trust that you are doing well today.

You are welcome to do your research at our resort. Please just inform us when you will be coming well in advance.

Kind regards

Pieter Erasmus I GENERAL MANAGER

Tshipise, A FOREVER RESORT

Cell: 072 624 2376

Tel: 015 539 0634

Fax to mail: 086 660 5040

Email: pieter@foreversa.co.za

Website: www.forevertshipise.co.za

GPS: -22 36' 20"S/ 30 10' 24"E

Physical Address: R525, Towards the Kruger National Park Pafuri Gate, Tshipise, Limpopo Province

Postal Address: PO Box 4, Tshipise, 0901

South African Weather Service
ISO 9001 Certified Organisation

Disclosure Statement

SCHEDULE 1

Please note: The South African Weather Service will only act upon customer requirements noted on this disclosure statement and not from any other correspondence.

FULL PERSONAL DETAILS OF USER

Full Names	DUROWOJU OLATUNDE SAMOD
University/school/organisation	UNIVERSITY OF VENDA
Student Number (if applicable)	11634830
Email address	durotunde@gmial.com
Cellphone	0780642299
Supervisor	Prof JO Odiyo
Project/Thesis Title	ISOTOPIC SIGNATURES IN GEOTHERMAL SPRINGS AND THEIR ENVIRONMENTAL MEDIA WITHIN SOUTPANSBERG
Current registered degree (e.g. BSc)	PhD
Expected finalization date (MMYYYY)	September, 2018

The South African Weather Service reserves the right to request, at any time, from the student proof of registration for the Degree at the University.

THE PURPOSE (*Please indicate a detailed description of the purpose for which the data will be used)*

The data set to consolidate with the isotopic composition of the precipitation and groundwater samples and to show spatial-temporal variations of the isotopes and their relationships with the regional annual hydrological cycle.

DATA REQUIRED *(Please include the weather elements (e.g. rain, temperature), place/s and time period)*

The data required are Monthly Rainfall, Temperature, and Altitude data for Thohoyandou, Sagole, Siloam, Mphephu and Tshipise from January 2015 to November 2017.

I hereby accept that:

- SAWS will be acknowledged in the resulting thesis/project or when published, for the data it provided.
- SAWS will be provided with a copy of the final results in printed or electronic format.
- The data received shall not be provided to any third party.

Signature of the User: 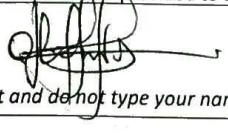 Date: 07/12/2017.

(*Please sign the document and do not type your name in as this is a legal document and requires a signature.*)

Private Document

Document Template Reference: CLS-Disclosure-001.10
Record Reference: CLS-CI-DS
Page 2 of 2

Gmail OLATUNDE DUROWOJU <durotunde@gmail.com>

FW: Climate Data Requests

Joe Matsapola <Joe.Matsapola@weathersa.co.za> 8 December 2017 at 08:24
To: "durotunde@gmail.com" <durotunde@gmail.com>
Cc: Elsa DeJager <Elsa.DeJager@weathersa.co.za>

Good morning, attached please find the data you requested. Please note most stations you requested are not opened but I added two more stations.

Kind regards

Joe Matsapola
Scientist: Climate Information
Tel: 0822338282/ 0123676029
Fax: 0123676031
e-mail: joe.matsapola@weathersa.co.za
Physical address: 442 Rigel Ave South, Erasmusrand, Pretoria
Postal adress: Private Bag X097, Pretoria 0001

Weatherlines: *120*555*3# or 083 123 0500
www.weathersa.co.za

"Creating a weather-smart nation – Innovating, Adapting and Facing the Future together"